Organization of cerebellar neuronal activity during motor action and rest in freely-moving rats

Hongying Gao

▶ **To cite this version:**

Hongying Gao. Organization of cerebellar neuronal activity during motor action and rest in freely-moving rats. Neurons and Cognition [q-bio.NC]. Université Pierre et Marie Curie - Paris VI, 2012. English. NNT : 2012PA066080 . tel-00829306

HAL Id: tel-00829306

https://theses.hal.science/tel-00829306

Submitted on 3 Jun 2013

HAL is a multi-disciplinary open access archive for the deposit and dissemination of scientific research documents, whether they are published or not. The documents may come from teaching and research institutions in France or abroad, or from public or private research centers.

L'archive ouverte pluridisciplinaire **HAL**, est destinée au dépôt et à la diffusion de documents scientifiques de niveau recherche, publiés ou non, émanant des établissements d'enseignement et de recherche français ou étrangers, des laboratoires publics ou privés.

PH.D. THESIS OF

UNIVERSITY PIERRE ET MARIE CURIE-PARIS VI

AND EAST CHINA NORMAL UNIVERSITY

Graduate School: Cerveau, Cognition, Comportement (ED3C), Paris VI
And Institutes for Advanced Interdisciplinary Research, ECNU

Specialist: Neuroscience

Presented by: Hongying GAO

To obtain the Doctor's degree of University Pierre et Marie Curie
And East China Normal University

Organization of cerebellar neuronal activity during motor action and rest in freely-moving rats

Defence predicted in may 2012 in front of the committee composed of
Mr. Clément LENA
Mr. Yinghe HU
Mr. Régis LAMBERT
Mr. Linlong NIAN
Mr. Jiping ZHANG

THESE DE DOCTORAT

DE L'UNIVERSITE PIERRE ET MARIE CURIE

ET DE L'UNIVERSITE NORMALE DE L'EST DE LA CHINE

Ecole Doctorale : Cerveau, Cognition, Comportement, Paris VI
et Institutes for Advanced Interdisciplinary Research, ECNU

Spécialité : Neuroscience

Présentée par Hongying GAO

Pour obtenir le grade de Docteur de l'Université Pierre et Marie Curie
et de l'Université Normale de l'Est de la Chine

Organisation de l'activité neuronale cérébelleuse lors de d'une tâche de préhension et reste dans des rats déplacant librement

Soutenqnce prévue au moins de mai 2012 devant le jury composé de
M. Clément LENA
M. Yinghe HU
M. Régis LAMBERT
M. Linlong NIAN
M. Jiping ZHANG

法国皮埃尔与玛丽居里与中国华东师范大学博士论文

博士生院：巴黎第六大学-脑，认知，行为
华东师范大学-科学与技术跨学科高等研究院

专业：神经生物学

博士生 高红英

自由活动大鼠在运动动作和休息状态下的小脑神经活动模式

2012 年 5 月答辩　答辩委员会成员
Clément LENA 先生
胡应和先生
Régis LAMBERT 先生
林龙年先生
张季平先生

Thanks!

During that 4 years of study, it's difficult to list everyone to whom I want to give my gratefulness.

I would like to give my sincere gratitude to Pr. Lambert, Pr. Zhang, Pr. Lin, who accepted to be the member of my jury and examine my work.

Clement Lena, who guided all along the thesis, opened many new points of view of the science. Your great intelligences and patience helped so much on my research and writing thesis. After 4 years of work with you, I learn a lot and I found it was a wise decision to choose you as my adviser. Thanks also for helping my life in Paris and introducing me a lot of French culture. I still remember the first day when I arrived in Paris, you came to pick me up although it was the same day for the defence of your previous student. I will miss the working days that you are shuttling among us with the demand sentences 'Clement, Clement'. Indeed, I am really grateful to be working with you.

The appreciativeness next go to my warm termmates: Remi, Daniela, Maria. You made the lab more like a big family. It was a pleasure to work in the same term with you. We always discussed and tried to find some solutions together as soon as a problem appeared. We inspired each other when we were disappointed with the results or when we met a trouble. Now, you become also my friends: the relaxed afternoon tea, the exciting films, the delicious dinners. We also shared some ideas about international food (French, Italian, Chinese...), music, movies, games and other culture. The new member, Robin, makes the team younger and more vivid.

Moreover, I want to thank everybody in the neuro lab. Each of you was so kind with me. Boris, Mariano, Anne, Stéphane D, Stéphane S, Pierre, Antonin, Romain, Guy, Eric, German, Angela, Shujia, Lu, Charly, David, Shixin, thank you for your discussions and suggestions. Eric

and Boris, as the only native English speakers, thank you for correcting my English writing every time.

I would like to thank also prof. Hu. Your support and help make it possible to finish my study and to arrange my defence.Thanks to Mme. Qian, Mrs. Li, Miss. Liu and all other people of East China Normal University who helped me make this co-orperation study.

Thanks to my friends who shared their time in France with me, Xin, Qi, Fan, Liang, Zhe, Cong, Qing, PingPing, Hong, Yingying, Yan. With you, the life in France is more colorful. I want to thank another friends in Germany, liangchi, who traveled several times with me and share his experiments with me. I would like to thank also my friends in Shanghai, Qin, Yinli and so many others, thanks so much for helping deal with the things in Shanghai and your words let me feel at home.

My dear parents, I am so grateful to be your child and wish you are also proud of me. I am sorry that I am far away from you since I am your only child. However, you know, your love, your support and understanding make my life still as near you.

Special thanks to Mauricette GIRARD and families JATTEAU, BICHON. Your great warmness and kindness touched my heart. Your patience and detailed introduction of the French language and culture helped me understand France better. I am also appreciated so much your understanding of my own culture.

Last, but not least, my rats, my lovely rats, without you, definitely there wouldn't be my thesis! I am quite happy about your performance and the results you gave to me. Hope you will have a happy lives in the heaven.

路漫漫其修远兮
吾将上下而求索

——屈原

Summary

The cerebellum is a brain structure involved in coordination complex motor actions such as voluntary movements. To achieve this function, the precise temporal control of a large population of neurons is required. While a large number of patterned population activity has been characterized in many major brain structures (thalamo-cortical system, basal ganglia, hippocampal formation, etc…), very little is currently known in the cerebellum. Therefore, I investigated the presence and characteristics of such an organization in freely-moving rats, especially when they perform a reach-and-grasp task. The cerebellar cortex has a strong topographical organization, such that neighboring cells share similar input sources and output targets. Therefore, studying the local network properties in the cerebellar cortex allows to access to functionally-relevant population activity.

First, I demonstrated that multi-wire electrodes, tetrodes, may be used to record multiple neighboring cells in chronic recordings of freely behaving animals using a custom-made microdrive.

Second, I examined in the area of the cerebellar cortex controlling limb movements how the principle cells (the Purkinje cells) coordinate their firing during rest and fast forelimb motor action. Using simultaneous electrophysiological recordings of multiple single cells, I found that neighboring Purkinje cells exhibit consistently a co-modulation of their firing rate at time scale of a few milliseconds. This correlated firing is observed during sleep and active exploration, and increases during motor execution. Our results thus indicate that during a fast and complex movement, local assemblies of Purkinje cells form dynamically at short time scales and will produce very transient episodes of inhibition in the deep cerebellar nuclei.

Third, in a collaboration with the group of Richard Courtemanche, we studied the link between neuronal firing and slow local field oscillations that are observed in the cerebellum at rest. We found that a large proportion of Golgi cells and Purkinje cells are modulated during the oscillations. These results indicate that these slow oscillations, that may be also observed in the motor cortex, are propagated in the cerebellar cortex.

Overall, my work has identified and characterized a number of state-dependent population activity patterns in the cerebellar cortex. How these patterns impact on the motor system largely remains to be understood and should be examined in future studies.

Résumé

Le cervelet est une structure du cerveau impliquée dans la coordination des actions motrices complexes telles que les mouvements volontaires. Pour remplir cette fonction, le contrôle temporel précis d'une large population de neurones est nécessaire. Alors qu'un grand nombre d'études ont été consacrées à l'étude de l'activité de réseau dans la plupart des grandes structures cérébrales (système thalamo-cortical, les noyaux gris centraux, hippocampe, etc ...), le cervelet reste très peu étudié. Par conséquent, j'ai examiné la présence et les caractéristiques d'une telle organisation chez les rats libres de leurs mouvements, en particulier lorsqu'ils accomplissent une tâche de préhension. Le cortex cérébelleux a une organisation topographique marquée, de sorte que les cellules voisines reçoivent les mêmes afférences et ont des efférences convergentes. Par conséquent, l'étude des propriétés du réseau local dans le cortex cérébelleux permet d'accéder à une activité populationnelle qui est fonctionnellement pertinente.

Tout d'abord, j'ai démontré que les multi-électrodes et particulièrement les tétrodes peuvent être utilisées, grâce à un « micro-drive » que j'ai conçu et réalisé, pour enregistrer plusieurs cellules voisines dans des enregistrements chroniques de comportement de rongeurs libres de leurs mouvements.

Deuxièmement, j'ai examiné dans la zone du cortex cérébelleux qui contrôle les mouvements des membres la façon dont les cellules principales (les cellules de Purkinje) coordonnent leur décharge pendant le repos et durant une action motrice des membres antérieurs. Par des enregistrements électrophysiologiques simultanés de plusieurs cellules individuelles, j'ai trouvé que les cellules de Purkinje voisines présentent toujours un co-modulation de leur taux de décharge à l'échelle de quelques millisecondes. Cette décharge corrélée est observée pendant le sommeil et d'exploration active, mais elle est accrue au cours de l'exécution de mouvements. Nos résultats indiquent donc que lors d'un mouvement rapide et complexe, les assemblées locales des cellules de Purkinje se forment dynamiquement à des échelles de temps courtes et produisent donc des épisodes très transitoires d'inhibition dans leur cible postsynaptique dans les noyaux cérébelleux.

Troisièmement, dans une collaboration avec le groupe de Richard Courtemanche, nous avons étudié le lien entre la décharge neuronale et les oscillations lentes du potentiel de champ local qui sont observées dans le cervelet au repos. Nous avons constaté qu'une grande proportion de cellules de Golgi et les cellules de Purkinje sont modulées pendant les oscillations. Ces résultats indiquent que ces oscillations lentes, qui peuvent également être observées dans le cortex moteur, se propagent dans le cortex cérébelleux.

Dans l'ensemble, mon travail a identifié et caractérisé un certain nombre de patrons d'activité populationnelle dans le cortex cérébelleux. L'impact de ces patrons sur le système moteur reste en grande partie à être compris et devrait faire l'objet de futures travaux.

摘要

小脑是涉及协调复杂运动，例如随意运动的大脑结构。要实现这个功能，对大量神经元活动的精确时间控制是必需的。在许多重要的大脑结构（丘脑 - 皮层系统，基底节，海马结构等）中，已经发现了大量的群体神经元活动模式，然而在小脑中还知之甚少。因此，我的课题是研究在自由活动大鼠中，特别是当它们进行抓取任务时，小脑神经活动模式的存在性及其特征。小脑皮层具有很强的局部结构组织性，例如相邻细胞有着类似的传入源和传出目标。因此研究小脑皮层的局部神经网络特性可以揭示功能相关的神经群体活动。

首先，我证明了通过特制的电极帽，四电极可以用于长期记录自由活动动物中多个相邻细胞的活动。

第二，我测试了在动物休息和快速前肢运动时，小脑皮层控制肢体运动区域中的主要细胞（浦肯野细胞）是如何协调它们的放电的。通过对多个单神经元的同时电生理记录，我发现相邻的浦肯野细胞显现出在毫秒水平上放电频率的联合改变。在动物睡眠，自由探索过程中都能观察到这种相关放电，并且这种相关性在运动执行时有所增加。我们的研究结果表明在一个快速复杂的运动过程中，局部浦肯野细胞群体在短时间尺度内会形成一个动态协作模块，并且它们的这种协作活动会对小脑深部核造成非常短暂的抑制。

第三，通过与 Richard Courtemanche 小组的合作，我们研究了神经元放电和局部低频波的联系。这种低频波通常在动物休息时能被观察到。我们发现大部分的高尔基细胞和浦肯野细胞受振荡波的调制。这些结果表明，这种在运动皮层中也能观察到的低频波会在小脑皮层中传播。

总体而言，我的工作确定并质化了小脑皮层中的一些状态依赖性神经群体活动模式。这些模式如何影响运动系统在很大程度上还有待研究，并应在今后的研究中检验。

Table of contents

FIRST PART: INTRODUCTION **1**

1 Structure of the cerebellum **2**

1.1 Anatomical structure 2

1.1.1 Location and structure of the cerebellum 2

1.1.2 Subdivisions of the cerebellum 2

1.1.3 Structure of the cerebellar cortex 2

1.2 Circuit 7

1.2.1 Circuit of cerebellum 7

1.2.2 Excitatory input of cerebellar cortex 10

1.2.3 Inhibition in the cerebellar cortex 11

1.2.4 Other elements in the cerebellar cortex 11

1.2.5 Output of cerebellar cortex 12

1.3 Functional organization 12

1.3.1 Division 12

1.3.1.1 Longitudinal zones 12

1.3.1.2 Microzones 13

1.3.1.3 Microcomplex 13

1.3.1.4 Multizonal microcomplex 13

1.3.2 Receptive Fields 18

1.3.2.1 Topography of climbing fiber afferents to microzone 18

1.3.2.2 Topography of mossy fiber afferents to microzone 18

1.3.2.3 Topography of parallel fiber afferents to microzone 19

1.3.2.4 Receptive field of interneurons 19

1.3.2.5 Interaction between receptive of climbing fiber and parallel fiber 19

1.3.2.6 Receptive field of the forelimb 22

1.3.2.7 The relationship between receptive filed of climbing fiber and that of spinal nociceptive withdrawal reflexes 24

1.4 Summary 26

2 Function of the cerebellum **27**

2.1 Function depends on regions 27

2.2 Voluntary motor control and motor learning 30

2.3 Non-motor functions 31

2.4 Timing 32

2.5 Conclusion 34

3 Purkinje cell activities 35

3.1 Simple spikes 35

3.2 Encode of simple spike for limb movement 36

3.3 Interactions of simple spike and complex spike 38

3.3.1 Inhibition of simple spike by complex spike 39

3.3.2 LTP of inhibition of simple spike by complex spike 39

3.4 Inhibitory input 42

3.5 Population and synchrony of Purkinje cell activities 42

4 Golgi cell activities 47

4.1 Structure 47

4.2 Basic activities 50

4.3 Functional activities 51

5 Oscillation in the cerebellum 52

5.1 High frequency oscillation 54

5.2 Low frequency oscillation 61

5.3 Gamma oscillation 65

5.4 Interaction and effect 68

6 Reach-grasp movement 69

6.1 Components 69

6.2 Similarities and differences of skilled forelimb among species 73

6.3 Brain regions involved in skilled reaching 74

7 The motor cortex **78**

7.1 The functional of motor cortex on voluntary movement 78

7.2 Connection between the motor cortex and the cerebellum 78

7.2.1 Anatomical connection 78

7.2.2 Two models of internal model based on connection ways between the motor cortex and the cerebellum 79

7.2.3 Coherence between the motor cortex and the cerebellum 84

8 Global conclusion and research proposal **85**

SECOND PART: METHODS **88**

1 Animal and training 89

1.1 Feeding 89

1.2 Recording table 90

1.3 Training schedule 90

2 Electrode Preparation 92

2.1 Preparation of headstage for the cerebellum 92

2.2 Preparation of bundle of single wire electrodes for the motor cortex 93

3 Surgery and implantation of electrodes 93

4 *In vivo* recording 94

5 Recording system 94

6 Data analysis 97

6.1 Single-unit isolation (clustering) 97

6.2 Video analysis 97

7 Histology 98

THIRD PART: RESULTS **99**

1 First article 100

2 Second article 110

3 Third article 140

4 Other results 186

FOURTH PART: DISCUSSION AND PERSPECTIVES 193

REFERENCES 203

First part
Introduction

1 Structure of the cerebellum

1.1 Anatomical structure

1.1.1 Location and structure of the cerebellum

The cerebellum is a part of the brain, which is posterior to the cerebral cortex and located above the pons (Figure 1.1A). The cerebellum includes a mass of external folded gray matter, the cerebellar cortex, around a core of white matter (Arbor vitae) (Figure 1.1B). Within the white matter, there are four clusters of gray matter called the deep nulei: the fastigial, the globose, the emboliform (the globose and the emboliform can be called together the interposed) and the dentate. In the rodent, these nuclei are contiguous. The cerebellar cortex is a very tightly folded 3-layer cortex which takes most of the volume of the cerebellum and in which the majority of the neurons in the cerebellum are located.

1.1.2 Anatomical divisions of the cerebellum

There are different ways to divide the cerebellum. From rostral to caudal, the cerebellar cortex can be divided into three parts separated by deep fissures: anterior lobe, posterior lobe and flocculonodular lobe (Figure 1.1B). From medial to lateral, leaving the vestibulocerebellum (also known as flocculo-nodular lobe) aside, the cerebellar cortex can be divided into two parts based on connections and functions: spino-cerebellum and cerebro-cerebellum (Figure 1.2A). Based on the folds, the cerebellar cortex is conventionally divided into ten lobules (Figure 1.2B). Larsell identified these ten lobules (I-X) in the vermis and corresponding ten lobules (HI-HX) in the hemispheres (Fig 2).

1.1.3 Structure of the cerebellar cortex

The cerebellar cortex has a uniform structure with the same basic neuronal circuitry repeated over the entire cerebellar cortex. This structure is composed by three layers: the molecular layer, the Purkinje cell layer and the granular layer (Figure 1.3). The molecular layer is located on the external side. Several types of interneurons such as stellate cells and basket cells are located in this layer. The Pukinje cell layer is a mono-layer of cells between molecular layer and granular layer. The soma of Purkinje cells, the principal cells of cerebellar cortex, are located in this layer. The granular layer is located below Purkinje cell layer and is named after the granule cells located in this layer.

Golgi cells are also located in granular layer. Except for the granule cells, which are glutamatergic, the other four main types of cells in the cerebellar cortex (Purkinje cell, stellate cells, basket cells and Golgi cells) are inhibitory.

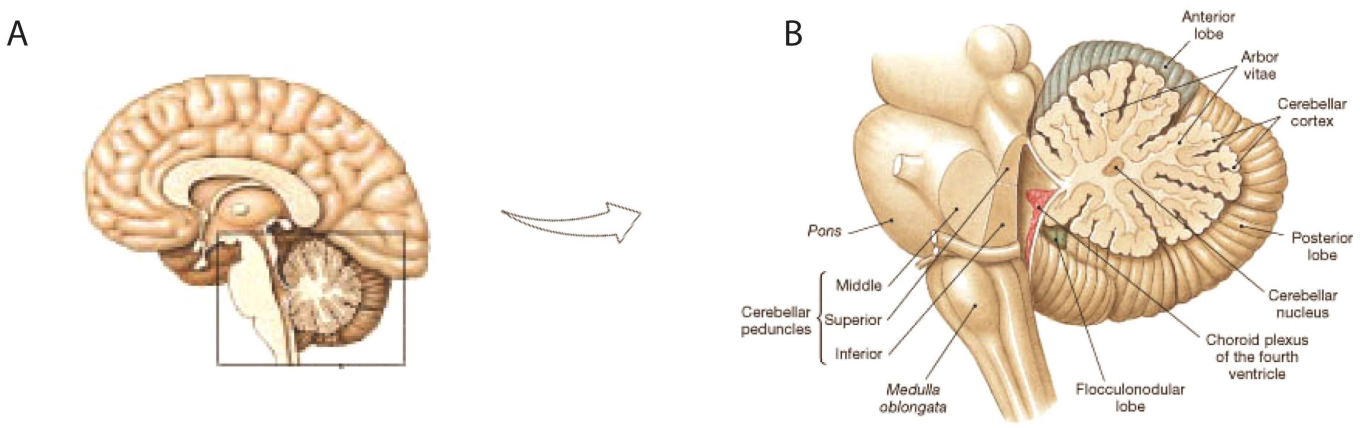

Figure 1.1 The location and the structure of the cerebellum
A: Sagittal view of the brain, showing the location of the cerebellum in the brain.
B: The structure of the cerebellum, showing 2 major structures (cerebellar cortex and cerebellar nuclei), 3 lobes (anterior lobe, posterior lobe and flocculonodular lobe).

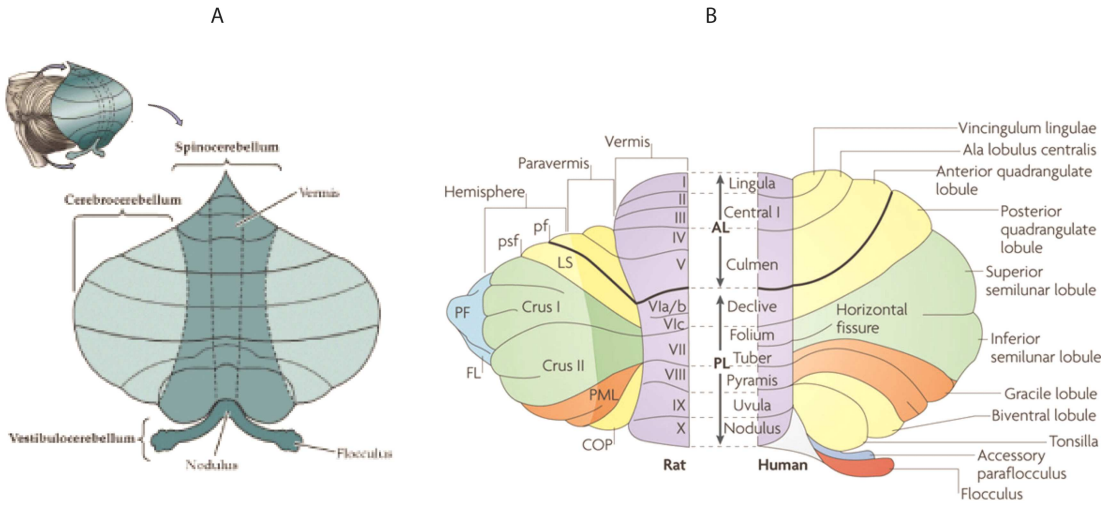

Figure 1.2 Subdivision of the cerebellum
A: Flattened view of the cerebellar surface, illustrating the three major subdivisions. Adapted from (Neuroscience. 2nd edition, 2001).
B: Dorsal view of the rat cerebellum to the left and simplified dorsal view of the human cerebellum to the right, indicating the comparative nomenclature. Equivalent regions in the rat and human cerebellum are given the same color. On the left, lobules in the ermis are numbered according to Larsell's schema, whereas on the right, the corresponding nomenclature as described by Bolk is shown. For both views the primary fissure dividing the anterior and posterior lobes is highlighted in bold. AL, anterior lobe; COP, copula pyramidis; Crus I and Crus II, ansiform lobule; FL, flocculus; LS, lobulus simplex; PF, paraflocculus; PL, posterior lobe; PML, paramedian lobule; psf, posterior superior fissure. Adapted from (Apps and Hawkes, 2009).

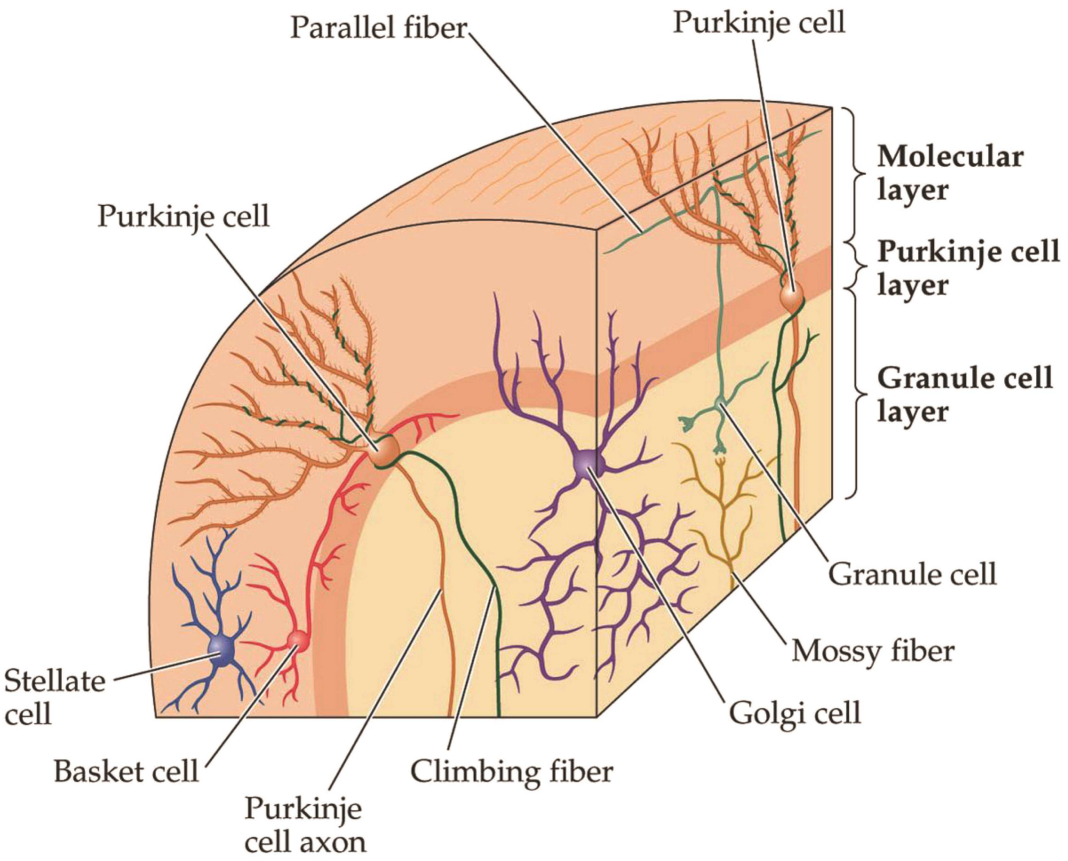

Figure 1.3 The structure of the cerebellar cortex
The figure shows 3 layer (molecular layer, Purkinje cell layer and Granule cell layer) and major cell types (Granule cell, Golgi cell, Purkinje cell, Stellate cell and Basket cell) in the cerebellar cortex. Adapted from (Neuroscience. 4nd edition).

1.2 Circuit

1.2.1 Circuit of cerebellum

Informations from sensory systems and from other parts of the brain and spinal cord enter the cerebellum through mossy fibers and climbing fibers, and excite deep cerebellar nuclei (Figure 1.4). The deep cerebellar nuclei, the source of cerebellar output fibers, send their axons towards many brain stem centers, and thalamic nuclei. The cerebellar nuclei neurons are excited by the mossy and climbing fibers and inhibited by Purkinje cell terminals from the cerebellar cortex. The cerebellar cortex also receives mossy and climbing fiber inputs and therefore, acts as a feed-forward inhibitory circuit on the deep nuclei (Figure 1.4B).

The inputs and outputs of the cerebellum are segregated in different areas of the cortex and nuclei. The information from the vestibular apparatus (semicircular canals and otolithic organs) travels along cranial nerve VIII to the vestibular nuclei in the medulla and directly enters into the vestibulo-cerebellum. The Purkinje cells in the flocculo-nodular lobe project to the vestibular nuclei (acting as deep cerebellar nuclei) which then send descending projections to the medial and lateral vestibulospinal tracts controlling posture. Projections also ascend to participate to the vestibulo-ocular reflex. Somatosensory inputs enter the spino-cerebellum through the cuneo-cerebellar and spino-cerebellar pathways, bringing proprioceptive and cutaneous information. Somatosensory inputs from the trunk and head, as well as inputs from the visual, vestibular and auditory systems enter the vermis. The intermediate zones receive projections from the distal extremities. Outputs from the vermis exit through the fastigial nuclei descending to the brain stem and lateral vestibular nuclei. Some projections also ascend to the thalamus and primary motor cortex. Outputs from the intermediate zone also project to the interposed nuclei and then descend through the red nucleus to the rubrospinal tract. Ascending projections go also to other parts of the brain such as the thalamus, the primary and supplementary motor cortex. Information from cortical areas are sent to the cerebro-cerebellum hemisphere through the pontine nuclei in the brainstem. Outputs descend in the corticospinal and reticulospinal pathways and project also through the dentate nuclei, to the thalamus continuing to the motor, premotor and prefrontal and

striatal areas.

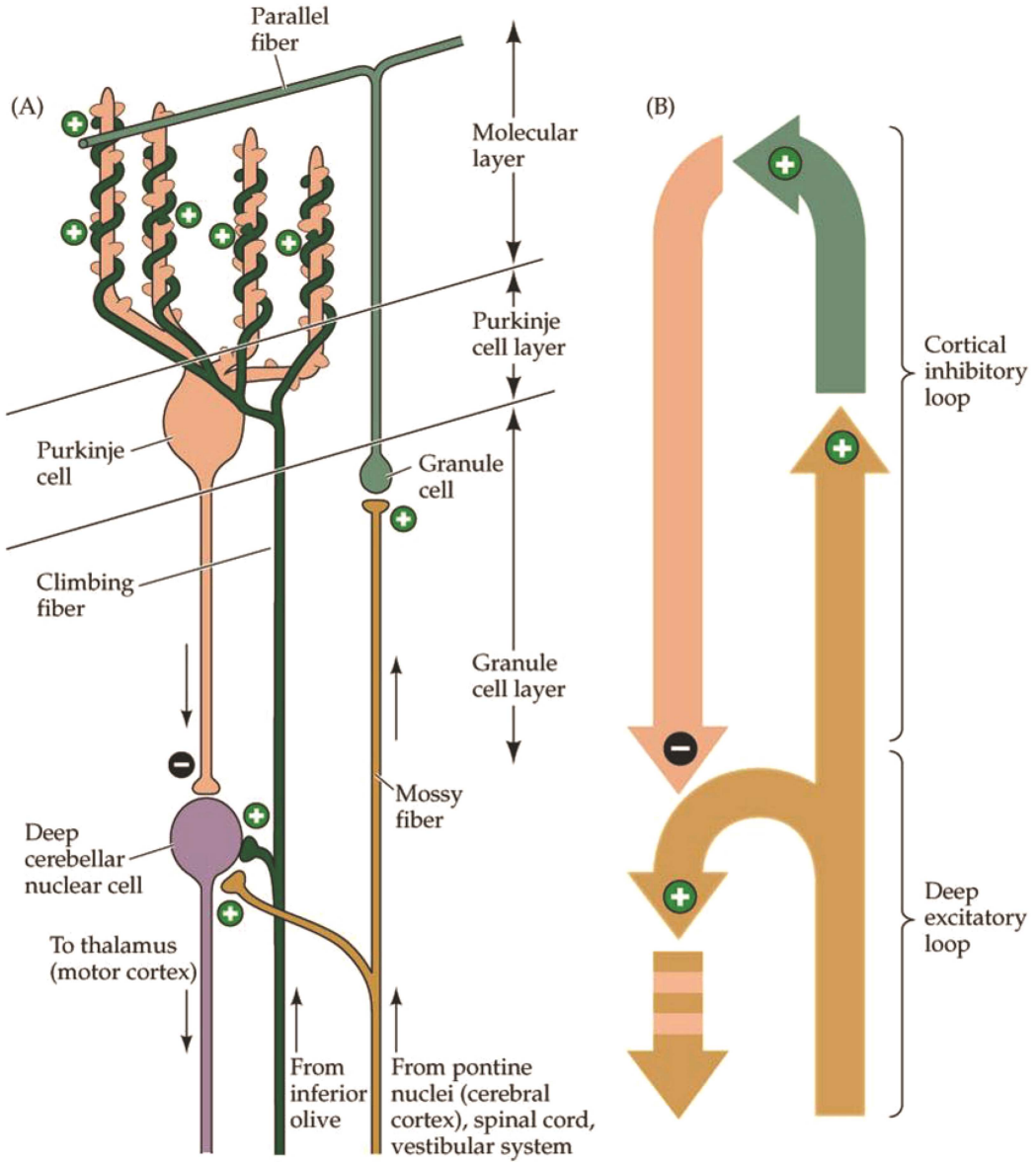

Figure 1.4 Circuit of the cerebellum
A Circuit of the cerebllum through different layers
B Diagram of the information loops in the cerebellum
Adapted from (Neuroscience. 4th edition, 2007).

1.2.2 Excitatory inputs of cerebellar cortex

The whole cerebellar cortex plays a role of feed-forward inhibition, thus it is quite determinant for the output of the cerebellum. The cerebellar cortex shares the same two main inputs with the cerebellar nuclei: the mossy fibers and climbing fibers.

The mossy fibers arise from a wide variety of sources, including the spinal cord, numerous brain stem nuclei (especially the pons) and the cerebellum itself. In the cortex, they target the granule cell dendrites where they form a characteristic rosette structure within a glomerulus. One mossy fiber contacts 400 to 600 granule cells in a folium. There is however only a small convergence on the granule cell, each granule cell receiving only a small number (four to five) of mossy fibers excitatory inputs (Chadderton et al., 2004; Eccles et al., 1967). Granule cells send their axons, known as parallel fibers, into the molecular layer and excite the Purkinje cells. A parallel fiber has a T shape and can be 4 to 7 mm long across the entire width of a folium in the mammals (Brand et al., 1976; Mugnaini, 1983; Pichitpornchai et al., 1994). It forms synaptic contacts with the dendritic spines of at least 300 Purkinje cells (Eccles et al., 1967). A Purkinje cell can make connection with a huge number of parallel fibers, 180000 in human (Fox and Bernard, 1957) or more than 60000 in rat (Napper and Harvey, 1988a,b; Palay and Chan-Palay, 1974). Only coincident granule cell inputs with a narrow time window can be summated effectively to excite a Purkinje cell. The whole-cell recording in the cerebellar cortex suggested that 50 simultaneously active granule cells are sufficient to excite a single Purkinje cell (Barbour, 1993).

The second main cerebellar afferents are the climbing fibers. Climbing fibers are projections from the inferior olivary nucleus located in the medulla oblongata. They carry information from various sources such as the spinal cord, vestibular system, red nucleus, superior colliculus, reticular formation, sensory and motor cortices. A climbing fiber forms numerous direct, excitatory synapses with the dendrites of one to ten Purkinje cells. Each Purkinje cell receives this powerful input from just one climbing fiber. The input of a single climbing fiber is so strong that an action

potential can reliably cause firing of a target Purkinje cell.

Besides mossy fibers and climbing fibers, the cerebellar cortex receives also several aminergic or peptidergic afferents. These afferents extend, throughout the granular and molecular layer, sparse and fine varicose fibers that form direct contact with Purkinje cells and other cerebellar neurons. Their role is to set the activity level or switch the operational mode of cerebellar microcomplexes, either locally or globally.

1.2.3 Inhibition in the cerebellar cortex

The principal excitatory connections of cerebellar cortex, the mossy, parallel and climbing fibers have been described above. There are also inhibitory elements in the cerebellar cortex. Basket and stellate cells, located in the molecular layer (Figure 1.3), mediate the feedforward inhibition of Purkinje cells supplemental to the direct parallel fiber-Purkinje cell pathway. The axonal initial segment of the Purkinje cell receives inhibitory synapses from basket cells in an unique pinceau complex structure and the dendrites of the Purkinje cell receive inhibitory synapses from stellate cells. These interneurons are also connected with each other through electrical synapses (Mann-Metzer and Yarom, 1999). The Purkinje cells also receive inhibition from neighboring Purkinje cells reciprocally via their recurrent collaterals (Orduz and Llano, 2007). These collaterals typically extend over 300um (Hawkes and Leclerc, 1989; O'Donoghue and Bishop, 1990). In the granular layer, Golgi cells are the only source of inhibition to granule cells by both feedforward and feedback inhibition, which might serve to increase the temporal precision and thereby reduce the randomness of cortical operation.

1.2.4 Other elements in the cerebellar cortex

At least two other cell types have been described in cerebellar cortex (review in Geurts et al., 2003), the excitatory unipolar brush cells (Dino et al., 1999) and the inhibitory Lugaro cells (Lane and Axelrod, 2002), but their roles in the cerebellar function is not well understood. The unipolar brush cells (UBCs), located primarily in the granular layer of vestibulo-cerebellum, are one of the only two kinds of excitatory neurons of the cerebellar cortex. They receive excitatory synaptic input on the dendritic brush from a single mossy fiber terminal in the form of a giant glutamatergic

synapse (Rossi et al., 1995) and send axons that contact granule cells and UBC dendrites within glomeruli. They can either fire high-frequency bursts of action potentials or discharge tonically (Diana et al., 2007). The UBC network contributes a powerful form of distributed excitation within the basic circuit of the cerebellar cortex. The Lugaro cells are characterized by a fusiform cell body with thick, horizontally oriented dendrites. The soma of Lugaro cells are located in or slightly below the Purkinje cell layer (Aoki et al., 1986; Sahin and Hockfield, 1990). An interesting possibility is that Lugaro cells play a role in synchronizing activity among Golgi cells situated along the parallel fiber beam, as observed in anesthetized rats (Vos et al., 1999). Lugaro cells may switch the operation of Golgi cells from the individual rhythmic mode to the synchronous mode.

1.2.5 Output of cerebellar cortex

The Purkinje cells are the sole output neurons of the cerebellar cortex, and therefore play a central role in cerebellar cortical information processing. They inhibit neurons in the vestibular and cerebellar nuclei (Ito and Yoshida, 1964; Ito et al., 1964). Gauck and Jaeger (2000) found that the timing of individual spikes in deep nuclear neurons is controlled precisely by brief decreases in inhibitory conductance, these being the consequence of the synchronous activation changes in a large population of Purkinje cell inputs. They also showed that spike rate is controlled linearly by the rate of inhibitory inputs. Thus, the inhibitory control exerted by the cerebellar cortex plays an important role on the final output of the cerebellum.

1.3 Functional organization

The cerebellum has a uniform structure and circuit, therefore, executes a unique algorithm. However, the spatial segregation of the various inputs to the cerebellar cortex allows us to subdivide the cortex in multiple functional zones.

1.3.1 Division

1.3.1.1 Longitudinal zones

Each side of the cerebellum is organized in seven mediolaterally parallel longitudinal functional

zones called: A, B, C1, C2, C3, D1, D2 (Voogd, 1964; Voogd, 1969) (Figure 1.5). Additional longitudinal zones have been subsequently added into this transverse lobular organization, for example, X (Ekerot and Larson, 1979) and Y (Ekerot and Larson, 1982) (Figure 1.7A). An individual zone is typically 1-2 mm wide in cat (Oscarsson and Sjölund, 1977). Each longitudinal zone receives climbing fiber inputs from discrete area of the inferior olive and projects Purkinje cell axons to a particular circumscribed area of cerebellar or vestibular nuclei. A parasagittally striped organization of the cerebellum consistent with the longitudinal functional zones is also reflected in the expression of various proteins, such as acetylcholinesterase (Marani and Voogd, 1977; Voogd et al., 1987), 5' nucleotidase (Marani,1982), Zebrin (Aldolase C) (Pijpers et al., 2005; Sanchez et al., 2002; Sillitoe et al., 2003; Sugihara and Shinoda, 2004) (Figure 1.6).

1.3.1.2 Microzones

The longitudinal zones can be divided further into microzones. Oscarsson (1976) defined a microzone as a functional unit of the cerebellar cortex. A microzone is a narrow longitudinal strip of cerebellar cortex usually 3 to 19 dendritic arbors wide (Schultz et al., 2009). All Purkinje cells within a microzone receive climbing fiber-mediated input with similar receptive field identity but receive inputs from several mossy fiber receptive fields. Non-adjacent cerebellar zones, sharing the same climbing fiber input and zebrin identity, can also share common mossy fiber inputs (Pijpers et al., 2006).

1.3.1.3 Microcomplex

The concept of microcomplex is posed by Ito (1984). A corticonuclear (olive-cortico-nuclear) microcomplex is a functional 'module', which contains not only the cerebellar cortex, but also inferior olivary and cerebellar deep nuclei. The existence of an olivocorticonuclear module has been confirmed by a combination of zebrin immunohistochemistry and tracer techniques (Pijpers et al., 2005). The cerebellum may contain thousands of microcomplexes (Ito, 1984). Microcomplexes perform similar computational operations but on different inputs.

1.3.1.4 Multizonal microcomplex

The stem of the axon of inferior olive cells, the climbing fiber, can branch to innervate microzones in different cerebellar cortical zones and/or in different parts of the same zone (Ekerot and Larson,

1982). Garwicz (1992) was the first to propose the term 'multizonal microcomplex'. He and his colleagues found that many, if not all, of the basic structural-functional units of the paravermal cerebellum are multizonal microcomplexes (Garwicz and Ekerot, 1994). The olivocerebellar divergence provides a structural basis for a functional linkage of two or more microzones with the same climbing fibre receptive field, but with an independent cerebellar cortical location; while the cerebellar corticonuclear convergence provides a structural basis that a certain group of neighboring cerebellar nuclear neurons receives the outputs from two or more cerebellar microzones, which have independent cerebellar cortical locations, with the same function (Figure 1.7B). Moreover, anatomical tracer studies found that there are differences in mossy fiber inputs at the zonal level of resolution (Herrero et al., 2002; King et al., 1998). Microzones belonging to an individual multizonal microcomplex might process in parallel and integrate information derived from mossy fiber inputs that arise from different origins, and thus perform parallel information processing. If this is the case, it means that the structural organization of the cerebellar cortex allows similar climbing fiber inputs to integrate with mossy fiber signals that arise from different sources.

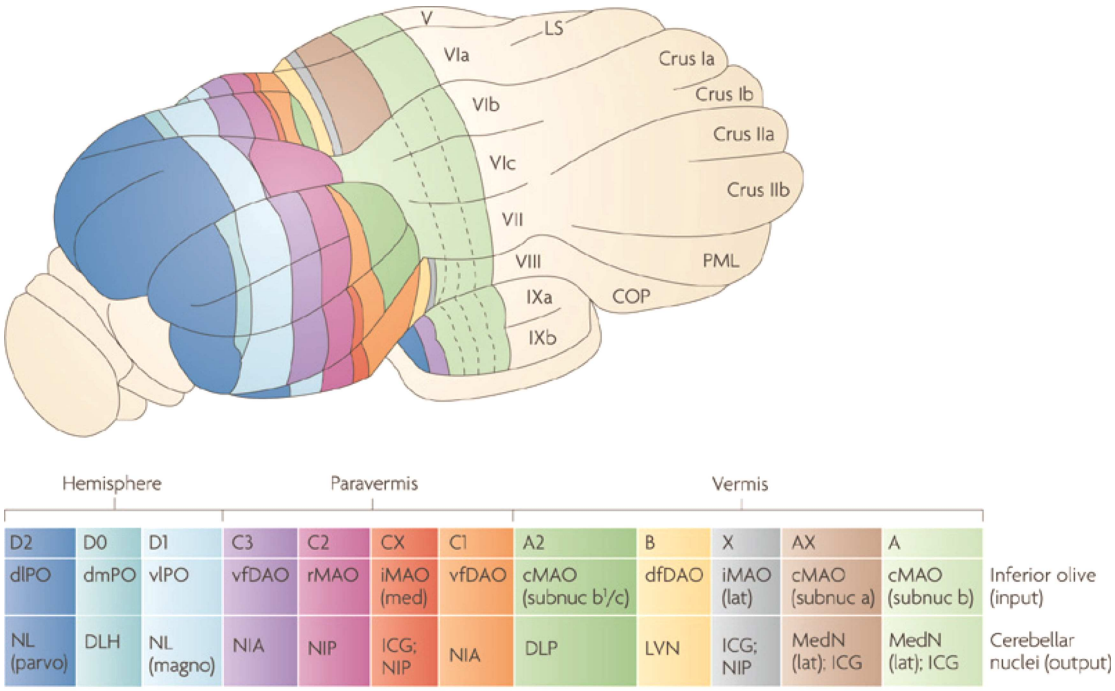

Figure 1.5 Cerebellar longitudinal zones.
Dorso-posterior view of the rat cerebellum, indicating the approximate location of different longitudinal zones on the cerebellar surface on the left hand side. Each longitudinal zone is defined by its inferior olive climbing fiber input and Purkinje corticonuclear output. cMAO (subnuc a), subnucleus a of caudal medial accessory olive; cMAO (subnuc b), subnucleus b of caudal medial accessory olive; cMAO (subnuc b1/c), subnucleus b1 and c of caudal medial accessory olive; COP, copula pyramidis; dfDAO, dorsal fold of dorsal accessory olive; DLH, dorsolateral hump; DLP, dorsolateral protuberance of medial nucleus; dlPO, dorsal lamella of the principal olive; dmPO, dorsomedial subnucleus of the principal olive; ICG, interstitial cell group; iMAO (lat), lateral part of intermediate medial accessory olive; iMAO (med), medial part of intermediate medial accessory olive; LVN, lateral vestibular nucleus; LS, lobulus simplex; MedN (lat), lateral part of medial nucleus; MedN (med), medial part of medial nucleus; NIA, nucleus interpositus anterior; NIP, nucleus interpositus posterior; NL (magno), magnocellular part of lateral nucleus. NL (parvo), parvocellular part of lateral nucleus; PML, paramedian lobule; rMAO, rostral medial accessory olive; vfDAO, ventral fold of dorsal accessory olive; vlPO, ventral lamella of the principal olive. Adapted from (Apps and Hawkes, 2009).

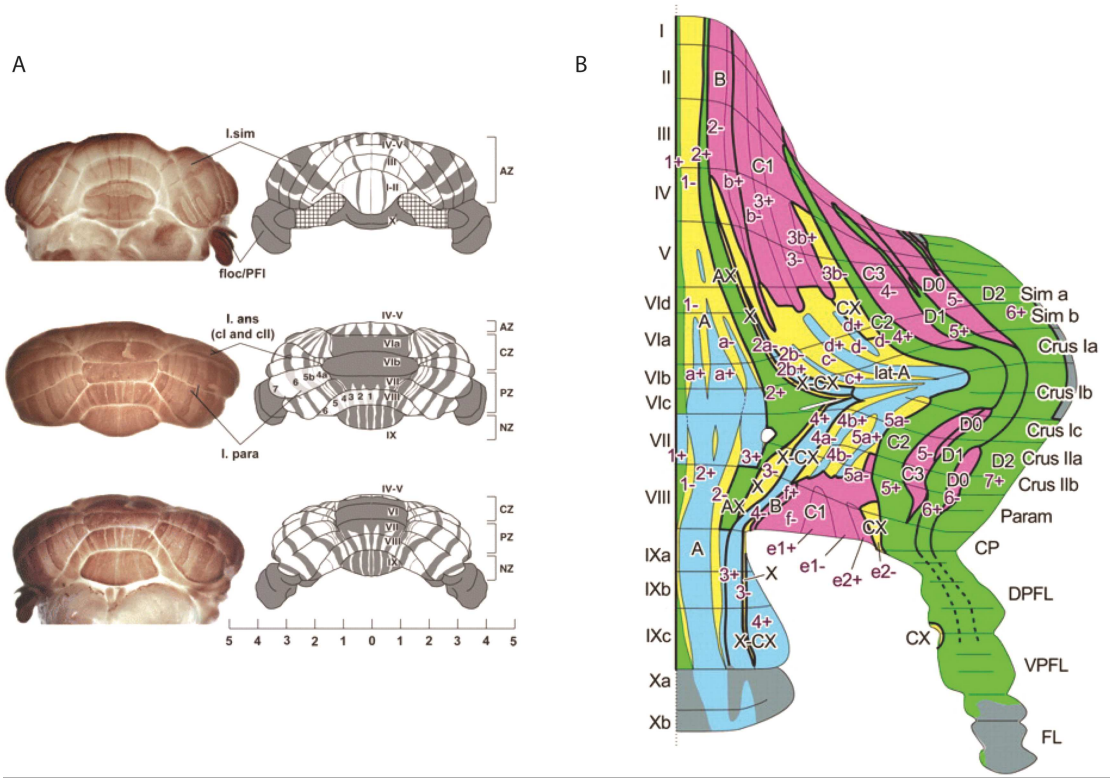

Figure 1.6 Immunohistochemistry of the cerebellum
A: whole-mount zebrin II of the adult mouse cerebellum. Left, whole mounts, showing staining of the Purkinje cell dendrites arranged parasagittally in the molecular layer. Right, schematics; upper, anterior views of the cerebellum; middle, dorsal views; bottem, posterior views. Cerebellar vermian lobules I-X are indicated by Roman numerals. The parasagittal zebrin II-immunoreactive stripes are labeled. The approximate extents of the transverse zones in the vermis are indicated in the schematics: anterior zone (AZ), central zone (CZ), posterior zone (PZ), and nodular zone (NZ). The scale (mm) applies to both whole mounts and schematics. Adapted from (Sillitoe and Hawkes, 2002).
B: Organization of zebrinII compartments and topographic olivocerebellar projection. Topographic organization explained with orientation axes. Areas belonging to each of the five groups (green, blue, yellow, red, and gray for groups I–V, respectively) were mapped on the zebrin II compartment pattern of the cerebellar cortex. Adapted from (Sugihara and Shinoda, 2004).

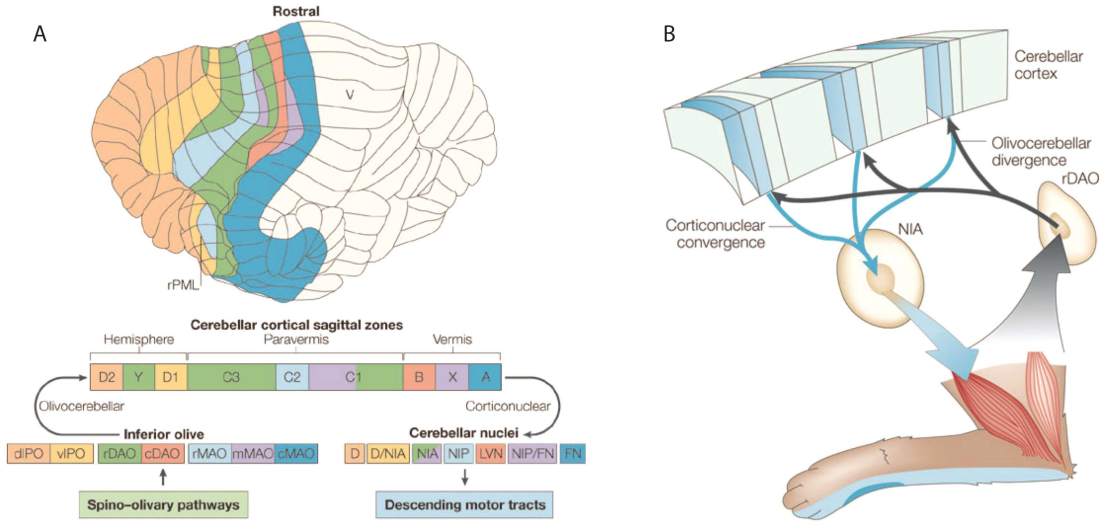

Figure 1.7 Cerebellar multizonal microcomplex (MZMC)
A: Connectivity of the cerebellum. The top panel shows a dorsal view of the cat cerebellum, indicating the approximate location of different sagittal zones on the cerebellar surface. In the simplified block diagrams below, matching colours show, for individual cerebellar cortical zones, the sites of origin of climbing fibres in the contralateral inferior olive, and the corresponding corticonuclear output targets in the ipsilateral cerebellar nuclei. dlPO, dorsal lamella of the principal olive; FN, fastigial nucleus; LVN, lateral vestibular nucleus; mMAO, middle part of medial accessory olive; NIP, nucleus interpositus posterior; rDAO, rostral part of dorsal accessory olive; rMAO, rostral medial accessory olive; rPML, rostral folia of the paramedian lobule of the posterior lobe; V, lobule Va–c of the anterior lobe; vlPO, ventral lamella of the principal olive. cDAO, caudal part of dorsal accessory olive; cMAO, medial accessory olive; D, dentate nucleus; Adapted from (Apps and Garwicz, 2005).

B: The basic structural design of a paravermal multizonal microcomplex (MZMC) as deduced from electrophysiological mapping studies and supported by neuroanatomical tract tracing experiments. Each paravermal MZMC is defined by divergence of information in the olivocerebellar projection and convergence of information in the corresponding corticonuclear projection. Adapted from (Apps and Garwicz, 2005).

1.3.2 Receptive Fields

The cerebellum is an interface, which uses sensory information to modulate motor actions. The organization of these inputs may be studied by searching the receptive fields of the cerebellar neurons. The somatic receptive field of a neuron in cerebellum is a region of body, where stimulation results in a change of firing of that neuron. According to the distribution of receptive fields in the cerebellar cortex, there is a special somatotopic map in the cerebellum. Through a large number of electrical stimulation experiments (e.g., Edge et al., 2003; Garwicz et al., 1992; Garwicz et al., 1998; Jörntell et al., 2000; Kolb et al., 1997) and some fMRI experiments (e.g., Peeters et al., 1999) in anesthetized animals (mainly in cats and rats) or human, researchers have been mapping out the organization of receptive fields in the cerebellum. The experimental results suggest that the olivocerebellar and corticonuclear zones are similarly organized in rat and cat, implying that the function of individual zones is conserved between species (Pardoe and Apps, 2002).

1.3.2.1 Topography of climbing fiber afferents to microzone

The zonal and microzonal organization of the cerebellar cortex and the information carried by climbing fibers have been studied over decades. Based on the climbing fiber-mediated input with similar receptive field identity, the cerebellar cortex is divided into thousands of microzones.

1.3.2.2 Topography of mossy fiber afferents to microzone

Although the receptive field of mossy fibers is less studied until now, some of their characters have still been found (e.g., Ekerot and Jörntell, 2003). Overall, the granule cells, which receive the mossy fibers to any given microzone, have receptive fields resembling the climbing fiber receptive field defining that microzone (Figure 1.8B). However, compared with the climbing fiber input, the mossy fiber input has a more intricate topographical organization, with a certain degree of overlap between neighboring areas (Garwicz et al., 1998). Rather than being somatotopically organized, cutaneous mossy fiber projections to granule cells in cats, like in rats, reveal a more complex mosaic pattern of organization (Kassel et al., 1984). These somatosensory projections of cerebellar granular layer exist widely among mammals (Welker et al., 1988).

1.3.2.3 Topography of parallel fiber afferents to microzone

The second level of climbing fiber and mossy fiber interactions is the relationship between climbing fiber and parallel fiber input to individual Purkinje cells, which can be represented by complex spikes and simple spikes respectively (Figure 1.8B). For the receptive field of limb, little excitation of the local mossy fibers to the Purkinje cells directly overlying them (Ekerot and Jörntell, 2001). Thus, the parallel fiber-mediated excitatory receptive fields of limb of the Purkinje cells differ from the underlying receptive field and therefore seem to be derived from mossy fibers that terminate in distant regions of cerebellar cortex. However, earlier studies in rats indicate that the ascending axons of granule cells make particularly powerful direct connections with Purkinje cells, which results in their parallel fiber-mediated receptive fields of face being similar to those of the underlying mossy fibers (Bower and Woolston, 1983; Cohen and Yarom, 1998). Unlike the wide receptive field of the mossy fiber, for both Purkinje cells and interneurons, the parallel fiber receptive fields are small and had distinct borders (Ekerot and Jörntell, 2001).

1.3.2.4 Receptive field of interneurons

Inhibitory cells also have their own receptive field. For example, each Golgi cell recorded in the C3 zone responds to stimulation of a small receptive field on the forelimb skin (Ekerot and Jörntell, 2011; Vos et al., 1999). Basket and stellate cells receive excitatory inputs from parallel fibers. These interneurons have excitatory receptive fields similar to those of subjacent mossy fibers (Figure 1.8B). In the C3 forelimb zone, they share the same receptive field with Purkinje cells in the same microzone. On the other side, the Purkinje cells in a given paravermal microzone have interneuron-mediated inhibitory receptive fields that are similar to those of the underlying mossy fibers (Ekerot and Jörntell, 2001; 2003).

1.3.2.5 Interaction between receptive fields of climbing fiber and of parallel fiber

The parallel fiber receptive field of Purkinje cell and interneuron are plastic and the direction of the plasticity depends on the interaction with the climbing fiber input. Conjunctive parallel fiber and climbing fiber activation leads to a long-lasting potentiation of parallel fiber synaptic input to interneurons (stellate and basket cells). Parallel fiber stimulation paired with climbing fiber

activity induced long-lasting decreases in the size of the receptive field of Purkinje cells in the C-zone (Within 5 min, all peripheral excitation of the simple spikes could be temporarily abolished. A small, restricted simple spikes receptive field similar in size and distribution to the original receptive field reemerged within 30 min, but the input from all other skin areas was persistently depressed) (Jörntell and Ekerot, 2002), but the same protocol enlarges the receptive field of the interneurons from a specific small skin area to the entire forelimb skin (Jörntell and Ekerot, 2003). Reciprocally, parallel fiber stimulations unpaired with climbing fiber activity induced long-lasting, very large increases in the receptive field size of Purkinje cells and induced long-lasting decreases in receptive field sizes of their afferent interneurons (Jörntell and Ekerot, 2002). These properties, and the fact that the mossy fiber receptive fields were unchanged, suggest that the receptive field changes are due to bidirectional parallel fiber synaptic plasticity in Purkinje cells and interneurons.

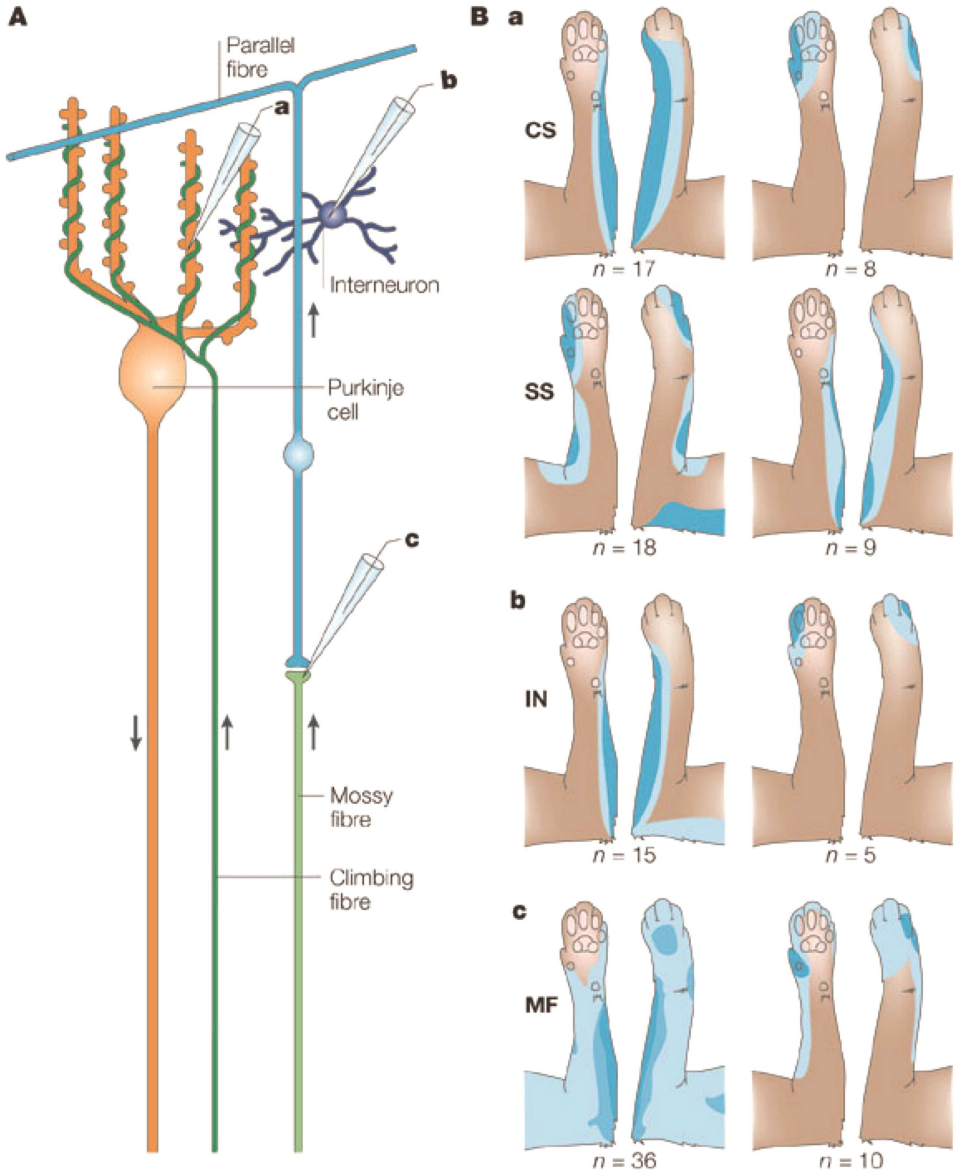

Figure 1.8 Summary of receptive fields in the cerebellar cortex.
A: Schematic diagram of recording sites in Purkinje cells, interneurons (IN) and mossy fibres (MF) at right angles to the surface through the C3 zone in the paravermal cerebellar cortex. Mossy fibre input was provided by the external component of the cuneo–cerebellar tract.
B: Typical receptive field characteristics of neuronal elements in two microzones (left and right columns) are depicted on the ventral and dorsal surface of the left cat forelimb. a: Complex spike (CS) and simple spike (SS) receptive fields of Purkinje cells. b: Receptive fields of nearby interneurons. c: Receptive fields of mossy fibre terminals immediately below the Purkinje cell layer. Note that in each microzone, the CS response (due to climbing fibre activity) of individual Purkinje cells has a similar receptive field on the skin of the ipsilateral forelimb as local inhibitory interneurons and mossy fibre terminals in the subjacent granular layer. By contrast, the excitatory SS receptive field of the same Purkinje cells (due to mossy fibre–granule cell–parallel fibre input) is different. Values shown with each pair of limb figurines denote the numbers of units that contributed to producing the average receptive field map.
Adapted from (Apps and Garwicz, 2005).

1.3.2.6 Receptive field of the forelimb

The receptive fields of the forelimb have been extensively studied in the cerebellum. The cerebellar control of forelimb movements is performed by a number of parallel subsystems-modules, each of which controls a relatively simple synergy (Ekerot et al., 1995). A fMRI experiment in anesthetized rats (Peeters et al., 1999) showed that there was no overlap between the cerebellar activations caused by forepaw and hindpaw (Figure 1.9A). Forelimbs are represented adjacent to both anterior lobe and the posterior lobe such as in the paramedian lobule in the cerebellum (Pardoe and Apps, 2002) (Figure 1.9B). The sensory afferents projectioning to the anterior lobe are strictly ipsilateral, whereas the afferents to the paramedian lobule are bilateral, although with a slight bias toward the ipsilateral projection. The cerebellar cortex is particularly well studied in the forelimb area of the paravermal C3 zone of the cat. 30 to 40 longitudinal microzones lye side by side in this zone. Each microzone (50 to 150 um wide) receives only one climbing fiber receptive field while several mossy fiber receptive fields in the forelimb skin.

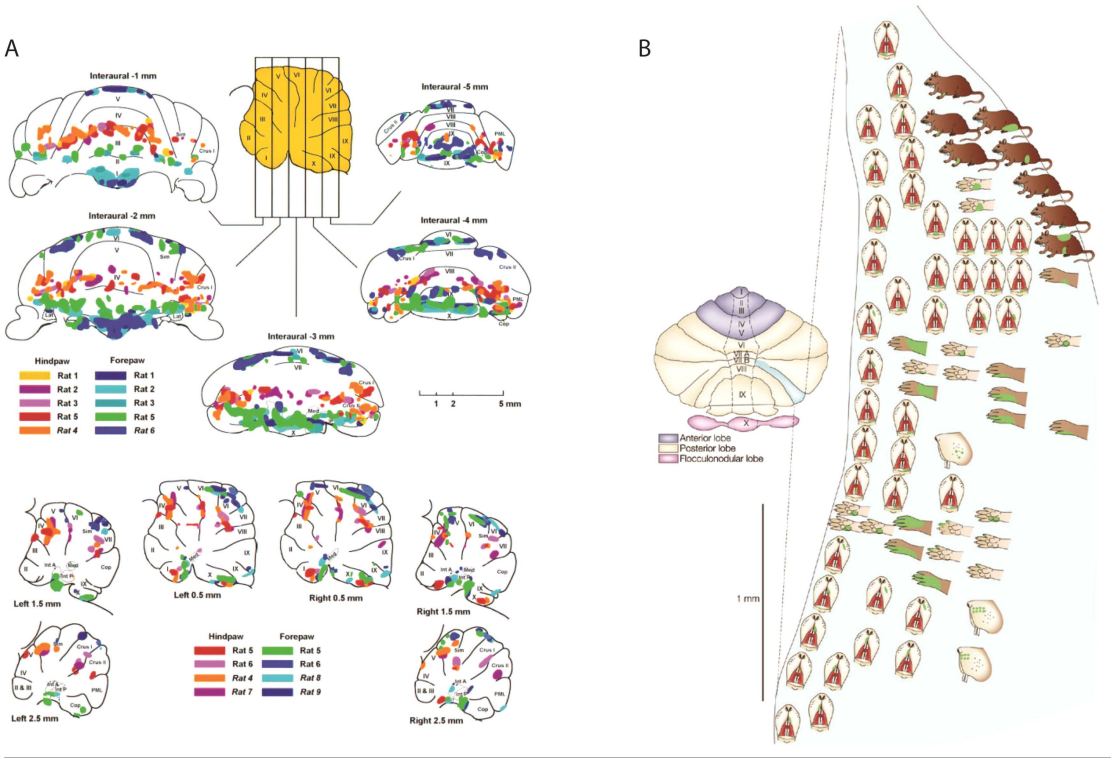

Figure 1.9 Receptive field representing forelimb
A: Composite maps of areas activated during hindpaw and forepaw stimulation, from all the imaged rat cerebellum. (Top) Coronal images. (Bottom) Sagittal images.
The red-tinted spots show activated areas resulting from hindpaw stimulation and those that are blue-green tinted result from forepaw stimulation. After hind or forepaw stimulation, several commonly activated areas are present in the different animals, with a clear separation of the fore- and hindpaw areas in the rostral cerebellum. Adapted from (Peeters et al., 1999).
B: The fractured somatotopy of the cerebellar cortex. Recordings of the receptive fields of granule cells in the rat cerebellar cortex (paramedian lobule) reveal multiple representations of the same body parts in different locations. Adapted from (Manni and Petrosini, 2004).

1.3.2.7 The relationship between receptive field of climbing fiber and that of spinal nociceptive withdrawal reflexes

The C3 zone has been intensively analyzed in connection with the withdrawal reflex (Ekerot and Jörntell, 2003; Ekerot et al., 1995; Garwicz et al., 1998). The skin receptive fields of climbing fibers that terminate in individual microzones in the paravermal cerebellar cortex and the receptive fields of individual modules of the spinal nociceptive withdrawal reflexes system are highly similar (Garwicz et al., 2002) (Figure 1.10). The cutaneous receptive fields in many cases are associated with input from muscles acting as dorsal or plamar flexors of the paw or digits. This input would tend to move the receptive field towards a stimulus applied to the skin (Jörntell et al., 1996). In general, the climbing fiber receptive field corresponded approximately to the area of the skin which would be withdrawn from an external stimulus by the movement controlled from the same module. The climbing fibers inputs reduce the excitation to Purkinje cell via LTD and indirect via LTP on interneurons, and therefore reduce the inhibitory effect of Purkinje cell to the target nuclei cells corresponding to the same module. The outputs of nuclei going to the premotor area which controlling corresponding muscles produce withdrawal (Ekerott et al., 1995).

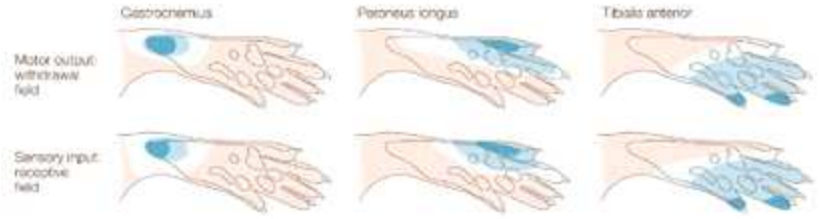

Figure 1.10 Sensorimotor transformations in spinal nociceptive withdrawal reflex modules
Comparison of quantified withdrawal fields and quantified skin receptive fields for three muscles in the rat hindlimb shows high levels of similarity. Adapted from (Apps and Garwicz, 2005).

1.4 Summary

The cerebellum has a mediolateral anatomic and functional organization. Based on different afferent inputs and cortico-nuclear connections, it is divided to microcomplexes. Each has a structure with uniform circuit and serves individual functional unit, which generally treats information in parallel with other microzones. This topographical organization is consistent with the distribution of various proteins, which present a particular immunohistochemistrical architecture and the distribution is overall consistent with the somatotopic mapping. Moreover, the plasticity and receptive fields of Purkinje cells can be altered bidirectionally based on the correlation or anti-correlation of parallel fiber and climbing fiber inputs. Although the similarity was shown between the withdrawal fields and skin receptive field for the muscles in rat hindlimb, the motor mapping is still comparatively less understood. More work is required to uncover the functional organization of motor output of the cerebellum.

2 Function of the cerebellum

The cerebellum has been shown to be involved in motor functions (postural control, motor control such as coordination and timing of movement, error detection, motor learning) and non-motor functions (control of emotions and cognitive functions).

The most important function of the cerebellum may be to coordinate motor actions so that movements are performed smoothly. Lesions of cerebellum do not change the sensory thresholds or the strength of muscle contraction, but disrupt the spatial accuracy and temporal coordination of movement. It impairs balance and reduces muscle tone. Thus the cerebellum is not necessary for basic elements of perception or movement, but for smoothness and effectiveness of movement.

The cerebellum is also known to be interconnected with the limbic system. Cerebellar stimulation can alter limbic function and elicit behaviors like sham rage, predatory attack, grooming, and eating (Schmahmann, 2001). The cerebellum projects also to multiple nonmotor areas in the prefrontal and posterior parietal cortex. Neuroimaging and neuropsychological data supply the nonmotor function of the cerebellum such as attention, language, working memory, emotion and addiction (review in Strick et al., 2009).

2.1 Function depends on regions

Although the cerebellum has an uniform circuit, different areas of the cerebellum have been identified as serving various functions (Fig 2.1), since each microcomplex has individual input and output.

The vestibulo-cerebellum (known as the flocculonodular lobe) regulates motion of the head and its position relative to gravity, controls eye movements and coordinates movements of the head and eyes by controlling the axial muscles involved in balance and coordination of eye, body and head movements. Dysfunction in this region can result in ataxic wide based gait, which is characterized by unsteady, uncoordinated walking (Damji et al., 1996). Other dysfunctions include postural sway and nystagmus (involuntary eye movements).

The spino-cerebellum regulates body and limb movements, modulates the descending motor system and voluntary movements in mammals such as pointing with a hand (Kitazawa et al.,

1998), visuomotor tracking with a computer mouse (Imanizu et al., 2000) or hand-grip control (Kawato et al., 2003). The main function of the spino-cerebellum may be the regulation of ongoing movements via error detection. By comparing the intended action with what is actually occuring, the spino-cerebellum integrates information from the motor cortex with sensory feedback. The spino-cerebellum is somatotopically organized. The axial muscles are located in the vermal region and the limbs in the intermediate regions. Dysfunction in these regions results in hypotonia (decreased muscle tone).

The cerebro-cerebellum, the most lateral part of the hemispheres, is involved in planning movement and evaluating sensory information for action and motor learning. The functions include preparation of intended movement, planning and timing of voluntary movements, as well as learned and skilled movements. It also controls higher level functions of motor and non-motor skills. This part of cerebellum contains the D1-D2 zones, is connected to the motor cortex in parallel. The most lateral zones of cerebellar hemispheres in primates are reciprocally connected to the cerebral cortex (Kelly and Strick, 2003), and have been proposed to contribute to cognitive function. In humans, these zones have also been suggested to be involved in speech (Leiner et al., 1986).

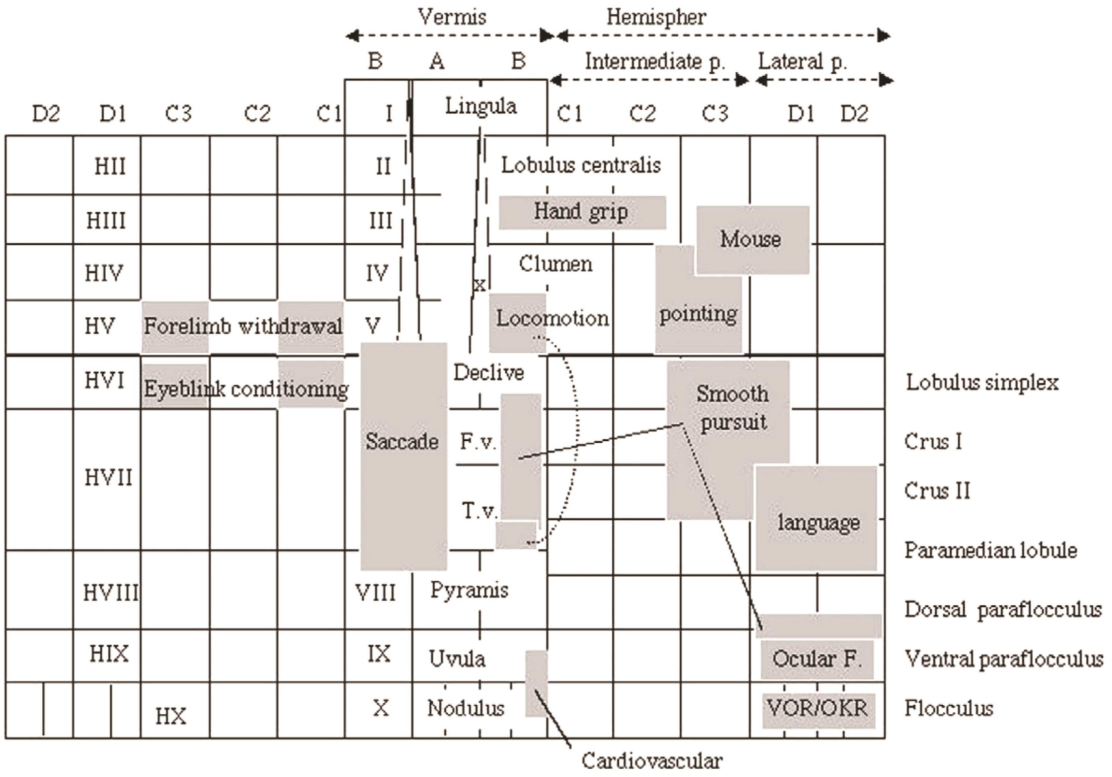

Figure 2.1 Surface functional map of the cerebellar cortex.
Dark areas represent approximate locations of the indicated functions. Multiply represented areas are connected by lines. Ordinate, lobule numbers. Abscissa, zone address. Adapted from (Ito, 2005).

2.2 Voluntary motor control and motor learning

A characteristic feature of voluntary motor control is that after repeating a task, one is able to perform the task precisely and without the feedback that was required before the task. The cerebellum has long been known to be involved in motor control because of the marked motor deficits associated with its damage (Brandauer et al., 2010; Lang and Bastian, 2002; Larkin, 2003). Besides that to accurately perform a quick movement in the absence of visual feedback needs the involvement of the cerebellum, learning voluntary movements requires also the involvement of the cerebral cortex. Motor learning is a function of the brain for acquiring new repertoires of movements and skills to perform them through practice, and it involves many areas of the brain. Marr (1969) and Albus (1971) were the first ones to conceptualize the cerebellum as a supervised learning system. In the cerebellum, the supervision of learning is performed via the error signal encoded in the climbing fibers (Kawato and Gomi, 1992). Ito showed that long-term depression (LTD) at the parallel fiber-Purkinje cell synapses produced by their coincident activation with the climbing fiber input is the neural substrate of such error-driven learning in vestibulo-ocular reflex (VOR) adaptation (Ito et al., 1982). The experiments during ocular-following response movements (optskinetic reflex) are in agreement with the hypothesis that the simple spike responses of Purkinje cells are shaped by LTD of Parallel fiber synapses with the error signal provided by the climbing fibers (Kobayashi et al., 1998).

The cerebellum operates in motor learning as an adaptive control system. The concept of adaptive control has been applied to various reflexes and compound movements such as vestibulo-ocular reflex (VOR), optokinetic eye movement response (OKR), ocular following response (OFR), eyeblink conditioning, saccadic eye movement, interlimb coordination during locomotion and operant conditioning of the H-reflex. Experiments on saccadic eye movements have shown that the adaptation of eye movement is input-dependent (Deubel, 1995), which is expected from supervised learning models of the cerebellum: only the synaptic weights for the inputs associated with the retinal error signal are modified (Gancarz and Grossberg, 1999). In arm-reaching movement in monkeys, the coding of end-point error is found to be consistent with the LTD

hypothesis (Kitazawa et al., 1998).

The cerebellum has been demonstrated to be necessary for the learning or execution of a number of voluntary movement, such as wrist flexion in response to a sudden load perturbation (Gilbert and Thach, 1977), the operant conditioning of wrist movements to lift a lever in response to visual stimuli (Sasaki and Gemba, 1982), throwing while looking through prisms (Martin et al., 1996a,b), reaching (Kitazawa et al., 1998; Kitazawa and Yin, 2002; Norris et al., 2004), the hand manipulation of a computer mouse (Imanizu et al., 2000), finger gripping (Kawato et al., 2003; Ulloa et al., 2003) and smooth pursuit eye movement (Kahlon and Lisberger, 2000; Shibata et al., 2005; Suh et al., 2000). During practice, climbing fiber carrying information regarding errors in the operation of neural control systems modifies the parallel fiber-Purkinje cell synaptic plasticity via LTD. Therefore, after learning, the cerebellum can performs as an internal feedback, which permits smooth movement in the absence of external feedback.

2.3 Non-motor functions

Three sorts of evidence have been put forward to support the idea that the cerebellum may also be involved in cognition. 1) Patients with cerebellar lesions are reported to have deficits in cognitive tasks. 2) Activation of the cerebellum has been found in functional imaging studies of normal subjects performing such tasks. 3) Substantial reciprocal connections exist between prefrontal cortex areas and the cerebellum. González and his colleagues (2005) have shown that after a cerebellar stroke, motor performance in both hands markedly slowed. This effect was accompanied by a slowing of motor imagery, suggesting an involvement of the cerebellum in motor execution and also in the planning and internal simulation of movements. Numerous brain-imaging studies have reported a cerebeller activation in non-motor tasks, such as mental imagery (Lotze et al., 1999; Parsons et al., 1995), sensory processing (Gao et al., 1996; Parsons et al., 2000), planning (Dagher et al., 1999; Kim et al., 1994), attention (Allen et al., 1997), language (Kim et al., 1999; Leiner et al., 1993; Price et al., 1999), personality, mood, intellect (Grill et al., 2004), spatial organisation, visual and long-term memory. The output to non-motor areas of the

cerebral cortex originates specifically from a ventral portion of the dentate nucleus. Several authors have argued that ventral dentate and related regions of the cerebellar hemispheres are selectively enlarged in great apes and humans. Indeed, the enlargement of the ventral dentate in humans is thought to parallel the enlargement of prefrontal cortex. These observations have led to the proposal that the dentate's participation in non-motor functions may be especially prominent in humans (Leiner et al., 1991). In summary, there are a lot of anatomical, neuroimaging, clinical, neuropsychological and modeling researches that provide compelling, although not conclusive, evidence that the human cerebellum has important nonmotor functions (Schmahmann, 1996). However, although a cerebellar contribution to cognitive processing seems strongly supported by a wealth of recent studies, there is still a debate on the cognitive function of the cerebellum. Some people still argue against a role of cerebellum in cognition (Glickstein and Doron, 2008). They suggest some of the imaging evidence may reflect the cerebellum's role in the control of eye movements rather than cognition.

2.4 Timing

Timing has been proposed as the basic function of the cerebellum underlying its contribution to both motor control and cognitive functions. Subjective or psychological time is the internal experience of how fast time is passing, or how much time has passed since the occurrence of some event. Subjective time estimation requires the participant to use an internal clock in order to measure objective time without the benefit of cues from external clocks. Estimating time intervals is an important adaptive skill, which can improve by learning, vital for making predictions and for motor control. In the timing hypothesis, the cerebellum is one important part working with other neural regions also associated with the operation of an internal clock such as the basal ganglia and regions of the frontal cortex, especially in the right hemisphere.

The cerebellum is responsible for rhythmic movements, such as walking, writing and scratching. A series of imaging studies by Sakai and his colleges (2000) showed that the memory of simple rhythms involves the anterior cerebellum, whereas the memory of complex rhythms and the adjustment of movement timing in response to irregular external triggers involve the posterior cerebellum. A possible reason for such differential involvement is the use of different

representations. The anterior cerebellum can provide internal models of body dynamics, which can be helpful in the prediction of regular timing as well as in the control of detailed movement parameters. The posterior cerebellum may provide internal models for prediction of sensory events, which may be useful in timing perception and adjustment. The cerebellum is able to make adjustments in the timing of these rhythmic movements and facilitates the action. The results of a series of elegant studies of ball throwing show that the timing of the opening of the fingers, required to release the gripped ball, is crucial for spatial accuracy. A breakdown in the temporal relationship between the forward movement of the limb and the ball release at the wrist is a cardinal feature of cerebellar damage (Timman et al., 1999). The results from precisely timed tasks, such as repetitive tapping following the presentation of an auditory metronome indicating the target interval, provide a more direct proof of the cerebellar timing hypothesis. Patients with cerebellar lesions are impaired on this simple tapping task (Ivry and Keele, 1989).

The timing capabilities of the cerebellum appear to extend beyond rhythmic movements into sensory events. The MEG study provided the evidence that the cerebellum in humans is activated in anticipation of somatosensory events, even when these events do not require overt responses, consistent with the hypothesis that the cerebellum is specialized for representing the temporal relationships between events, motor or otherwise (Tesche and Karhu, 2000). The cerebellum plays an active role in coordination and the timing of movement through integrating sensory information with learned information (Mauk et al., 2000). For example, in eyeblink conditioning, such learning is only adaptive if the animal is able to learn the precise timing between the conditioned and unconditioned stimuli. Thus, the fundamental association is not only between two stimulus events, but also the precise temporal relationship of these events. Lesions of the cerebellum produce profound impairments on such forms of conditioning. It seems that the cerebellar cortex appears to play a critical role in regulating the fine timing of the conditioned response (Perrett et al., 1993).

The timing function of the cerebellum is also involved in nonmotor function such as perception or speech. Perceptual tasks that require precise timing also have been associated with the cerebellum. Patients with cerebellar lesions are impaired when asked to judge the duration of intervals in the range of 400 ms to 4 s (Mangels et al., 1998). The cerebellum is proved to be involved in both

speech production and speech perception (review in Ackermann et al., 2007). The cerebellar patients performed normally in categorizing speech sounds that could be identified on the basis of either spectral or temporal cues. However, when only a temporal cue was available, their performance fell to near chance, reflecting the stringent demands placed on an internal timing system in this condition. Patients with bilateral cerebellar degeneration are unable to discriminate between speech contrasts that involve purely temporal cues. A fMRI study found that such sounds produce increased activation only in the cerebellum and the inferior left frontal gyrus compared to speech perception conditions in which similar word contrasts required the analysis of spectral cues (Mathiak et al., 2002). Behavioral and modeling studies suggest that the cerebellar timing system is best characterized as providing a near-infinite set of interval-type timers rather than as a single clock with pacemaker or oscillatory properties, but this is controversial.

2.5 Conclusion

Analysis of a large sample of damage experiments has revealed that the function of the cerebellum has a mediolateral organization. While non-motor function of the cerebellum in still debated, it is clear that the cerebellum is involved in the smoothness and accuracy of the motor control, even in the absence of visual feedback. It seems that timing is a key concept for understanding the mechanism of the cerebellar motor function. The posterior cerebellum has been shown to be processing the internal feedforward computations used for prediction of sensory events, which may be useful in timing perception and adjustment of a movement of complex rhythm. Thus, It's interesting to research how is the temporal control of the cerebellum in voluntary movement on a level of population units.

3 Purkinje cell activities

As described above, Purkinje cells are the output of the cerebellar cortex and thus transmit the result of the computation in the cerebellar cortex. Studying Purkinje cell activity is thus crucial to decipher the cerebellum function.

The occurence of spikes in Purkinje cell in vivo is determined by the interaction between intrinsic and network properties. Purkinje cells are intrinsically active, they can fire in a highly regular and fast (30-150 Hz) way in the absence of synaptic input (Häusser and Clark, 1997) or in dissociated preparations (Raman and Bean, 1999). This is mainly due to resurgent sodium conductances and potassium conductances (Roman and Bean, 1999; Womack and Khodakhah, 2003). Besides the intrinsic properties of Purkinje cells themselves, the patterns of spike activity are determined also by excitatory inputs from the climbing fiber and parallel fibers, and by inhibiotory inputs from molecular layer interneurons. Purkinje cells discharge two kinds of spikes (simple spikes and complex spikes) due to two different sources of excitatory inputs (parallel fiber and climbing fiber, respectively).

3.1 Simple spikes

The mossy fiber-granule cell-parallel fiber pathway causes the Purkinje cells to discharge 'simple spikes'. The spontaneous steady simple spikes activity produced by the mossy fibers has a high frequency during the rest state and the frequency can be modulated largely by sensory stimuli (such as somatosensory, vestibular stimuli) or motor movements (such as voluntary eye or limb movement), sometimes the frequency of simple spikes can reach very high levels up to several hundreds spikes per second. The frequency of simple spikes can readily encode the magnitude and duration of peripheral stimuli or centrally-generated behaviors.

Simple spikes of Purkinje cells have been found encoding global kinematic parameters of limb movement such as position (Roitman et al., 2005; Marple-Horvat and Stein, 1987), velocity (Coltz et al., 1999; Marple-Horvat and Stein, 1987), direction (Roitman et al., 2005; Fortier et al., 1989;

Mano and Yamamoto, 1980), movement distance (Fu et al., 1997), force (Smith and Bourbonnais, 1981) and surface texture or weight of the object which animals grasped (Espinoza and Smith, 1990). Some studies support the idea that the firing of Purkinje cells represents kinematically the integrated information about the whole limb movement rather than encode single parameter of the movement (Pasalar et al., 2006). Simple spikes of Purkinje cells can encode other movement such as the eye movements (Stone and Lisberger, 1990; Shidara et al., 1993; Medina and Lisberger, 2009; Gomi et al., 1998).

3.2 Complex spikes

Single climbing fibers contact extensively with Purkinje cells so that they can generate an extremely powerful synapic excitation, resulting in a complex spike. And therefore, both single action potentials and high-frequency bursts in the climbing fiber are reliably transmitted to Purkinje cell (Maruta et al., 2007). Unlike simple spikes, complex spikes have a firing rate at very low frequency, usually less than 1 Hz in spontaneous condition. Despite the low frequency of firing, complex spikes can alter the rate of simple spikes and their synchronization might signal the timing of peripheral events or act as triggers for behavior (Llinás, 2009).

Climbing fibers convey information regarding errors in the operation of neural control systems. The information can include sensory signals, which may be evoked by a sudden loud sound (Mortimer, 1975) or pain (Jörntell et al., 1996), and these sensory signals inform the cerebellum of a harmful consequence of an inadequately executed movement. For examples, in vestibulo-ocular reflex, optokinetic reflex, and ocular following responses, the retinal slip causes retinal error signals, which are mediated by accessory optic system and inferior olive and finally conveyed by climbing fiber activity to the flocculus, where complex spikes are then induced. During eyeblink conditioning, climbing fiber activity is evoked by corneal stimulation when the eye failed to close in time to protect the cornea from an aversive stimulus such as an air puff. In a voluntary movements, such as the reaching-by-hand movement of a wedge-prism-wearing monkey, learning critically depends on the visual information of the error, which is provided shortly after accomplishment of the reaching movement (Kitazawa and Yin, 2002). However, the errors carried

by the climbing fiber can be induced not only by sensory information but also motor information. Individual climbing fiber signals cutaneous sensory events reflecting activity of a single muscle conditional upon the functional state of the muscle itself and that of functionally-related muscles. Climbing fibers projecting to the paravermal cerebellum mediate highly integrated sensorimotor information derived from spinal withdrawal reflex modules acting on single forelimb muscles (Garwicz et al., 2002). One study in another voluntary movements of hand and arm also supports this idea that climbing fiber signals encode not only the errors detected through sensory systems, but also other types of errors arising from the internal mechanisms of the motor systems (Kitazawa et al., 1998). They find that climbing fiber signals indeed arise in three phases of movement: at the beginning, before and after the end. Discharges of complex spikes in the third phase of movement encode the errors arising from sensory systems, whereas, discharges in the first and second phases are not due to the sensory information but to internal mechanisms of the motor systems. Thus, climbing fibers may convey motor signals as well: that is, signals representing a movement or its preparatory state caused by sensory stimuli. Winkelman and Frens (2006) detected climbing fiber signals, which likely represented motor commands for an OKR, to an even greater extent than the sensory components.

Complex spike patterns can 'restart' after a strong, unexpected sensory input, thereby triggering a new motor program (Llinás, 2009). When a perturbation of an ongoing motor program occurs, a new motor program may be activated rapidly through a new synchronized complex spike pattern (Van Der Giessen et al., 1997). The two mechanisms, switching to a different motor program and modifying the current motor program, could in principle be used individually or successively to correct motor activity.

Error signals encoded by the climbing fibers can produce motor learning via synaptic plasticity at parallel fiber-Purkinje cell synapse, although other plasticity mechanisms may also contribute to motor learning (Boyden et al., 2004). This idea was first proposed by Marr (1969) and Albus (1971). In their model, the climbing fiber provides the instructive signal, which Marr believed to be a positive reinforcer whereas Albus believed it to be an error signal. The signal regulates the strength of parallel fiber-Purkinje cell synapses and thereby guides the encoding of new

stimulus-response associations. Later, the finding by Ito (Ito et al., 1982) that electrical stimulation of climbing fibers induces a decrease in synaptic strength in parallel fibers which are active simultaneously is consistent with Albus's idea. The observation that the blockade of LTD impairs motor learning further support these theories. Nitric oxide (NO) is required for LTD induction (Shibuki and Okada, 1991). Injection of a NO-synthase inhibitor into the cerebellum led to learning deficits in the conditioned eyeblink response in rabbits (Chapman et al., 1992) and blocked the adaptation of walking on a treadmill following a sudden increase in the speed of the running belt in decerebrate cats (Yanagihara and Kondo, 1996).

Because inferior olive neurons discharge with a highly regular rhythm under selected conditions, a hypothesis has been proposed that climbing fibers provide a periodic clock for coordinating movements or motor timing (Kazantsev et al., 2004; Llinás and Welsh, 1993). Although, climbing fiber signals have been reported to occur randomly in awake monkeys (Keating and Thach, 1995), several lines of evidence support this idea. First, with the tremor triggered by injection of harmaline, complex spikes discharge rhythmically at a rate around 10 Hz. Secondly, in slice conditions, inferior olive neurons exhibit spontaneously a marked oscillation of their membrane potential. Olivary neurons also exhibit oscillations in their membrane potential during rest in vivo (Khosrovani et al., 2007). Such subthreshold oscillations occur at preferred frequencies of around 2-4 Hz or 6-9 Hz, and these frequencies are also observed in the complex spikes during rest. Third evidence came from the studies on skilled tongue movements in rats: Welsh and his colleagues (1995) found that climbing fibers discharged rhythmically and time-locked to licking movement at about the time when the tongue was fully extended, and some Purkinje cells firing of complex spikes synchronizes with each other. They suggested that the climbing fiber activities are transferred to cerebellar nuclear neurons via Purkinje cell axons to eventually aid tongue motoneurons entraining the movement.

3.3 Interactions of simple spikes and complex spikes

The patterns of complex spikes and simple spikes can influence one another. The occurrence of one complex spike can totally inhibit simple spikes during a short time. Complex spikes can alter

the synaptic plasticity in Purkinje cell and induce short-term or long-term inhibitory of synaptic inputs. Generally, for most Purkinje cells, the frequencies of simple spike and complex spikes are modulated reciprocally: an increase in complex spikes is associated with a decrease in simple spikes and vice versa (Ebner et al., 2002). Simple spike activity can modify climbing fiber activity pattern through GABAergic feedback from the cerebellar nuclei to the inferior olive (Miall et al., 1998).

3.3.1 Modification of simple spike after the occurrence of a complex spike

Immediately after the initiation of a complex spike, the Purkinje cell does not elicit any simple spikes for a short period of time around ten or more milliseconds (Sato et al., 1992), which known as the climbing fiber pause (it likely reflects a reset of the pacemaker). Immediately after the climbing fiber pause, a transient increase in simple spike activity which lasts 20-40 ms is often observed (Sato et al., 1992), which known as simple spike facilitation. After the simple spike facilitation, many Purkinje cells show a phase of simple spike suppression that lasts several tens of milliseconds (Bosman et al., 2010). Simple spike suppression comprises a ~30% reduction in simple spike firing which lasts hundreds of milliseconds. Moreover, it can also occur following complex spike activity of not only the same Purkinje cell, but also other local Purkinje cells (Schwarz and Welsh, 2001). This implies that a climbing fiber affects more Purkinje cells than the one with which it forms direct synaptic contact. Because simple spike suppression is most prominent in sagittal plane (Bosman et al., 2010), it is possible that it is supported by the sagittally-oriented axons of the molecular layer interneurons and/or by the similarly oriented climbing fiber ramification of neurons that are coupled in the inferior olive.

3.3.2 LTD of inhibition of simple spike by complex spike

A postsynaptic long-term potentiation can be induced by repetitive (1 Hz) parallel fiber stimulation without concomitant climbing fiber activation (Coesmans et al., 2004; Lev-Ram et al., 2002). However, combined climbing fiber and parallel fiber activity can induce postsynaptic long-term depression (LTD) at the parallel fiber-Purkinje cell synapse (Ito and Kano, 1982). Thus, LTD at parallel fiber synapses is a unique and characteristic form of synaptic plasticity whose

induction requires the convergence of signals from both granule cell axons and climbing fibers to a Purkinje cell and plays an essential role in the cerebellum's error-driven learning mechanism. For example, climbing fiber input inducing LTD modifies the mossy fiber input-Purkinje cell output relationship of the flocculus and thereby adaptively alters the gain of the VOR to minimize the control error of eye movements.

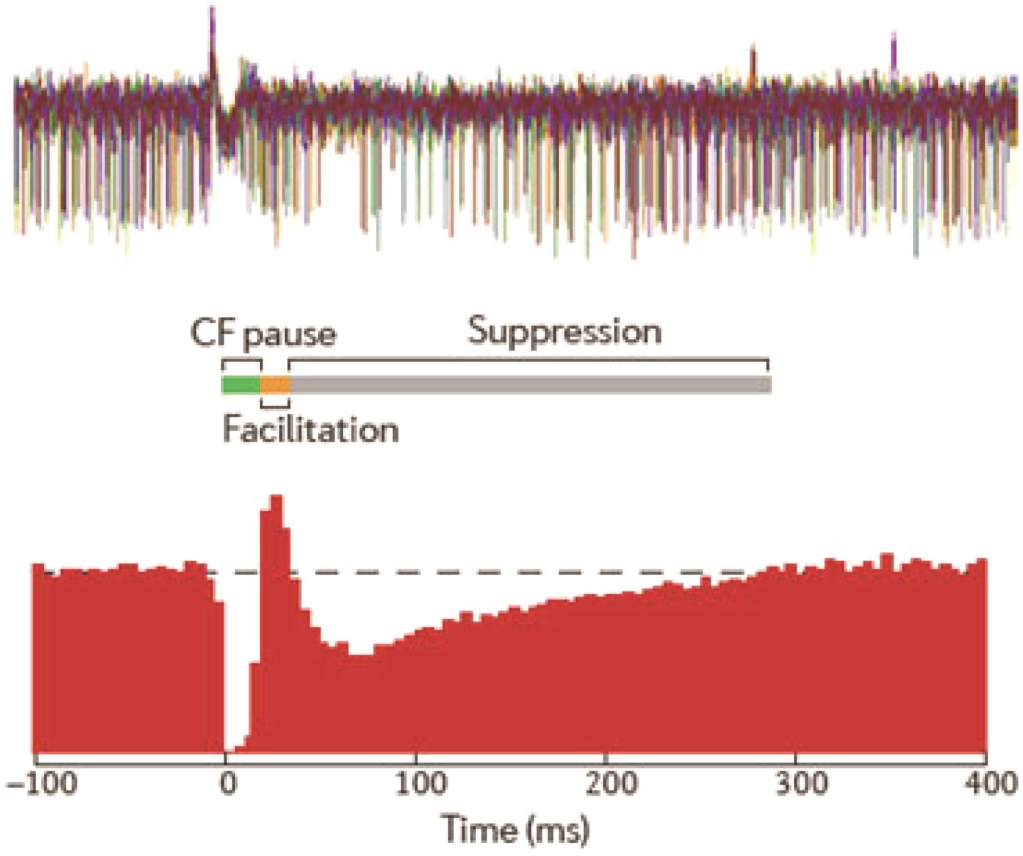

Figure 3.1 Simple-spike firing patterns can be influenced by complex spikes
An overlay of eight fragments of an extracellular recording of a Purkinje cell in an awake, adult mouse aligned on the onset of the complex spike (time = 0 ms) shows three phases following a complex spike (top and middle panels): pause, increase and suppression of simple-spike firing. The lower panel is a histogram of simple-spike times of the same Purkinje cell relative to the firing of complex spikes (time = 0ms), using 5 ms bins. The dashed line shows the average number of simple spikes per bin during the 200 ms before the complex spike. Adapted from (De Zeeuw et al., 2011).

3.4 Inhibitory input

Besides of excitatory input, the discharge of Purkinje cells is also modulated by the inhibitory interneurons (Hausser and Clark, 1997), which cause the highly irregular spontaneous discharge of Purkinje cell in vivo (Eccles et al., 1967). Interestingly, the chronic reduction of excitatory inputs from granule cells or of inhibitory inputs from molecular layer interneurons in vivo increases the regularity of simple spike firing without affecting the simple spike firing frequency (Wulff et al., 2009). Conversely, in the mutant mice, chronic enhancement of the inhibitory control of excitatory inputs to Purkinje cells increases the irregularity of simple spike activity, with only a mild concomitant increase in firing frequency (Hoebeek et al., 2005). Following parallel fiber stimulation in vitro, a transient, short latency increase in Purkinje cell firing is immediately followed by feedforward inhibition induced by activation of molecular layer interneurons (Mittmann et al., 2005).

Purkinje cells recurrent axon collaterals may also inhibit the inhibitory output of Purkinje cell inhibition (Orduz and Llano, 2007), but their control of Purkinje cell firing is not well understood. However, these connections have been proposed to underlie fast population oscillation (de Solages et al., 2008).

In general, the intrinsic activity of Purkinje cells seems to set the basal simple spike frequency at tens of Hz, whereas the inhibitory and excitatory inputs are essential for the precision of simple spike timing.

3.5 Population Purkinje cell activities and synchrony

The postsynaptic targets of Purkinje cells receive convergent inputs from hundreds of Purkinje cells (Llinas et al., 2004) and individual Purkinje cell-deep cerebellar nucleus connections have a small amplitude size (Bengtsson et al., 2011). Therefore, the influence of single Purkinje cell on the output of the deep cerebellar nuclei is limited. The impact of the cortex on the deep cerebellar

nuclei is determined by the population activity of the cortex. Indeed, the timing of eye movement can hardly been inferred from the activity of a single Purkinje cell, but it may be predicted from the activity of a population of tens of Purkinje cells (Thier et al., 2000). Likewise, the decoding of movements needs also the Purkinje cell population (Medina and Lisberger, 2009). Thus, understanding the role of Purkinje cell in motor control requires to describe and understand the factors that determine the coordination of discharge of the Purkinje cell population.

The coordination of discharge at short time-scale, the synchrony, is a type of firing coordination that favors synaptic summation and thus favors a tight temporal control of the postsynaptic target. Spontaneous and stimulation-triggered synchrony has been reported in the cerebellar cortex in anesthetized animals. Both the complex spikes (Welsh et al., 1995; De Zeeuw et al., 1997) and simple spikes (De zeeuw et al., 1997) of Purkinje cells are found to discharge synchronously. The most documented case of coordinated discharge in the cerebellum is the synchronization of complex spikes (Welsh et al., 1995). This coordination is not the result from intra-cerebellar integration of information, but directly reflects the synchrony between the inferior olive cells that generate the complex spikes in Purkinje cells. All climbing fibers trigger complex spikes and arise from the inferior olive, thus the synchrony of complex spikes of the Purkinje cells are determined by the properties of the olivary neurons. Dendritic spines of neighboring olivary neurons are electrotonically coupled within glomeruli by gap junctions composed of connexin 36, which enhances the synchrony of complex spikes. The synchrony of complex spikes which occurs within 2 ms is usually restricted to the parasagittal zones (up to ~500 um) or microzones (up to ~100 um) (Ozden et al., 2009; Wylie et al., 1995), whereas the synchrony which occurs in the range of 3 to 10 ms can be found among Purkinje cells across larger parts of the cerebellar cortex (Bosman et al., 2010; De Zeeuw et al., 1996; De Zeeuw et al., 1997; Welsh et al., 1995). Complex-spike activities within a microzone are characterized by a common sensitivity to particular internal or external stimuli. The spatial boundaries of synchronously activated Purkinje cells within a microzone that occur during rest are largely maintained following sensorimotor activation. Complex spike synchrony can also occur between different zones and microzones for which two mechanisms may contribute (shared excitatory and inhibitory input to inferior olivary neurons

which project to different zones). Olivary neurons projecting to different microzones may share common excitatory afferents, thus the activation of these afferents will trigger complex spikes in different microzones simultaneously (De Zeeuw et al., 1998). The interzonal and intermicrozonal synchrony can be increased during motor activity and/or sensory stimulation (Van Der Giessen et al., 1997; Welsh et al., 1995). The coupling of olivary neurons which project to different microzones in the cerebellar cortex is controled by the GABAergic input from the cerebellar nuclei (Long et al., 2002). The terminals of cerebellar nuclei to the olive are adjacent to the electrically coupled dendritic spines in olivary glomeruli (De Zeeuw et al., 1996) and their activation should shunt the electical synapse.

In general, the synchrony of simple spikes is likely to occur within a 'patch' of Purkinje cells that is fed by the numerous varicosities of the ascending parts of a set of granule cell axons. The formation of these patches might be enhanced by inhibitory input from stellate cells, which may be predominantly excited by the more distal parts of parallel fibers. However, simple spike synchrony can also occur between Purkinje cells that are distributed over longer distances, often in particular planes (De Zeeuw et al., 1997). By contrast, synchronous simple spike activity in Crus II, which can be time-locked to whisker stimulation and enhanced by peripheral stimulation (Wise et al., 2010), is largely restricted to Purkinje cells oriented along the parallel fiber beam (Bosman et al., 2010). In wild type animals, on beam-synchronization does not occur spontaneously (Goossens et al., 2001; Cheron et al., 2004). The patchy and longitudinal organizations of simple-spike synchrony are not mutually exclusive and can occur at the same time as a result of shared excitation. This could explain why simple spike synchrony can occur along the parallel fiber beams and sagittal zones but is most prominent within small patches. In a recent computer model, synchrony of Purkinje cells at time scale of 10ms could be found when they share excitation (Jaeger, 2003). Such slightly broader synchrony is indeed observed between Purkinje cells (Bosman et al., 2010; De Zeeuw et al., 1997; Wise et al., 2010), mostly in cases where the cells also exhibit synchronized complex spikes indicating that they belong to a common functional ensemble.

Neighboring Purkinje cells are also known to exhibit spontaneously synchronized simple spikes. Synchronization of neighboring Purkinje cells has been noted in early recordings of pairs of cells in anesthetized and decerebrate animals (Bell and Grimm, 1969; Ebner and Bloedel, 1981). De Solages and her colleagues (2008) have shown that at least some of this synchrony may result in part from a fast cerebellar oscillation (Adrian, 1935) arising from a population oscillation of Purkinje cells, associated with millisecond-scale synchrony and 5-ms delayed coordination of discharge. Shin and De Schutter (2006) also suggested a synchronizing role for local inhibitory neurons, since synchrony appeared associated with episodes of slowed firing rate of Purkinje cells.

Synchrony of simple spikes and of complex spikes do not occur independantly. In the vestibulo-cerebellum, simple spike synchrony is correlated to complex spike synchrony during the optokinetic reflex and accordingly, mainly occurs in the sagittal plane (De Zeeuw et al., 1997).

There are few reports on task-related synchrony in awake animals. Synchrony of multi-units in Purkinje cell layer has also been observed in the rats during a reaching task (Heck et al., 2007). These authors found that multi-unit signals of Purkinje cell pairs in the paramedian lobule showed tightly synchrony at sub-millisecond scale (almost without any delay) along the parallel fiber during a reaching task in head-fixed animals. Even though the signals were from the Purkinje cell layer (as determined by the presence of complex spikes), only multi-unit activity was used to perform all the data analysis. Moreover, the rats were under head-fixed condition. These results are suprising since the parallel fiber conductions time between the recording time is of several millisecond. The actions invoke them the synchrony of granule cell along parallel fiber but this is also surprising since mossy fiber collaterols rather display action posterier extension (Leergaard? I found only his anatomy studies). A possible explanation could be that the multiunit signal contailed spikes from fast-conduct spikes (such as from Lugaro cells). Thus, activities from individual Purkinje cells during a freely-moving reach may be necessary to better study the role of synchrony in timing and voluntary coordinating movement.

Purkinje cell synchronization is likely to substantially affect the activity in the downstream structures, the deep cerebellar nuclei (Gauck and Jaeger, 2000), allowing to modulate the deep

cerebellar cells at very short time scales. At the level of the cerebellar and vestibular nuclei, tens to several hundreds of Purkinje cells from single microzones converge upon a single neuron (De Zeeuw and Berrebi, 1995). Retrograde transneuronal tracing with rabies virushave demonstrated that several cerebellar modules may be involved in the control of individual muscles (Ruigrok, 2011). Thus, synchronized simple spikes could thus strongly influence the timing of spike in neurons in the cerebellar nuclei. The organization of Purkinje cell population maybe orchestrate the coordinated motor movement indirectly through forming important timing signals to cerebellar nuclei cells.

4 Golgi cell activities

The majority spikes of Purkinje cells, simple spikes, are emitted under the tight control of impulses from granule cells directly via parallel fibers and indirectly via molecular layer interneurons. However, since a Purkinje cell can make connection with huge number of parallel fibers, only coincident granule cell inputs within a narrow time window can be summated effectively to excite a Purkinje cell. The Golgi cell in the most important element for inhibitory modulate firing of granule cells by both feedforward and feedback pathway. Thus, studies on Golgi cells can help to better understand the firing pattern and functional mechanism of Purkinje cells, which will in turn effect the downstream structure.

4.1 Structure

Golgi cells receive excitatory inputs from mossy fibers and parallel fibers (the granule cell axons) and give inhibitory outputs to granule cells into the glomeruli. The glomerus is a complex structure, enclosing the mossy fiber and Golgi cell terminals, several tens of granule cell dendrites (Ito, 1984), the Golgi cell basal dendrites (Hámori and Szentágothai, 1966) and also the climbing fibers collaterals to the Golgi cell (Scheibel and Scheibel, 1954) (Figure 4.1). The Golgi cell-granule cell synapses consist of small boutons located proximally to the granule cell dendritic endings, which in turn, receive the excitatory mossy fiber terminals. Simat and his colleagues (2007) found several neurochemical phenotypes of Golgi cells. The majority of Golgi cells are GABAergic and glycinergic (80%), some are only GABAergic (15%), and others are only glycinergic (5%). In general, Golgi cells inhibit the granule cells by activation GABAergic currents and the unipolar brush cells by activation glycinergic (and GABAergic) currents in the vestibulo-cerebellum.

Golgi cells exhibit a relatively large (10-20 um) soma (Barmack and Yakhnitsa, 2008). The dendrites present variable morphologies (not rigorously organized in a plane but rather irregular and with a three-dimensional extension) and often two to four dendrites emerging as thin

processes from a single point in the soma and terminated with several varicosties. The Golgi cell axonal plexus extends exclusively in the granular layer over ~650 um sagittally and ~180 um medio-laterally and, through thin branches, can form secondary plexuses in the same or even in neighboring laminae (Eccles et al., 1967). The Golgi cell axon expands preferentially in the parasagittal plane, as confirmed by confocal imaging (Barmack and Yakhnitsa, 2008). The axonal organization matches the parasagittal distribution of mossy fiber ramification (Sultan, 2001). Moreover, the entire Golgi cells, comprising their axon and dendrites, are segregated into parasagittal compartments defined by markers of granular layer neurons or Purkinje cells such as zebrin-2, aldolase C, nitric oxide synthase (Sillitoe et al., 2008). This parasagittal organization is related to a major issue of cerebellar organization, in which mossy fiber inputs coherently activate certain granular layer areas, certain sets of Purkinje cells and specific portions of the olive-nuclear complex, thus forming structural and functional modules. The presence of gap junctions among the inhibitory interneurons (stellate, basket and Golgi cells) was early observed both within and across classes of Golgi cells (Sotelo and Llinás, 1972). Therefore, it seems that Golgi cells, through mossy fiber (and potentially climbing fiber) inputs to their dendrites, are wired within microcircuits involving specific cortico-nuclear modules, while through their parallel fiber connections they can be interconnected with multiple modules.

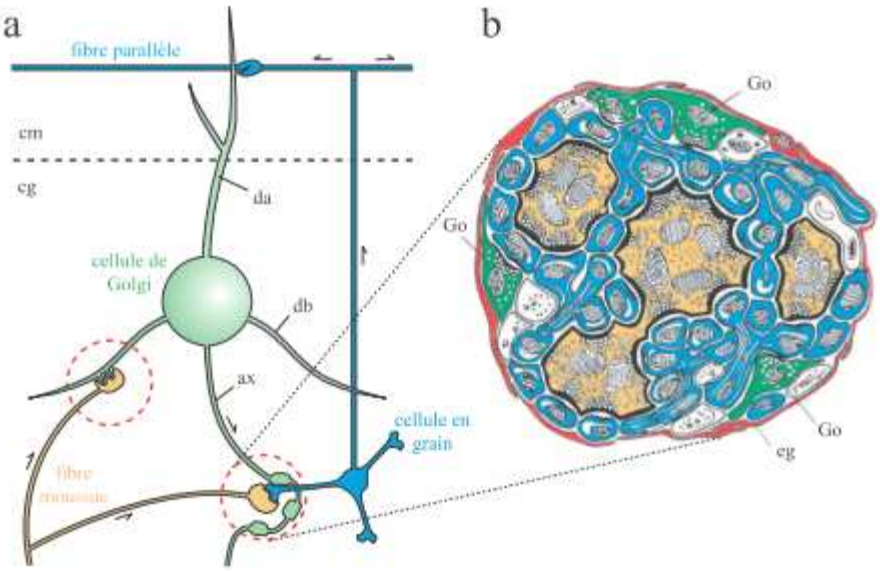

Figure 4.1 The structure of a glomerus

a: A scheme shows that the glomerus is a complex structure, enclosing the mossy fiber and Golgi cell terminals, and granule cell dendrites. ax: axon; cg: the granular layer; cm: the molecular layer; da: apical dendrite; db: basolateral dendrite;

b: A drawing of the ultrastructure of a glomerus observed under an electronic microscope. eg: glial envelope; Go: axonal varicosities of a Golgi cell.

Adapted from (Dugué, 2006).

4.2 Basic activities

There is a debate on the regularity of firing of Golgi cells. Some studies supported that the Golgi cells are spontaneously active and have a highly regular, typical, firing rhythm without bursts (Chadderton et al., 2004; Miles et al., 1980; Van Kan et al., 1993; Vos et al., 1999) while the others appraised the Golgi cell firing pattern as 'rather irregular' (Atkins et al., 1997; Eccles et al., 1966). Functional studies have shown that Golgi cell activity can be influenced both by mossy fibers, parallel fibers and climbing fibers and by molecular layer interneurons (Barmack and Yakhnitsa, 2008; Eccles et al., 1967; Holtzman et al., 2006; Ros et al., 2009; Vos et al., 1999; Xu and Edgley, 2008). However, resent study debates on the regulation of molecular layer interneurons feedback to the Golgi cell cells (Hull and Regehr, 2012). The inputs to Golgi cells from granule cell, interneurons in the molecular layer and Lugaro cell have been well charaterized (Bureau et al., 2000; Dieudonné, 1998; Dieudonné and Dumoulin, 2000; Dumoulin et al., 2001; Heine et al., 2010; Holtzman et al., 2011; Maex and De Schutter, 1998), but less is known on mossy fiber and climbing fiber inputs. The mossy fiber to Golgi cell connection is glutamatergic, and it rapidly and efficiently excites the Golgi cell (Kanichay and Silver, 2008). Climbing fibers have an excitatory effect on Purkinje cells but an inhibitory effect on Golgi cells (Schulman and Bloom, 1981). This may be because 1) the climbing fibers activate first the stellate cells, which in turn inhibit the Golgi cells (Xu and Edgley, 2008); 2) the climbing fibiers activate mGluR2 glutamate receptors on Golgi cell dendrites, which activate an inward rectifier current preventing depolarisation (Watanabe and Nakanishi, 2003).

Since the structure of Golgi cell dendrites is more three-dimensional than restrained to a plane, Golgi cells can both precisely respond to topographically organized inputs and perform an extended spatio-temporal integration of parallel fiber information modulating their basal activity state (De Schutter, 2002; review in De Schutter and Bjaalie, 2001; Vos et al., 2000). Recent studies demonstrated that the gap junctions can facilitate the synchronization of vast areas of the cerebellar cortex (Dugué et al., 2009).

4.3 Functional activities

According to patch-clamp recordings, the Golgi cells have a pacemaker activity that causes a 1-10 Hz spontaneous firing (Dieudonné, 1998; Forti et al., 2006). Golgi cells are resonant around their oscillation frequency, making them suitable to enhance responses in the theta-frequency band (Solinas et al., 2007). Rhythmic activity is also observed in vivo both in awake (Miles et al., 1980) and anesthetized animals (Holtzman et al., 2006; Vos et al., 1999), probably as a reflection of pacemaking modulated by synaptic activity. It has been recently proposed that electrical coupling between Golgi cells could be critical to allow the emergence of low-frequency synchronized oscillations in neighboring Golgi cells (Dugué et al., 2009). Golgi cells show 'loose synchrony' over hundreds of micrometers along the coronal axis (Tahon et al., 2005; Vos et al., 1999), possibly reflecting shared excitatory inputs along the parallel fiber beam, feed back inhibition onto granule cell or gap junctions.

The Golgi cells present two well-defined responses to the two main modalities of the mossy fiber inputs: long frequency-modulated discharges and short high frequency bursts. First, Golgi cells can continuously follow peripheral signals by modulating their frequency with the intensity of the stimulus (Miles et al., 1980). Secondly, Golgi cells respond to punctuate stimulation with a short burst of spikes. The bursts occur very rapidly (in about 10 ms upon facial stimulation) and consist of one to three well timed spikes in short sequence (Vos et al., 1999). The first spike corresponds to the trigeminal input (trigemino-cerebellar mossy fibers), the second spike to sensory-motor cortical input (cortico-ponto-cerebellar mossy fibers), and the third one may reflect the parallel fiber input. Following the bursts, the Golgi cell generates a long-lasting inhibitory period (Holtzman et al., 2006; Xu and Edgley, 2008) or silent pause lasting for about 100 ms, probably reflecting both intrinsic membrane properties and synaptic inputs (Solinas et al., 2007).

In summary, the Golgi cell, by shifting from a rhythmic discharge to an event-driven state (review in D'angelo, 2008), can both entrain and be entrained in network oscillations demonstrating an intimate relationship with both local and long range circuit.

5 Oscillation in the cerebellum

Oscillatory activity is a hallmark of neuronal network function in various brain regions. The frequency of network oscillations covers more than three orders of magnitude, from slow oscillations in the delta (1.5-4 Hz), theta (4-8 Hz), alpha (8-12 Hz) and beta (10-30 Hz) ranges to fast oscillations in the gamma (30-80 Hz), high gamma (80-200 Hz) and up to ultrafast (>200 Hz) ranges (Buzsáki and Draguhn, 2004). Oscillations have been commonly reported in the motor system. The spectral content of oscillations can be enhanced in specific bands depending on the animal's behavior state. Theta (DeCoteau et al., 2007), alpha (Babiloni et al., 1999; Gunji et al., 2007), beta (Courtemanche and Lamarre, 2005; Pfurtscheller, 1981), and gamma oscillations (Muthukumaraswamy, 2010; Pei et al., 2011) have been reported when the animal is preparing or performing a movement. Fast Oscillations (>200 Hz) are reported in the hippocampus during slow-wave sleep and in the rat barrel cortex during whisking, which is thought to be associated with very rapid integration of multiwhisker stimuli (Jones and Barth, 1999).

In the cerebellum, all these three ranges (slow, fast, ultrafast) of oscillatory activity have been reported (Table 1). At the lower frequencies, the oscillations may reflect inferior-olive-driven complex spike activities of Purkinje cells at a stable frequency around 10 Hz in the awake resting rat (Lang et al., 1999), or slowly bursting activities of granule cells occurring at 2 to 10 Hz (delta band and theta band) (D'Angelo et al., 2001; Van Der Giessen et al., 2008), or the granular layer oscillations of the local field potentials that occur at 10 to 30 Hz (beta band) (Courtemanche and Lamarre, 2005). At higher frequencies, they vary from field oscillations at 30 to 80 Hz (gamma band) or 80 to 160 Hz (high-gamma band) to low amplitude field potentials that oscillate at even higher frequencies of 160 to 260 Hz (high-frequency oscillation (HFO)). The oscillations in the cerebellum have been the subject of many modelisation studies aimed at understanding their mechanism. For example, feedback inhibition from the Golgi to the granule cells may be responsible for 10-50 Hz oscillations and the reccurent connections between interneurons may induce fast oscillations (100-250 Hz) in the molecular layer (de Solage et al., 2008; Maex and De Schutter, 2005).

Oscillation Type	Frequency Band	Main Causal Substrates	Orientation in Cerebellar Cortex	Putative Functional Consequences	References
Complex spike oscillations (Delta/Theta)	1–4 Hz 4–9 Hz	olivary coupling and conductances	sagittal	- learning-dependent timing	Lang et al., 2006 Van Der Giessen et al., 2008
Theta oscillations	4–9 Hz	granule cell conductances	patchy	- assessment of sensory state - intermittent control of continuous movements	Hartmann and Bower, 1998 D'Angelo et al., 2001
Beta oscillations	10–30 Hz	granule cell and Golgi cell network	patchy	- cerebello-cerebral communication during sensorimotor processing and active and passive movements	Courtemanche and Lamarre, 2005 Seteropoulos and Baker, 2006
Gamma oscillations	30–80 Hz	molecular layer interneurons and Purkinje cells	transversal beam-like	?	Middleton et al., 2008
Very Fast Oscillations (VFO)	80–160 Hz	cerebellar cortical gap junctions	parasagittal-like	?	Middleton et al., 2008
Very High-Frequency Oscillations (VHFO)	160–260 Hz	recurrent collaterals	patch-like	?	de Solages et al., 2008

Table 1 Overview of oscillatory activities in cerebellar cortex and their presumptive causes and consequences
Adapted from (De Zeeuk et al., 2008).

5.1 High frequency oscillation

The fastest oscillatory activity reported in the cerebellum can be classified in the ultrafast (90-200 Hz) range of physiological oscillation, as previously described in the hippocampus (Buzsaki et al.,1992; Buzsaki and Draguhn, 2004). In the cerebellum, oscillatory rhythms faster than 160 Hz have been observed for more than 70 years. High frequency oscillations were first reported in anesthetized or decerebrate mammalian cerebellum by Adrian (1935) and Dow (1938). Adrian reported low-amplitude, high-frequency (150-250 Hz) oscillations in the electroencephalogram on the cerebellum surface (Fig 5.1A). Later, this oscillation was also observed in avian and reptilian cerebellum by Brookhart, Moruzzi, Snider (1951) and Joynt (1958). A decade later, Pellet and his colleagues (1974) reported first in the chronic animal the presence of cerebellar high frequency oscillations. The oscillations were observed across several different states including calm relaxed waking, attentive waking without movements, slow-wave sleep and paradoxical sleep, and the intensity of the oscillation increased during the active waking and paradoxical sleep. In recent years, the study in mutant animals renewed the interest on high frequency oscillations in the cerebellum. Cheron observed fast oscillations in pathological conditions (Cheron et al., 2004). He and his colleagues used several kinds of Ca-binding protein gene knockouts mice. Since Ca-binding proteins are differently expressed in the cerebellar neurons cell types, altering a type of Ca-binding protein will selectively perturb Ca homeostasis and thereby modulate excitability of selected neuronal types. Calretinin (Cr) is present in Golgi, Lugaro and unipolar brush cells. Calbindin D-28 K (Cb) is present only in Purkinje cells and parvalbumin (Pv) is present in both molecular interneurons and Purkinje cells. The KO mice for these proteins have a normal cerebellar morphology and the most remarkable electrophysiological feature in these Ca-binding protein-deficient mice is the presence of a strong, spontaneous oscillations around 160-200 Hz, which is not seen in wild type mice (Fig 5.1B). Network 160 Hz oscillations also emerged in slices prepared from the cerebellum of mature rats when bathed in zero-calcium media (Traub et al., 2007) and could also been observed in other ataxic mice such as a model of Angelman syndrome carrying the *Ube3a* null mutation (Cheron et al., 2005) and a model of fetal alcohol syndrome

(Servais et al., 2007).

In all these mutant mice, the amplitude of local field potential high frequency oscillations always increased when the recording electrode approached the Purkinje cell layer, reaching its maximum just beneath the Purkinje cell bodies, suggesting that assemblies of Purkinje cell are the major generator of the 160 Hz oscillations (Cheron et al., 2004; review in Cheron et al., 2008). Spatial coherence analysis demonstrated that HFOs were perfectly synchronized at sites along the coronal plane but not along rostro-caudal axis. However, there is no coherence along the parallel fiber in anesthetized rat and the amplitude of the high frequency oscillations observed in anesthetized rat is smaller than the one in mutant mice. De Solages and her colleagues (2008) used linear silicon electrodes in penetrations orthogonal to the layers to record simultaneously extracellular potentials in the different layers of the cerebellar cortex and found that high-frequency oscillations could be seen in all the layers (Fig 5.1C). The Purkinje cell and the granular layer display a uniform phase but a reversal of phase in the molecular layer. The amplitude of the oscillations was maximal in the Purkinje cell layer and decreased with distance from the Purkinje cell layer. The current-source density analysis revealed a source-sink pair in the Purkinje cell layer and the proximal molecular layer, indicating that the oscillations observed in the extracellular potential throughout the cerebellar cortex are generated in the layers containing the somata and proximal dendrites of the Purkinje cells.

In all knockout mice for genes encoding Ca-binding proteins, in which 160 Hz oscillations were observed, microinjection of GABAA antagonist, such as bicuculline or gabazine, reversibly reduced the power of the 160 Hz oscillation (Cheron et al., 2004; Servais et al., 2005), indicating the involvement of inhibitory synapses. Application of gap-junction blocker carbenoxolone (CBX) in mutant mice in vivo blocked 160 Hz oscillation efficiently, suggesting that a gap junction-coupled network support the emergence of this fast oscillation. In contrast, after pentobarbital (a GABAA receptor positive modulator) injection, the HFOs were maintained, and even facilitated through enhanced Purkinje cells synchrony. Interestingly, in the absence of HFOs, the injection of pentobarbital never induced the emergence of HFOs. However, the precise site which is accounting for HFOs wasn't tested in these experiments, since there are at least two

possible sites where gap junctions would be relevant to the 160 Hz oscillation: at the level of stellate and basket cells and the level of the axonal plexus of Purkinje Cell collaterals. The experiments in anesthetized rats (de Solages et al., 2008) confirmed the contribution of inhibitory connections and further suggested that HFOs are due to the axonal recurrent connection between Purkinje cells. Intravenous administration in vivo of GYKI 52466, an antagonist of the AMPA receptors that mediate climbing and parallel fiber inputs to Purkinje cells, increased the oscillation power. Thus, the oscillations do not require glutamatergic transmission to Purkinje cells. They confirmed that the oscillations did not require glutamatergic or other extracerebellar inputs by verifying the presence of oscillations after pedunculotomy. They tested picrotoxin, a noncompetitive antagonist of GABAA receptors. Picrotoxin reduced the power of the high-frequency oscillations. These experiments indicate that GABAergic but not glutamatergic transmission is required for the genesis of the ultrafast oscillations. To investigate further the source of the synaptic inputs responsible for the oscillations, they applied the agonist of CB1 receptors WIN 55,212-2, which acts presynaptically to suppress inhibitory inputs from local interneurons and excitatory inputs from climbing and parallel fibers. This treatment inhibit all the inputs to Purkinje cells except that of the recurrent collateral input itself, and should thus preserve the GABAergic recurrent connections between Purkinje cells, because they do not express CB1 receptors. WIN induced an increase in the oscillation power. This indicates that WIN spares the GABAergic transmission responsible for the oscillations. In summary, their results suggest that the high-frequency are not driven by excitatory inputs but rather that they are mediated by cannabinoid-insensitive GABAergic synapses, most probably those of the recurrent collaterals of Purkinje cells. However WIN 55,212-2 also directly affects P-type calcium currents, which are responsible for the majority of calcium influx in cerebellar Purkinje cells (Hartmann and Konnerth, 2005; Usowicz et al., 1992), but this effect is reported at much higher concentration used by de Solages and her colleagues. However, there are no direct evidence, since no more direct way to manipulate specifically the output of the recurrent collaterals of Purkinje cells is available until now. A lack of calretinin and calbindin also directly leads to high-frequency oscillations, suggesting that a disturbance in calcium homeostasis in Purkinje cells can indeed also contribute

to the generation of high-frequency oscillations.

The frequency of oscillation showed no significant differences between the different single knockout mice. In contrast to mice deficient for either one of the genes or the double Cr-/-Cb-/-, HFOs in Pv-/-Cb-/- mice showed two frequency peaks during approximately 50% of the oscillation recording time (Servais et al., 2005). Reciprocal Purkinje-cell synapses are predicted by computer simulations to allow the emergence of such oscillations (Maex and De Schutter, 2005; de Solages et al., 2008).

Fluctuation of the local field potential reflect the collective behavior of the surrounding neurons. Oscillatory activity has been shown to be a fundamental emergent property of neural networks (Bartos et al., 2007; Destexhe and Contreras, 2006). The relationship between local field potential oscillations and neural discharge is central to understanding the type of information carried by oscillations. In the mice with invalidated calcium-binding protein genes, the anomalous fast oscillations are associated with the emergence of the synchrony of Purkinje cells (Cheron et al., 2004). Further pharmacological research showed that when Purkinje cells synchronicity was abolished, the fast oscillation was simultaneously inhibited, by contrast Purkinje cells synchronicity increased when fast oscillation facilitated (Servais and Cheron, 2005). These phenomenons suggested that fast cerebellar oscillations involve synchronous rhythmic firing of Purkinje cells population. Cross-correlograms between Purkinje cell pairs in mutant mice demonstrates a remarkable synchrony of the high-frequency simple spike firing along the parallel fiber beam. In contrast, cross-correlograms of distant Purkinje cells are flat in WT mice. De Solages and her colleagues (2008) demonstrated that the activity of neighboring Purkinje cell is synchronized by the high frequency population oscillation in the anesthetized and head-restrained unanesthetized rats. The cross-correlograms of neighbouring Purkinje cells pairs displayed a central peak, indicating the presence of synchronous (<2 ms) firing, associated with 5 ms side peaks (Figure 5.2). The spectral density of multiunit spike trains showed that a high-frequency peak was often present in the spectrum of the multiunit spike trains, revealing an emergent organization of the population at a high frequency. The temporal relationship between the HFOs and simple spike and complex spike firing was shown to be phase-locked in the mutant mice.

Simple spike discharges occurred on the negative phase of the HFOs, whereas the complex spike discharge appeared during the ascending phase of the HFOs. In contrast, there was no phase locking between HFOs and Golgi cell spikes, although increased Golgi cell firing rate was correlated with a significant reduction of concomitant HFOs (Cheron et al., 2004). In the anesthetized rat, the spikes recorded in the Purkinje cell layer were phase-locked to the negative phase of the oscillations in the granular layer. After blocking the AMPA receptors or activating the CB1 receptors, simple spikes remained time locked to the negative phase of the oscillations. In summary, HFOs in normal (de Solages et al., 2008) and mutant (Cheron et al., 2004) animals present a number of similarities, but differ mostly by their spatial extension, suggesting a loss of spatial confinement of the HFOs in mutant animals.

Little is known on the link between fast oscillations and cerebellar function. In KO mice models, the HFOs were suppressed in response to an air puff on the whiskers, regardless of whether this stimulus caused a facial movement, but only if the Purkinje Cell also responded to stimulus (Cheron et al., 2004). The HFOs were also suppressed during spontaneous muscle activity but only if the simple spike firing was also modulated. The duration of the HFOs suppression was strongly correlated with the duration of the Purkinje Cell response.

The oscillations could help to retrieve information embedded in the termporal patterns of the simple spike activities by synchronizing their impact in the cerebellar nuclei neurons (Shin and De Schutter, 2006). However the function of the HFOs remains to be study in more physiological condition. It will be interesting to find out whether the high-frequency oscillations can indeed serve, just like the low frequency oscillations, as a fundamental computational mechanism for the implementation of a temporal coding scheme that enables fast processing and memory retrieval. Moreover, whether the link between Purkinje cells and high frequency oscillation presents across the different states in the freely-moving animal is still unclear. For better study on the neuron population, a large number of simultaneously-recorded neurons is necessary.

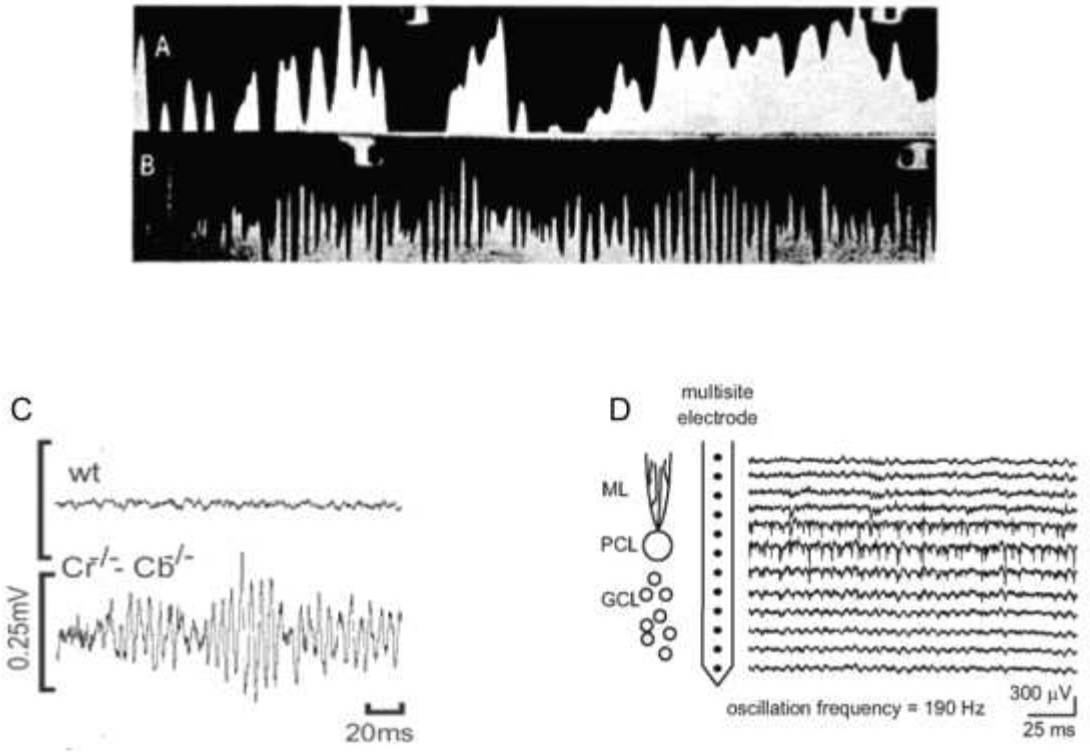

Figure 5.1 High frequency oscillations observed in cerebellar cortex.

A, B: Surface recording from cerebral (A) and cerebellar (B) cortex shows oscillation at gamma range (60 Hz) and high frequency range (180 Hz) in the two region respectively. Adapted from (Adrian, 1935).

C: High frequence oscillations can be observed in Calcium binding protein mutant mice (Cr-/-Cb-/-; bottom), but not in wild type mice (wt; top trace). Adapted from (Cheron et al. 2004).

D: Simultaneous recording across layers performed with a linear multisite electrode indicate that high-frequency oscillations could be seen in all the layers of cerebellar cortex. The amplitude of the oscillations was maximal in the Purkinje cell layer and decreased with distance from the Purkinje cell layer. Adapted from (de Solages et al., 2008).

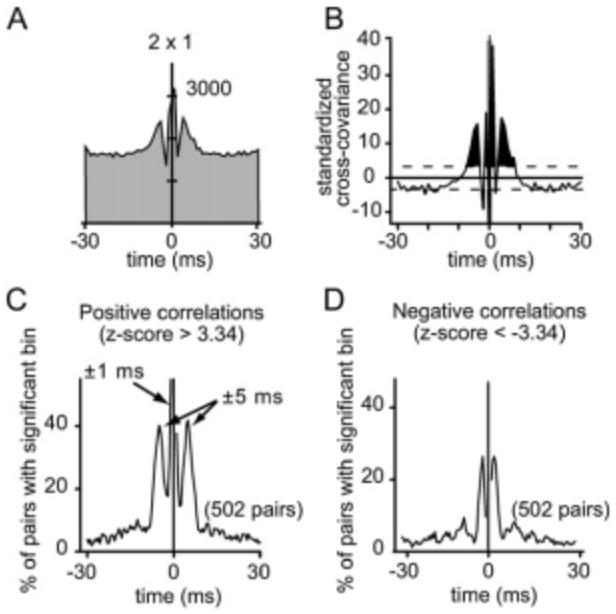

Figure 5.2 Short-Term Correlations between Purkinje Cells

A: Crosscorrelogram of two neighboring Purkinje cells recorded simultaneously from a single tetrode.

B: Principle of identification of the bins with significant correlation in the standardized crosscovariance histogram (whose values are analogous to z scores). The dashed lines indicate the lower and upper limits of the confidence interval. Filled parts of the histogram indicate the presence of correlations departing significantly from the expectation for independent spike trains.

C, D: Fraction of pairs with significant correlations for time bins between -30 and +30 ms. Positive correlations (C) and negative correlations (D) correspond to observed correlations larger and smaller than expected, respectively.

Adapted from (de Solages et al., 2008).

5.2 Low frequency oscillation

A computer simulation has predicted that feedback inhibition from Golgi to granule cells induces 10-50 Hz oscillations in spike discharges from the latter (Maex and De Schutter, 2005). This may account for the large-amplitude oscillation recorded in the granular layer of freely moving animals: 10-25 Hz range in the primate (Courtemanche and Lamarre, 2005; Courtemanche et al., 2002; Pellerin and Lamarre, 1997) (Figure 5.3) and 4-12 Hz range in the rodent (Hartmann and Bower, 1998) (Figure 5.4).

Granule cells appear to have rhythm-permissive cellular properties, and could be part of a resonant network (D'Angelo et al., 2009). Feedback loops (via mossy fiber-granule cell-Golgi cell interactions) and feedforward circuits (via mossy fiber-Golgi cell-granule cell interactions) could generate oscillations or at least resonate in response to entraining excitation. Such interactions imply that Golgi cells would also be entrained by the rhythm. Golgi cells also appear to have cellular properties that could entrain or maintain rhythmicity in the granular layer. Computational modeling has predicted that the granular layer can generate theta-frequency oscillations (Kistler and De Zeeuw, 2003) and may also undergo cycles of activity at relatively higher frequencies (Maex and De Schutter, 1998). The theta band oscillations seems predominant in the cerebellum and there are not only neurons in the granular layer operating in the theta band. Other loops within the same system may operate within the same frequency range. The recurrent circuitry passing through the deep cerebellar nuclei may reactivate the granular layer in about 100 ms (Kistler and De Zeeuw, 2003). Since the Golgi cells presumably receive various direct and indirect inputs (either excitatory or inhibitory) from the climbing fibers derived from the inferior olive, the granular layer may also be tuned toward the dominant frequencies of the olivo-cerebellar modules. Now, it is clear that slow theta and beta rhythms originate in the granular layer and these oscillations influence local cell firing. Multi-unit activity in the granular layer is phased-locked with the negative phase of the LFP oscillations (Courtemanche et al., 2002) and Golgi cells are also phase-locked to the oscillations (Dugue et al., 2009). However, the question whether Golgi cells will prevent the propagation of the the oscillation from the granular layer to other layers

hasn't been answered, some authors arguing on theortical ground that the oscillations will be depressed by incoming activity.

So far, functional hypotheses have been mostly proposed for cerebellar oscillatory activities that operate in the low frequency range. For example, synchronized delta and theta oscillations of complex spike activities generated in the inferior olive may be required for learning-dependent timing in response to unexpected events (Van Der Giessen et al., 2008), and local field potentials oscillating in the theta and beta band that are generated in the granular layer may be involved in preparing the system prior to the execution of movements (Courtemanche and Lamarre, 2005; Hartmann and Bower, 1998). The low frequency oscillations are state-dependent. They occurred preferentially when the animal is immobile and attentive to its environment. They decrease during drowsiness, and are modulated during the behavioral motor task. In a task requiring the monkey to move the arm 1 second after an auditory cue, the oscillations stopped 150-200 ms after the cue, resumed 200-300 ms later, and stopped again 50-100 ms before movement onset (Pellerin and Lamarre, 1997). Low frequency oscillations, specifically in the the theta band, are involved in sensorimotor processing. A remarkable coherence in low frequency oscillations between the sensorimotor cortex and cerebellum has been observed in the rat and monkey (Courtemanche et al., 2002). The cerebellar cortical oscillations in the beta band synchronize optimally with those in the primary somatosensory cortex when the animal is expecting a signal to perform an active movement (Courtemanche and Lamarre, 2005), while single-unit activities of cerebellar nuclei neurons can synchronize with beta band field potentials in the primary motor cortex during the execution of a movement (Soteropoulos and Baker, 2006). These results indicate that at the lower frequencies, cerebellar oscillations can act in concert with oscillations in the cerebral cortex during specific stages of behavior. Low frequency activity may also represent a suitable band for communication between the cerebellum and the thalamo-cortical system (O'Connor et al., 2002). Although the low frequency oscillation has been comparatively well studied in the cerebellar cortex, it is still not clear how much the 4-12 Hz granular cell layer oscillations can exert their influence across the cerebellar cortex, if these oscillations can reliably influence other granular layer units and if they can influence cerebellar cortex output.

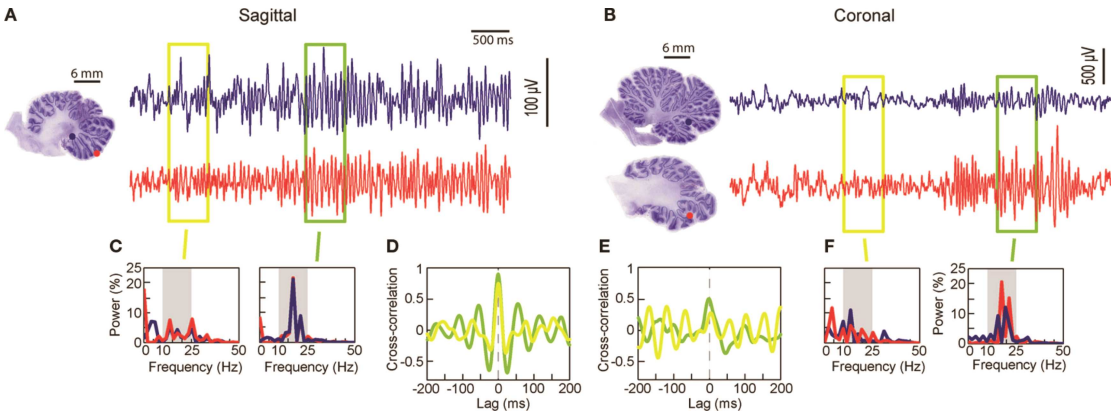

Figure 5.3 10-25 Hz oscillations observed in granular layer of cerebellar cortex at rest in a monkey.

A, B: Simultaneous LFPs recorded sagittally or coronally. Estimated positions of the recording pairs shown, based on reconstruction from electrolytic lesions. Two periods are highlighted, one with low (yellow box) and one with strong (green box) oscillations.

C,F: Fast Fourier Transforms (FFT) for each recording site, for each selected period.

D,E: Cross-correlation for each selected period. Recording sites, field potential and FFT traces are color-matched.

Adapted from (Courtemanche et al., 2009).

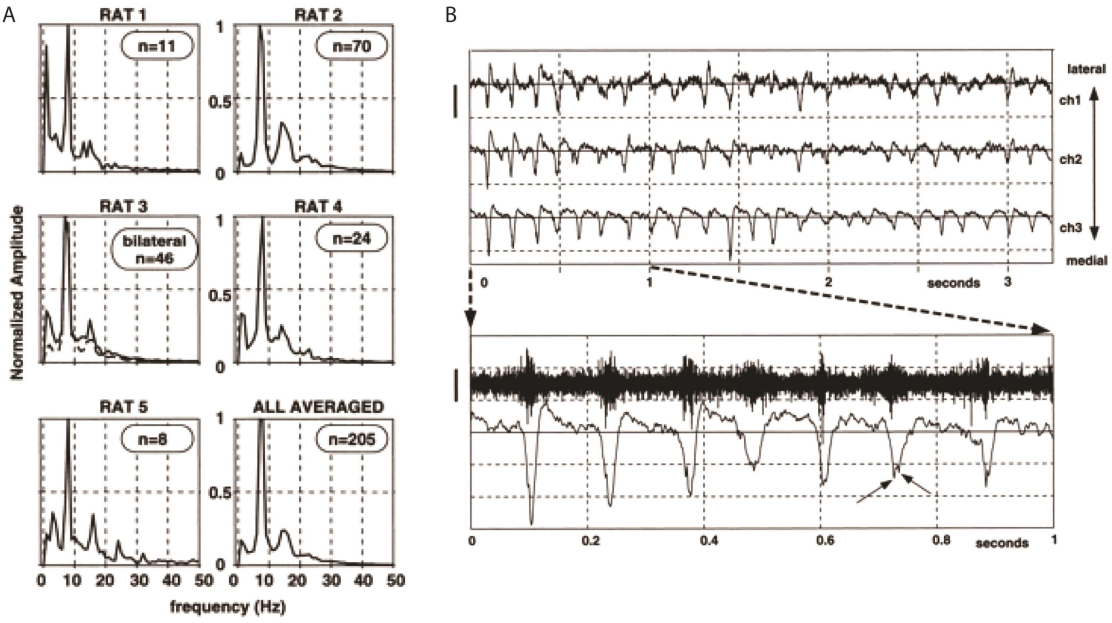

Figure 5.4 Theta oscillations observed in granular layer of cerebellar cortex in rats.
A: Oscillation frequency comparedamong 5 rats. Oscillatory activity in all rats exhibited a central peak, 8 Hz, with subsidiary peaks near 1.2 and 15.0 Hz.
B: Oscillatory activity seen in left Crus IIa during awake immobility. Top 3 trace: 3 s of typical oscillatory activity (scale bar: 250 mV top trace, 500mV bottom 2 traces) recorded from 3 electrodes spaced, 500 mm apart mediolaterally. Data were filtered between 1 and 300 Hz. Bottom 2 traces: expanded timescale of the data from the most medial electrode in top. Field potential oscillation (scale bar: 200 mV) was accompanied by a burst of multiunit activity (filtered 300 - 3,000 Hz; Scale bar: 50 mV).
Adapted from (Hartmann and Bower, 1998).

5.3 Gamma oscillation

Activity within the gamma and high gamma range has been reported in cerebellar recordings (Niedermeyer, 2004) (Figure 5.5). However, the origin layer which generates the gamma band oscillations is so far unclear (Dalal et al., 2008).

In slice of mouse and human tissue, one can induce field oscillations at the gamma and high-gamma band in coronal slices of Crus I and II in the cerebellar cortex following application of a cholinergic stimulation with physostigmine or nicotine, but not in coronal slices of other cerebellar regions or in sagittal slices in general (Middleton et al., 2008). By using pharmacological blockade of GABAA receptors, Middleton and his colleagues suggested that a combined input from GABAergic interneurons and Purkinje cells may be required to generate the gamma field potentials. The gamma oscillations, on the other hand, may specifically require electrotonic coupling within a zonal region; Middleton and his colleagues used five different types of gap junction blockers, and all of them affected the power of the gamma oscillations. Moreover, they observed, in intracellular recording from both molecular layer interneurons and a subset of Purkinje cells, spikelets which are subthreshold postjunctional potentials that usually reflect prejunctional full action potentials filtered by electrical synapses. Combined with dye-coupling experiments, their data thus suggest that at least a subpopulation of Purkinje cells is directly coupled to molecular layer interneurons.

These oscillations in the cerebellum may also be related to behavioral paradigms. Dalal and colleagues (2008) showed that the cerebellum reveals activities in the 65-90 Hz band or the 90-115 Hz band during a self-paced finger movement task. In the cerebral cortex, the dynamic synchronization of gamma rhythms is linked to precision sensorimotor tasks (Tecchio et al., 2007) and selective attention to tactile stimuli (Bauer et al., 2006). More specifically, event-related synchronization at gamma frequencies is observed during the onset and execution of motor commands (Szurhaj et al., 2005). In general, the gamma rhythms appear to serve as a temporal code in the cortex, facilitating the dynamic formation of neuronal assemblies by permitting synchronous firing among neurons.

These high-frequency activities in the cerebellum seem to have the possibility to occur in coherence with those in other brain regions. Thalamocortical cells show gamma band activities that are facilitated by their input from the cerebellar nuclei (Timofeev and Steriade, 1997). Corticocerebellar coherence at gamma frequencies is observed in monkeys during manual precision grip tasks (Soteropoulos and Baker, 2006). Depending on their results, the lack of a time delay between DCN and M1 activity suggests that the cerebellum and cortex may form a pair of phase coupled oscillators. The extensive oscillatory synchronization observed between cerebellum and motor cortex may have functional importance in sensorimotor processing.

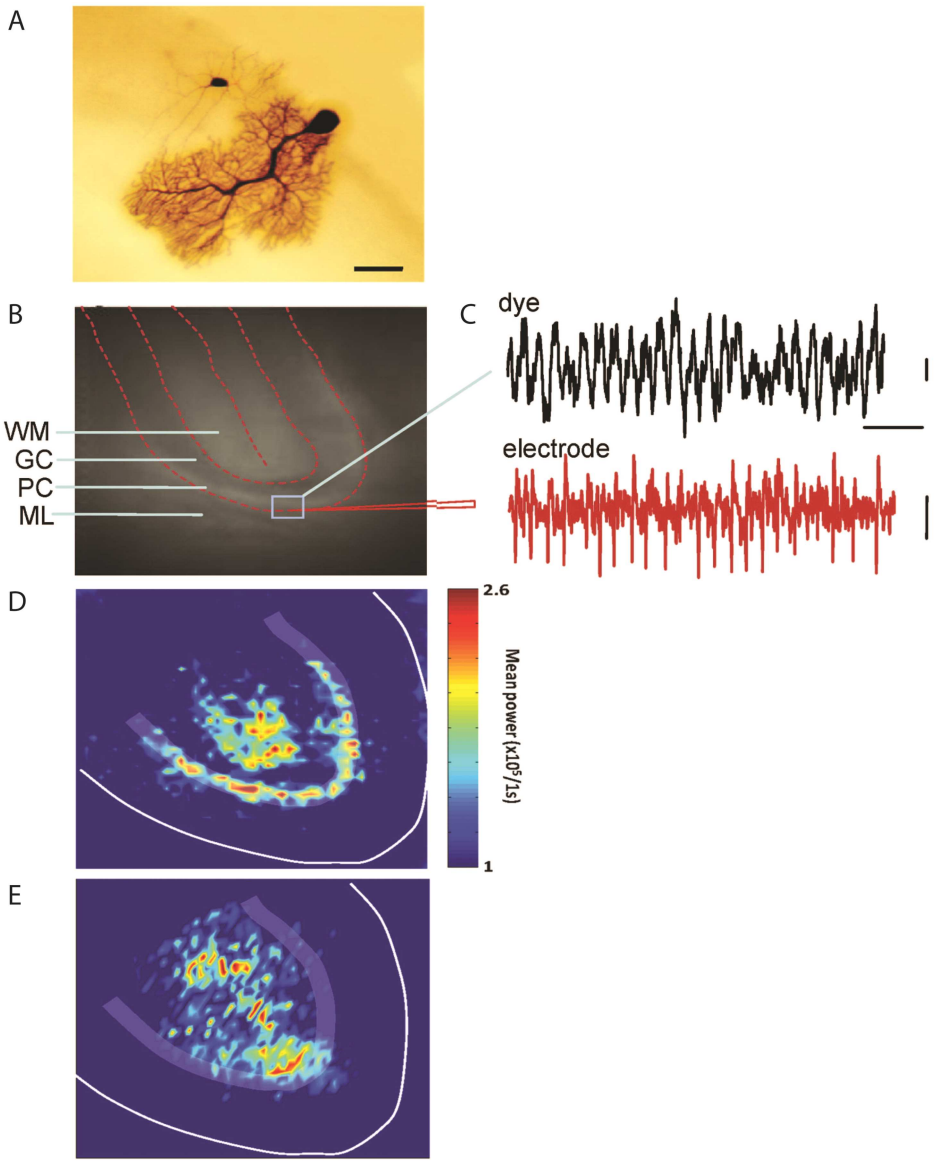

Figure 5.5 Optical recordings show differential origin of gamma and high gamma rhythms
A: An example of heterocellular dye-coupling between a Purkinje cell and an inhibitory interneuron. Note: biocytin was injected only into the Purkinje neuron during extracellular high frequency oscillations and is presumed to diffuse to the other cell via gap junctions. Adapted from (Akemann et al., 2009).
B: Comparison of electrophysiology and voltagesensitive dye recordings. Fluorescence image of a dye-stained cerebellar slice with indication of the main anatomical features (WM, white matter; GC, granule cell layer; PC, Purkinje cell layer; ML, molecular layer) and the location of an extracellular field electrode and overlaid region of interest for fluorescence signal.
C: Example traces show concurrent field and dye recordings of high-frequency oscillations induced by nicotine.
D, E: Pooled peak power in the gamma band (20–60 Hz) and high gamma band (80–160 Hz) from power spectra of the optical data morphed onto an idealized lobule slice. Note that peak gamma power is mainly confined to the Purkinje cell layer around the apex of the lobule, but with additional signal in the gamma band in distal white matter. In contrast, high gamma peak power was seen in the granule cell layer at the lobule apex and diffusely in white matter.
Adapted from (Middleton et al., 2009).

5.4 Interaction and effect

High frequencies could, under particular circumstances, act well together with oscillations of lower frequencies (Canolty et al., 2006; Jacobs et al., 2007). Such cross-frequency phase synchronization could even occur within the olivocerebellar system itself (Lang et al., 2006). So, different cerebellar rhythms may coexist and their underlying networks can still, at least partly, be shared.

Regardless of the underlying mechanisms, questions remain as to what functions the various cerebellar oscillations may serve. Clearly, all oscillations generated in the cerebellar cortex, independent from whether they operate at low or high frequencies, will exert their effects in the end through the cerebellar and vestibular nuclei. The Purkinje cells form the sole output of the cerebellar cortex, and the neurons in the cerebellar and vestibular nuclei form, apart from the recurrent connections, their only target neurons. Since the firing rate and spike timing of these target neurons depend relatively strongly on the level of synchrony in their Purkinje cell inputs, synchronized cerebellar oscillations may well in general evoke their effects downstream.

6 Reach-to-grasp movement

Voluntary movements are good models for investigating specific mechanisms underlying cerebellar function as motor control and motor learning. Among these models, voluntary eye movements such as saccade provide powerful models, since they are precise and their brain-stem circuitry is already well understood (Hopp and Fuchs, 2004). With this model, the basic principles of how the cerebellum may control movement in general are starting to be uncovered (Prsa and Their, 2001; Robinson and Fuchs, 2001). However, this model is difficult to apply to the rodents.

6.1 Components

Reach and grasp movements are also among of the best characterized rat skilled voluntary movement, and it can serve as a movement model in rodents. Thus, in our experiments, the reach-to-grasp-food motor task is chosen as a model for studying cerebellar function. In this task, rats need use their preferring forepaw to catch, hold and manipulate food pellets (Whishaw, 2003; Whishaw and Pellis, 1990) (Figure 6.1). Learning reaching skilled movement involves the adaptation of natural muscle synergies to novel circumstances, such as positioning the forelimb, so it can project through a narrow slot (L. Hermer-Vazquez et al., 2004). This skilled forelimb reaching movement needs the coordination of a number of shoulder, elbow, wrist, paw and digital muscles (Hylalnd and Jordan, 1997). Multiple muscles are active at all stages of the reach, and no unique muscle relationships to initiation of individual movement components could be identified. On average, movements in the upward and medial directions occurred together, prior to forward movement. Latissimus dorsi activivation is the earliest muscle event, occurring approximately 150 ms prior to movement, whilst onset of teres major activity, possibly related to paw elevation, has the highest temporal correlation with movement onset. Triceps activity is strongly time-locked to the end of the reach, and may provide the final extensor thrust to complete the reaching movement. It is concluded the reaching movements are produced by temporal variation in distributed activity among all available muscles. According to analysis of Eshkol-Wachman Movement Notation (EWMN), a reach-grasp movement consists of 10 component movements (Whishaw and Pellis, 1990; Whishaw et al., 2003) (Figure 6.2).

1. digits to the midline. Using mainly the upper arm, the reaching limb is lifted from the floor so that the tips of the digits are aligned with the midline of the body.

2. digits flexed. As the limb is lifted, the digits are flexed, the paw is supinated, and the wrist partially flexed.

3. elbow in. Using an upper arm movement, the elbow is adducted to the midline while the tips of the digits retain their alignment with the midline of the body.

4. advance. The limb is advanced directly through the slot toward the food target.

5. digits extend. During the advance, the digits extend so that the digit tips are pointing toward the target.

6. arpeggio. When the paw is over the target, the paw pronates from digit 5 (the outer digit) through to digit 2, and at the same time the digits open.

7. grasp. The digits close and flex over the food, with the paw remaining in place, and the wrist is slightly extended to lift the food.

8. supination 1. As the paw is withdrawn, the paw supinates by almost 90 degrees.

9. supination 2. Once the paw is withdrawn from the slot to the mouth, the paw further supinates by about 45 degrees to place the food in the mouth.

10. release. The mouth contacts the paw and the paw opens to release the food.

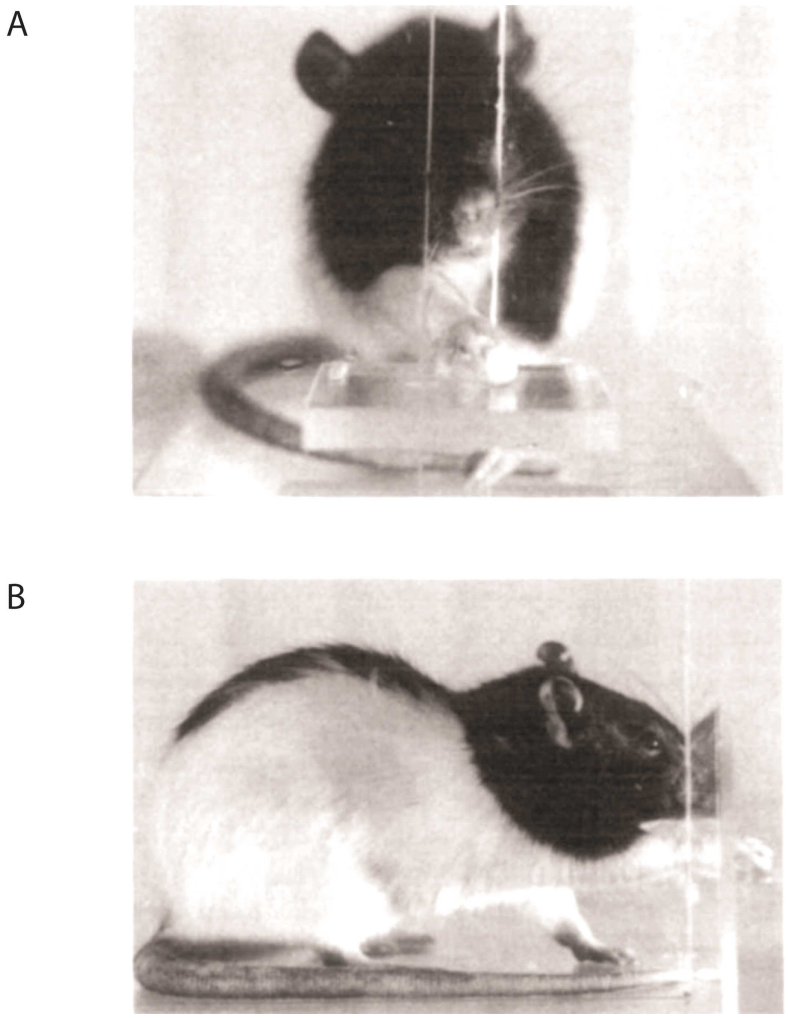

Figure 6.1 The reach-to-grasp-food task
A: Front view of a rat performing a reach-to-grasp-food task. A food pellet is placed on the shelf. To obtain food the rat reaches through an aperture. Since the apparatus is clear, the rat can be filmed.
B: Side view of a rat performing a reach-to-grasp-food task.
Adapted from (Whishaw and Pellis, 1990).

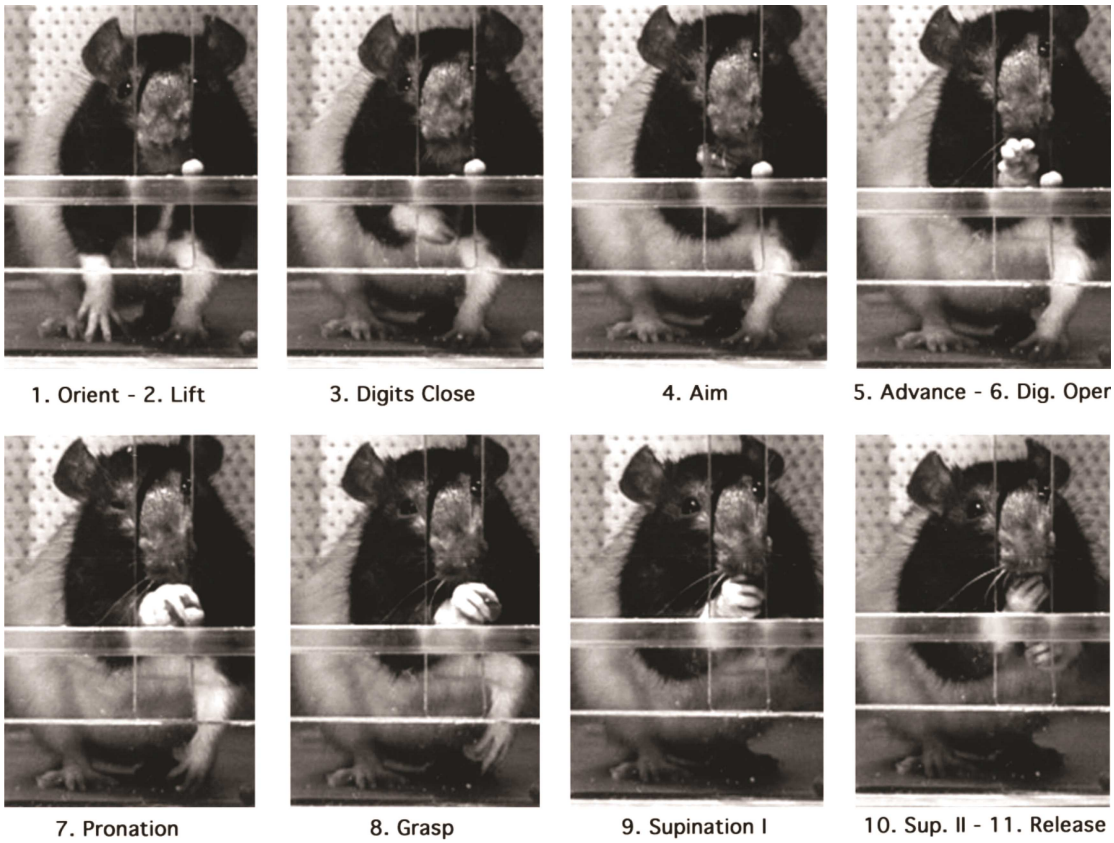

Figure 6.1 10 movement components of a typical reaching movement.
Adapted from (Metz and Whishaw, 2000).

6.2 Similarities and differences of skilled forelimb among species

Skilled forelimb movements were initially thought to originate in the primate lineage but in fact are common among tetrapod taxa and probably share a common origin in early tetrapods. Furthermore, skilled movements are likely to have been derived from, and elaborated through, food-handling behavior (review in Iwaniuk and Whishaw, 2000). There are many similarities in skilled reaching between rodents and primates. They share similarities in behaviors, skeletal structure, musculature, neural pathways, and in the subcortical and cortical brain regions that mediate skilled reaching (Green, 1963). This makes rats useful models for the study of human neurological conditions that compromise skilled reaching. For example, rat skilled reaching is used to model such conditions as spinal cord injury, cortical stroke, Parkinson's disease, and Huntington's chorea. The most striking difference in the skilled reaching of rodents and primates is that primates use vision, whereas rodents use only olfaction to locate food, even when visual or other disambiguating information that the rats can perceive is available (Whishaw and Tomie, 1989).

The neural organization of the motor system is also similar within rodent species. Both rats and mice could use a single forelimb to reach for food, although performance is better and more consistent in rats than in mice (Whishaw, 1996). Both species locate the food using olfaction, and move from a diagonal supporting pattern in which support and postural adjustments come mainly from the contralateral to reaching forelimb and the ipsilateral to reaching hindlimb. Kinematic measures indicate that despite the initial slower velocity of reaching in mice than in rats, the shape of the velocity curve and the trajectory of the limb movement, above and beyond the food pellet, are similar in both species. The motor control of reaching in two rodent species is almost the same. Although there are many similarities, there are still differences even among the rat strains when they perform a reach-to-grasp task. Whishaw and his colleges compared three rats trains during a reach-to-grasp-food task (VandenBerg et al., 2002; Whishaw et al., 2003): the Long-Evans, the Fischer-344 and the Sprague-Dawley. They found that there are difference in both performance score and movement. The Fischer-344 rats learn much slower than the Long-Evans and the

Sprague-Dawley rats, whereas between the two latter rat trains, there is no difference in the acquisition. Among all these three rats trains, movement differences exist in the phases of the movement. For example, when lifting the limb, the Fischer-344 rats do not bring the digits or elbow to the midline of the body; When entering the slot, the paw of the Long-Evans rats is significantly higher than that of the Fischer-344 or Sprague-Dawley rats; During the grasp, the Sprague-Dawley rats appear to grasp the food with the digits incompletely extended during the arpeggio and incompletely flexed; The grasp duration is shorter in the Long-Evans rats. Nikkhah and his colleges (1998) found also strain-differences, which were prominently during the acquisition phase and at the full performance level between five different rat strains (DA/Ztm, LEW/Ztm-ci, LEW.1W/Ztm, SD/Ztm, SPRD/Ztm-Cu3) by using another grasp task: 'staircase test'. There are also individual differences in performance, but they are not related to the measures, training, movement ability, locomotor activity, or anatomy (e.g., brain with cortical thickness, acetylcholinesterase and neuron density, pyramidal tract size). Success is negatively related to numbers of gestures used on a reach (Gholamrezaei and Whishaw, 2009). Individual differences in response strategy may bias some rats to use a more successful goal strategy and others to use a less successful habit strategy for skilled reaching. Changes in the food pellet's diameter (weighing between 20 and 1000 mg) do not induce changes in animal's the grip size as they move to grasp the pellet (Metz and Whishaw, 2000).

Despite of the variarance of performance of reach-to-grasp task among rats trains or among Muridae animals, rats indicate similar performance, which has been well characterized though movement analysis (Whishaw and Pellis, 1990), and neural circuit for reach-to-grasp task. Moreover, sharing similarities in behaviors, musculature and nerual organization of the motor system makes rats a good model for studying neural acitivity during a reach-to-grasp task, whose results may also apply to the human being.

6.3 Brain regions involved in skilled reaching

Rat skilled reaching is relatively inflexible, supporting the opinion that it is produced by a complex, relatively fixed neural circuitry. In general, most of the major structures of the primate motor system are present also in rodents. Like primates, rats use motor cortex, caudate nucleus,

red nucleus, and descending pathways to the spinal cord, including corticospinal tracts and a rubrospinal tracts. A number of studies have demonstrated that the movement elements are altered by motor system damage, including damage to the motor cortex (Alaverdashvili and Whishaw, 2008; Whishaw, 2000), basal ganglia (Bennett et al., 1998; Wenger et al., 1999), brainstem (Whishaw et al., 1993), and spinal cord (Ballermann et al., 2001). In addition, it is now thought that the role played by the lateral and medial descending pathways of the spinal cord in the execution of skilled forelimb movements could be synergistic, rather than the exclusive responsibility of an individual pathway. The electrophysiological results also indicate that interpositus, the output nucleus of intermediate cerebellum, and magnocellular red nucleus, which connects interpositus to the spinal cord, are involved primarily in grasp control during the reach-to-grasp movement (Gibson et al., 1998).

The motor cortex plays a very important role in skilled reaching (Whishaw et al., 1986). No matter the size of a damaged region in the motor cortex, it will impair the skilled movement (Moon et al., 2009). The rats, which switched from using the contralateral-to-lesion paw to the ipsilateral-to-injury paw after motor cortex injury, make very few attempts to reach and have very few successes during the first few days following motor cortex stroke. Over a period of about 14 days, they start to recover and become persistent in attempting to reach and their success rate recovers almost to preoperative levels but the success in obtaining food on a first reach remains extremely poor (Whishaw, 2000). Motor cortex damage reduces individual digit movement, both as the paw is pre-shaped for grasping and in the the grasping action itself (Alaverdashvili and Whishaw, 2008).

The red nucleus (RN) is a prominent structure in the motor system of mammals and is thought to play a role in the control of limb movement. Its cells receive projections from the cerebral cortex and the cerebellum and send projections to many brainstem nuclei as well as to the spinal cord, and then further project toward inferior olive. The lesions of the red nucleus do not impair reaching or grasping success with the limb contralateral to the lesion but reaching movements are changed (Whishaw and Gorny, 1996). While motor cortex lesions impaired subsequent use of the contralateral limb, additional red nucleus lesions did not change total reaches or reaching success.

However, it produced moderate qualitative changes in limb accuracy and paw opening during grasping (Whishaw et al., 1990). These results suggest that in the rat, the RN is not essential for the ballistic component of reaching but may contribute to fine motor control such as may provide the tonic mechanism that momentarily immobilizes the limb so that arpeggio and grasping movement can occur. Recordings of task-related red nucleus neurons in chronically implanted freely moving rats have demonstrated that peaks of increased activity occur before, during and after the reach, and there were clear peaks between reach-onset and reach-end (Jarratt and Hyland, 1999). Both excitations and inhibitions showed a strong tendency to end in close temporal association with reaching. The spread of neural activation onset times throughout the course of the complex reach-to-grasp movement is consistent with a relationship of individual neurons in the rat red nucleus with movements of all parts of the forelimb. The disproportionate number of modulations that occur during the reach and their strong alignment with time of reaching suggests there is a bias in red nucleus function towards the control of distal motions associated with accurate grasp.

The corticospinal (pyramidal) tract is thought to be the main substrate of voluntary movement. It is important in pronation and supination (Passingham et al., 1983), independent finger movements (Lawrence and Kuypers, 1968), contactual hand orienting responses and reflex adjustments (Schwartzman, 1978). Unilateral lesions of pyramidal tract caused impairment of almost all movements involved in reaching, including lifting, aiming, pronating and supinatingthe limb and releasing food, except digit opening. Rats with additional damage to adjacent structures, such as the medial lemniscus and olivary complex, are much more severely impaired on the reaching tasks (Whishaw et al., 1993).

Recent studies demonstrated that the cerebellum is also involved in the control of voluntary movement. To identify cerebellar regions that are involved in the control of limb muscles, rabies virus was injected into the tibialis anterior and gastrocnemius muscles of the rat (Ruigrok et al., 2008). They find labelled cells of the cerebellar nuclei as well as of several strips of Purkinje cells. The experiments of reach-to-grasp movements of patients with pathology restricted to the cerebellum indicate that the cerebellum contributes substantially to the coordination of movements

required to perform reach-to-grasp movements (Rand et al., 2000). In another experiment, cerebellar subjects showed abnormalities in the sequence of the reach and grasp movement and highly variable timing of peak grip aperture (Zackowski et al., 2002). Their results indicate that cerebellar damage can cause a specific breakdown in the coupling of reach and grasp movements. The cerebellum may be particularly involved in combining reach and grasp movements into a single motor program. On the level of cell, the gating of cutaneous inputs to cerebellar climbing fibers during a reaching task also been studied (Apps et al., 1997). Cerebellar nuclei cells are reported to correlated with the arm reaching (Fortier et al., 1989). Inactivation of deep cerebellar nuclei will impair the reaching movement (Martin et al., 2000). Increasing simple spikes in subdivision of cerebellar cortex inhibits output to specific cerebellar nuclei, therefore produces unique behavioral deficits during a reach-to-grasp task (Horn et al., 2010). However, deep nuclei cell is not controlled by a single Purkinje cell, but by local Purkinje cell population, which is less studied now during a reaching task. Therefore, these studies indicate a substantial contribution of the cerebellum to reach-and-grasp movements, with strong modulation of neuronal discharge in this structure. It thus offers a good model to study processes of neuronal coordination that may occur in the cerebellum during voluntary movements.

.

7 The motor cortex

As discussed above, the motor cortex is necessary for voluntary movements. It is involved in the planning, control, and execution of voluntary movement. However, how the primary motor cortex works together with the cerebellum contributing to the voluntary movements are far to be understood.

7.1 The function of the motor cortex in voluntary movement

In the early research, electrical stimulation experiments found the motor cortex is an orderly arrangement of areas caussing, upon stimulation, movements of muscles of different regions of the body such as the face, digits, hand, arm, trunk, leg, and foot. Activity in individual neurons in the primary motor cortex is modulated when monkeys either flex or extend the individual joints of their contralateral limbs (Evarts and Tanji, 1976). The modulation of individual neurons begins ~100 ms or more before the onset of movement during movement of a particular joint and particular direction of movement (Tanji and Evarts, 1976). Since most voluntary movements involve multiple joints and require sequential and temporally precise activation of multiple muscles, cells in the motor cortex are demonstrated to encode more global features of the movement such as its direction, extent, or joint angle changes. All the neurons recorded in the motor cortex fired briskly before and during movements in a broad range of directions, when monkeys were asked to move a joystick toward different directions (Georgopoulos et al., 1982). Thus, Georgopoulos and his colleagues proposed that movement in a particular direction is determined by the net action of a large population of neurons. The important role of the motor cortex in skilled reaching has been specifically discussed in the previous section: Reach-to-grasp movement.

7.2 Connection between the motor cortex and the cerebellum

7.2.1 Anatomical connection

The cerebellum has recurrent connections with the cerebral cortex (Allen and Tsukahara, 1974). On the one hand, the cerebellar connections with the cerebral cortex are viewed as a means of

collecting information from widespread regions of the cerebral cortex, including portions of the frontal, parietal, temporal, and occipital lobes (Glickstein et al., 1985; Legg et al., 1989; Schmahmann, 1996). Thus, the cerebellum is thought to perform a sensorimotor transformation on its inputs. On the other hand, the intermediate part of the hemisphere including the C1-C3 zones, is connected not only to the brainstem and the spinal cord via the projection from the interpositus nucleus to the red nucleus and other nuclei, but also to multiple subdivisions of the ventrolateral thalamus, which in turn project to a myriad of cortical areas, including the motor domains such as the primary motor area (M1) (Dum and strick, 2003), the premotor area (PMA) (Middleton and Strick, 1998), the supplementary motor area (SMA) and the presupplementary motor area (PreSMA) (Akkal et al., 2007) and the nonmotor domains such as frontal cortex, prefrontal cortex (Middleton and Strick, 2001) and posterior parietal cortex (Clower et al., 2001). Thus, the outputs from the cerebellum influence widespread regions of the cerebral cortex.

7.2.2 Two models of internal model based on connection ways between the motor cortex and the cerebellum

Control system modeling is helpful for understanding the role of the neural systems that control voluntary movements. In models of voluntary movements, the cortical areas (higher motor centers) devoted to motor planning and preparation, the motor cortex receives instruction signals directly from the anterior cingulate gyrus (ACC), supplementary motor area (SMA) and premotor area (PMA), and indirectly from pre-SMA via SMA. The primary motor cortex (controller) receives these signals and generates commands to drive lower motor centers in the brainstem and spinal cord that are connected to a motor apparatus, the controlled object (Ito, 2006). From the theories of movement control, Ito (1970) proposed the concept of internal model in the cerebellum. Based on the two principles, follow which the connections of the motor cortex and the cerebellum are organized: in a loop and in parallel, two different models of internal model of motor control have been proposed, respectively, forward and inverse model.

The experiments using both retrograde and anterograde transneuronal transport of rabies virus in monkeys showed that the arm area of the primary motor cortex (M1) receives input from Purkinje cells located primarily in lobules IV-VI of the cerebellar cortex via thalamus and neurons in the

arm area of M1 project via the pons to granule cells primarily in lobules IV-VI, indicating that the regions of the cerebellar cortex that receive input from M1 are the same as those that project to M1 (Kelly and Strick, 2003). Considering the loop connections between the cerebellum and the primary motor cortex, Kawato and his colleagues (1987) proposed that the function of this loop is to build an internal model of the movement. In the model, the command signals generated by the motor cortex return via the cerebellum to the motor cortex before the actual results of the performed movement are fed back to the motor cortex through the sensory system. With the feedback information, the motor cortex should be able to provide precise instructions to the motor apparatus by referring to the prediction given by the cerebellar forward model, even without referring to the consequences of the actual movement through external feedback via the sensory system.

The second relationship of primary motor cortex and the cerebellum, instead of in loop, is in parallel. Anatomical studies using transported viruses have clearly shown that the projections from the cerebellum through the thalamus to the cortex constitute multiple 'parallel' channels (Middleton and Strick, 1998). Neurons in the supplementary motor cortex and premotor cortex project to the motor cortex (Fang et al., 2005), at the same time, they project also to the cerebellum via the pontine nucleus (Wiesendanger et al., 1979). Tracing experiments with viruses in monkeys found the the regions of the cerebellar cortex that receive inputs from the prefrontal cortex (area 46) are the same as those that project to the area 46. Thus, similarly to M1, the prefrontal cortex forms separately closed-loop circuits with the cerebellar cortex. Based on parallel path connections between the cerebellum and the primary motor cortex with higher motor centers, a inverse model for control and learning of voluntary movements was proposed by Kawato and his colleagues (1987) and afterwards developed by Kawato and his coworkers (Kawato and Gomi, 1992; Shidara et al., 1993). In this model, output from cerebellar microcomplexes are incorporated in parallel to the motor cortex. The cerebral output and cerebellar output converge in the lower motor centers. Such a convergence is noted in the rubrospinal tract neurons, which receive inputs from the interpositus nucleus (Toyama et al., 1970) and the motor cortex (Tsukahara and Kosaka, 1968). Thus, the inverse model can play the role of a feedforward controller.

Both computational forward and inverse models match the previous concept of internal feedback from an internal model of the controlled object formed in the cerebellum via cerebrocerebellar communication loops (Ito, 1970; Ito, 1984) (Figure 7.1). In the forward model, the command copy arises from the primary motor cortex. The cerebellum as a forward model receives motor commands via the mossy fibers and sensory signals via the climbing fibers. In the inverse model, the command copy arises from higher motor centers. The cerebellum as an inverse model receives instruction signals via the mossy fibers and motor signals via the climbing fibers. The former fits model with a decorrelation control algorithm, while the latter is the typical case of feedback-error learning. The nuclear output of a microcomplex usually represents motor commands, but in the forward model, it represents sensory signals. In these models, the internal feedback can in a way replaces the external feedback and makes the system perform effectively after learning even if the external feedback is unavailable or too slow to guide motor execution.The internal model is conceived to mimic the learning capability, since a characteristic feature of voluntary motor control is that after repeating a task, one is able to perform the task precisely and without the feedback that was required before the task and that a normally functioning cerebellum is required to accurately perform a quick movement in the absence of visual feedback (Ito, 1970).

An internal model can be regarded as a predictor of the consequences of motor commands. When common input signals drive both a microcomplex and a neuronal circuit, and when the difference in their outputs is returned to the microcomplex via the climbing fibers, the input-output relationship of the microcomplex will gradually be modified due to the induction of synaptic plasticity until it closely mimics the other neuronal circuit. Thus, a microcomplex is capable of forming a internal model by copying the signal transfer characteristics of another system running in parallel. For the voluntary movements, the actual movements of the motor apparatus are observed through a sensory system and compared with the predicted movements by the internal model, probably through the inhibitory connection from the cerebellar nuclei to the inferior olive (see Ito, 2001). The internal feedback, through a forward model and/or an inverse model of the cerebellum, explains how we eventually learn to move in an increasingly more accurate and smooth manner, even with our eye closed, through repeated practice. The explanation can also be

applied to finger-to-noise or finger-to-finger test (Holmes, 1939) and the speech-motor activity prediction (Fox et al., 2000). Internal feedback can also predict the sensory consequences of a movement and act to cancel it, which otherwise induces a sensation that disrupts the execution of the movement. The observation in fish cerebellum-like areas, which cancel the disruptive signals caused by swimming in electrosensation support this mode (Bell et al., 1997). The use of internal models of the body and the environment can improve the performance of motor control (Kawato, 1999).

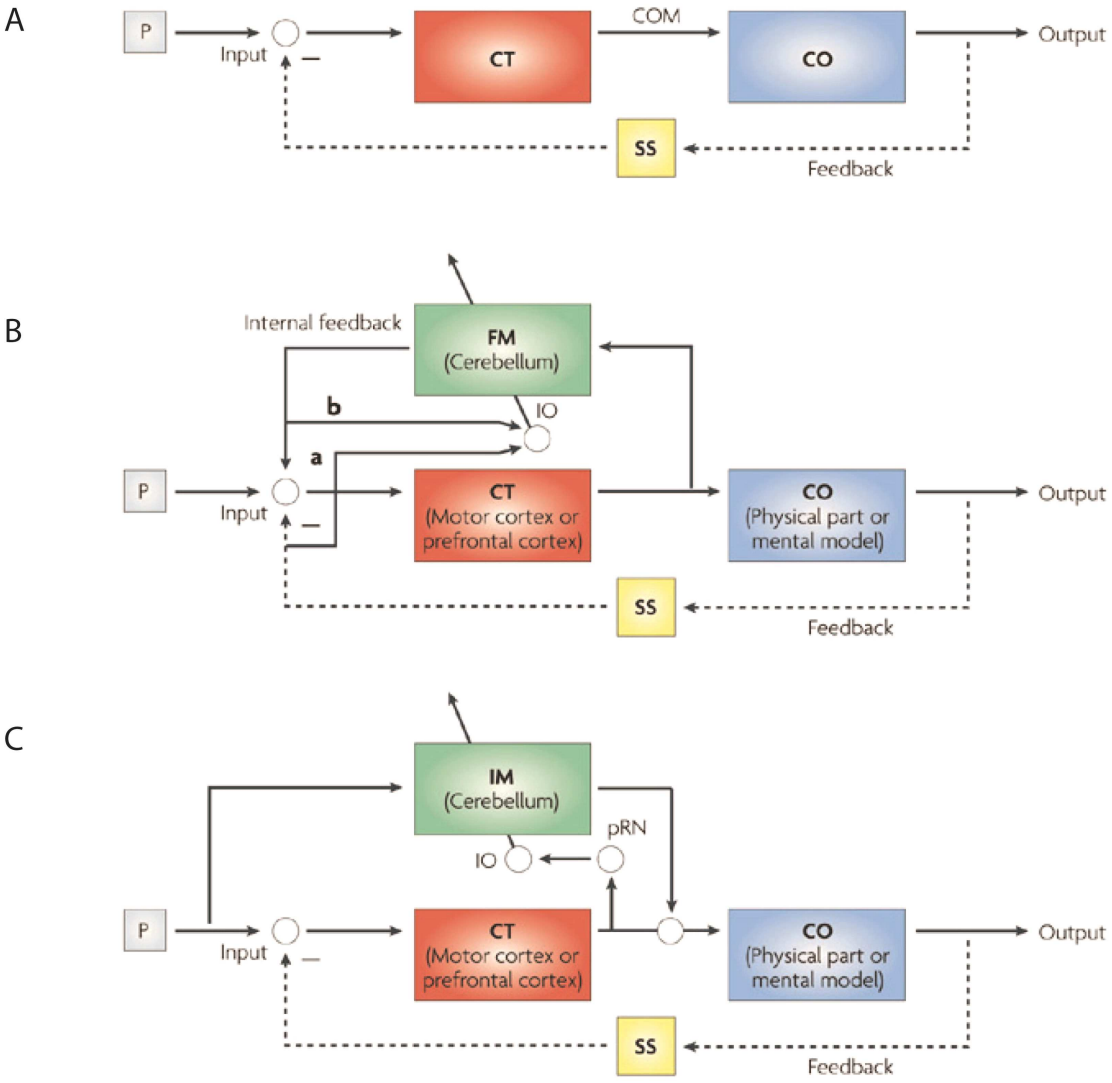

Figure 7.1 Block diagrams for internal-model control
A: The basic structure of a control system, consisting of a controller (cT) that manipulates a controlled object (cO), an instructor (P) that gives an instruction to the controller, and a sensory system (ss) that mediates feedback (indicated by –) to the controller. This external feedback is represented using a dashed line as it can be spared when internal models are functioning. circles indicate junctions at which signals converge or are relayed.
B: A forward-model (FM) control system. In this system a forward model mimics the dynamic properties of the cO. error signals are derived by comparing the outputs of the cO (monitored by the ss; a) with those of the forward model (b) in the inferior olive (IO), and are sent into the forward model to modify it.
C: An inverse-model (IM) control system. An inverse model mimics the reciprocal of the dynamic properties of the controlled object. For learning in the inverse model, feedback errors are derived from the command signals (cOM) that are generated by the cT. The arrows that obliquely cross the forwardmodel and inverse-model boxes represent the pathway signals that tune the dynamics of the forward model or the inverse dynamics of the inverse model. prN, parvocellular red nucleus. Adapted from (Ito, 2008)

7.2.3 Coherence between the motor cortex and the cerebellum

In vivo recording experiments have shown the functional connection between the motor cortex and the cerebellum. The recordings made in arm-related areas of the cerebellar nuclei and primary motor cortex in monkeys during a reaching and button pressing task demonstrated a spatially specific, short latency, primarily excitatory pathway from cerebellar nuclei to M1 at the single neuron level (Holdefer et al., 2000). The control of precise slow finger movements in human is maintained by a 6-9 Hz motor cortical drive, arising in a cerebello-thalamo-cortical loop and probably realizing a control loop with a feedback adjustment of precise movements (Gross et al., 2002).

8 Global conclusion and research proposal

The cerebellum is one of the earliest brain structure investigated, and consequently its fundamental circuit and mode of operation is now well characterized. As exposed in the introduction, the cerebellar cortex has been studied in great detail: it is a three-layer cortex and a two-layer neuronal network with an input stage, the granular layer, and an output stage, the Purkinje cell layer, with extensive connectivity between the layers carried by the parallel fibers. This circuit implements a supervised learning algorithm, with the climbing fibers (an extra-cerebellar afferent) carrying a learning ('error') signal to the Purkinje cells. This algorithm allows to adjust the synaptic weights in the cerebellar cortex in order to optimize the motor output and reduce the 'error' signal. This computation is thought to implement an implicit 'internal model' of the movement which continuously determines the cerebellar cortex output.

Recording the activity of the cerebellar cortex provides access to the implementation of the cerebellar internal model. Recordings from single cell have provided large amounts of information on the time course of firing rate in relation with movement; however, it is difficult to reconstruct with a good temporal precision the population firing from cells recorded on separate trials; there is thus a need to record simultaneously the neurons to describe the fine temporal structure of the neuronal populations.

The functional organization of the cortex provides hints on how to record cells that belong to the same neuronal assembly: substantial evidence indicates indeed that the cortex is organized in many thin parasagittal bands, or microzones; the neurons within these microzones share similar instructive signals, since climbing fibers make multiple collaterals within the bands and the neurons in the inferior olive that give rise to the climbing fibers of a band are electrically coupled. Moreover, axons from the neurons in each band converge in small territories of the cerebellar nuclei. Therefore, understanding how neurons combine their activity in each microzone requires to record simultaneously groups of neurons in narrow bands. The easiest way to perform such recordings is to target groups of neighboring cells. Since these cells share not only the same

climbing fiber signals but also the same parallel fiber inputs, these recordings should maximize the chance to observe events of coordinated discharge of cells belonging to the same micro-zone. Another method to access to population activity is to look in the local field potential for hits of combined activity of multiple neuronal elements. Studying the link between cell firing and local field potential patterns may reveal the presence of coordinated activity. This can be studied for fast cerebellar oscillations, that have been recently analyzed in anesthetized animals, but scarcely in awake animals. The other main known patterns of local field potential are slow oscillations observed in the granular layer and that are presumably reflecting patterned inputs from the motor cortex embedded in slow theta-frequency oscillations. It is currently unknown to which extent this discharge is propagated in the cerebellar network.

My project was thus first designed to 1) solve a number of technical challenges in order to perform recordings of neighboring Purkinje cells in freely moving animals 2) characterize the presence of coordinated discharge in various conditions 3) examine the link between the patterns of local field potential and Purkinje cells firing.

Setting up a technique which can provide stable, simultaneous recordings of neighboring cells is essential for my project. Multi-contact electrode recordings are indeed powerful tools in many brain structures. Tetrode recordings have been recently introduced in the study of cerebellar function. They have proved helpful in demonstrating that the fast cerebellar oscillation arise from a Purkinje cell population oscillation, notably associated with short-term correlations between neighboring Purkinje cells. However, these results were obtained from anesthetized or head-fixed animals. Thus, the first purpose of my thesis is to set up this technique to allow multi-units recording in freely-moving rats. To achieve this, I tested two kinds of tetrodes: traditional wire tetrode and pointed quartz tetrode. I showed that the quartz electrodes produce the most satisfactory recording in the cerebellar layers. Then, I designed a headstage, which can hold several independent movable tetrodes in freely-moving rats, and demonstrated that stable recordings can be obtained in active animals.

With this technique, I investigated the organization of local Purkinje cells *in vivo*, with a particular

focus on the short term coordination of discharge. Such coordination has been reported in anesthetized and head-fixed animals. However, there are few reports on task-related synchrony in awake animal. Thus, the second part of my thesis is to examine in the area of the cerebellar cortex controlling limb movements how the neighboring Purkinje cells coordinate their firing during a reach-to-grasp-food task in freely-moving rats. To achieve this, I firstly examined the region of the cerebellar cortex involved in forelimb control. Then, I developed a training schedule, following which rats can learn the reach-to-grasp-food task. After the surgery, during which a headstage was implanted above the cerebellar area controlling the forelimb, I observed the Purkinje cells activities and studied their temporal organization across states and during the learned skilled task. We are also interested in the interaction and propagation of local field potential oscillations, which represent the integrated local neural population activities, in cerebellar different layers across states and the relationship of oscillations and single neural activity. Cerebellar theta oscillation has been demonstrated to originate in the granular layer and have influence local cell firing. However, there is still debate whether Golgi cells will prevent the propagation of the oscillation from the granular layer to other layers. In collaboration with the group of Richard Courtemanche, we recorded the local field potential and cells activity in the same site both in the granular layer and the Purkinje cell layer during awake immobility. We examined how Golgi cells and Purkinje cells activities were affected by the local theta oscillation in both layers. With these results, we suggest that theta oscillations can propagate across cerebellar layers.

In the following chapter 'Methods', I provide a detailed description of the methods, followed by the three manuscripts describing the main results of my thesis.

Second part
Methods

Methods

My Ph.D. research mainly focuses on organization of the cerebellar neurons in freely-moving animals. Thus, for this propose, in most experiments I record activities of cerebellar cells in different vigilance states in rats including sleep, active exploration and a skilled motor task. Rats are implanted with a headstage holding several quartz tetrodes in paramedia lobule of the cerebellar cortex and sometimes with a bundle electrodes in the motor cortex. These electrodes allow observing and recording cells' activities during extended periods of time. Further analysis is performed in matlab or R.

1Animal and training

The experimental procedures are conducted in conformity with institutional guidelines and in compliance with national and European laws and policies. Male adult Long-Evens rats (3-5 months old at the start of the experiment; 350-500g; Charles River Laboratories, France) are used in these experiments. They are housed individually on a 7 AM to 7 PM reversed light/dark schedule.

1.1 Feeding

For the rats which are in the schedule of training to perform a reach-to-grasp task, in which they should grasp food pellet through a small slot, a special feeding schedule is used. These rats are initially housed in the same condition as usual with ad libitum food. Once rats are familiar with their cage and one week before behavioral training, they are placed on a food deprivation schedule (gradually food restricted until their weight reached 85-90% of their normal body weight). Then, during the training schedule, the total weight of pellets (dustless precision pellets 45mg, banana flavor, Bio-Serv, France) given to the rat during training is removed from the weight of food fed to the rat in the cage, so that their body weight is maintained at 85-90% of their normal body weight. After rats learned the task and one week before the surgery, the rats are fed unrestrictedly until

they totally recover from surgery. Then the food deprivation schedule is reinstated for recording sessions.

1.2 Training and recording table

Rats are trained and recorded in a special table. The table is 65cm long, 50cm wide and 80cm above the ground. In the front of the table, there is a vertical plastic transparent clear Plexiglas wall allowing to film the rat's movements. At the center of the front wall, there is a 1cm wide slit that extended from the floor of the table to a height of 5 cm. On the outside of the wall, in front of the slit, mounted 3 cm above the floor of the table, is a 2 cm wide by 4 cm long shelf. On the shelf there are 3 shallow indentations which are 2 cm away from the inside front wall aligned with the edges of the slit. The food pellet is usually placed on the contralateral indentation to the preferred paw of rats, so that the rats have to use always their preferred paw to grasp pellets.

1.3 Training schedule:

Rats are trained to learn a reach-to-grasp task, in which they should grasp a pellet through a slot only with the preferred paw and find another pellet on the floor in the other side of the table in turn, so that successive trials are separated by several seconds. Successful reaching involves the achievement of four stages, in which the rat need to: 1) orient to the slot for each pellet presentation; 2) transport its forelimb through the slot to grasp the food pellet; 3) withdraw its forelimb through the slot and present grasped food to the mouth (Gharbawie et al., 2007); 4) search for another pellet on the floor at the rear of the apparatus and after eating the pellet, go back to prepare the first stage for the next trial.

The training lasts about 2 weeks, and the schedule is as below:

1) Day 1-3: habitation with the training table

Training begins when a food-restricted rat is individually placed in a training table. The aim of the first day is the habitation to the training table. Pellets are placed randomly on the floor of the table, so that the rat can explore all over the table when searching for food . On day 2 and 3, usually rats do not need food to encourage their exploration on the table.

2) Day 4-7: learning to remember the two reinforced places and to face on the slot

The pellets are placed on the floor of the table in front of the shelf and at the rear part of the table so that the rat can collect food in these two place. After 2 days training, rats can usually learn that these two places are the only places where they can find food. Then to encourage a naive rat to orient to the slot at the front of the table, a number of food pellets are placed on the shelf and directly in front of the slot (Gharbawie et al., 2008). The objective is to make the pellets accessible to the tongue or paw through the slot. In addition, crushed food pellets are placed on the shelf to intensify the scent of the pellets and to prompt rat's interest. Once the rat seems to have interest in collecting food from the slot, pellets are moved far enough away from the slot to prevent the rat from using its tongue to collect the food while allowing the rat to reach the pellet with its paw.

3) Day 8-11: learning the normal grasp only by one preferring paw

From day 8 (the second week of training), the rat receives daily training sessions of 25 pellets, but for no longer than 30 min. A pellet is placed on the shelf, in front of slot in the beginning, so that it's easier for a rat to grasp. Once the rat shows its capacity to grasp pellets, a pellet is moved gradually to a more lateral side and farther from the slot to encourage the rat to use only its preferred paw (which is determined from the observation during the previous trials) and to encourage forelimb transport for pellet retrieval, until individual pellets are placed into the indentation contralateral to the preferred paw.

4) Day 12-14: learning the 'in-turn' task

If the rat has already learned how to grasp the pellet which is placed on the contralateral indentation through the slot only with the preferred paw, the rat is then taught to grasp a pellet on the shelf and eat a pellet on the floor at the rear part of the table in turn. This design provides more time between two trials of grasping, which allows the replacement of a food pellet on the shelf. Moreover, the data collected when the rat eats the pellets without grasping can also be used as a control to ensure that the results we get from the grasp task are not from eating. To achieve this, after the rat grasps a pellet on the shelf, a pellet is randomly placed on the floor at the rear part of the table. Usually the rat initially continues to grasp for a while even there is no more pellet. But after a certain of time, it gives up and search food all over the floor of the table. When the rat finds the pellet which is placed at the rear part of the table and eats it, another pellet is placed again in

the indentation on the shelf. After several times, the rat remembers the two available places of food and start to do the whole task voluntarily.

Usually, after two weeks of training, the rat learns how to perform the whole skilled motor task.

2 Electrode Preparation

In our experiments, two kinds of electrodes are used: tetrodes for recordings in the cerebellum and bundle of single wire electrodes for recordings in the motor cortex.

2.1 Preparation of a headstage for the cerebellum

In the anesthetized rats, we compared the recording from hand-made wire tetrode and commercial quartz tetrode and found that quartz tetrodes have a much easier penetration and provide satisfactory separation of cells in Purkinje cell layer. Moreover the quartz tetrodes provide stable recordings in freely-moving rats for a long time (Gao et al., 2011). Thus, we choose quartz tetrodes for recording cerebellum cells in our experiments in freely-moving animals. In order to well perform these experiments *in vivo*, we manufactured an implantable, stable and light-weight tetrode headstage (Figure 8.1), which holds multiple microdrives, each allowing controlling independently a reference or one quartz tetrodes. Each microdrive has a micro-machined backbone holding at its top and bottom a threaded rod that is allowed to rotate freely. A small cubic screw is mounted on the rod and translates when the rod is turned. The screw carries a stainless steel tube to which the tetrode is attached. Quartz tetrodes are obtained from 4 platinum/tungsten-cores in a quartz rods, sculpted with a sharp tip (Thomas Recording Gmbh, Germany). A 30 gauge quartz tube is used to guide each electrode to the brain. The upper ends of the tetrodes are silver plated to the pins of the connector and secured with heat shrink tubing. The whole drive is enveloped by a conic piece of cardboard covered with aluminum foil connected to the ground to reduce electromagnetic interference during the recordings. Before recording, the tips of the tetrodes are cleaned (Microelectrode Tip Cleaner, Thomas Recording Gmbh) and gold-plated (gold solution, Sifco) to lower their impedance to 200-300 kΩ for improving the signal-to-noise ratio. A dye (cell-labeling solution, Invitrogen) is applied to the tip of tetrodes to visualize the track of the electrodes in the cerebellum.

2.2 Preparation of bundle of single wire electrodes for the motor cortex

Hand-made bundle is obtained by gathering sixteen 12µm Nickel-Chrome wires (Goodfellow, Kanthal Palm Coast, Florida, USA) in a 28 gauge metal tube. One side of each electrode is connected with a signal connection through an electrode interface board (Neuralynx, Montana, USA). The other end of the bundle is cut by a sharp fine scissors to ensure a good shape of the tip. The tips of the electrodes are gold-plated to lower their impedance (gold solution, Sifco) and dye-coated to show the position of electrodes in the motor cortex and in the cerebellum.

3 Surgery and implantation of the electrodes

After a rat learned the task, one headstage including 1-4 movable commercial quartz tetrodes (Thomas Recording) and one movable reference electrode are fixed in the skull above the surface of the paramedian lobule of the cerebellum and sometimes a bundle of wire electrode is also implanted in the skull above the motor cortex by a standard surgery. During the surgery, the rats are maintained anesthetized during the whole experiment with a mixture of isoflurance (0.5~2%) and O_2. Animals are mounted in a stereotaxic frame (David Kopf Instruments, CA) with bars in the ears and mouth. Heart rate and blood O_2 concentration are monitored to adjust the level of anesthesia. A heating device controlled by rectal temperature is used to maintain the rat at physiological core temperature. Before incision of the scalp, 3% lidocaine is injected subcutaneously at the site of incision. The skull and dura over the para-vermian part of paramedian lobule (3 mm lateral to the midline and 4 mm posterior to the lambda) in the hemisphere ipsolateral to the preferred paw are removed using a dental drill, a curved syringe needle, and fine forceps. Subdural meninges are gently removed where the electodes are to be advanced. A headstage is implanted and fixed in the skull just above the cerebellar cortex by dental cement. A bundle of 16 Nickel-Chrome wires is in some cases also implanted into the primary somatomotor cortex (the center is Lateral 3 mm, and Bregma 3.5 mm) in the hemisphere contralateral to the preferred paw during the surgery. The wounds are carefully stitched and spread with fusidic acid cream (bacteriostatic antibiotic). After the surgery, the animals are carefully

taken care of and are allowed to recover totally before recoding.

4 In vivo recording

After the rat has fully recovered from the surgery (the weight of the rat rose and stayed stable; and the rat could explore actively without staggering), it is replaced on the training and recording table. A recording system is connected to the electrodes implanted in the rat for recording from the cerebellum and the motor cortex. We advance tetrodes until cell signals are obtained from the Purkinje cell layer, the granular layer or deep cerebellar nuclei. Once the tetrodes are near or in a layer, they are adjusted more carefully to optimize the signal/noise ratio of the extracellular cell spikes. The activities are continuously monitored through loudspeakers and displayed on a computer screen monitor. Once the signals are stable, they are first filtered 0.1 Hz to 8 kHz with a Butterworth filter, then differentially amplified, sampled at 25 kHz. Filtered and amplified signals are recorded for several minutes when the rat is sleeping, actively exploring or performing a grasp task, and stored to disk for off-line analysis. When the rat is performing the reach-to-grasp task, a camera (Allied Vision Technologie, Germany), which is positioned orthogonally to the table such that the animal's behavior is filmed from the front, captures the movement of the rat with a frame rate of 50 Hz.

5 Recording system

Real-time signals are captured by Tucker-Davis Technologies (TDT) system, which includes two chronic splice connectors, a motorized commutator, two preamplifiers, a base station (including five digital signal processors (DSPs)), a camera, a monitor speaker and a computer (Fig).

Electrical signals from the cerebellum and the motor cortex are conveyed to two preamplifiers respectively through a chronic splice connector which includes 16 channels and links to a motorized commutator. The motorized commutator is used for freely, behaving animals. Sensors on the commutator continuously measure the torque applied to the headstage cable, and spin a motor to replace the connector and eliminate the torque at the animal's end of the cable. Thus, when the animals are freely-moving during observation and recording, the cables are not twisted by motion. The 16 channels of analog signal are then amplified and digitized at a 24,414 kHz

sampling rate. The amplified digital signal is sent to the base station via a noiseless fiber optic connector. The base station is a multiple DSP device. In our case, the base station collects data from two preamplifiers, each digitizing 16 channels. The multiprocessor architecture is equipped with five DSPs and provides simultaneous ~25 kHz sampling on every channel with a 16-bit precision. The DSPs include one master and four auxiliary DSP. Each DSP communicates with an internal bus to send and receive information from the I/O controller and the shared memory. The master DSP acts as the main data interface between the zBus (host PC) and the multi-DSP environment. The base station is also linked to a camera (Allied Vision Technologie, Germany) and a monitor speaker so that we can monitor the electrophysiological recordings and record the video at the same time. The software triggers each frame of the camera and thus allow synchronizing the recording electrical signals with the video. Finally, the software platform allows controlling the hardware and the visual interface makes it flexible to observe and record the data in real-time.

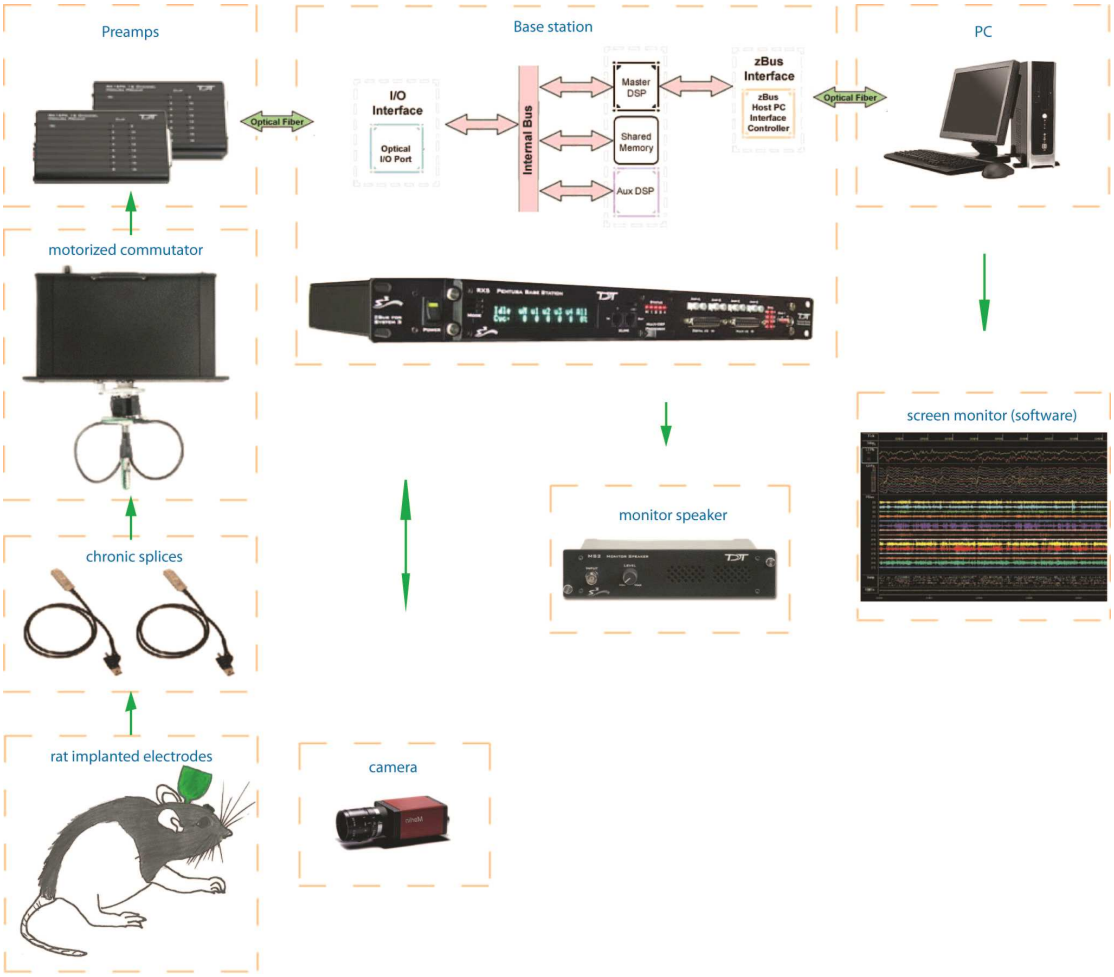

Figure 8.1: Recording system

6 Data analysis

6.1 Single-unit isolation (clustering)

Continuous recordings are first high-pass filtered at 300 Hz with a Butterworth filter before thresholding (typically at 80μV). The transformation from raw data of extracellular recordings into spike train estimates is the operation of spike sorting. There is currently no 'standard' method to perform spike sorting, despite an extensive literature (e.g., Brown et al., 2004; Fee et al., 1996; Franke et al., 2010; Kim and Kim, 2003; reviews in Lewicki, 1998; Pouzat et al., 2004; Shoham et al., 2003; Takahashi et al., 2003; Vargas-Irwin and Donoghue, 2007), and a number of methods supplemented in commercial and free softwares: e.g., klusters (http://klusters.sourceforge.net/, Hazan et al., 2006), mclust (A. D. Redish, http://redishlab.neuroscience.umn.edu/MClust/MClust.html), KlustaKwik (K. Harris, http://klustakwik.sourceforge.net/), SpikeOmatic (e.g. Delescluse and Pouzat, 2006). In our lab, single-unit spikes are isolated off-line using manual clustering ('xclust', M.A. Wilson), mostly using peak amplitudes recorded from the four channels of the tetrodes. Usually, three to seven units could be isolated per tetrode and the quality of isolation is would be verified by testing the distribution of inter-spike intervals and the existence of a 1-2 ms refractory period devoid of spikes in the auto-correlogram to reduce miss-clustering (Gao et al., 2011). However, this procedure can't allow the sorting of overlapping waveforms arising from coincident spikes from two or more different units, i.e., within an interval of less than 0.5 ms (the width of the Purkinje cells spikes being less than 0.3 ms). Once the timestamps of spikes for all units have been obtained, further analysis is performed with GNU R (R Development Core Team, 2004) and Matlab.

6.2 video analysis

When rats are performing the reach-to-grasp task, a camera (Allied Vision Technologie, Germany) in front of the training/recording table captures the movement information of rats with a rate of 50 Hz. Each frame of the video recoding is synchronized with the neurophysiological signals. The

video is analyzed off-line afterwards frame by frame. Three components of movement in each successful grasp trial are manually scored: lift (the inception of lifting the forepaw), cover (rotation around the wrist and the digits are opened for grasping) and grasp (closing the digits around the food while flexing the wrist to lift the food). Although up to 10 components may be distinguished during the movement, we limited our analysis to the three most obvious steps, other components being difficult to time accurately too variable across animals.

7 Histology

After the behavior and electrophysiological experiments, the rats are killed by overdose of anesthesia. The brain is carefully taken out and fixed in 4% formalin solution. After the tissue is totally fixed, it is sliced sagittally with a 30-40 um thickness using a microtome slicer (Leica VT1000 S), then dehydrated, cleared, and infiltrated with wax. The embedded slices are inspected in fluorescence microscopy (Leica DM LB). Fluorescent signals from the dye applied on the electrodes allow reconstructing the trajectory of the tetrodes in the cerebellum and the position of wire electrodes of the bundle in the motor cortex.

Third part
Results

First article

Journal of Physiology - Paris xxx (2011) xxx–xxx

Contents lists available at SciVerse ScienceDirect

Journal of Physiology - Paris

journal homepage: www.elsevier.com/locate/jphysparis

Tetrode recordings in the cerebellar cortex

HongYing Gao [a,b,c,d,e], Camille de Solages [a,b,c,d], Clément Lena [a,b,c,d,*]

[a] Institut de Biologie de l'Ecole Normale Supérieure, IBENS, Paris F-75005, France
[b] CNRS, UMR 8197, Paris F-75005, France
[c] Inserm, U1024, Paris F-75005, France
[d] Ecole Normale Supérieure, Paris F-75005, France
[e] Institutes for Advanced Interdisciplinary Research, East China Normal University, Shanghai 200062, China

ARTICLE INFO

Article history:
Available online xxxx

Keywords:
Cerebellum
Tetrode
In vivo recording
Purkinje cells
Synchrony

ABSTRACT

Multi-unit recordings with tetrodes have been used in brain studies for many years, but surprisingly, scarcely in the cerebellum. The cerebellum is subdivided in multiple small functional zones. Understanding the proper features of the cerebellar computations requires a characterization of neuronal activity within each area. By allowing simultaneous recordings of neighboring cells, tetrodes provide a helpful technique to study the dynamics of the cerebellar local networks. Here, we discuss experimental configurations to optimize such recordings and demonstrate their use in the different layers of the cerebellar cortex. We show that tetrodes can also be used to perform simultaneous recordings from neighboring units in freely moving rats using a custom-made drive, thus permitting studies of cerebellar network dynamics in a large variety of behavioral conditions.

© 2011 Elsevier Ltd. All rights reserved.

1. Introduction

The cerebellar cortex consists of three layers and is divided into many functional zones. Most incoming information reaches the cortex via mossy fibers terminating in the granule layer, and is then relayed to the output layer formed by the Purkinje cells. Granule cell axons, referred to as parallel fibers, ascend to the molecular layer and synapse onto Purkinje cell dendrites. This relatively simple organization is repeated throughout the cerebellar cortex, concealing the topography of the functional organization of the cerebellum. Indeed, the cerebellar cortex is divided into multiple functional zones (Apps and Hawkes, 2009). These zones may be evidenced by molecular markers, the zebrins (Brochu et al., 1990), whose expression is organized in roughly parasagittal bands perpendicular to the parallel fibers and results from developmental processes (Larouche and Hawkes, 2006). Since parallel fibers propagate the information across the boundaries of the zones (e.g. Gao et al., 2006), the zebrin zonation might not reflect functional divisions. However, the bands receive distinct inputs from mossy fibers and specific input from climbing fibers to the Purkinje cells that, in turn, project to specific areas of the deep cerebellar nuclei (Buisseret-Delmas and Angaut, 1993; Sugihara and Shinoda, 2004; Voogd and Bigaré, 1980; Voogd and Glickstein, 1998; Voogd and Ruigrok, 2004). Studies of sensory receptive fields suggest an even finer functional organization of the inputs and outputs of the cerebellar cortex (Bower and Woolston, 1983; Cohen and Yarom, 1998; review in Garwicz et al., 1998). The functional importance of the parasagittal zonation of the cerebellar cortex is also reflected by the temporal organization of inputs from the inferior olive. These inputs take the form of unitary climbing fibers contacting the Purkinje cells and their activation produces an extremely powerful excitation that drives complex spikes in these cells. Multiple single-electrode (Lang et al., 1999; Lou and Bloedel, 1992; Sasaki et al., 1989) and optical (Ozden et al., 2008; Schultz et al., 2009) recordings have shown a strong synchrony of activation of climbing fibers in narrow parasagittal bands which correspond to zebrin bands (Sugihara et al., 2007). This circumscribed functional topography of the cerebellar extrinsic connectivity is complemented by the stronger efficiency of local granule cells to excite neighboring Purkinje cells (Isope and Barbour, 2002) and by the structure of the intrinsic inhibition, characterized by a relatively limited spatial extension of the territory innervated by most inhibitory interneurons (e.g. Dizon and Khodakhah, 2011) and a compartmentalization of local inhibition by the zebrin zones (Gao et al., 2006; Ozden et al., 2009; Sillitoe et al., 2008). Specific cerebellar computations are thus likely to be operated in small functional zones within the network, and are thus best analyzed by studying the dynamics of neuronal activity in local cerebellar network. *In vivo* recordings of neighboring cerebellar cells with pairs of electrodes are difficult experiments in

* Corresponding author at: Institut de Biologie de l'Ecole Normale Supérieure, IBENS, 46 rue d'Ulm, Paris F-75005, France.
E-mail address: lena@biologie.ens.fr (C. Lena).

0928-4257/$ - see front matter © 2011 Elsevier Ltd. All rights reserved.
doi:10.1016/j.jphysparis.2011.10.005

anesthetized/decerebrate preparations (Bell and Grimm, 1969; Ebner and Bloedel, 1981; Shin and De Schutter, 2006), and even harder in awake animals. The combination of *in vitro* and modeling approaches of the local networks provides an alternate approach, which has brought much insight (e.g. Dugué et al., 2009; Maex and De Schutter, 1998; Medina et al., 2000; Solinas et al., 2007; Vervaeke et al., 2010); however further understanding the cerebellar network dynamics will require studying experimentally how neighboring cells, which are likely to collaborate in signal processing, may coordinate their activity to collectively encode information (Thier et al., 2000).

In the last two decades, multi-contact electrode recordings have proved a key technique to study population activity in the brain. These electrodes allow the sampling of extracellular potential at multiple neighboring points in space. The contacts of the electrodes may be spread around an axis (Gray et al., 1995) or arranged linearly (e.g. Bragin et al., 2000; Csicsvari et al., 2003), the former being particularly efficient for recording simultaneously multiple neighboring cells. In configurations where the distance between the multiple contacts of the electrodes corresponds roughly to the distance over which the extracellular spike decays, the extracellular spikes of individual cells are recorded by several channels of the electrode with a unique distribution of amplitudes over the channels: largest amplitude for the contact closest to the cell and smallest amplitude for the farthest. The relative amplitude over the channels thus provides a signature of the physical position of the cell relative to the different contacts of the electrode and allows discrimination of spikes from different cells. While multi-contact electrodes, and particularly tetrodes, have been used intensively to study the patterns of activity in some brain structures such as the hippocampus (e.g. Wilson and McNaughton, 1993) or neocortex (e.g. Jung et al., 1998), other neural structures like the cerebellum have been scarcely investigated with such electrodes.

Linear multi-site electrode (Delescluse and Pouzat, 2006; de Solages et al., 2008; Tahon et al., 2011) and tetrode (de Solages et al., 2008; Halverson et al., 2010; Soteropoulos and Baker, 2008) recordings have been recently introduced in the study of cerebellar function. Linear electrodes are well suited to identify current sources and sinks in a laminar structure such as the cerebellum. Tetrode recordings improve the yield of experiments, and allow studying the coordination of discharge between neighboring neurons. They have proved helpful in demonstrating that the fast cerebellar oscillations, first reported by Adrian (1935), arise from a Purkinje cell population oscillation notably associated with short-term (~5 ms) correlations between neighboring Purkinje cells (de Solages et al., 2008). Here, we show that tetrodes can be used to record in the other layers of the cerebellar cortex, and that they can be adapted to record neuronal activity from freely-moving animals. We discuss the benefits and limitations of these electrodes and finally briefly discuss the relevance of such recordings for the study of neuronal firing coordination in the Purkinje cell layer.

2. Cerebellar recordings with tetrodes

2.1. Methods

2.1.1. Drive and electrodes

We manufactured an implantable, stable and light-weight tetrode headstage which holds multiple microdrives, holding a reference and one to four quartz tetrodes. Each microdrive has a micro-machined backbone holding at its top and bottom a threaded rod that is allowed to rotate freely. A small cubic screw is mounted on the rod and translates when the rod is turned. The screw carries a stainless steel tube to which the tetrode is attached. A 30 gauge quartz tube is used to guide each electrode to the brain and the upper part of the tube is beveled to facilitate the insertion of the electrode without damaging its tip. The free ends of the tetrodes are connected to the pins of connector with silver paint and secured with heat shrink tubing. The whole drive is enveloped by a conic piece of cardboard covered with aluminum foil connected to the ground to reduce the electromagnetic interference during the recordings.

Hand-made tetrodes are obtained by twisting four polymide-insulated 12 μm Nickel-Chrome wires (Goodfellow, Kanthal Palm Coast, Florida, USA). The four wires are fused together by heating, the bundle is cut with sharp fine scissors to ensure good shape of the tip. Quartz tetrodes are obtained from 4 platinum/tungsten-cores in a quartz rod, sculpted with a sharp tip (Thomas Recording Gmbh, Germany). Before recording, the tips of the tetrodes are cleaned (Microelectrode Tip Cleaner, Thomas Recording Gmbh) and gold-plated (gold solution, Sifco) to lower their impedance to 200–300 kΩ and improve the signal-to-noise ratio.

2.1.2. Surgery and recordings

The Experimental Procedures are conducted in conformity with institutional guidelines and in compliance with national and European laws and policies. After the induction of anesthesia with a ketamine-xylazine mixture, animals are mounted in a stereotaxic frame (David Kopf Instruments, CA) with bars in the ears and mouth and maintained anesthetized during the whole experiment with a mixture of isoflurance (0.5–1.5%) and O_2. Heart rate and blood O_2 concentration are monitored to adjust the level of anesthesia. A heating device, controlled by rectal temperature, is used to maintain the rat at physiological temperature. Before the incision of the scalp, 3% lidocaine is injected subcutaneously at the site of incision. The skull and dura over the vermian part of lobule V and VI are removed using a dental drill, a curved syringe needle, and fine forceps. Subdural meninges are gently removed at the location the electodes are to be lowered. For experiments in anesthetized animals, a commercial quartz tetrode is inserted in the cerebellar cortex and advanced through different layers. The surface of the cerebellum is maintained moist with a saline solution. For experiments in awake rodents, a headstage is implanted and fixed in the skull just above the cerebellar cortex with dental cement. The wound is carefully sutured and covered with fusidic acid cream (bacteriostatic antibiotic). After surgery, animals are allowed to recover several days before recording. Extracellular potentials are acquired with a Tucker Davis Technologies system 3. During tetrode adjustment and recordings, the activities of cerebellar neurons are continuously monitored through loudspeakers and displayed on a computer screen monitor.

2.1.3. Data analysis

To isolate spikes, continuous wide-band extracellular recordings are first filtered off-line with a 2-pole Butterworth 500 Hz high pass filter. Spikes are then extracted by thresholding the filtered trace and the main parameters of their wave form extracted (width and amplitude on the 4 channels). The data are hand-clustered by polygon-cutting in 2-dimension projections of the parameter space using Xclust (Matt Wilson, MIT). The quality of clustering is evaluated by inspecting the auto-correlograms of the units. The discrimination of complex spikes is performed as in de Solages et al. (2008) by searching spikes followed by large stereotyped positive wave, and the shared cellular origin of complex spike and simple spikes is verified by inspection of their cross-correlogram.

Please cite this article in press as: Gao, H., et al. Tetrode recordings in the cerebellar cortex. J. Physiol. (2011), doi:10.1016/j.jphysparis.2011.10.005

2.2. Results

2.2.1. Comparison of tetrode types

Wire tetrodes are inexpensive and well suited for the study of dense, layered areas such as the hippocampal pyramidal cell layer. In the cerebellum, these electrodes should also be well suited for recordings in the Purkinje cell layer (Fig. 1A–C); however, we found that the penetration of these electrodes in the cerebellar cortex is often difficult and damaging (substantial neuronal death is generated when electrodes are moved), and the fine adjustment of the position of these electrodes is difficult to perform. Moreover, the amplitude of spikes tend to be similar on the four channels of the electrodes indicating an insufficient distance between the four recording sites and often rendering the separation of spikes arduous. This problem could be circumvented by using wires with larger diameter, but at the cost of even worse penetration properties. An alternative is to use pointed quartz tetrodes. The tetraedric position of the contacts on these electrodes is optimal for triangulating the spikes from sources distributed in three dimensions. These electrodes have a much easier penetration in the brain and provide satisfactory separation of cells in the Purkinje cell layer (Fig. 1D–F), often allowing discrimination of more than 3 cells. When recorded on the four channels of the tetrode, the waveform of the initial spike of the complex spikes is very similar to that of the simple spikes of individual Purkinje cells, so it is easy to attribute these two sorts of spikes to the same unit in spike sorting (see Section 3.2 below). Complex spikes recorded from Purkinje cells are multiphasic events starting with a (normal) negative spike followed by a positive wave with multiple negative spikelets that differ in number and shape across cells (Fig. 2); it is therefore possible to distinguish complex spikes from simple spikes by searching these features after the occurrence of each spike (de Solages et al., 2008).

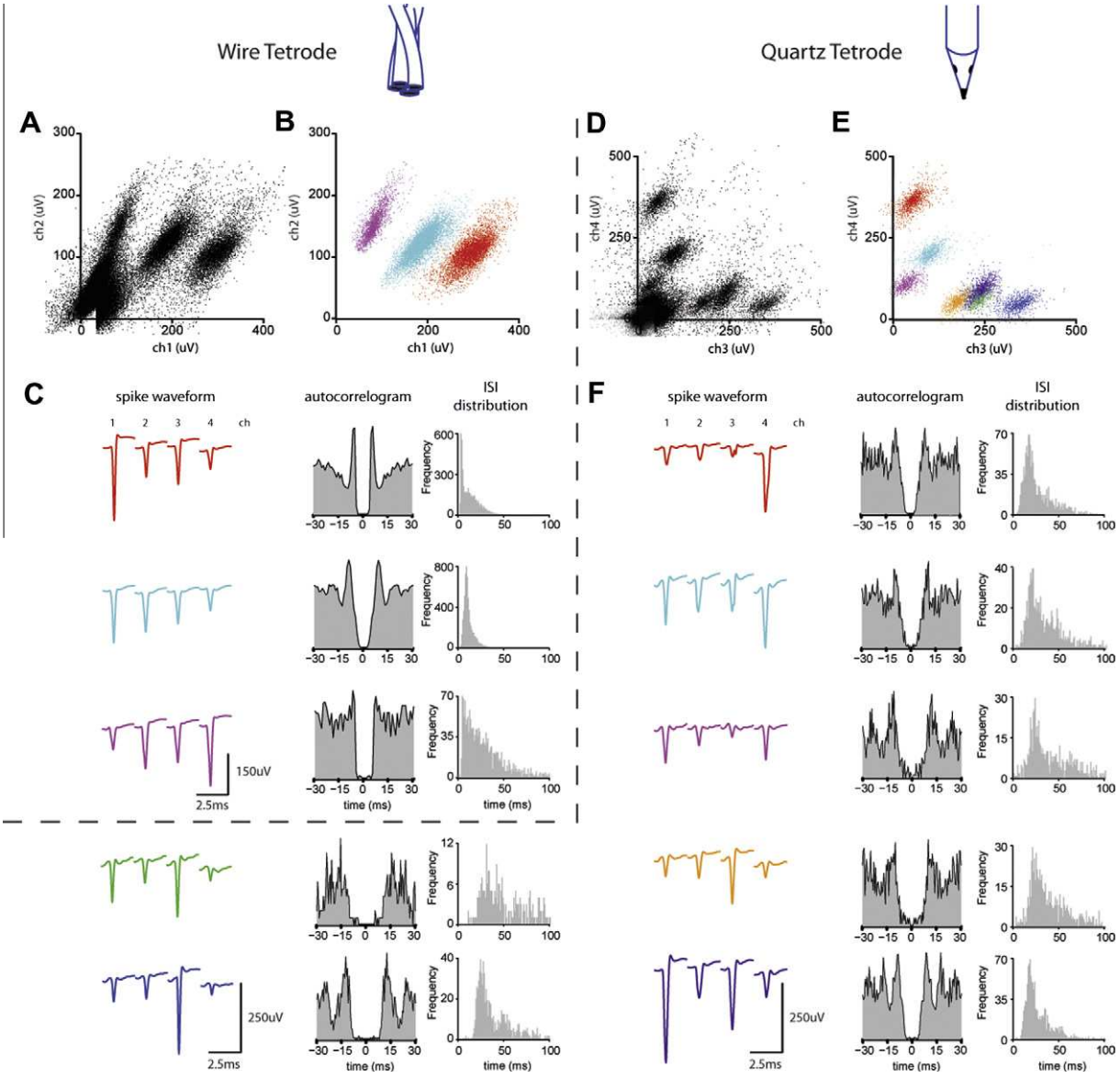

Fig. 1. Comparison of isolation of units recorded in the Purkinje cell layer in anesthetized rats with a hand-made tetrode and a commercial tetrode (Thomas recording). (A–C) Recording with a hand-made tetrode where 3 units were isolated. (A) Plot of amplitude of unsorted spikes on a pair of channels. (B) Same plot after sorting, 3 different units (shown in different colors) were isolated using the amplitudes of signals recorded from the 4 channels of the same tetrode. (C) Average unfiltered waveforms, auto-correlograms and ISI distributions of the 3 different cells. (D–F) Recording with a tetrode with a sharp tip. 7 units were isolated. (D) Plot of unsorted spikes. (E) Same plot after sorting, the different units are plotted in different colors. (F) Average unfiltered waveforms, auto-correlograms and ISI distributions of the 7 cells.

Please cite this article in press as: Gao, H., et al. Tetrode recordings in the cerebellar cortex. J. Physiol. (2011), doi:10.1016/j.jphysparis.2011.10.005

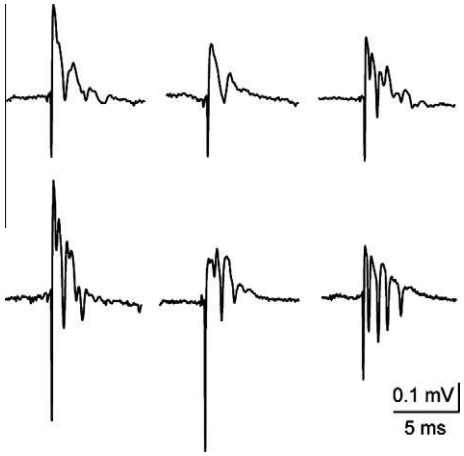

Fig. 2. Inter-cellular variability of complex spikes waveform. Plots from the average unfiltered waveforms recorded from six different Purkinje cells in anesthetized rats. The variability may result from many factors including differences in dendritic geometry and distribution of membrane currents across cells, and differences in position of the recording site relative to the dendrites.

2.2.2. Tetrode recordings in the layers of the cerebellar cortex

The quartz electrodes may also be used to record in the other layers of the cerebellar cortex. In the molecular layer, slow-firing units (presumably molecular-layer interneurons) are sometimes encountered but the extracellular spikes are often small and difficult to discriminate from the background noise. The most distinctive feature of molecular layer recordings is the presence of transient negative waves, 'fat spikes', lasting more than 1 ms and occurring at low frequency (~1 Hz) (Fig. 3A–E). This activity is best seen in the bottom of the molecular layer, close to the Purkinje cell layer, and may be easily interpreted as the extracellular signature of complex spikes produced by the climbing fiber synaptic inputs to the Purkinje cell dendrites. Indeed, when one contact of the tetrode is located in the molecular layer and another is located in the Purkinje cell layer (and these contacts aligned with the main axis of the Purkinje cells), the complex spikes recorded in the Purkinje cell layer are showing up as a 'fat spike' in the molecular layer (Fig. 3D–G). The negative wave of the 'fat spikes' mirrors the initial positive wave observed in the Purkinje cell layer. Such a topography of extracellular signal is consistent with the presence of a dipole of current sinks and sources in the dendrites and soma respectively, corresponding to the dendritic inward currents (due to glutamate receptor activation and/or subsequent calcium currents caused by the climbing fiber input) and the subsequent depolarization of the soma.

In the granule cell layer, the recorded cells exhibit in general a low firing rate (interspike interval larger than 30 ms) and no bursts in resting conditions (Fig. 3K–M). These cells are likely to be Golgi cells (Barmack and Yakhnitsa, 2008; Edgley and Lidierth, 1987; Holtzman et al., 2006; Miles et al., 1980; Prsa et al., 2009; van Kan et al., 1993; Vos et al., 1999b). The average (unfiltered) waveform of these cells is clearly multiphasic, with the main negative wave followed by a transient positive wave (Fig. 3L). The spikes

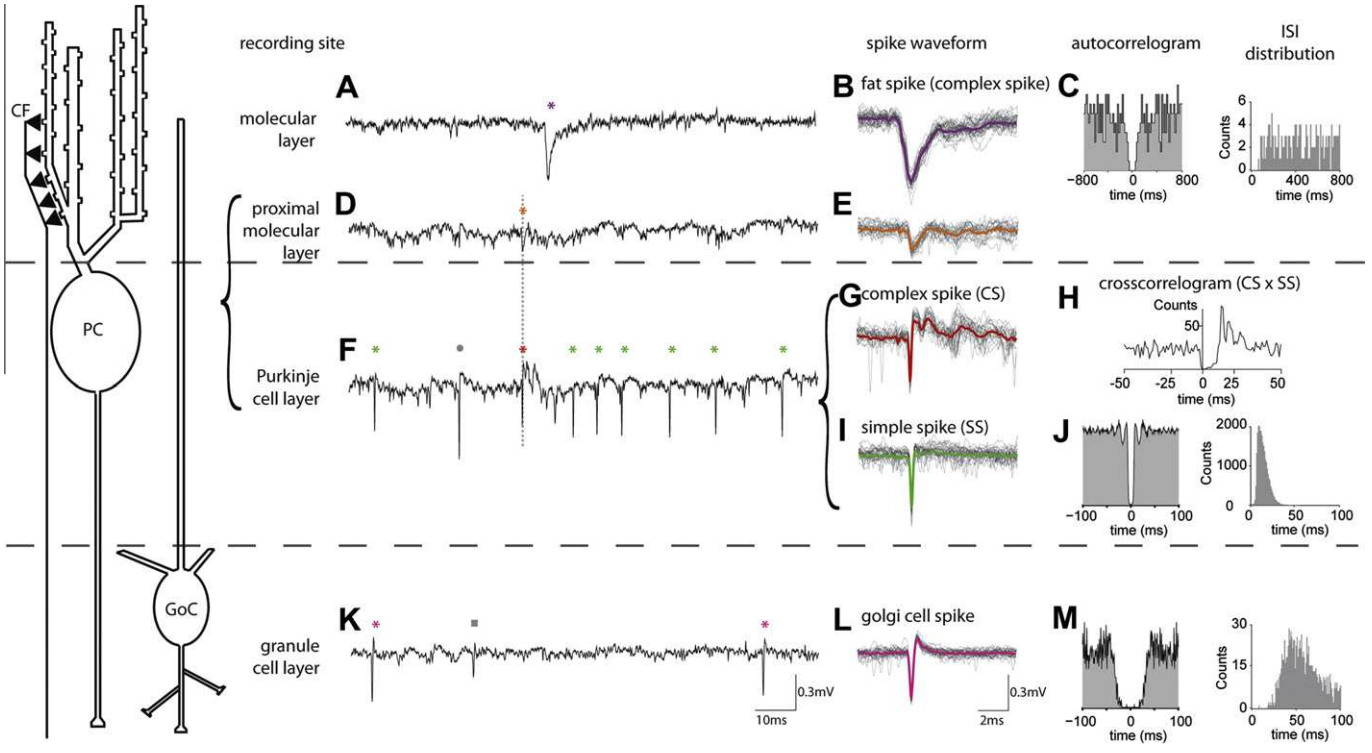

Fig. 3. Example of recordings from different cell types in the layers of the cerebellar cortex. (A) Raw trace of continuous recording from the molecular layer. (B) 30 successive (gray) and average (purple) unfiltered waveforms of 'fat spikes' (complex spikes recorded in the molecular layer). (C) Auto-correlogram and ISI distribution of the 'fat spikes'. (D, F) Simultaneous recording from 2 channels of one tetrode in the proximal molecular layer and the Purkinje cell layer respectively. The complex spike shows up as a 'fat spike' (orange star) in the molecular layer, while it has the classical shape of a complex spike (red star) in the Purkinje cell layer. The 'fat spikes' in D and in A are from two different cells and are not recorded simultaneously. The simple spikes from two units (green star and gray circle) are observed in the Purkinje cell layer. Average and 30 individual unfiltered waveforms of 'fat spikes' (E), complex spikes (G) and simple spikes of one Purkinje cell (I) are shown aside. (H) Cross-correlogram of complex spikes and simple spikes, showing a pause of simple spikes firing after the occurrence of complex spikes. (J) Auto-correlogram and ISI distribution of simple spikes of one Purkinje cell. (K) Raw trace of continuous recording from granule cell layer. Spikes from 2 different cells (pink star and gray square) could be observed. (L) Average and 30 successive unfiltered waveforms of spikes from one Golgi cell (pink) recorded in molecular layer. (M) Auto-correlogram and ISI distribution of the Golgi cell spikes. Braces indicate simultaneous recordings of the traces plotted. All traces are from anesthetized animals. PC: Purkinje cell. CF: climing fiber. GoC: Golgi cell.

Please cite this article in press as: Gao, H., et al. Tetrode recordings in the cerebellar cortex. J. Physiol. (2011), doi:10.1016/j.jphysparis.2011.10.005

are sometimes followed by a small (~10–20 uV) slow negative wave with a rapid decay (tau ~1–2 ms), which could be an extracellular signature of the synaptic currents produced in the postsynaptic targets by the firing of the Golgi cell, as has been reported in other brain structures (e.g. Csicsvari et al., 1999). Multiple Golgi cells may occasionally be recorded from the same tetrode (Fig. 3K). Juxtacellular recordings in the granule cell layer have allowed recordings from granule cells, unipolar-brush cells and mossy-fibers (e.g. Barmack and Yakhnitsa, 2008), which exhibit distinctive features, but we failed to record activity from these small cells with quartz tetrodes, possibly because of the large surface of their contacts. Such units are however occasionally encountered with classical wire tetrodes.

Finally, we also found that multiple units may easily be recorded simultaneously in the deep cerebellar nuclei.

2.2.3. Tetrode recordings in freely moving animals

So far, we have shown that quartz tetrodes may be used in anesthetized and head-fixed animals (de Solages et al., 2008), but it was unclear whether they could also be used in chronically implanted animals. Specifically, their stiffness might prevent them from behaving like 'floating electrodes' and thus preclude the stable recordings when the animal is moving. To test this, we mounted these electrodes on a simple implantable microdrive and recorded the cerebellar activity during free exploration (Fig. 4). We found that stable recordings of multiple units (Fig. 4E) could be obtained on a daily basis (although significant movement could take place across days). The main difference with recordings in anesthetized and resting animals was the presence, in all the layers of the cerebellar cortex, of an increased background activity that could not be resolved into single cells and that hindered the proper sorting of the smallest units. Nevertheless, the ability to record multiple units in awake animals opens the way for studies of local patterns of activity in the cerebellar cortex during behaviors.

3. Discussion

3.1. Data recording

Multi-channel extracellular recordings with tetrodes are nowadays relatively standard procedures, and may be accomplished with commercial setups. We found that recordings in the cerebellum generally do not require very specific alterations, except when neuronal activity is the highest (notably in the Purkinje cell layer). In this case, it may be preferable to record continuously the extracellular potential and perform off-line the filtering, the spike detection and sorting. This also prevents the introduction of unwanted

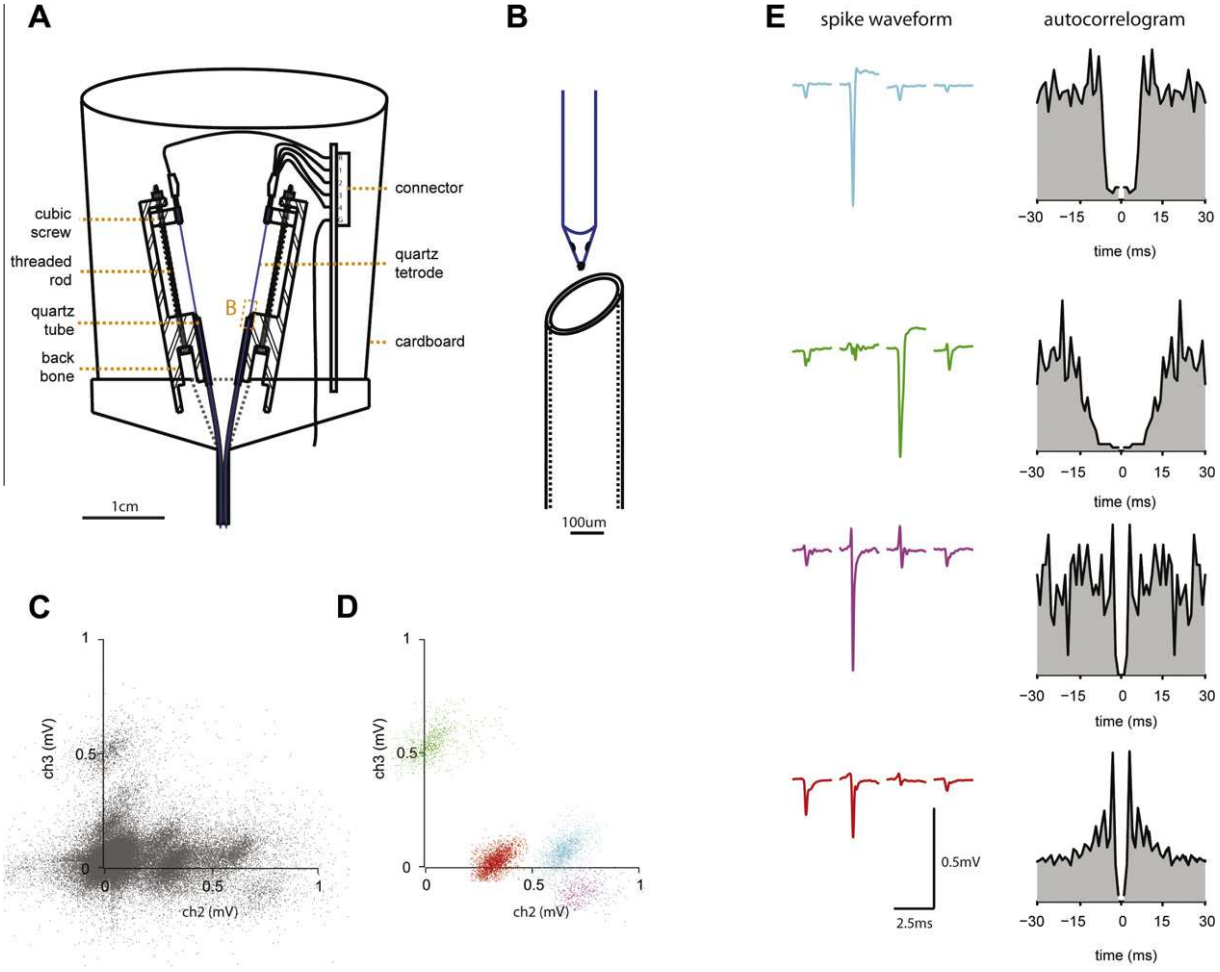

Fig. 4. Cells recorded in the Purkinje cell layer in freely-moving rat with a custom-made implantable headstage consisting of multiple microdrives controlling independently the position of quartz tetrodes and a reference electrode. (A) Diagram of the headstage. (B) The upper part of the 30 g quartz tube guiding the electrode is beveled in order to facilitate the insertion of the tetrode. (C–E) Recording in which 4 units were isolated in a freely-moving rat implanted with the headstage during free exploration. (C) Plot of unsorted spikes on a pair of channels. (D) Same plot after sorting, 4 different units (shown in different colors). (E) Average unfiltered waveforms and auto-correlograms of the 4 different cells.

Please cite this article in press as: Gao, H., et al. Tetrode recordings in the cerebellar cortex. J. Physiol. (2011), doi:10.1016/j.jphysparis.2011.10.005

distortions by the sub-optimal filters in use in on-line spike detection systems (Quian Quiroga, 2009).

The choice of the electrode influences the yield in cerebellar recordings. Tetrodes are usually metal electrodes and as such share the characteristics of their single-channel counterparts (Robinson, 1968): the uninsulated part of the electrode is coupled to the extracellular medium via a complex impedance with a pseudo-capacitive behavior (Lempka et al., 2011; McAdams et al., 1995); this coupling is normally linear for the range of signal amplitudes (below 1 mV) and bandwidth (1–10 kHz) used in extracellular recordings (Onaral and Schwan, 1982). Provided that the input impedance of the amplifier is high enough (G Ω range), and that the shunting capacitance of the electrodes is much smaller than the electrode impedance, these electrodes allow to record the average of the extracellular potential facing the uninsulated part of the electrode (Nelson et al., 2008). A large uninsulated surface will limit the thermal noise at the cost of a spatial filtering which may result in an increased multi-unit background if the density of neurons is high. Reciprocally, a small uninsulated surface will limit the spatial averaging at the cost of increasing the thermal noise due to the high impedance (Lempka et al., 2011). However, the deposition of a noble metal at the electrode tip allows lowering its impedance by an order of magnitude (e.g. Franks et al., 2005) without increasing the cross-section of the wire, therefore improving the signal-to-noise ratio (and eventually improving the biocompatibility in chronic recordings). Finally, the multicontact electrodes have one more important degree of freedom than their single channel counterparts: the spatial distribution of the contacts, which will determine the efficiency to triangulate and thus discriminate the spike sources (Mechler et al., 2011). While the linear and planar layout of contacts can be obtained with hand-crafted electrodes, they are less optimal than the tetrahedral layout of contacts from commercial tetrodes. Ultimately, each brain area/cell type may require adjustments to optimize the yield of recordings.

We compared two types of multi-site electrodes allowing the discrimination of multiple units in the cerebellar cortex *in vivo:* hand-made tetrodes (made of conventional tetrode wire: polymide-insulated 12 um Nichrome wire) are inexpensive and easily assembled (Nguyen et al., 2009); Alternatively, commercial quartz tetrodes – obtained from 4 platinum/tungsten-cores in a quartz rods, sculpted with a sharp tip – are more expensive but superior in the number of units simultaneously recorded that may be discriminated in the Purkinje cell layer and in the deep cerebellar nuclei. In our experiments, the 1 kHz impedance of each channel of the electrodes is above 1 MΩ, but is lowered to 200–300 kΩ by gold-plating before being used *in vivo*. These electrodes proved suitable to record Purkinje cells (simple and complex spikes), Golgi cells, and deep cerebellar nuclei units, but may be less optimal to record molecular layer interneurons, and even worse at recording granule cells and mossy fibers, possibly because the surface of the contact is too large to record very local spikes in the extracellular medium. Linear electrodes have provided satisfactory results for Purkinje cell recordings *in vitro* (Delescluse and Pouzat, 2006), but did not appear suitable for discriminating cellular activity in the Purkinje cell layer *in vivo* (de Solages et al., 2008); they might however be useful to explore the relation between neuronal activity/field potential across the layers *in vivo* (Lu et al., 2005).

To study neuronal activity in non-anesthetized preparations, recordings may also be performed in head-restrained or chronically implanted animals. In the latest case, the tetrodes are mounted on a drive attached to the skull. A number of drive designs for adjustable multi-electrode recordings are available in the literature (Jog et al., 2002; Kloosterman et al., 2009; Krüger, 1983; Szabó et al., 2001; Wilson and McNaughton, 1993). Quartz electrodes have a larger diameter than wire tetrodes, but we found that they may be mounted in similarly-designed drives and they allow stable recordings over single sessions.

3.2. Spike sorting

The transformation from raw data of extracellular recordings into spike train estimates is the operation of spike sorting. There is currently no 'standard' method to perform spike sorting, despite an extensive literature (e.g. Brown et al., 2004; Fee et al., 1996; Franke et al., 2010; Kim and Kim, 2003; reviews in Lewicki, 1998; Pouzat et al., 2004; Shoham et al., 2003; Takahashi et al., 2003; Vargas-Irwin and Donoghue, 2007), and a number of methods supplemented in commercial and free softwares: e.g. klusters (http://klusters.sourceforge.net/, Hazan et al., 2006), mclust (A.D. Redish, http://redishlab.neuroscience.umn.edu/MClust/MClust.html), KlustaKwik (K. Harris, http://klustakwik.sourceforge.net/), SpikeOmatic (e.g. Delescluse and Pouzat, 2006). The simplest sorting algorithms operate on the measurement of several parameters of the spikes (typically amplitude and shape parameters -but wavelet coefficients may be used instead (Letelier and Weber, 2000)-, possibly transformed via principal component analysis in order to reduce the dimensionality of the data). The sorting aims at identifying 'clusters' in the parameter space that represent groups of spikes that resemble one another and seem to emanate from the same physical position, which is reflected by the relative amplitude over the channels of the electrode. The timestamps of spikes belonging to each cluster are taken as estimates of spike trains from individual neurons. A good estimate of the spike train should thus be obtained from clusters of points well isolated in the parameter space and thus unlikely to contain misclassified spikes from neighboring clusters (de Solages et al., 2008). Specific measures have indeed been designed to assess the degree of cluster isolation (Joshua et al., 2007; Schmitzer-Torbert et al., 2005). An isolated cluster may still contain spikes from two units with very similar extracellular amplitude; however the distribution of the inter-spike intervals may then contain intervals shorter than the refractory period of individual neurons (if the two spikes belong to different units), and the proportion of such events may then be used to estimate the rate of contamination of the clusters (e.g. Harris et al., 2000). While this method allows tracking easily the presence of 'false positive' errors (extraneous spikes), the 'false negative' errors (missing spikes of a unit) are much harder to track.

Spikes will be missed by the clustering procedure if their waveform differs significantly from the spikes in the main cluster of the cell. In the cerebellum, this is the case of Purkinje cells that produce two sorts of spikes, the simple and complex spikes. We found that the initial negative spike of the complex spike may either be very similar to the simple spikes or, in some instances, form a cluster of slightly smaller spikes (de Solages et al., 2008); the complex spike is also often followed by a positive wave that is not observed after simple spikes. The complex spikes exhibit a typical crosscorrelogram with simple spikes which may be used to associate with the same unit these two types of spikes when they are found in two neighboring clusters. Another classical source of discrete changes in waveforms is bursts of action potentials, during which the waveform may change considerably (reduction of size, broadening) (e.g. Harris et al., 2000). The smallest spikes may be lost or, worse, attributed to another unit and therefore introduce spurious correlations between units (e.g. Quirk and Wilson, 1999). Specific algorithms that take into account the relation between the instantaneous firing rate and the waveform may however be used to circumvent this type of error in spike sorting (Delescluse and Pouzat, 2006; Pouzat et al., 2004). However, this source of error is less of a concern in the cerebellum than in cortical tissue where spike adaptation may be very prominent.

Please cite this article in press as: Gao, H., et al. Tetrode recordings in the cerebellar cortex. J. Physiol. (2011), doi:10.1016/j.jphysparis.2011.10.005

Another important cause of mis-clustering is the overlap of extracellular spikes due to near-synchronous firing of neighboring units. In the Purkinje cell layer, overlap is more likely to occur, as many units fire continuously at a high rate (~50 Hz), and is even further increased by the synchronization of spikes (Bell and Grimm, 1969; de Solages et al., 2008; Ebner and Bloedel, 1981). The overlap of spike waveforms will result in spikes of various amplitudes and shape depending on the individual waveforms and temporal offset between the spikes. Unless one unit has a much larger amplitude than the others, this overlap may lead to mis-clustering of the spikes (which will be omitted from the spike trains of the units that fired together). Since most of the energy of the spikes recorded in the cerebellum is concentrated in a short window of 200–300 μs, the overlap of waveforms should mostly take place for events spaced by this interval or less. The filtering procedure used to remove the low frequencies from the recordings may sensibly increase the temporal window of interaction of extracellular waveforms of spikes occurring at short delays. After filtering with the IIR (Infinite Impulse Response) high-pass filters commonly used (Butterworth or Bessel filters), the negative wave of the spike in the filtered extracellular potential will be followed by an exaggerated positive wave whose amplitude and duration will depend on the filter parameters. Lowering the order and cutoff of the high-pass filter will minimize these effects, so that the interaction between waveforms separated by more than 1 ms will be negligible (de Solages et al., 2008). Alternatively, wavelet filters may be used instead in order to improve the preservation of the extracellular waveforms (Wiltschko et al., 2008). Several algorithms already exist to handle overlapping spikes (Takahashi et al., 2003; Vargas-Irwin and Donoghue, 2007) but to our knowledge none have yet been applied to cerebellar recordings.

In summary, errors in spike sorting may degrade the quality of the estimation (in the statistical sense) of multiple spike trains, and therefore, the known sources of misclustering should be kept in mind while drawing any scientific conclusion from tetrode recordings.

3.3. Tetrode use for the study of coordinated activity in the cerebellum

The first benefit of tetrode recordings may just be to increase the yield of experiments, allowing recording more cells with fewer penetrations. However, since these electrodes allow recording simultaneously neighboring neurons, they may also help studying patterns of activity involving multiple cells. The most documented case of coordinated discharge in the cerebellum is the synchronization of complex spikes (Welsh et al., 1995, see Introduction above). This coordination is not the result from intra-cerebellar integration of information, but directly reflects the synchrony between the inferior olive cells that generate the complex spikes in Purkinje cells. Neighboring Purkinje cells are also known to exhibit synchronized simple spikes. Purkinje cell synchronization is likely to affect substantially the activity in the downstream structures, the deep cerebellar nuclei (Gauck and Jaeger, 2000), allowing to modulate the deep cerebellar cells at very short time scales. Synchronization of neighboring Purkinje cells has been noted in early recordings of pairs of cells in anesthetized and decerebrate animals (Bell and Grimm, 1969; Ebner and Bloedel, 1981). We have recently shown (de Solages et al., 2008) that some of this synchrony may result from a fast cerebellar oscillation (Adrian, 1935) arising from a population oscillation of Purkinje cells, associated with millisecond-scale synchrony and 5-ms delayed coordination of discharge (de Solages et al., 2008); such oscillations were indeed visible (but not noted) in the early studies, as pointed out by Isope et al. (2002). Shin and De Schutter also suggested a synchronizing role for local inhibitory neurons, since synchrony appeared associated with episodes of slowed firing rate of Purkinje cells (Shin and De Schutter, 2006). Since inhibitory neurons are known to contact multiple neighboring Purkinje cells, combined recordings with tetrodes of neighboring interneurons and Purkinje cells should help to analyze the effect of local inhibition on neighboring cells (de Solages and Léna, in preparation). Shared excitation could also favor synchronization (Jaeger, 2003) at time scales of the order of 10 ms. Such slightly broader synchrony is indeed observed between Purkinje cells (Bosman et al., 2010; De Zeeuw et al., 1997; Wise et al., 2010), mostly in cases where the cells also exhibit synchronized complex spikes indicating that they belong to a common functional ensemble. Broad coordination is also found between Golgi cells, and is likely due to shared excitatory inputs and gap junctions (Vos et al., 1999a). A much tighter synchrony at the sub-millisecond scale has also been observed along the parallel fiber axis in the cerebellar cortex during a reaching task (Heck et al., 2007). But, instead of single-unit spikes, only multi-unit signals were used in this study. Tetrode recordings in such experiments could indeed help identifying the units responsible of these correlations.

4. Conclusion

Tetrode recordings are relatively easy to set up in the cerebellum and, provided a few caveats are taken into account, they allow studying patterns of activity in groups of neighboring cells in the cerebellum. Synchronization is an activity pattern commonly observed in the cerebellar cortex, but its prominence between neighboring units underlines the importance of studying the cerebellar local networks. More elaborated forms of patterned activity have also been observed in the cerebellar cortex, with notably a number of normal and pathological rhythmic activities (reviews in Cheron et al., 2008; De Zeeuw et al., 2008). Multi-electrodes studies (e.g. Bosman et al., 2010; Cheron et al., 2004; Heck et al., 2007; Mostofi et al., 2010; Vos et al., 1999a; Welsh et al., 1995; Wise et al., 2010) and tetrode recordings (de Solages et al., 2008) have already proven the interest of recordings multiple cells at the same time to study patterned neuronal discharge. Bringing tetrode recordings to freely moving animals holds great promise in characterizing the contribution of these phenomena to cerebellar function and revealing their underlying mechanisms during a variety of behavioral conditions in awake animals.

Acknowledgements

This work was supported by ANR (08-SYSC-005-02 DALTPAC, 09-MNPS-038-01 Cecomod, 07-NEURO-025-03 Natacs), the Centre National de la Recherche Scientifique (CNRS), the Institut National de la Santé et de la Recherche Médicale (INSERM, C.L.), the Ecole Normale Supérieure (ENS), the Ministère des Affaires Etrangères (H. G.).

References

Adrian, E.D., 1935. Discharge frequencies in the cerebral and cerebellar cortex. Journal of Physiology – London 83, 32–33.

Apps, R., Hawkes, R., 2009. Cerebellar cortical organization: a one-map hypothesis. Nature Reviews Neuroscience 10, 670–681.

Barmack, N.H., Yakhnitsa, V., 2008. Functions of interneurons in mouse cerebellum. Journal of Neuroscience 28, 1140–1152.

Bell, C.C., Grimm, R.J., 1969. Discharge properties of Purkinje cells recorded on single and double microelectrodes. Journal of Neurophysiology 32, 1044–1055.

Bosman, L.W.J., Koekkoek, S.K.E., Shapiro, J., Rijken, B.F.M., Zandstra, F., Van de Ende, B., Owens, C.B., Potters, J.W., De Gruijl, J.R., Ruigrgok, T.J.H., De Zeeuw, C.I., 2010. Encoding of whisker input by cerebellar Purkinje cells. Journal of Physiology 588, 3757–3783.

Bower, J.M., Woolston, D.C., 1983. Congruence of spatial organization of tactile projections to granule cell and Purkinje cell layers of cerebellar hemispheres of the albino rat: vertical organization of cerebellar cortex. Journal of Neurophysiology 49, 745–766.

Bragin, A., Hetke, J., Wilson, C.L., Anderson, D.J., Engel, J., Buzsáki, G., 2000. Multiple site silicon-based probes for chronic recordings in freely moving rats: implantation, recording and histological verification. Journal of Neuroscience Methods 98, 77–82.

Brochu, G., Maler, L., Hawkes, R., 1990. Zebrin II: a polypeptide antigen expressed selectively by Purkinje cells reveals compartments in rat and fish cerebellum. Journal of Comparative Neurology 291, 538–552.

Brown, E.N., Kass, R.E., Mitra, P.P., 2004. Multiple neural spike train data analysis: state-of-the-art and future challenges. Nature Neuroscience 7, 456–461.

Buisseret-Delmas, C., Angaut, P., 1993. The cerebellar olivo-corticonuclear connections in the rat. Progress in Neurobiology 40, 63–87.

Cheron, G., Gall, D., Servais, L., Dan, B., Maex, R., Schiffmann, S.N., 2004. Inactivation of calcium-binding protein genes induces 160 Hz oscillations in the cerebellar cortex of alert mice. Journal of Neuroscience 24, 434–441.

Cheron, G., Servais, L., Dan, B., 2008. Cerebellar network plasticity: from genes to fast oscillation. Neuroscience 153, 1–19.

Cohen, D., Yarom, Y., 1998. Patches of synchronized activity in the cerebellar cortex evoked by mossy-fiber stimulation: questioning the role of parallel fibers. In: Proceedings of the National Academy of Sciences of the United States of America, vol. 95. pp. 15032–15036.

Csicsvari, J., Hirase, H., Czurkó, A., Mamiya, A., Buzsáki, G., 1999. Oscillatory coupling of hippocampal pyramidal cells and interneurons in the behaving rat. Journal of Neuroscience 19, 274–287.

Csicsvari, J., Henze, D.A., Jamieson, B., Harris, K.D., Sirota, A., Barthó, P., Wise, K.D., Buzsáki, G., 2003. Massively parallel recording of unit and local field potentials with silicon-based electrodes. Journal of Neurophysiology 90, 1314–1323.

de Solages, C., Léna, C., in preparation. Modulation of Purkinje cell firing and coordination by molecular layer interneurons in the cerebellar cortex in *vivo*.

de Solages, C., Szapiro, G., Brunel, N., Hakim, V., Isope, P., Buisseret, P., Rousseau, C., Barbour, B., Léna, C., 2008. High-frequency organization and synchrony of activity in the purkinje cell layer of the cerebellum. Neuron 58, 775–788.

De Zeeuw, C.I., Koekkoek, S.K., Wylie, D.R., Simpson, J.I., 1997. Association between dendritic lamellar bodies and complex spike synchrony in the olivocerebellar system. Journal of Neurophysiology 77, 1747–1758.

De Zeeuw, C.I., Hoebeek, F.E., Schonewille, M., 2008. Causes and consequences of oscillations in the cerebellar cortex. Neuron 58, 655–658.

Delescluse, M., Pouzat, C., 2006. Efficient spike-sorting of multi-state neurons using inter-spike intervals information. Journal of Neuroscience Methods 150, 16–29.

Dizon, M.J., Khodakhah, K., 2011. The role of interneurons in shaping purkinje cell responses in the cerebellar cortex. The Journal of neuroscience 31, 10463–10473.

Dugué, G.P., Brunel, N., Hakim, V., Schwartz, E., Chat, M., Lévesque, M., Courtemanche, R., Léna, C., Dieudonné, S., 2009. Electrical coupling mediates tunable low-frequency oscillations and resonance in the cerebellar Golgi cell network. Neuron 61, 126–139.

Ebner, T.J., Bloedel, J.R., 1981. Correlation between activity of Purkinje cells and its modification by natural peripheral stimuli. Journal of Neurophysiology 45, 948–961.

Edgley, S.A., Lidierth, M., 1987. The discharges of cerebellar Golgi cells during locomotion in the cat. Journal of Physiology 392, 315–332.

Fee, M.S., Mitra, P.P., Kleinfeld, D., 1996. Automatic sorting of multiple unit neuronal signals in the presence of anisotropic and non-Gaussian variability. Journal of Neuroscience Methods 69, 175–188.

Franke, F., Natora, M., Boucsein, C., Munk, M.H.J., Obermayer, K., 2010. An online spike detection and spike classification algorithm capable of instantaneous resolution of overlapping spikes. Journal of Computational Neuroscience 29, 127–148.

Franks, W., Schenker, I., Schmutz, P., Hierlemann, A., 2005. Impedance characterization and modeling of electrodes for biomedial applications. IEEE Transactions on Biomedical Engineering 52, 1295–1301.

Gao, W., Chen, G., Reinert, K.C., Ebner, T.J., 2006. Cerebellar cortical molecular layer inhibition is organized in parasagittal zones. Journal of Neuroscience 26, 8377–8387.

Garwicz, M., Ekerot, C.F., Jörntell, H., 1998. Organizational principles of cerebellar neuronal circuitry. News in Physiological Sciences 13, 26–32.

Gauck, V., Jaeger, D., 2000. The control of rate and timing of spikes in the deep cerebellar nuclei by inhibition. Journal of Neuroscience 20, 3006–3016.

Gray, C.M., Maldonado, P.E., Wilson, M., McNaughton, B., 1995. Tetrodes markedly improve the reliability and yield of multiple single-unit isolation from multi-unit recordings in cat striate cortex. Journal of Neuroscience Methods 63, 43–54.

Halverson, H.E., Lee, I., Freeman, J.H., 2010. Associative plasticity in the medial auditory thalamus and cerebellar interpositus nucleus during eyeblink conditioning. Journal of Neuroscience 30, 8787–8796.

Harris, K.D., Henze, D.A., Csicsvari, J., Hirase, H., Buzsáki, G., 2000. Accuracy of tetrode spike separation as determined by simultaneous intracellular and extracellular measurements. Journal of Neurophysiology 84, 401–414.

Hazan, L., Zugaro, M., Buzsáki, G., 2006. Klusters, NeuroScope, NDManager: a free software suite for neurophysiological data processing and visualization. Journal of Neuroscience Methods 155, 207–216.

Heck, D.H., Thach, W.T., Keating, J.G., 2007. On-beam synchrony in the cerebellum as the mechanism for the timing and coordination of movement. In: Proceedings of the National Academy of Sciences of the United States of America, vol. 104. pp. 7658–7663.

Holtzman, T., Rajapaksa, T., Mostofi, A., Edgley, S.A., 2006. Different responses of rat cerebellar Purkinje cells and Golgi cells evoked by widespread convergent sensory inputs. Journal of Physiology 574, 491–507.

Isope, P., Barbour, B., 2002. Temporal organization of activity in the cerebellar cortex: a manifesto for synchrony. Journal of Neuroscience 22, 9668–9678.

Isope, P., Dieudonné, S., Barbour, B., 2002. Temporal organization of activity in the cerebellar cortex: a manifesto for synchrony. Annals of the New York Academy of Sciences 978, 164–174.

Jaeger, D., 2003. No parallel fiber volleys in the cerebellar cortex: evidence from cross-correlation analysis between Purkinje cells in a computer model and in recordings from anesthetized rats. Journal of Computational Neuroscience 14, 311–327.

Jog, M.S., Connolly, C.I., Kubota, Y., Iyengar, D.R., Garrido, L., Harlan, R., Graybiel, A.M., 2002. Tetrode technology: advances in implantable hardware, neuroimaging, and data analysis techniques. Journal of Neuroscience Methods 117, 141–152.

Joshua, M., Elias, S., Levine, O., Bergman, H., 2007. Quantifying the isolation quality of extracellularly recorded action potentials. Journal of Neuroscience Methods 163, 267–282.

Jung, M.W., Qin, Y., McNaughton, B.L., Barnes, C.A., 1998. Firing characteristics of deep layer neurons in prefrontal cortex in rats performing spatial working memory tasks. Cerebral Cortex 8, 437–450.

Kan, P.L.V., Gibson, A.R., Houk, J.C., 1993. Movement-related inputs to intermediate cerebellum of the monkey. Journal of Neurophysiology 69, 74–94.

Kim, K.H., Kim, S.J., 2003. Method for unsupervised classification of multiunit neural signal recording under low signal-to-noise ratio. IEEE Transactions on Biomedical Engineering 50, 421–431.

Kloosterman, F., Davidson, T.J., Gomperts, S.N., Layton, S.P., Hale, G., Nguyen, D.P., Wilson, M.A., 2009. Micro-drive array for chronic in vivo recording: drive fabrication. Journal of Visualized Experiments 26, 2–5.

Krüger, J., 1983. Simultaneous individual recordings from many cerebral neurons: techniques and results. Reviews of Physiology, Biochemistry and Pharmacology 98, 177–233.

Lang, E.J., Sugihara, I., Welsh, J.P., Llinás, R., 1999. Patterns of spontaneous purkinje cell complex spike activity in the awake rat. Journal of Neuroscience 19, 2728–2739.

Larouche, M., Hawkes, R., 2006. From clusters to stripes: the developmental origins of adult cerebellar compartmentation. Cerebellum 5, 77–88.

Lempka, S.F., Johnson, M.D., Moffit, M.A., Otto, K.J., Ripke, D.R., McIntyre, C.C., 2011. Theoretical analysis of intracortical microelectrode recordings. Journal of Neural Engineering 8, 045006.

Letelier, J.C., Weber, P.P., 2000. Spike sorting based on discrete wavelet transform coefficients. Journal of Neuroscience Methods 101, 93–106.

Lewicki, M.S., 1998. A review of methods for spike sorting: the detection and classification of neural action potentials. Network: Computation in Neural Systems 9, 53–78.

Lou, J.S., Bloedel, J.R., 1992. Responses of sagittally aligned Purkinje cells during perturbed locomotion: synchronous activation of climbing fiber inputs. Journal of neurophysiology 68, 570–580.

Lu, H., Hartmann, M.J., Bower, J.M., 2005. Correlations between purkinje cell single-unit activity and simultaneously recorded field potentials in the immediately underlying granule cell layer. Journal of Neurophysiology 94, 1849–1860.

Maex, R., De Schutter, E., 1998. Synchronization of Golgi and granule cell firing in a detailed network model of the cerebellar granule cell layer. Journal of Neurophysiology 80, 2521–2537.

McAdams, E.T., Lackermeier, A., McLaughlin, J.A., Macken, D., Jossinet, J., 1995. The linear and nonlinear electrical-properties of the electrode–electrolyte interface. Biosensors and Bioelectronics 10, 67–74.

Mechler, F., Victor, J.D., Ohiorhenuan, I., Schmid, A.M., Hu, Q., 2011. Three-dimensional localization of neurons in cortical tetrode recordings. Journal of Neurophysiology 106, 828–848.

Medina, J.F., Garcia, K.S., Nores, W.L., Taylor, N.M., Mauk, M.D., 2000. Timing mechanisms in the cerebellum: testing predictions of a large-scale computer simulation. Journal of Neuroscience 20, 5516–5525.

Miles, F.A., Fuller, J.H., Braitman, D.J., Dow, B.M., 1980. Long-term adaptive changes in primate vestibuloocular reflex. III. Electrophysiological observations in flocculus of normal monkeys. Journal of Neurophysiology 43, 1437–1476.

Mostofi, A., Holtzman, T., Grout, A.S., Yeo, C.H., Edgley, S.A., 2010. Electrophysiological localization of eyeblink-related microzones in rabbit cerebellar cortex. Journal of Neuroscience 30, 8920–8934.

Nelson, M.J., Pouget, P., Nilsen, E.A., Patten, C.D., Schall, J.D., 2008. Review of signal distortion through metal microelectrode recording circuits and filters. Journal of Neuroscience Methods 169, 141–157.

Nguyen, D.P., Layton, S.P., Hale, G., Gomperts, S.N., Davidson, T.J., Kloosterman, F., Wilson, M.A., 2009. Micro-drive array for chronic in vivo recording: tetrode assembly. Journal of Visualized Experiments 26, 7–9.

Onaral, B., Schwan, H.P., 1982. Linear and non-linear properties of platinum electrode polarization part I. Frequency dependence at very low frequencies. Medical and Biological Engineering and Computing 20, 299–306.

Ozden, I., Lee, H.M., Sullivan, M.R., Wang, S.S.H., 2008. Identification and clustering of event patterns from in vivo multiphoton optical recordings of neuronal ensembles. Journal of Neurophysiology 100, 495–503.

Ozden, I., Sullivan, M.R., Lee, H.M., Wang, S.S.H., 2009. Reliable coding emerges from coactivation of climbing fibers in microbands of cerebellar Purkinje neurons. Journal of Neuroscience 29, 10463–10473.

Please cite this article in press as: Gao, H., et al. Tetrode recordings in the cerebellar cortex. J. Physiol. (2011), doi:10.1016/j.jphysparis.2011.10.005

Pouzat, C., Delescluse, M., Viot, P., Diebolt, J., 2004. Improved spike-sorting by modeling firing statistics and burst-dependent spike amplitude attenuation: a Markov chain Monte Carlo approach. Journal of Neurophysiology 91, 2910–2928.

Prsa, M., Dash, S., Catz, N., Dicke, P.W., Thier, P., 2009. Characteristics of responses of Golgi cells and mossy fibers to eye saccades and saccadic adaptation recorded from the posterior vermis of the cerebellum. Journal of Neuroscience 29, 250–262.

Quian Quiroga, R., 2009. What is the real shape of extracellular spikes? Journal of Neuroscience Methods 177, 194–198.

Quirk, M.C., Wilson, M.A., 1999. Interaction between spike waveform classification and temporal sequence detection. Journal of Neuroscience Methods 94, 41–52.

Robinson, D.A., 1968. The electrical properties of metal microelectrodes. Proceedings of IEEE 56, 1065–1071.

Sasaki, K., Bower, J.M., Llinás, R., 1989. Multiple Purkinje cell recording in rodent cerebellar cortex. European Journal of Neuroscience 1, 572–586.

Schmitzer-Torbert, N., Jackson, J., Henze, D., Harris, K., Redish., A.D., 2005. Quantitative measures of cluster quality for use in extracellular recordings. Neuroscience 131, 1–11.

Schultz, S., Kitamura, K., Post-Uiterweer, A., Krupic, J., Häusser, M., 2009. Spatial pattern coding of sensory information by climbing fiber-evoked calcium signals in networks of neighboring cerebellar Purkinje cells. Journal of Neuroscience 29, 8005–8015.

Shin, S.L., De Schutter, E., 2006. Dynamic synchronization of Purkinje cell simple spikes. Journal of Neurophysiology 96, 3485–3491.

Shoham, S., Fellows, M.R., Normann, R.A., 2003. Robust, automatic spike sorting using mixtures of multivariate t-distributions. Journal of Neuroscience Methods 127, 111–122.

Sillitoe, R.V., Chung, S.H., Fritschy, J.M., Hoy, M., Hawkes, R., 2008. Golgi cell dendrites are restricted by Purkinje cell stripe boundaries in the adult mouse cerebellar cortex. Journal of Neuroscience 28, 2820–2826.

Solinas, S., Forti, L., Cesana, E., Mapelli, J., De Schutter, E., D'Angelo, E., 2007. Fast-reset of pacemaking and theta-frequency resonance patterns in cerebellar Golgi cells: simulations of their impact in vivo. Frontiers in Cellular Neuroscience 1, 4.

Soteropoulos, D.S., Baker, S.N., 2008. Bilateral representation in the deep cerebellar nuclei. Journal of Physiology 586, 1117–1136.

Sugihara, I., Shinoda, Y., 2004. Molecular, topographic, and functional organization of the cerebellar cortex: a study with combined aldolase C and olivocerebellar labeling. Journal of Neuroscience 24, 8771–8785.

Sugihara, I., Marshall, S.P., Lang, E.J., 2007. Relationship of complex spike synchrony bands and climbing fiber projection determined by reference to aldolase C compartments in crus IIa of the rat cerebellar cortex. Journal of Comparative Neurology 501, 13–29.

Szabó, I., Czurkó, A., Csicsvari, J., Hirase, H., Leinekugel, X., Buzsáki, G., 2001. The application of printed circuit board technology for fabrication of multi-channel micro-drives. Journal of Neuroscience Methods 105, 105–110.

Tahon, K., Wijnants, M., De Schutter, E., Maex, R., 2011. Current source density correlates of cerebellar Golgi and Purkinje cell responses to tactile input. Journal of Neurophysiology 105, 1327–1341.

Takahashi, S., Anzai, Y., Sakurai, Y., 2003. Automatic sorting for multi-neuronal activity recorded with tetrodes in the presence of overlapping spikes. Journal of Neurophysiology 89, 2245–2258.

Thier, P., Dicke, P.W., Haas, R., Barash, S., 2000. Encoding of movement time by populations of cerebellar Purkinje cells. Nature 405, 72–76.

Vargas-Irwin, C., Donoghue, J.P., 2007. Automated spike sorting using density grid contour clustering and subtractive waveform decomposition. Journal of Neuroscience Methods 164, 1–18.

Vervaeke, K., Lorincz, A., Gleeson, P., Farinella, M., Nusser, Z., Silver, R.A., 2010. Rapid desynchronization of an electrically coupled interneuron network with sparse excitatory synaptic input. Neuron 67, 435–451.

Voogd, J., Bigaré, F., 1980. Topographical distribution of olivary and cortico-nuclear fibres in the cerebellum: a review. In: Courville, J., de Montigny, C., Lamarre, Y. (Eds.), The inferior olivary nucleus: anatomy and physiology. Raven Press, New York, pp. 207–234.

Voogd, J., Glickstein, M., 1998. The anatomy of the cerebellum. Trends in Neurosciences 21, 370–375.

Voogd, J., Ruigrok, T.J.H., 2004. The organization of the corticonuclear and olivocerebellar climbing fiber projections to the rat cerebellar vermis: the congruence of projection zones and the zebrin pattern. Journal of Neurocytology 33, 5–21.

Vos, B.P., Maex, R., Volny-Luraghi, A., De Schutter, E., 1999a. Parallel fibers synchronize spontaneous activity in cerebellar Golgi cells. Journal of Neuroscience 19, RC6.

Vos, B.P., Volny-Luraghi, A., De Schutter, E., 1999b. Cerebellar Golgi cells in the rat: receptive fields and timing of responses to facial stimulation. European Journal of Neuroscience 11, 2621–2634.

Welsh, J.P., Lang, E.J., Suglhara, I., Llinás, R., 1995. Dynamic organization of motor control within the olivocerebellar system. Nature 374, 453–457.

Wilson, M.A., McNaughton, B.L., 1993. Dynamics of the hippocampal ensemble code for space. Science 261, 1055–1058.

Wiltschko, A.B., Gage, G.J., Berke, J.D., 2008. Wavelet filtering before spike detection preserves waveform shape and enhances single-unit discrimination. Journal of Neuroscience Methods 173, 34–40.

Wise, A.K., Cerminara, N.L., Marple-Horvat, D.E., Apps, R., 2010. Mechanisms of synchronous activity in cerebellar Purkinje cells. Journal of Physiology 588, 2373–2390.

Please cite this article in press as: Gao, H., et al. Tetrode recordings in the cerebellar cortex. J. Physiol. (2011), doi:10.1016/j.jphysparis.2011.10.005

Second article

Title

Millisecond processing in the cerebellum

HongYing Gao [a,b,c,d,e], Christophe Pouzat [f], Clément Lena [a,b,c,d,*]

a Institut de Biologie de l'Ecole Normale Supérieure, IBENS, Paris F-75005, France

b CNRS, UMR 8197, Paris F-75005, France

c Inserm, U1024, Paris F-75005, France

d Ecole Normale Supérieure, Paris F-75005, France

e Institutes for Advanced Interdisciplinary Research, East China Normal University, Shanghai 200062, China

f Laboratoire de Physiologie Cérébrale, CNRS, UMR 8118, UFR biomédicale de l'Université René Descartes (Paris V), Paris-F75006, France

* corresponding author

Abstract

Voluntary movements require a precise temporal control of the motor system. The cerebellum is involved in the timing of complex actions. Here, we examine in the area of the cerebellar cortex controlling limb movement how the principal cells (the Purkinje cells) coordinate their firing during a fast forelimb motor action. Using simultaneous electrophysiological recordings of multiple individual cells, we show that neighboring Purkinje cells, which are known to converge in the cerebellar nuclei, exhibit correlated modulation of firing at short and long time scales. At the millisecond time scale, the correlated firing increases during motor execution but is maintained during sleep and active exploration embedded in high frequency oscillations. At longer time scales, neighboring cells only exhibit a mild preference for parallel modulation of their firing rate along behavior. Our results thus indicate that during a fast and complex movement, local assemblies of Purkinje cells form dynamically at short time scales and will produce very transient episodes of inhibition in the deep cerebellar nuclei.

Introduction

The motor system in mammals controls the execution of movement with an exquisite temporal precision at time scales of few tens of milliseconds or below (eye movements, throwing watts, speech production Ackermann). The cerebellum is a part of the motor system that plays an essential role in the accurate timing of movement (eyeblink medina, thatch). Its function has been proposed to rely on internal models of the movement elaborated on the knowledge of past experiences; these models allow to overcome the delays of the sensory feedback used to guide movement learning, and thus shape the motor command with an optimal temporal precision (Ito, 1970). The computational properties of the cerebellar circuit have been proposed to rely on its associative capabilities, notably by the Purkinje cells that select through supervised learning the relevant information in their hundred thousands of inputs carrying contextual sensory-motor information (Albus, 1971; Dean et al., 2002; Marr, 1969). Each Purkinje cell exerts only a small inhibition on the cerebellar nuclei neurons (Gauck and Jaeger, 2000), and the shaping of the motor command is obtained by the combination of the activity of many Purkinje (Medina and Lisberger, 2009; Thier et al., 2000) through the summation of their inputs on their target in the cerebellar nuclei.

Population of neurons that control individual motor units are not spread on the whole surface of the cerebellum but instead are topographically organized in narrow parasagittal bands (Ruigrok, 2011) that define 'microzones' (Apps and Hawkes, 2009), which may be considered as the minimal functional unit of the cerebellar cortex (Deanet al., 2010). This organization is aligned with the topography of the learning signal carried by the climbing fibers, which collaterals extend along thin parasagittal bands of Purkinje cells (Apps and Garwicz, 2005; Jörntell et al., 2000; Voogd et al., 1987). In contrast, the contextual information is distributed in the orthogonal (transverse) plan by the parallel fibers. Therefore groups of neighboring Purkinje cells are located at the intersection of the two types of inputs and thus share similar instructive signal (carried by the climbing fibers) and associative information (carried by the paralell fibers). Neighboring Purkinje cells are known to exhibit spontaneously coordinated activities. Spontaneous synchronization has been noted in early recordings of pairs of proximal cells in anesthetized and decerebrate animals (Bell and Grimm, 1969; Ebner and Bloedel, 1981); more recent experiments (de Solages et al., 2008) showed that fast (>200Hz) cerebellar oscillations (Adrian, 1935) arising from populations of Purkinje cells are associated with millisecond-scale synchrony (de Solages et al., 2008). Shin and De Schutter also suggested a synchronizing role for local inhibitory neurons, since synchrony appeared associated with episodes of reduced instantaneous firing rate of Purkinje

cells (Shin and De Schutter, 2006). However, whether neighboring Purkinje cells -which axons converge in the cerebellar nuclei- coordinate their discharge during a motor task is currently unknown.

Here, we examined the firing patterns of neighboring Purkinje cells in a task of food retrieval (Whishaw and Pellis, 1990). In this task, the animals have to generate a voluntary multi-segmental movement of the forelimb in order to reach and grasp a food pellet. Ample evidence from pharmacological micro-injections indicate that the intermediate cerebellum contributes to reaching and grasping (Apps and Garwicz, 1997; Cooper et al., 2000, Ekerot et al., 1997; Horn et al., 2010), and recordings in the intermediate cerebellum have demonstrated strong modulations of the firing rate of Purkinje cell layer units (Heck et al., 2007). We therefore recorded simultaneously neighboring Purkinje cells and examine the organization of discharge during the movement.

Results

Modulation of Purkinje cells during a voluntary skilled movement

We trained 13 rats to perform a voluntary and skilled movement of grasping to retrieve food pellets through a slot. This movement is composed by a complex sequence of actions (Whishaw and Pellis, 2003). Using fast video recordings synchronized with the electrophysiological recordings, we scored three landmarks events in this movement : 1) “lift” : time at which the forepaw left the ground, 2) “cover” : contact of the forepaw with the pellet, taking place immediately after the rotation of the wrist, and opening of the digits, and 3) “grasp” : closing the digits around the food while flexing the wrist to lift the food (Figure 1A). The duration from lift to grasp was 598 +/- 40 ms, the average duration from lift to cover and cover to grasp were 292 +/- 23 ms and 306 +/- 37 ms respectively (mean+-sd). Chronic tetrode recordings allowed us to record simultaneously neighboring Purkinje cells in the paramedian lobule of the cerebellum ipsi-lateral to the limb used. We identified the Purkinje cells modulating their firing rate during the movement by searching in event-triggered averages of the firing rate the presence of significant deviations from the (inter-trial) baseline. 110 out of 122 (90%) Purkinje cells recorded had a significant modulation of their firing rate around at least one of landmark events of the movement, either lift (n=93), cover (n=92) , or grasp (n=90) (three different examples are shown in Figure 1B). The modulation could be an increase or/ and decrease of the firing rate relative to baseline.

Figure 1C summarize the responses of all the Purkinje cells around the lift of the forelimb, 93 cells were significant modulated around this landmark, among which 44 cells significantly increased, 35 cells significantly decreased and 14 both significantly increased and decreased (Figure 1D). While most cells (n=73) were modulated in relation with the three landmarks of movement, only one third of the cells responded only to one (n=18) or to two (n=19) phases of the movement. In most cases (14/18 recording sites) all cells recorded from the same tetrode where modulated during the movement. Neighboring cells recorded from the same tetrode tended to exhibit similar profile of firing rate during movement, although strict parallel covariation was the exception rather than the rule (Figure 2A). To assess the significance of co-variation of pairs of cells, we computed the correlation coefficient of their profile of firing rate (i.e. peri-event histogram) around the landmark events (Figure 2B). In average, the time course of firing was positively correlated around the lift event for the pairs of neighboring cells but not for pairs of distant cells (correlation coefficient for firing profile +/- 150ms around lift (mean +- sem): neighboring cells 0.23+-0.08 (significantly different from 0, p=0.011), distant cells: 0.032+-0.047 (p=0.46) with a significant difference between neighboring vs distant pairs: p=0.031); neither neighboring nor distant pairs had preferentially positively-correlated peri-event histograms around cover and grasp events (correlation coefficient for neighboring pairs of cells cover: 0.14+- 0.08 p=0.11; grasp 0.007+-0.052 p=0.54 distant pairs of cells cover: 0.074+-0.091 p=0.83; grasp: 0.054+-0.045 p=0.26). The average distance between recording sites for distant pairs was 0.88 +/- 0.45 mm (mean +/- sd), thus indicating an upper limit for the functional segregation of cells in this part of the cerebellum. However, assessing the variation of firing rate around an event over multiple trials with event-triggered averages is limited by the uncertainty on the timing of the event (the frame rate of the video used to identify the events was 50Hz, yielding a 20ms uncertainty on the actual timing of the event), and more critically by the inter-trial variability in the speed of the execution of the movement around the landmark event. To circumvent these limitations, we analyzed the covariance of the instantaneous firing rate of pairs of cells around the landmark events. We found that neighboring cells in average had positively correlated instantaneous firing rate around all three landmark events (+/- 150ms), while distant units did not (Figure 2C). Overall, these results indicate that neighboring cells in the paramedian lobule tend to modulate their firing rate similarly along the reach-and-grasp movements.

Short-term synchrony of Simple spikes of Purkinje cells pairs modulated during the motor task

So far, we only provided evidence for the presence of a co-modulation of the firing rate of neighboring cells; however, this does not indicate whether the timing of spikes is coordinated between cells. To examine this question, we analyzed the relative timing of the spikes from the pairs of cells in

cross-correlograms during the periods of time of the movement when the cells significantly increased their firing rate compared to the average baseline inter-trial firing rate. The variations of firing rate during the movement are expected to produced (broad) peaks in the cross-correlograms (Brody, 1998), but we consistently observed a narrow central peak in the cross-correlograms of neighboring cells (Figure 3H). This peak had a width of a few milliseconds and an amplitude corresponding to an excess of ~20% of near-coincident spikes (Figure 3J); when expressed in rate of events, the average rate of occurrence of pairs of spikes from neighboring cells with a delay of 3ms or less, was 34.4+/-4.7Hz, and the central peak indicated an excess rate of synchronous events of 4.4+/-1.8Hz. The central peak was absent from the correlogram of spikes trains from distant pairs of cells with a modulation of their firing rate during the movement (Figure 3I), suggesting that the presence of a modulation of the firing rate in the pair of cells is not a sufficient cause to observe short-term correlations. [Figure K, L (both neighboring cell pairs with or without co-modulation can indicate short-term synchrony) are not in the text]

To test explicitly to which extent correlations resulted from the profile of firing rate around movement, we computed the cross-correlograms between actual spike trains and surrogate spike trains which reproduced the inter-spike interval distribution and time-dependent modulation of firing rate of actual neighboring cells. Surrogate spike trains were obtained by estimating the distribution of the cells inter-spike intervals along time using smoothing splines; the quality of this estimate was verified by a battery of tests and the spike trains were subsequently generated using a thinning procedure. The generation of multiple surrogate spike trains allowed to extract confidence interval for the expected correlations. We found that the crosscorrelograms between the spike train from a first real cell and a surrogate spike train modeled after a second neighboring cell predicted the right level of observed correlation except at short time scales, where the narrow peak around zero was not reproduced. These results indicate that the central peak observed in the correlogram from pairs of real neighboring cells do not simply result from the inter-spike interval distributions of the cells and their changes of firing rate along time (i.e. from a co-variation of the firing rate). These results suggest instead that neighboring cells do not discharge independently from another.

To test for the independence of the firing of neighboring cells, we compared the ability of two types of smooth spline models of single cell spike trains to account for the real firing patterns around the behavioral events: the first model was identical to the one used above to generate surrogate data and produced an estimate of the interspike distribution and the time dependency of the firing probability of the cell; the second model had a supplementary term corresponding to the delay to the nearest spike from a (real) neighboring cell thus providing an estimate of the temporal relationship of firing of the

neighboring cells (Figure 4). These models were fitted to the spike trains from each pair of cells using one half of the behavioral trials and their ability to account for the other half of the trials was then tested. In 39 out of 43 pairs, we found that the model taking into account the delay to the nearest spike from a neighboring cell produced a better prediction of the actual spike train (Figure 5A), confirming the inter-dependence of the instantaneous firing probability of neighboring cells. Moreover, the smooth spline fitting procedures allow to easily derive a confidence interval for the fits. We therefore examined the term of the model corresponding to delay to the nearest spike from a neighboring cell and identified, in the fits of this term, the significantly positive peaks; these peaks indicated the time delays to the neighboring cells spikes that were associated with a significant increase of probability of firing, and hence provided an estimate of the width of the temporal association of neighboring cell spikes: in about 80% of the cells, the significant temporal association was shorter than 5ms (Figure 5B), and the peak association time was shorter than 4ms (Figure 5C). Such results were not found for distant pairs (Figure 5D-F). Overall, these results demonstrate that, during movement, neighboring cells tend to fire in near synchrony with typical delays inferior to 5ms.

Complex spikes are also known to be synchronized in narrow parasagittal bands. Indeed, we observed a clear correlation of complex spikes of neighboring cells during the recording sessions (Figure 6D). In our conditions, we did not observe a modulation of complex spike firing during the movement (Figure 6C) and the firing rate remained at an average frequency of 0.50 +/- 0.29 Hz (mean +/- sd). Most of our recordings were indeed performed after learning the movement, in well-trained animals; the animals generally succeeded in retrieving the food and there were consequently too few failures in successful food retrieval to allow the analysis of complex spike firing for these failed trials.

Relation with basal synchrony

Neighboring Purkinje cells are known to be spontaneously synchronized (see Introduction). We then compared the level of cell pairs synchronization observed during periods of increased firing of the cells to the basal synchrony observed (Figure 7). We found that the short-term correlations between cell pairs during the inter-trial periods of time were approximately two fold higher than the correlations of the same pairs during the task-related modulation of firing, and this difference was significant at the shortest time scales. Interestingly the shape of the central peak between and during the task were quite similar raising the possibility that the inter-trial level of cell pairs synchrony is due to the ongoing (task-unrelated) motor activity. We therefore compared the synchrony observed during free spatial exploration (similar to the inter-trial activity during the task) with the synchrony recorded during quiet

awakening or light sleep (when the animals exhibited no motor activity and the cortical EEG spectrum did not contain theta oscillations). Surprisingly, there was no difference in the shape or level of short-term correlations in these two conditions (Figure 7J). We have previously reported that the basal synchrony between pairs of Purkinje cells is related to fast oscillations; the correlations observed in the present study in both conditions were indeed very similar to the fast-oscillations reported previously (peaks in crosscorrelogram around 4ms); The shape of the cross-correlograms remained similar independently from the detection of a peak in the power spectrum of the local field potential; this suggests that the oscillations has little impact on local field potential, as expected if only it is a relatively local phenomenon that occurs independently at short term distances (de Solages). Oscillations were however detected as a peak in the power spectrum of the local field in 48% of the cases, although the amplitude tended to be smaller during active exploration (possibly due to increased 'background' activity observed in cerebellar extracellular recordings during active behavior). Similar peaks (and shapes) of crosscorrelogram between pairs of adjacent cells were observed independently from the detection of a peak in the spectrum of the local field potential. The detected peaks were smaller when the rats were actively exploring the environement; however the background activity increased in these condition (compared to the resting state), suggesting that the peaks were hidden by the overall activity of the network.

Discussion

The present study demonstrates that neighboring Purkinje cells, which share similar learning signal as demosntrated by the synchrony of their complex spikes, exhibit only a mild similarity of their firing profile during a reaching movement but consistenlty expressed a correlated firing at short time scales (<5ms). These correlations are expressed at the same time scale as the spontaneous correlations expressed at rest and associated with fast oscillation, but they are stronger during the movement. Since neighboring Purkinje cells likely belong to the same microzone, these results indicate that the cerebellar cortex produces very transient events of inhibition of their postsynaptic targets during movement and rest.

Movement encoding in the Purkinje cell layer

Purkinje cells in the intermediate and lateral cerebellum are known to encode the global kinematic parameters of limb movement such as position (Marple-Horvat and Stein, 1987; Roitman et al., 2005), velocity (Coltz et al, 1999; Marple-Horvat and Stein, 1987), direction (Roitman et al., 2005; Fortier et al., 1989; Mano and Yamamoto, 1980), movement distance (Fu et al., 1997), surface texture or weight of the object which animals grasped (Espinoza and Smith, 1990). The encoding of force by Purkinje cell firing has also been proposed (Smith and Bourbonnais, 1981); however, when the force required to complete a movement was varied while keeping the movement constant, it was found that Purkinje cells preferentially encode the kinematics rather than the force required to produce the limb movent (Pasalar et al., 2006).-In these studies, the firing profile of the Purinje cells during the task exhibited a wide variety across cells, even when recorded on the same beam of parallel fibers (Heck et al., 2007); however the cells were sampled throughout large areas of the cerebellar cortex, likely encompassing many microzones (Ekerott et al., 1997) and thus controlling several different motor units. Our study reveals that neighboring cells exhibit weakly similar firing profiles, thus suggesting that individual units within a microzone only encode related but distinct subsets of the elements that compose the movement. This is consistent with experiments of paired recordings from connected pairs of Purkinje and nuclear cells (McDevitt et al., 1987), which showed that the firing profile of these cells were only reciprocal for elementary (square) but not for continuous (sinusoidal) forepaw deplacements, suggesting that individual Purkinje cells firing profile did coincide with the total inhibition of nuclear cells only in specific short temporal windows. Similarly, all eye saccade parameters could not be extracted from the activity of the Purkinje cells in the oculomotor vermis, while they could be inferred from the population activity of many Purkinje cells (Thier et al., 2000). Overall, movements parameter encoding in a microzone are likely to be distributed throughout the population of Purkinje cells enclosed in this functional unit.

Local synchrony during the task and rest

While neighboring Purkinje cells may exhibit very diverse time course during the movement, they consistently express correlated firing at short time scale (3ms) during periods of increased firing. These correlations occurred at a time scale shorter than than the interspike intervals of the cells, and could not be predicted when only the time course of firing of each cell was taken into account, suggesting that they reflect very transient coincident increase of firing probability of neighboring cells. Only a few studies examined the synchrony in awake animals: a previous study reported such short term correlations between cells in the same functional zone of the flocculus in awake rabbits during optokinetic stimulations (De Zeeuw et al., 1997), but it was unclear to which extent this synchrony

were due to the ongoing task. Spontaneous synchrony does not seem to occur between distant sites in awake animals, even if the cells are situated on the same beam of parallel fibers (Cheron et al., 2004). However, another study reported synchrony between distant recording sites along the parallel fibers in the cerebellar hemispheres during a reaching task suggesting that units in distant microzones may also synchronize during the movement (Heck et al., 1997); this synchrony however was only observed in the multi-unit signal and took place at sub-millisecond time scales, thus shorter than the propagation delay in the parallel fibers between the recording sites; this suggested that these events were due to a powerful synchronous activation of the granule cells under each recording site (with virtually no jitter in the triggering of the spikes in the granule and Purkinje cells). The presence of such sub-millisecond synchrony could not be resolved in our recordings since extracellular spike waveforms overlap at this time scale and prevent proper sorting of spikes. Correlations at few milliseconds may be observed in anesthetized or decerebrate animals in response to physiological sensory stimulations (Ebner and Bloedel, 1981; Wise et al., 2010) suggesting that incoming information to the cerebellar cortex may cause co-actvitaion of Purkinje cells with such delays. Multiple mechanisms may contribute to the appearance of correlated discharge at the time scale of a few milliseconds.: numerical stimulations indicate that shared excitation via parallel fibers or shared inhibition from local interneurons will produce correlated discharge in the range of 5-10ms (Jaeger, 2003), suggesting that feedforward inhibition might contribute to narrow the correlated firing down to few milliseconds (Brunel et al., 2004).

Recurrent inhibition could also help sharpen the correlations between neighboring neurons. Multiple pathways exist for recurrent inhibition in the Purkinje cell layer: recurrent collaterals of Purkinje cells axons (Larramendiand Lemkey-Johnston, 1970) may directly connect to, and inhibit, neighboring Purkinje cells (Bishop, 1982; Orduz and Llano, 2007). They also contact Lurago and globular cells (Hirono et al., 2012), which connect to molecular layer interneurons inhibiting the Purkinje cells (Laine and Axelrad 1998, 2002; Simat et al., 2007) and possibly Purkinje cells directly (Dean et al., 2003). Inhibitory recurrent networks may spontaneously generate synchronous activities associated with fast oscillations, and such oscillations are indeed present at rest in the Purkinje cell layer (Adrian, 1935; de Solages et al., 2008); they are responsible, at least in part, for the basal correlations observed at rest between neighboring cells. In the present study, we have confirmed the presence of such population oscillations in resting unanesthetized animals (de Solages et al., 2008), but also shown that the oscillations are present in awake behaving animals; very similar patterns of cell firing correlations were observed at rest and during behavior. These correlations were observed even when the oscillations were

not visible as peaks in the spectrum of the local field potential, presumably because they were masked by increased background local field potential activities. Interestingly, the correlation patterns of neighboring cells recorded during the reach-and-grasp task and inter-trial periods of time had also very similar shape but were simply scaled up during the task. This is consistent with the properties of sparse oscillations in recurrent inhibitory networks, which frequency (reflected in the width of synchrony peaks) is unchanged when the firing frequency of the cells increase (Brunel and Hakim, 1999; de Solages et al., 2008). Therefore, the recurrent inhibitory network in the output layer of the cerebellum may continously generate sparse ultra-fast oscillations and therfore substantially contribute to sharpen the Purkinje cell layer to the cerebellar nucleus target.

Functional impact of correlations

Purkinje axons from individual microzones converge in the cerebellar nuclei (Ruigrok, 2011). Nuclear cells receive excitatory inputs from the mossy fibers and inhibitory inputs from local interneurons and Purkinje cells. The excitatory inputs are, for a large part, mediated by NMDA receptors (Anchisi et al., 2001; Audinat et al., 1992) whose slow kinetics low-pass-filter the incoming excitation (Gauck and Jaeger, 2003), while the fast inhibitory inputs from Purkinje cells precisely time the spikes (Person and Raman, 2012). Purkinje cell synchrony with delays under 3ms such as observed in the present study will favor summation of the inhibitory currents in the postsynaptic nuclear cell, since their decay time is around ~2.5ms. The synchronous firing of Purkinje cell will then create very transient windows of powerful inhibition. Such spontaneous events, likely due to spontaneously synchronous climbing fiber inputs to functionally-related Purkinje cells. are indeed observed in intracellular recordings from nuclear neurons, and may occur in ~200Hz bursts (Bengtsson et al., 2011). Such inhibitory events, which provide a upper estimate of the effect of synchronous activation of the presynaptic Purkinje cells of a nuclear neuron, were not sufficient to produce rebound responses in the nuclear cells, an event that has been linked to synaptic plasticity in the cerebellar nuclei (Aizenman et al., 1998). It is therefore unlikely that the synchrony observed in our study correspond to learning events. Rather, in combination with recent studies of the nuclear neurons, it indicates that the cerebellum output is controlled with a time scale of a few (3-5) milliseconds.

Conclusion

Overall, these results indicate that movement representation in the cerebellar cortex is heavily fragmented over many different Purkinje cells, even if they belong to the same elementary functional

microzone. However, cell firing is not entirely independent, since periods of increased firing activity during the movement are associated with an enhanced synchrony. This synchrony will favor synaptic summation in the postsynaptic nuclear neurons and allow to control the postsynaptic targed with an accuracy of a few milliseconds.

Methods

Animal and training

The experimental procedures were conducted in conformity with institutional guidelines and in compliance with national and European laws and policies. 14 male adult Long-Evens rats (350-500g; Charles River Laboratories, France) were used in these experiments. They were housed individually on a 7 AM to 7 PM reversed light/dark schedule. 13 rats were trained to perform a food-grasp task, in which they should grasp food pellet through a small slot. These rats were initially housed in the same condition as usual. After rats were familiar with their cage, they were placed on a food deprivation schedule until the weight maintained at 80-90% of the normal weight. Then they were trained 20-50 trials once or twice everyday in a special training and recording table. The table was 65cm long, 50cm wide and 80cm above the ground. In the front of the table, there was a plastic transparent wall, which the rat couldn't pass. At the center of the front wall, there was a 1cm wide slit that extended from the floor of the table to a height of 15 cm. On the outside of the wall, in front of the slit, mounted 3cm above the floor of the table, was a 2cm wide by 4 cm long shelf. On the shelf there were 3 indentations which were 2 cm away from the inside front wall aligned with the edges of the slit. The food pellet (dustless precision pellets 45mg, banana flavor, Bio-Serv) was placed on the contralateral hole to the preferring paw of rats. Rats were trained to learn to grasp pellets through slot always by the preferring paw and to find another pellet in the other side of the table in turn. Usually after being trained for 5-7 days, rats could learn to perform task.

Surgery and implantation of the headstage

After the rat learned the task, one headstage including 1-4 movable commercial tetrodes (Thomas Recording) and one movable reference electrode (Gao et al., 2011) was fixed in the skull above the surface of the paramidian lobule of the cerebellum of the rat by a standard surgery. During the surgery, rats were maintained anesthetized during the whole experiment with a mixture of isoflurance (0.5~2%) and O2. Animal were mounted in a stereotaxic frame (David Kopf Instruments, CA) with bars in the ears. Heart rate and blood O2 concentration were monitored to adjust the level of

anesthesia. A heating device controlled by rectal temperature was used to maintain the rat at physiological core temperature. Before incision of the scalp, 3% lidocaine was injected subcutaneously at the site of incision. The skull and dura over the vermian part of paramedian lobule in the hemisphere ipsolateral to the preferring paw were removed using a dental drill, a curved syringe needle, and fine forceps. Subdural meninges were gently removed where the electodes were to be advanced. Then the headstage was implanted and fixed in the skull just above the cerebellar cortex by dental cement. Animals were allowed to fully recover before recording.

in vivo recording

After rats' recovery from the surgery, we advanced tetrodes to its reaching Purkinje cell layer. The Purkinje cell layer was characterized by an intense cellular activity and distinctive complex spikes. Once the tetrodes were near or in the right layer, they were adjusted more carefully to get the signals of cell activities out of noise. The activities, which were first filtered 0.1 Hz to 8 kHz with a Butterworth filter, then differentially amplified, sampled at 25 kHz, were continuously monitored through loudspeakers and displayed on a computer screen monitor. Once the signals were stable, they would be recorded when the rats were active-exploring, sleeping or performing a grasp task and be stored to disk for off-line analysis.

Single-unit isolation (clustering)

Continuous recordings were first high-pass filtered at 300 Hz with a Butterworth filter before thresholding (typically at 80μV). Single-unit spikes were isolated off-line using manual clustering ('xclust', M.A. Wilson), mostly depending on differences of peak amplitudes recorded from four channels. Usually, three to seven units could be isolated per tetrode and they would be verified by testing the distribution of inter-spike intervals and the existence of a 1-2 ms refractory period devoid of spikes in the auto-correlogram to reduce miss-clustering. However, this procedure can't allow the sorting of overlapping waveforms arising from coincident spikes from two or more different units, i.e., within an interval of less than 0.5 ms (the width of the Purkinje cells spikes being less than 0.3 ms).

Further analysis was performed with GNU R (R Development Core Team, 2004).

video analysis

When rats were performing the reach-to-grasp task, a camera (Allied Vision Technologie, Germany) in front of the training/recording table captures the movement information of rats with a rate of 50 Hz. Each frame of the video recoding was synchronized with the neurophysiological signals. The video was

analyzed off-line afterwards frame by frame. Three components of movement in each successful grasp trial were manually scored: lift (the inception of lifting the forepaw), cover (rotation around the wrist and the digits are opened for grasping) and grasp (closing the digits around the food while flexing the wrist to lift the food). Although up to 10 components may be distinguished during the movement, we limited our analysis to the three most obvious steps, other components being difficult to time accurately too variable across animals.

Histology

After the behavior and electrophysiological experiments, the rats are killed by overdose of anesthesia. The brain was carefully taken out and fixed in 4% formalin solution. After the tissue was totally fixed, it was sliced sagittally with a 30-40 um thickness using a microtome slicer (Leica VT1000 S), then dehydrated, cleared, and infiltrated with wax. The embedded slices were inspected in fluorescence microscopy (Leica DM LB). Fluorescent signals from the dye applied on the electrodes allowed reconstructing the trajectory of the tetrodes in the cerebellum.

Acknowledgements

This work was supported by ANR (08-SYSC-005-02 DALTPAC, 09-MNPS-038-01 Cecomod, 07-NEURO-025-03 Natacs), the Centre National de la Recherche Scientifique (CNRS), the Institut National de la Santé et de la Recherche Médicale (INSERM, C.L.), the Ecole Normale Supérieure (ENS), the Ministère des Affaires Etrangères (HY. G.).

References

Adrian, E.D. Discharge frequencies in the cerebral and cerebellar cortex. *J. Physiol. (London)* **83**, 32-33 (1935).

Aizenman, C.D., Manis, P.B. & Linden, D.J. Polarity of long-term synaptic gain change is related to postsynaptic spike firing at a cerebellar inhibitory synapse. *Neuron* **21**, 827-35 (1998).

Albus, J. A theory of cerebellar function. *Mathematical Biosciences* **10**, 25-61 (1971).

Anchisi, D., Scelfo, B. & Tempia, F. Postsynaptic currents in deep cerebellar nuclei. *Journal of neurophysiology* **85**, 323-31 (2001).

Apps, R., Atkins, M.J. & Garwicz, M. Gating of cutaneous input to cerebellar climbing fibres during a reaching task in the cat. *The Journal of physiology* **502 (Pt 1**, 203-14 (1997).

Apps, R. & Garwicz, M. Anatomical and physiological foundations of cerebellar information processing. *Nat. Rev. Neurosci.* **6**, 297-311 (2005).

Apps, R. & Hawkes, R. Cerebellar cortical organization: a one-map hypothesis. *Nature reviews. Neuroscience* **10**, 670-81 (2009).

Audinat, E., Gähwiler, B.H. & Knöpfel, T. Excitatory synaptic potentials in neurons of the deep nuclei in olivo-cerebellar slice cultures. *Neuroscience* **49**, 903-11 (1992).

Bell, C.C. & Grimm, R.J. Discharge properties of Purkinje cells recorded on single and double microelectrodes. *Journal of neurophysiology* **32**, 1044-55 (1969).

Bengtsson, F., Ekerot, C.-F. & Jörntell, H. In vivo analysis of inhibitory synaptic inputs and rebounds in deep cerebellar nuclear neurons. *PloS one* **6**, e18822 (2011).

Bishop, G.A. The pattern of distribution of the local axonal collaterals of Purkinje cells in the intermediate cortex of the anterior lobe and paramedian lobule of the cat cerebellum. *The Journal of comparative neurology* **210**, 1-9 (1982).

Brody, C.D. Slow covariations in neuronal resting potentials can lead to artefactually fast cross-correlations in their spike trains. *Journal of neurophysiology* **80**, 3345-51 (1998).

Brunel, N. & Hakim, V. Fast global oscillations in networks of integrate-and-fire neurons with low firing rates. *Neural computation* **11**, 1621-71 (1999).

Brunel, N., Hakim, V., Isope, P., Nadal, J.-P. & Barbour, B. Optimal information storage and the distribution of synaptic weights: perceptron versus Purkinje cell. *Neuron* **43**, 745-57 (2004).

Cheron, G. *et al.* Inactivation of calcium-binding protein genes induces 160 Hz oscillations in the

cerebellar cortex of alert mice. *The Journal of neuroscience : the official journal of the Society for Neuroscience* **24**, 434-41 (2004).

Coltz, J.D., Johnson, M.T. & Ebner, T.J. Cerebellar Purkinje cell simple spike discharge encodes movement velocity in primates during visuomotor arm tracking. *The Journal of neuroscience : the official journal of the Society for Neuroscience* **19**, 1782-803 (1999).

Cooper, S.E., Martin, J.H. & Ghez, C. Effects of inactivation of the anterior interpositus nucleus on the kinematic and dynamic control of multijoint movement. *Journal of neurophysiology* **84**, 1988-2000 (2000).

de Solages, C. *et al.* High-frequency organization and synchrony of activity in the purkinje cell layer of the cerebellum. *Neuron* **58**, 775-88 (2008).

De Zeeuw, C.I., Koekkoek, S.K., Wylie, D.R. & Simpson, J.I. Association between dendritic lamellar bodies and complex spike synchrony in the olivocerebellar system. *Journal of neurophysiology* **77**, 1747-58 (1997).

Dean, I., Robertson, S.J. & Edwards, F.A. Serotonin drives a novel GABAergic synaptic current recorded in rat cerebellar purkinje cells: a Lugaro cell to Purkinje cell synapse. *The Journal of neuroscience : the official journal of the Society for Neuroscience* **23**, 4457-69 (2003).

Dean, P., Porrill, J., Ekerot, C.-F. & Jörntell, H. The cerebellar microcircuit as an adaptive filter: experimental and computational evidence. *Nature reviews. Neuroscience* **11**, 30-43 (2010).

Dean, P., Porrill, J. & Stone, J.V. Decorrelation control by the cerebellum achieves oculomotor plant compensation in simulated vestibulo-ocular reflex. *Proceedings. Biological sciences / The Royal Society* **269**, 1895-904 (2002).

Ebner, T.J. & Bloedel, J.R. Correlation between activity of Purkinje cells and its modification by natural peripheral stimuli. *Journal of neurophysiology* **45**, 948-61 (1981).

Ekerot, C.F., Garwicz, M. & Jörntell, H. The control of forelimb movements by intermediate cerebellum. *Progress in brain research* **114**, 423-9 (1997).

Espinoza, E. & Smith, A.M. Purkinje cell simple spike activity during grasping and lifting objects of different textures and weights. *Journal of neurophysiology* **64**, 698-714 (1990).

Fu, Q.G., Flament, D., Coltz, J.D. & Ebner, T.J. Relationship of cerebellar Purkinje cell simple spike discharge to movement kinematics in the monkey. *Journal of neurophysiology* **78**, 478-91 (1997).

Gauck, V. & Jaeger, D. The control of rate and timing of spikes in the deep cerebellar nuclei by inhibition. *The Journal of neuroscience : the official journal of the Society for Neuroscience* **20**, 3006-16 (2000).

Gauck, V. & Jaeger, D. The contribution of NMDA and AMPA conductances to the control of spiking in neurons of the deep cerebellar nuclei. *The Journal of neuroscience : the official journal of the Society for Neuroscience* **23**, 8109-18 (2003).

Heck, D.H., Thach, W.T. & Keating, J.G. On-beam synchrony in the cerebellum as the mechanism for the timing and coordination of movement. *Proceedings of the National Academy of Sciences of the United States of America* **104**, 7658-63 (2007).

Hirono, M. *et al.* Cerebellar globular cells receive monoaminergic excitation and monosynaptic inhibition from Purkinje cells. *PloS one* **7**, e29663 (2012).

Horn, K.M., Pong, M. & Gibson, A.R. Functional relations of cerebellar modules of the cat. *The Journal of neuroscience : the official journal of the Society for Neuroscience* **30**, 9411-23 (2010).

Ito, M. Neurophysiological aspects of the cerebellar motor control system. *International journal of neurology* **7**, 162-76 (1970).

Jaeger, D. No parallel fiber volleys in the cerebellar cortex: evidence from cross-correlation analysis between Purkinje cells in a computer model and in recordings from anesthetized rats. *Journal of computational neuroscience* **14**, 311-27 (2003).

Jörntell, H., Ekerot, C., Garwicz, M. & Luo, X.L. Functional organization of climbing fibre projection to the cerebellar anterior lobe of the rat. *The Journal of physiology* **522 Pt 2**, 297-309 (2000).

Lainé, J. & Axelrad, H. Lugaro cells target basket and stellate cells in the cerebellar cortex. *Neuroreport* **9**, 2399-403 (1998).

Lainé, J. & Axelrad, H. Extending the cerebellar Lugaro cell class. *Neuroscience* **115**, 363-74 (2002).

Larramendi, L.M. & Lemkey-Johnston, N. The distribution of recurrent Purkinje collateral synapses in the mouse cerebellar cortex: an electron microscopic study. *The Journal of comparative neurology* **138**, 451-9 (1970).

Marple-Horvat, D.E. & Stein, J.F. Cerebellar neuronal activity related to arm movements in trained rhesus monkeys. *The Journal of physiology* **394**, 351-66 (1987).

Marr, D. A theory of cerebellar cortex. *The Journal of physiology* **202**, 437-70 (1969).

McDevitt, C.J., Ebner, T.J. & Bloedel, J.R. Relationships between simultaneously recorded Purkinje cells and nuclear neurons. *Brain research* **425**, 1-13 (1987).

Medina, J.F. & Lisberger, S.G. Encoding and decoding of learned smooth-pursuit eye movements in the floccular complex of the monkey cerebellum. *Journal of neurophysiology* **102**, 2039-54 (2009).

Orduz, D. & Llano, I. Recurrent axon collaterals underlie facilitating synapses between cerebellar

Purkinje cells. *Proceedings of the National Academy of Sciences of the United States of America* **104**, 17831-6 (2007).

Pasalar, S., Roitman, A.V., Durfee, W.K. & Ebner, T.J. Force field effects on cerebellar Purkinje cell discharge with implications for internal models. *Nature neuroscience* **9**, 1404-11 (2006).

Person, A.L. & Raman, I.M. Purkinje neuron synchrony elicits time-locked spiking in the cerebellar nuclei. *Nature* **481**, 502-5 (2012).

Roitman, A.V., Pasalar, S., Johnson, M.T.V. & Ebner, T.J. Position, direction of movement, and speed tuning of cerebellar Purkinje cells during circular manual tracking in monkey. *The Journal of neuroscience : the official journal of the Society for Neuroscience* **25**, 9244-57 (2005).

Ruigrok, T.J.H. Ins and outs of cerebellar modules. *Cerebellum (London, England)* **10**, 464-74 (2011).

Shin, S.-L. & De Schutter, E. Dynamic synchronization of Purkinje cell simple spikes. *Journal of neurophysiology* **96**, 3485-91 (2006).

Simat, M., Parpan, F. & Fritschy, J.-M. Heterogeneity of glycinergic and gabaergic interneurons in the granule cell layer of mouse cerebellum. *The Journal of comparative neurology* **500**, 71-83 (2007).

Smith, A.M. & Bourbonnais, D. Neuronal activity in cerebellar cortex related to control of prehensile force. *Journal of neurophysiology* **45**, 286-303 (1981).

Thier, P., Dicke, P.W., Haas, R. & Barash, S. Encoding of movement time by populations of cerebellar Purkinje cells. *Nature* **405**, 72-6 (2000).

Voogd, J., Hess, D.T. & Marani, E. The parasagittal zonation of the cerebellar cortex in cat and monkey: topography, distribution of acetyhcholinesterase, and development. *New Concepts in Cerebellar Neurobiology.* 183-220 (1987).

Whishaw, I.Q. & Pellis, S.M. The structure of skilled forelimb reaching in the rat: a proximally driven movement with a single distal rotatory component. *Behavioural brain research* **41**, 49-59 (1990).

Wise, A.K., Cerminara, N.L., Marple-Horvat, D.E. & Apps, R. Mechanisms of synchronous activity in cerebellar Purkinje cells. *The Journal of physiology* **588**, 2373-90 (2010).

Figure legends

Figure 1 Purkinje cells are modulated during a skilled reaching task

A: Three frames of video show the landmark events of the movement, respectively: ‘lift’, ‘cover’ and ‘grasp’. Yellow arrows indicate the position of the paw. The numbers on the bar indicate average duration between phases.

B: Examples of three Purkinje cells, which are modulated during motion. Spikes of cells in all the trials and average firing rate during one session are aligned to time of three phases respectively. Red point: time of ‘lift’. Green points: time of ‘cover’. Blue points: time of ‘grasp’.

C: Peristimulus time histogram of all Purkinje cells for one component of the movement: ‘lift’. Color encodes the z-score of firing rate. Each line corresponds to one Purkinje cell, whose averaged firing rate of all trials in one session is aligned to the time of ‘lift’. Cells are arranged by deacrising values of z-score.

D: time course of average firing rate during ‘lift’ for 3 population of Purkinje cells: all Purkinje cells (shown in black), significant increased Purkinje cells (shown in red) and significant decreased Purkinje cells (shown in blue)

Figure 2 neighboring Purkinje cells are weakly co-modulated during task.

A: 6 examples of neighboring cell pairs (shown in solid or dotted line), showing high (Top), middle (Middle), and low (Bottom) similarity of profile of modulation, respectively.

B: Co-variation of the profile of firing rate of pairs of neighboring (shown in red) or remote (shown in yellow) cells around landmark event.

C: Co-variation of the instantaneous firing rate of pairs of neighboring (shown in red) or remote (shown in yellow) cells around landmark event.

Figure 3 Short-term synchrony of neighboring Purkinje cell pairs during period of increased firing during the task.

A-G: One example of neighboring Purkinje cell pair, showing short-term synchrony during their modulation.

A, D: Average waveforms of simple spikes and complex spikes for a pair of neighboring Purkinje cells from 4 channels of one tetrode (shown in black, red, green and blue, respectively). B, E: Auto-correlation of simple spikes of this pair. C, F: discharge profile of this pair of all trials in one cell

during the task. Average firing rate during one session is aligned to time of 'cover'. Black bar: simple spikes; Orange star: complex spikes; Green points: time of ‘cover’; Red block: time of significant modulation. G: Cross-correlations of the cell pair in A-F during modulation (red line) and during the whole session (black line). The time period used to compute the cross-correlation are shown in red block in C and F.

H: average cross-correlation of all neighboring Purkinje cell pairs during modulation. SEM is shown in light red.

I: average cross-correlation of all distant Purkinje cell pairs. SEM is shown in light grey.

J: short-term synchrony of neighboring Purkinje cell during modulation are larger than during the whole task. Dots are average cross-correlation during modulation. Its smoothed line is shown in green line. The average cross-correlation during whole task is shown in black.

K-L: neighboring Purkinje cell pairs without co-modulation (K) exhibit also short-term synchrony, similar to the pairs with co-modulation (L).

Figure 4 Penalized likelihood modeling of the firing of neighboring Purkinje cell pair allows to quantify their temporal interaction

A, B: actual rasters and PSTH of one neighboring Purkinje cell pair.

: the smooth PSTH of this pair produced by simple and complex models; the inter-dependence of this pair.

C, F: raster and PSTH of cell 1 of this pair produced by simple model or by complex model.

D, E: time since last spikes (D) and interval spike related to 'lift' (E) produced by simple model.

G, H: time since last spikes (G) and interval spike related to 'lift' (H) produced by complex model.

I: time delaying to the neighboring cell spikes computerized by complex model. This panel indicates that the firing probability of the cell 1 is increased when the cell 2 fires in a short window of 3 ms.

J: cross-correlation of actual spikes trains (shown in blue), spikes trains produced by simple model (red), or complex model (green). 2SD of average cross-correlation of 5 cases of simple model are shown in gray.

Figure 5 neighboring cells , not remote cells, will help predict the spike time of the other by penalized likelihood models

A, D: distribution of which model can better mimic real spike trails of neighboring pairs (A) or remote pairs (D).
B, E: distribution of peak interaction delays of pairs of neighboring pairs (B) or remote pairs (E).
C, F: distribution of ranges of significant cell interaction delays of pairs of neighboring pairs (C) or remote pairs (F).

Figure 6 Complex spikes during a skilled reaching task
A: waveform of complex spikes and simple spikes of one Purkinje cell.
B: cross-correlogram of complex spikes and simple spikes. Simple spikes are inhibited by complex spikes during tens of milliseconds.
C: rasters and average firing of this cell during task. All 18 trials in one session are aligned to time of 'lift'. Simple spikes are shown in black; Complex spikes are shown in red.
D: average cross-correlogram of complex spikes pairs.
E: time course of average firing rate during 'lift' for complex spikes of Purkinje cells.

Figure 7 synchronous firing of neighboring Purkinje cells during sleep and active exploration.
A: waveforms, auto-correlations of one Purkinje cell pair during sleep.
B: cross-correlogram of the cell pair shown in A.
C: z score plot of cross-correlation of all neighboring Purkinje cell pairs.
D: histogram of significant positive (shown in red) and negative (shown in red) cross-correlation for each bin time
E: average cross-correlation of all neighboring Purkinje cell pairs during sleep.
F: average cross-correlation of all distant Purkinje cell pairs during sleep.
G: average cross-correlation of all neighboring Purkinje cell pairs during active exploration.
H: average cross-correlation of all distant Purkinje cell pairs during active exploration.
I: comparison of average peak of cross-correlation between 3-5 ms of neighboring and distant Purkinje cell pairs across different states.

Figure 8 High frequency oscillations in local field potential across different vigilance states.

A: spectrum analysis of local field potential in motor cortex during one session.

B: histogram of peak frequency of high frequency oscillation during sleep.

C: coherence analysis of LFPs recorded in neighboring sites in Purkinje cell layer during one session

D: coherence analysis of LFPs recorded in distant sites in Purkinje cell layer during one session

E: spectrum analysis of local field potential during one active exploration session.

F: histogram of peak frequency of high frequency oscillation during active exploration.

G: comparison of peak frequency and peak amplitude of high frequency oscillation observed in local field potential across two states. Data during sleep are shown in purple. Data during active exploration are shown in red.

H: comparison of average peak of cross-correlation between 3-5 ms of neighboring and distant Purkinje cell pairs across different states.

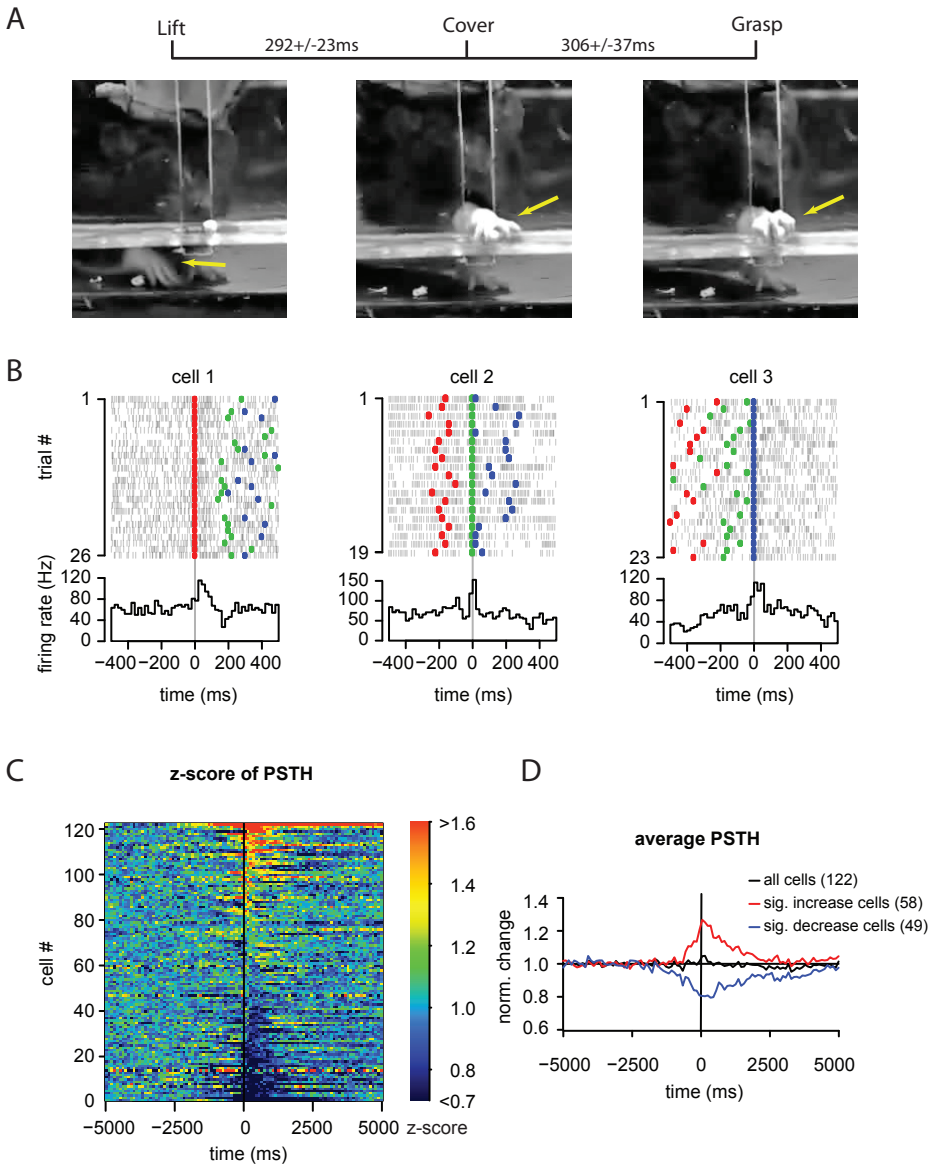
A
Lift
Cover
Grasp
292+/-23ms
306+/-37ms
B
cell 1
cell 2
cell 3
trial #
firing rate (Hz)
time (ms)
C
z-score of PSTH
cell #
time (ms)
z-score
D
average PSTH
all cells (122)
sig. increase cells (58)
sig. decrease cells (49)
norm. change
time (ms)

Figure 1

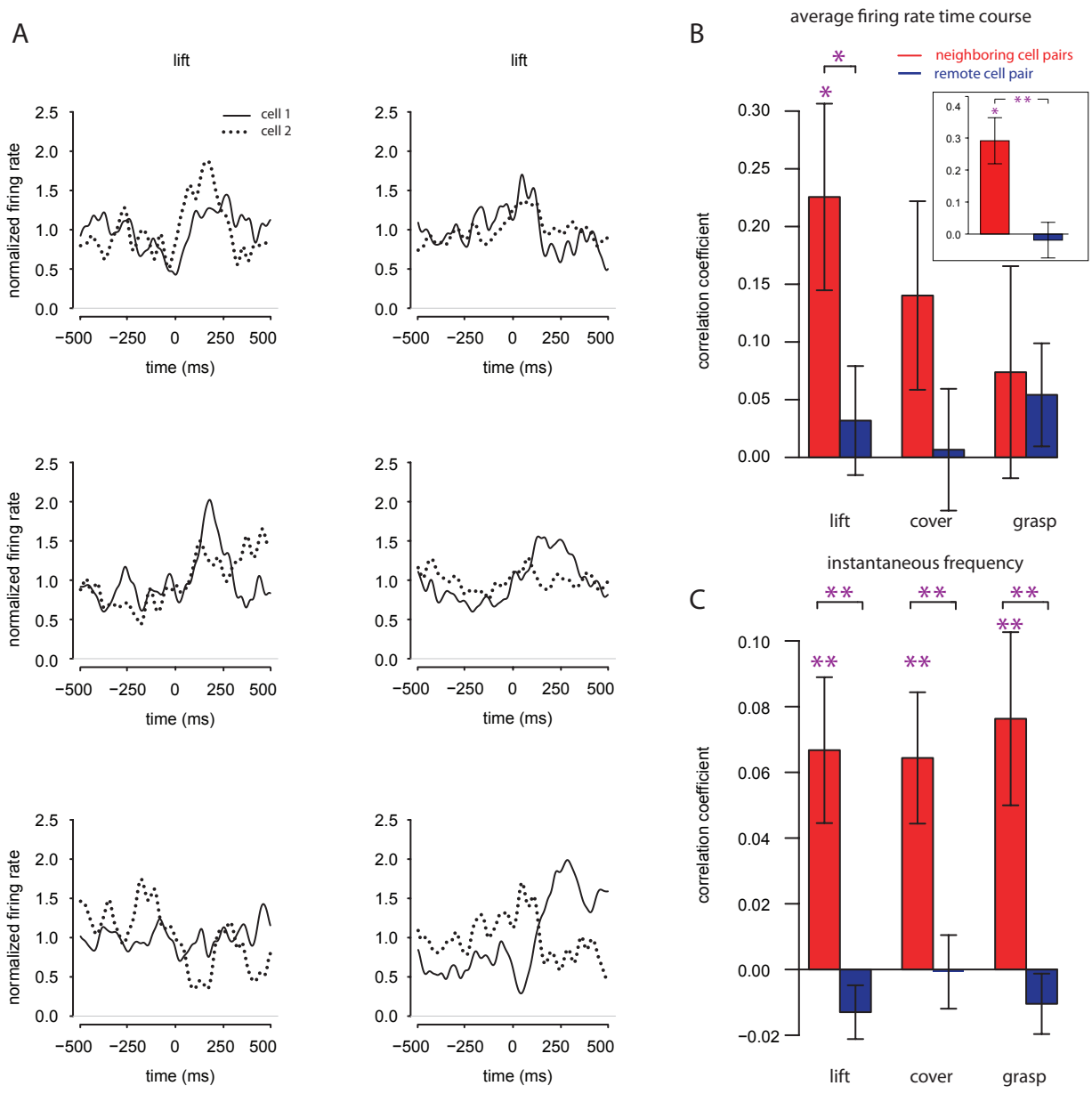
A
lift
lift
cell 1
cell 2
normalized firing rate
time (ms)
B
average firing rate time course
neighboring cell pairs
remote cell pair
correlation coefficient
lift
cover
grasp
C
instantaneous frequency
correlation coefficient
lift
cover
grasp

Figure 2

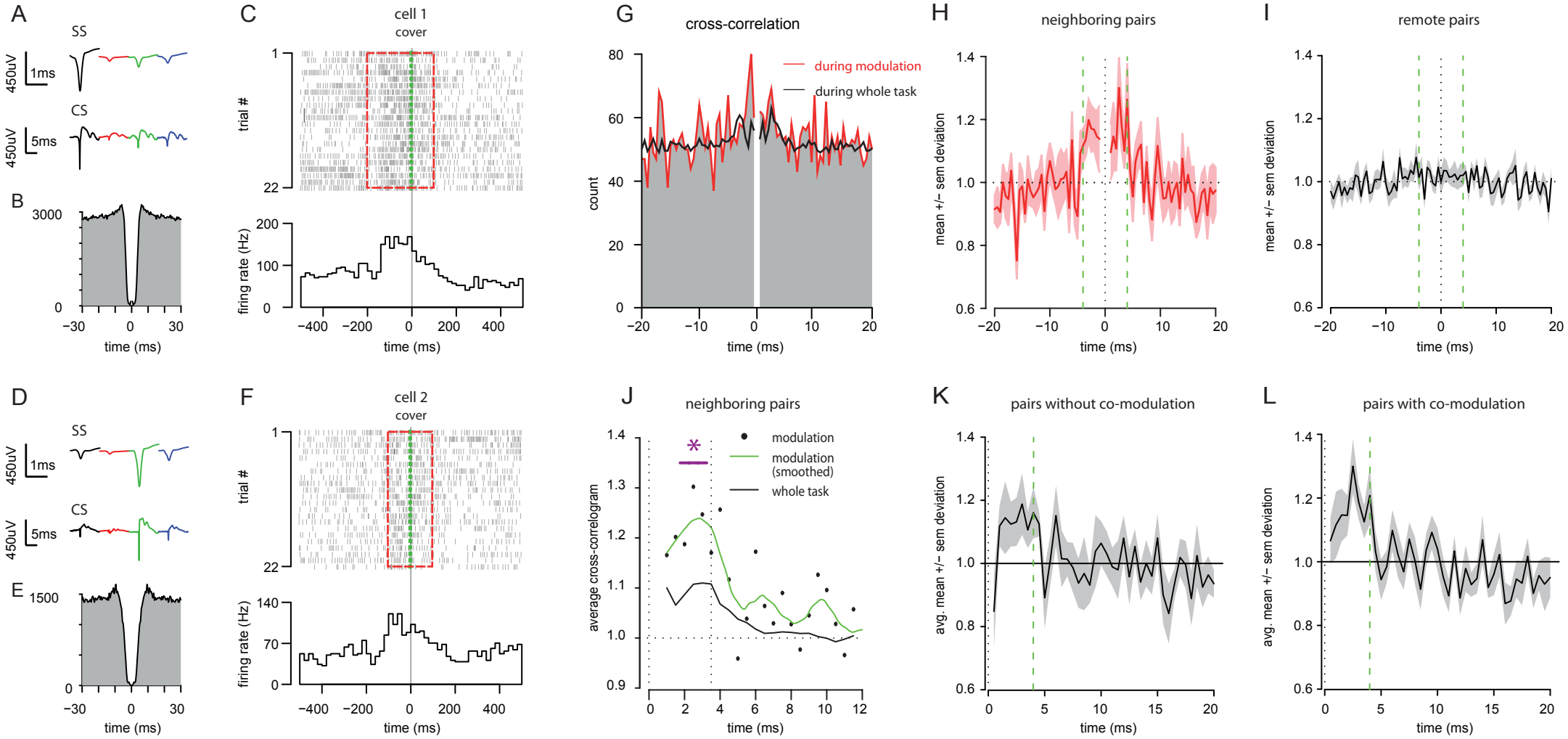
A
SS
450uV
1ms
CS
450uV
5ms
B
3000
0
−30
0
30
time (ms)
C
cell 1
cover
trial #
1
22
firing rate (Hz)
200
100
0
−400
−200
0
200
400
time (ms)
G
cross-correlation
during modulation
during whole task
count
80
60
40
20
0
−20
−10
0
10
20
time (ms)
H
neighboring pairs
mean +/− sem deviation
1.4
1.2
1.0
0.8
0.6
−20
−10
0
10
20
time (ms)
I
remote pairs
mean +/− sem deviation
1.4
1.2
1.0
0.8
0.6
−20
−10
0
10
20
time (ms)
D
SS
450uV
1ms
CS
450uV
5ms
E
1500
0
−30
0
30
time (ms)
F
cell 2
cover
trial #
1
22
firing rate (Hz)
140
70
0
−400
−200
0
200
400
time (ms)
J
neighboring pairs
modulation
modulation (smoothed)
whole task
average cross-correlogram
1.4
1.3
1.2
1.1
1.0
0.9
0
2
4
6
8
10
12
time (ms)
K
pairs without co-modulation
avg. mean +/− sem deviation
1.4
1.2
1.0
0.8
0.6
0
5
10
15
20
time (ms)
L
pairs with co-modulation
avg. mean +/− sem deviation
1.4
1.2
1.0
0.8
0.6
0
5
10
15
20
time (ms)

Figure 3

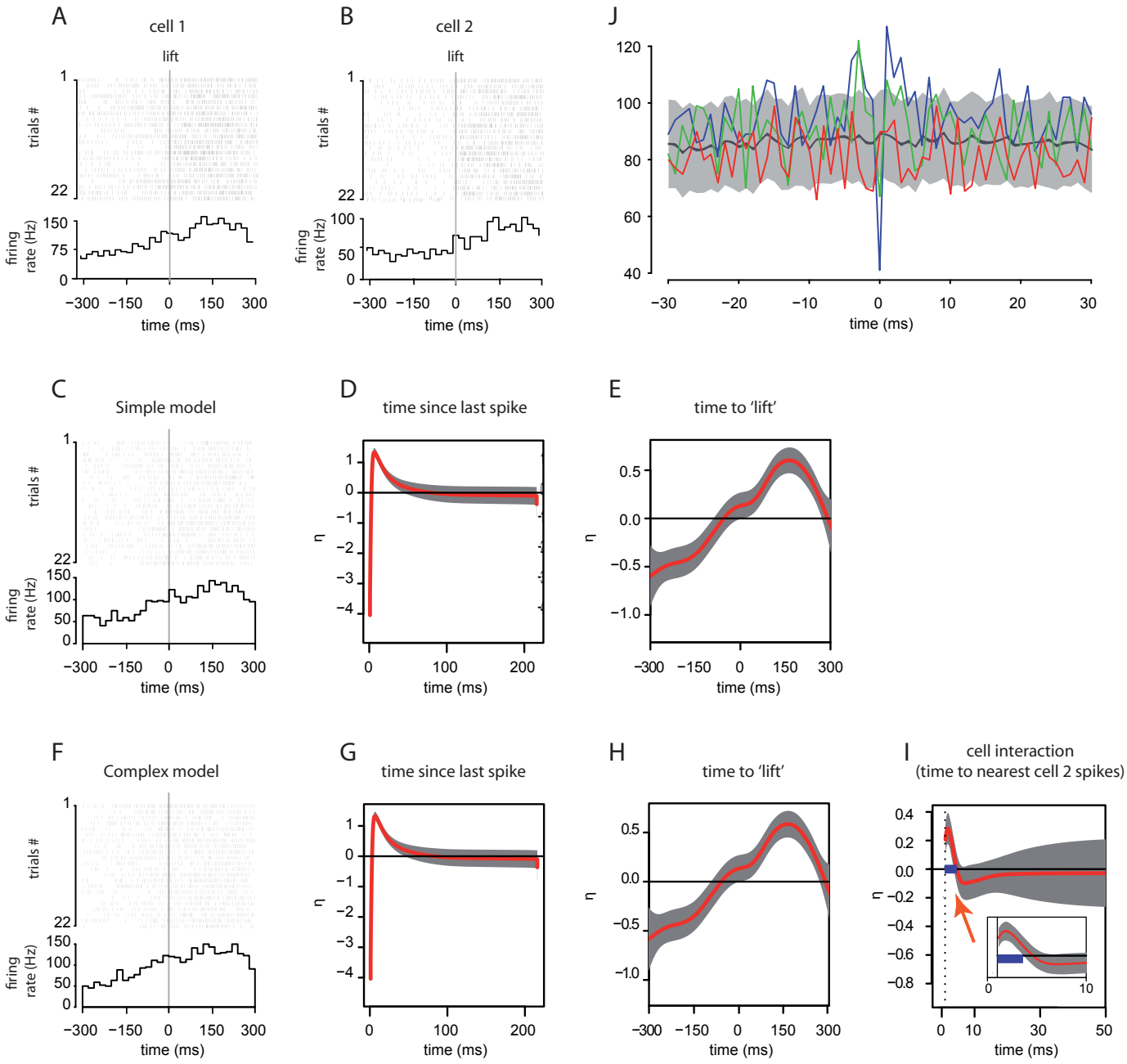
A
cell 1
lift
trials #
firing rate (Hz)
time (ms)
B
cell 2
lift
J
time (ms)
C
Simple model
D
time since last spike
η
E
time to 'lift'
F
Complex model
G
time since last spike
H
time to 'lift'
I
cell interaction
(time to nearest cell 2 spikes)

Figure 4

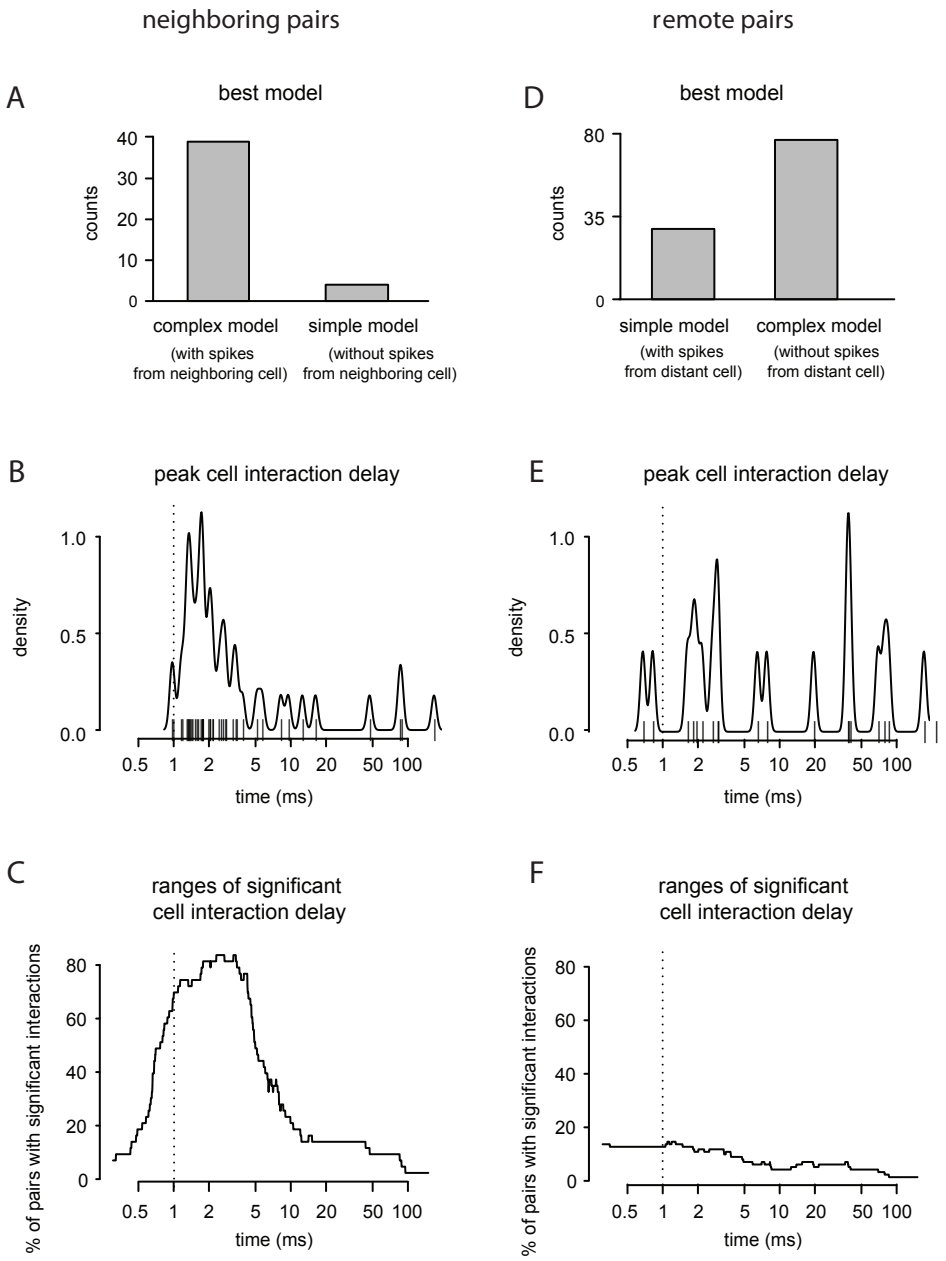
neighboring pairs
remote pairs
A
best model
counts
40
30
20
10
0
complex model
(with spikes
from neighboring cell)
simple model
(without spikes
from neighboring cell)
D
best model
counts
80
35
0
simple model
(with spikes
from distant cell)
complex model
(without spikes
from distant cell)
B
peak cell interaction delay
density
1.0
0.5
0.0
0.5 1 2 5 10 20 50 100
time (ms)
E
peak cell interaction delay
density
1.0
0.5
0.0
0.5 1 2 5 10 20 50 100
time (ms)
C
ranges of significant
cell interaction delay
% of pairs with significant interactions
80
60
40
20
0
0.5 1 2 5 10 20 50 100
time (ms)
F
ranges of significant
cell interaction delay
% of pairs with significant interactions
80
60
40
20
0
0.5 1 2 5 10 20 50 100
time (ms)

Figure 5

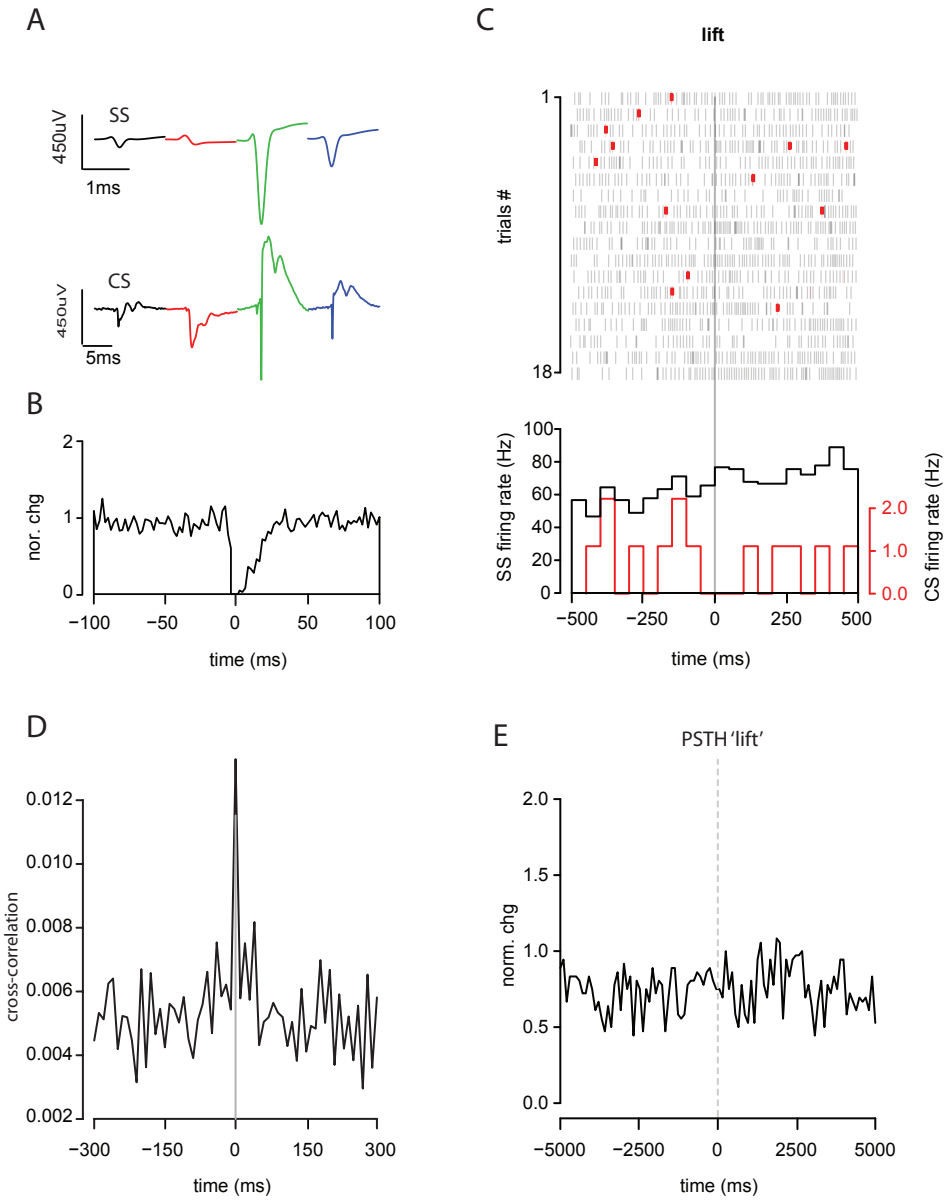
A
SS
450uV
1ms
CS
450uV
5ms
B
nor. chg
2
1
0
−100
−50
0
50
100
time (ms)
C
lift
trials #
1
18
SS firing rate (Hz)
100
80
60
40
20
0
2.0
1.0
0.0
CS firing rate (Hz)
−500
−250
0
250
500
time (ms)
D
cross-correlation
0.012
0.010
0.008
0.006
0.004
0.002
−300
−150
0
150
300
time (ms)
E
PSTH 'lift'
norm. chg
2.0
1.5
1.0
0.5
0.0
−5000
−2500
0
2500
5000
time (ms)

Figure 6

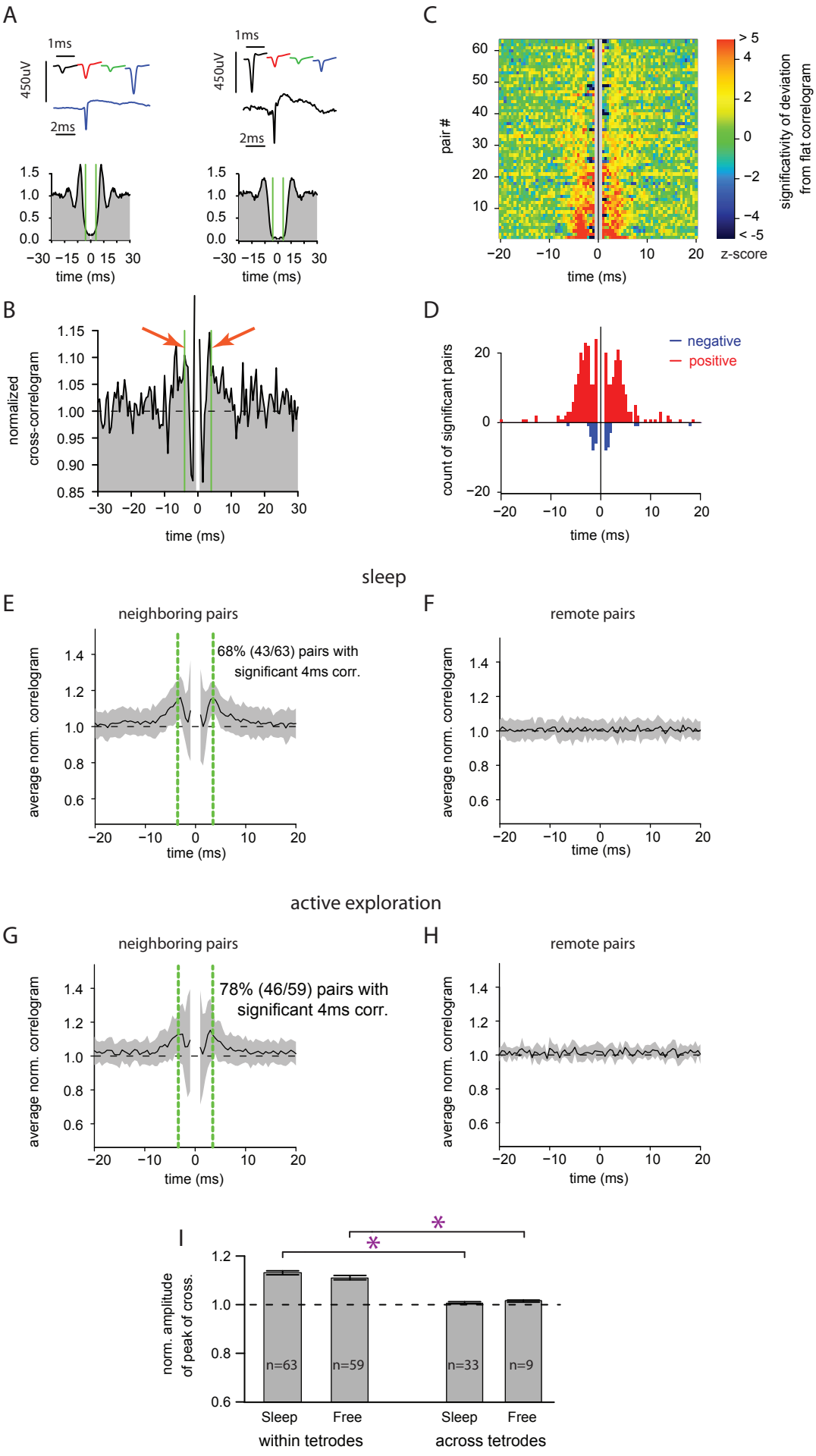
A
1ms
450uV
2ms
time (ms)
B
normalized cross-correlogram
time (ms)
C
pair #
time (ms)
significativity of deviation from flat correlogram
z-score
D
negative
positive
count of significant pairs
time (ms)
sleep
E
neighboring pairs
68% (43/63) pairs with significant 4ms corr.
average norm. correlogram
time (ms)
F
remote pairs
average norm. correlogram
time (ms)
active exploration
G
neighboring pairs
78% (46/59) pairs with significant 4ms corr.
average norm. correlogram
time (ms)
H
remote pairs
average norm. correlogram
time (ms)
I
norm. amplitude of peak of cross.
n=63
n=59
n=33
n=9
Sleep
Free
Sleep
Free
within tetrodes
across tetrodes

Figure 7

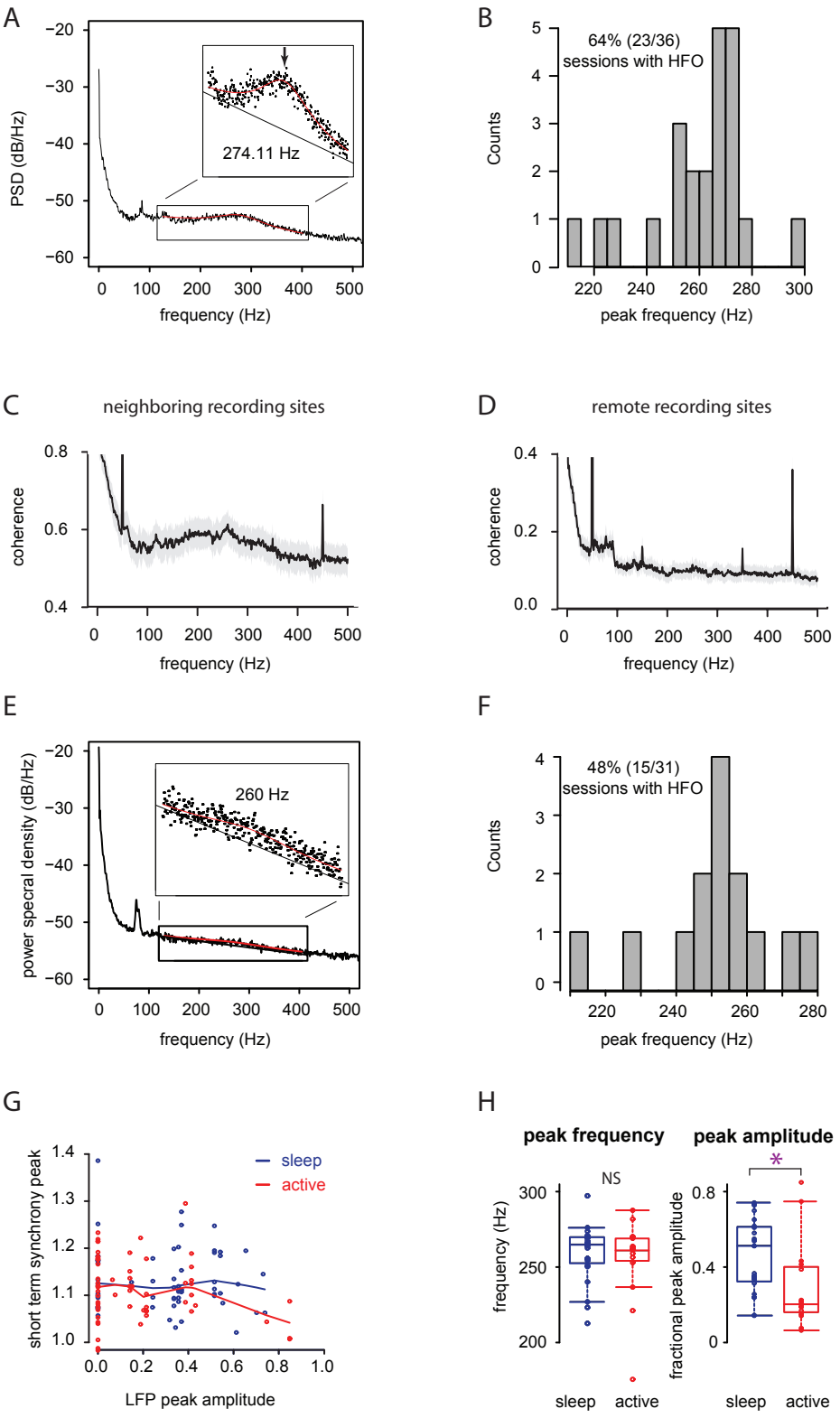
A
PSD (dB/Hz)
274.11 Hz
frequency (Hz)
B
64% (23/36)
sessions with HFO
Counts
peak frequency (Hz)
C
neighboring recording sites
coherence
frequency (Hz)
D
remote recording sites
coherence
frequency (Hz)
E
power specral density (dB/Hz)
260 Hz
frequency (Hz)
F
48% (15/31)
sessions with HFO
Counts
peak frequency (Hz)
G
short term synchrony peak
sleep
active
LFP peak amplitude
H
peak frequency
peak amplitude
NS
*
frequency (Hz)
fractional peak amplitude
sleep
active
sleep
active

Figure 8

Third article

Penetrability of 4-12 Hz oscillations across the cerebellar cortex layers in the awake rat

Maxime Lévesque[1*]

HongYing Gao[2*]

Carla Paz Arasanz[1]

J.M. Pierre Langlois[3]

Clément Léna[2]

Richard Courtemanche[1]

[1]Department of Exercise Science & FRSQ Groupe de Recherche en Neurobiologie Comportementale/Center for Studies in Behavioral Neurobiology (CSBN) Concordia University, Montréal (Qc) Canada, H4B 1R6

[2]Institut de Biologie, IBENS UMR 8197 – U 1024, École Normale Supérieure, Paris Cedex 05, France, 75230

[3]Département de Génie Informatique et Génie Logiciel, École Polytechnique, C.P. 6079, Succ. Centre-Ville, Montréal (Qc), Canada, H3C 3A7

[*]These authors contributed equally to this work.

Abbreviated title: Influence of GCL oscillations across the cerebellar cortex
40 text pages, 7 figures, 1 table
Abstract: 231 words, Introduction: 1144 words, Discussion: 2296 words, Total: 8307 words.

Corresponding author: Richard Courtemanche, Ph.D.
Center for Studies in Behavioral Neurobiology
Department of Exercise Science
SP-165-17, Richard J. Renaud Science Complex
7141 Sherbrooke Street West
Concordia University
Montréal (Qc) Canada H4B 1R6
Phone: (514) 848-2424 ext. 3302
Fax: (514) 848-8681
e-mail: rcourt@alcor.concordia.ca

Abstract

There is an increasing amount of evidence for the variety, richness and influence of cerebellar oscillations in neuronal coding and in neuronal population formation. One type of oscillation present during awake immobility, the 4-12 Hz rodent cerebellar cortex granule cell layer-specific local field potential (LFP) oscillations, could influence network operations and cell firing across the cerebellar networks. Granule cell layer (GCL) LFPs and simultaneous single neuron activity were studied during LFP oscillatory periods in the cerebellar cortex of rats at rest. During those oscillations, about 30 % of the Golgi cells and 25 % of the Purkinje cells were phase-locked and displayed a clear phase relationship with the LFPs. In contrast, most Golgi cells and Purkinje cells did not show strong oscillatory firing patterns. During LFP oscillatory episodes, spike firing occurred during a particular phase of the cycle, which, for most of the Golgi and Purkinje units, was around the peak of the LFP cycle. Overall, our results present a remarkable constancy of the oscillatory influence on unit discharge when transitioning from the granule cell layer to the Purkinje cell layer. In the resting state, GCL LFP oscillations appear to influence neural population patterns and could prepare population activity for an upcoming phasic sensory or motor change. The GCL LFP oscillations in the resting state could have an important neural network shaping capacity serving as a neural baseline for cerebellar operations.

Introduction

With its impressive regularity and massively parallel circuits, the cerebellar cortex has been the subject of elaborate scientific inquiry, for determining the fine details of its singular anatomy, but also notably in determining its inherent operations supporting the flow of information (Eccles et al. 1967; Ito 2010; Llinás et al. 1981; Llinás et al. 2004; Voogd and Glickstein 1998). The cerebellar cortex presents many recurrent circuits that could harbor rhythmic activity (Isope et al. 2002), even if such a fact had previously been held in doubt (Bullock 1997). In truth, the cerebellar cortex is a structure that has shown an impressive array of oscillatory phenomena *in vivo*. For instance, olivo-cerebellar afferents carry a 6-10 Hz rhythmic signal that can influence the temporal coordination of Purkinje cell complex spikes across the cerebellar cortex (Lang et al. 2006; Lang et al. 1999; Llinás 2009; Welsh et al. 1995). The granule cell layer (GCL) also presents rhythmic activity in its local field potential (LFP), namely at 10-25 Hz in the monkey (Courtemanche et al. 2002; Pellerin and Lamarre 1997), and 4-12 Hz in the rodent (Dugué et al. 2009; Hartmann and Bower 1998; O'Connor et al. 2002). High-frequency oscillations have also been detected in the Purkinje cell and molecular layers (Cheron et al. 2004; de Solages et al. 2008; Middleton et al. 2008). Finally, slower (<1 Hz) oscillations have been recorded in the cerebellar cortex of normal rodents (Ros et al. 2009) and the tottering mouse (Chen et al. 2009). The evidence for how these oscillations from multiple levels of the cerebellar input-output systems could be produced by, or produce an influence on, cerebellar cortex processing has recently been reviewed (D'Angelo et al. 2009; De Zeeuw et al. 2011; de Zeeuw et al. 2008). Overall, these oscillations can influence how cellular elements respond to stimulation or organize into temporary networks (De Zeeuw et al. 2011).

The GCL of the cerebellar cortex shows strong LFP oscillations that are dynamic (D'Angelo et al. 2009). Both oscillations in the 10-25 Hz range in the primate (Courtemanche et al. 2009; Courtemanche and Lamarre 2005; Courtemanche et al. 2002; Pellerin and Lamarre 1997), and the 4-12 Hz range in the rodent (Dugué et al. 2009; Hartmann and Bower 1998; O'Connor et al. 2002) appear in

the attentive immobile state, with a multi-site spatial anisotropy in their synchronization; the LFP synchrony follows a dynamic parasagittal modularity (Courtemanche et al. 2009). In addition, these LFP oscillations could potentially link cerebro-cerebellar interactions (Courtemanche and Lamarre 2005; O'Connor et al. 2002), to the point of influencing motor cortical rhythms (Soteropoulos and Baker 2006). Slower oscillatory phenomena can also link together cerebral and cerebellar networks (Ros et al. 2009; Rowland et al. 2010): the theta and beta bands have been nonetheless heavily studied for dynamically linking distant systems (Buzsaki 2006; Buzsaki and Draguhn 2004; Senkowski et al. 2008). Such oscillatory activity has the potential to be information-rich (Bullock 1997; Senkowski et al. 2008). While the GCL oscillations are readily observable in the LFPs, which should correspond to local or synaptic input activity (Buzsaki and Draguhn 2004), the fact that they can synchronize with cerebral cortex oscillations via recurrent loops (Allen and Tsukahara 1974; Voogd and Paxinos 2004) begs to the fact that the GCL oscillations must have an influence on the cerebellar cortex downstream units.

The network-shaping capacity of those oscillations could be a basic property of the networks corresponding to various states (Llinás 2001). An example are the “up and down states” such as seen in cerebral cortex and basal ganglia (Stern et al. 1998; Wilson and Kawaguchi 1996). An analogous bi-stability phenomenon has been recently identified in the Purkinje cell, providing for a difference in responsivity of those neurons, affecting cerebellar processing (Loewenstein et al. 2005; Schonewille et al. 2006; Shin et al. 2007), and a slower rhythmicity influence on units (Ros et al. 2009). From a circuit perspective, faster oscillatory phenomena can be seen as an extension of the state effect, felt by the network on faster timescales (Buzsaki 2006). In the monkey and rodent, GCL oscillations in the theta and beta ranges appear related to the behavioral correlate of an awake, immobile, yet attentive animal that is “ready” and monitoring the environment (Courtemanche et al. 2002; Dugué et al. 2009; O'Connor et al. 2002; Pellerin and Lamarre 1997).

It is also an open question how far the GCL oscillations can exert their influence across the cerebellar cortex. If these oscillations are linked to cerebral cortex oscillations, there must be a neural

signature across the cerebellar cortex units. Can these oscillations influence the cerebellar cortex Purkinje cells, or does their influence remain into the GCL? The GCL oscillations do not have a readily established substrate, though some elements have been postulated (Courtemanche et al. 2002; D'Angelo and de Zeeuw 2009; Maex and De Schutter 2005). They definitely influence granule cell firing (Courtemanche et al. 2002; Hartmann and Bower 1998; Pellerin and Lamarre 1997). In fact, granule cells appear to have rhythm-permissive cellular properties (D'Angelo et al. 2001), and could be part of a resonant network (D'Angelo et al. 2009). Overall, there are a few hints that show that the GCL has intrinsic circuit oscillatory capacities, such as shown in network modeling (Dugué et al. 2009; Honda et al. 2011; Maex and De Schutter 2005). For instance, feedback loops (via mossy-granule-Golgi cell interactions) and feedforward circuits (via mossy-Golgi-granule interactions) could generate or at least resonate oscillations. Such interactions imply that Golgi cells would also be entrained by the rhythm. Golgi cells also appear to have cellular properties that could entrain or maintain rhythmicity in the GCL (D'Angelo 2008; Dugué et al. 2009; Forti et al. 2006; Galliano et al. 2010). Golgi cells can synchronize their activity through electrical synapses, forming local networks that can participate in the rhythm formation (Dugué et al. 2009; Vervaeke et al. 2010). Despite preliminary reports (Courtemanche et al. 2002), however, the quantitative extent of the relationship of LFP oscillations with non-granule GCL neurons or Purkinje cells is still not firmly established, so their influence might stay fairly local.

This report focuses on the relationship between units recorded using single sharp tungsten electrodes (or tetrodes) and the simultaneously recorded GCL LFPs in the awake rat. We recorded from Golgi cells spikes and Purkinje cell simple spikes and evaluated their firing patterns during 4-12 Hz GCL LFP oscillations. A first hypothesis was that cell firing in the cerebellar cortex would be related to those oscillations, meaning that the oscillatory phenomenon would have a strong enough influence on the cell subpopulations to influence cell firing; a second hypothesis was that the Golgi cell firing would be more phase-locked to the oscillatory LFPs than the Purkinje cell simple

spike firing, since the local circuits in the GCL might preserve the oscillatory influence better than the diverging/converging connections from the GCL reaching the Purkinje cells.

Materials and methods

Animals and behavior

Seven (7) male Sprague-Dawley rats (4 rats/Charles River, St-Constant, QC; 3 rats/Institut de Biologie vivarium, École Normale Supérieure - ENS, Paris, France, ~ 400-500 g) were initially handled to remain calm in the recording environment. Once implanted, they were housed individually on an 8:00 AM to 8:00 PM reversed light/dark schedule in the Concordia University (4 rats) or the École Normale Supérieure Institut de Biologie (3 rats) animal care facilities. Recording sessions were conducted in a 28L x 22W x 20H cm test chamber (Lafayette Instruments, Lafayette, IN), or in a small open opaque dark plexiglas field arena. Rats were kept in the test area for a period of one to two hours, in relative dim-lighting conditions, and most subjects explored the area for the first few minutes, until they calmed down and kept relatively immobile. They were kept attentive by the experimenter. All animal handling, care and surgical procedures were in accordance with the guidelines of the respective animal welfare councils (Canada: CCAC, approved by the Concordia University Animal Research Ethics Committee; France: in compliance with national and European laws and policies, approved by the École Normale Supérieure).

The surgery and electrophysiological methods followed were similar to Dugué et al. (2009) and Gao et al. (2011). At Concordia, rats were mounted with a Neuralynx 12-drive electrode holder (Bozeman, MO) for recordings in the posterior cerebellum; at ENS, animals were mounted with one to four quartz tetrodes for access of the cerebellar cortex.

General surgery measures

Very similar procedures were followed for surgery at the two institutions.
Body temperature was continuously monitored with a rectal probe and maintained with a heating pad. Rats were mounted on a stereotaxic instrument so that lambda and bregma lay in the same horizontal plane. General anesthesia was induced for certain rats with an i.m. injection of ketamine hydrochloride

(Ketaset, 100 mg/kg) and xylazine (AnaSed, 2.2 mg/kg) and maintained by supplemental injections as required. Other rats were initially anesthetized with a ketamine-xylazine mixture, and maintained with a mixture of isoflurane (0.5–1.5%) and oxygen. To reduce bronchial secretions, certain rats were injected with 0.04 mg/kg s.c. of atropine sulfate before inducing anesthesia. The skull and dura over the posterior cerebellum were removed using a dental drill and precision forceps. A headstage was implanted and fixed in the skull just above the cerebellar cortex with dental cement. At the end of surgery, the wound was carefully sutured and covered with antibiotic cream. After surgery, animals were allowed to recover several days before recording.

Recordings with multiple single electrodes (Concordia)

Multiple single electrode implantation was made using a Neuralynx 12-drive headstage (Neuralynx, Bozeman, MT), with 6 screws serving as anchors into the frontal and parietal bones. The implantation target was at Bregma -12, Lateral 2.5 to 3, aiming for the crus II/paramedian lobule. One bone screw served as the ground contact and a stainless-steel needle (19 G) placed in brain tissue served as reference. Tungsten microelectrodes with shank diameters of 75 μM and impedances around 1 MΩ (0.2-1.5 MΩ – FHC Inc., Bowdoin, ME) were inserted into individual drives, mounted into the headstage. Each microelectrode could be moved independently using a small screwdriver to advance-retract the electrode, into the cerebellum, at any time. Between three and seven electrodes were implanted in each rat.

Both local field potentials (LFP) and single isolated units were recorded simultaneously. LFP data were on-line filtered between 1 and 475 Hz and sampled at 2003 Hz. Multiunit and single unit activity were filtered between 600 and 6000 Hz and sampled at 32 kHz. Spike isolation was achieved by slowly moving the electrode tip, lowering or retracting the individual microdrives (160 μm/turn precision, with increments of about ¼ or ½ turn), and achieving spike isolation from (a) the oscilloscope and sound output for the general waveform of the spike and corresponding spike sound

coming from the amplifiers, before digitization, and (b) from the Neuralynx DAS software 32-point digitized thresholded waveform, overlaid to verify reproducibility. A single unit would be isolated at a time, from the noise on one microelectrode, and rarely 2 spikes could be isolated simultaneously on a given electrode. Methods for LFP and unit recordings closely followed published procedures (Dugué et al. 2009).

Recordings with tetrodes (ENS)

Tetrodes were implanted in a lightweight tetrode headstage holding multiple microdrives, each with a reference and one to four quartz tetrodes. The microdrives were moved via a cubic screw mounted on a threaded rod. Tetrodes were protected by a stainless steel tube and a 30 G beveled guide tube. Drives were enveloped in a grounded conic piece of cardboard and aluminium foil. Quartz tetrodes from Thomas Recording GmbH (Giessen GER) were used, constructed as 4 platinum/tungsten-cores in a quartz rod, sculpted with a sharp tip. The tips of the tetrodes were cleaned and gold-plated to lower their impedance to 0.1-0.3 MΩ.

Extracellular potentials were acquired with a Tucker-Davis Technologies System 3 (TDT, Alachua, FL). The signal from each channel was first filtered 0.1 Hz to 8 kHz with a Butterworth filter, then differentially amplified, sampled at 25 kHz, and stored to disk for off-line analysis. During tetrode adjustment and recordings, the activities of cerebellar neurons were continuously monitored through loudspeakers and displayed on a computer screen monitor. To isolate spikes, continuous wide-band extracellular recordings were first filtered off-line with a two-pole Butterworth 500 Hz high-pass filter. Spikes were then discriminated by thresholding the filtered trace and extracting the main parameters of their waveform (width and amplitude on the 4 channels). LFPs were also recorded from the same signal, with the initial tetrode signal downsampled at xx Hz and filtered with a low-pass filtered at yy Hz. Methods for LFP recordings and unit identification closely followed published procedures (de Solages et al. 2008; Gao et al. 2011).

Recordings of LFP oscillations and single unit activity

Quality of the LFPs was evaluated so that each LFP was free of sector noise, or was affected by artifact. The quality of the LFP oscillations would be sensitive to tip displacement across the layers. As the microelectrode progressed through the layers, it was stopped at the level of clear-cut GCL activity with oscillatory LFPs. When it was possible to isolate a putative Golgi cell, the electrode would be further adjusted: however, if not, the electrode would be left at the recording site. The other microelectrodes could then be independently moved to seek other units. LFP activity was monitored on-line for oscillatory quality, supported by the audio signal from multiunit activity, phasically related to the LFPs during oscillatory episodes. Data was recorded during quiet rest, as the rat stayed quiet without apparent movement, but kept periodically attentive by providing small food pellets and water in the recording area, for durations of up to 90 min. As this study was about the rest condition, optimal for 4-12 Hz LFP oscillations, periods when the rat was grooming or exploring the area were removed from the analysis, and movement artifacts were taken out. Recordings were kept for periods of optimal oscillatory behavior, with our longest recording period lasting 20 min.

Data analysis

Analyses were performed using NeuroExplorer (Nex Technologies, Littleton MA) and MATLAB (MathWorks, Natick MA), the latter with routines based on standardized functions (e.g., signal processing toolbox).

LFPs. Local field potential oscillations were detected using spectrograms, calculated using the discrete short-time Fourier transform to evaluate rhythmicity. In certain cases, coherence spectrograms were also used to evaluate LFP synchronization. For spectogram analysis, data sampled at 2003 Hz were decimated by a factor of 15 after being low-pass filtered by a 100th order FIR filter. The

spectrogram was then elaborated from the dataset, separated into one-s intervals (134 points) to which a Hamming window was applied, and the windows were overlapped by 50%. The discrete Fourier transforms were evaluated over 256 points with zero padding. LFPs were explored to establish detected time periods of strong oscillations, in contrast with periods when oscillations were weaker. To enhance the detection of significant oscillation periods, a gamma correction with a factor of 0.2 was applied to the spectrogram to improve their contrast to random noise. An example of those spectrograms is given in Fig. 2.

A multi-parametric algorithm was then used to identify oscillatory periods in the 4-12 Hz band of the spectrogram. The band of 4 to 12 Hz was chosen in correspondence with rodent GCL oscillations from other *in vivo* studies (Dugué et al. 2009; Hartmann and Bower 1998; O'Connor et al. 2002). For each time window, the algorithm identified the peak frequency in the band of interest and calculated the energy within a 1 Hz band centered on this peak. To be considered a valid candidate, a peak must have met time and frequency domain criteria. The energy within the peak must have been at least 30% of the largest peak within a 60-s window (time domain criterion), and contain at least 40% of the band energy at that time (frequency domain criterion). An oscillatory period was then identified by a succession of peaks with a determinate track in time and frequency. The relative peak intensities must not have varied in time by more than 100% per second, successive peak frequencies must not have varied by more than 7.5 Hz per second, and there must have been a continuous track of candidate peaks at least 5 s long. The parameters listed here were selected through systematic data analysis and had the advantage of standardizing the detection of oscillation events over all data sets, eliminating any bias. The end result was a list of “oscillation periods” throughout the recording file, and interspersed in between those, periods of weaker or no oscillation. Fig. 2 illustrates detected periods for 50 s of recordings, delineated with a red box.

Units. Isolated, identifiable units were sought for these experiments. For single-electrode

recordings, the digitized spike was processed for single-unit identification in SpikeSort (Neuralynx, Bozeman MT) in manual mode. Unit identification was essentially based on the shape of the extracellular action potential. In SpikeSort, the basic template of the spike waveform was estimated from the overlaid spikes (based on > 100 detections), and the spike selection was based on the matching of the spike shapes with this general template. Secondary elements were also used such as the 2-D distribution of the spike amplitude and duration values (e.g., peak height, valley depth, action potential duration), and ISIs of less than 1 ms were removed. Special attention was paid to spike reproducibility, centering on both the amplitude and temporal measures. With this method, the edited spike time series were thus cleaned up, removing potential noise (neural or artifactual), from the spike train. For tetrode recordings, the data were hand-clustered by polygon-cutting in two-dimension projections of the parameter space using Xclust (Matt Wilson, MIT). Parameter space was centered on spike amplitude and width properties. The quality of clustering was evaluated by inspecting the auto-correlograms of the units.

Spike-LFP relationships. Relation between the timing of single-unit activity and LFPs was established by cross-correlating the spike train with events representing detected LFP peaks during oscillatory periods. During those detected periods of oscillation, each spindle was identified and the peak of the LFP was established as a unitary event (Courtemanche et al. 2003), to identify peaks of cycles (FindPeaks, Tom O'Haver, U. Maryland), which was set as the zero delay phase. In order to establish the temporal correlation, the cross-correlation between the LFP peak events and the spike events was calculated, with the LFP used as the reference point (Courtemanche et al. 2003; Courtemanche et al. 2002; Gerstein 1999; Lamarre and Raynauld 1965).

To establish the significance of the spike-LFP relationship, the cross-correlogram between the spikes and the LFP peaks was compared to a spike-shuffled control analysis. In oder to do this , and the number of crossings of the 95% (2 SD) confidence interval of the cross-correlogram between -240 ms and 240 ms (two cycles on each side of the zero, the center LFP peak) was determined. A correlated

spike was established if two peaks, separated by an interpeak delay between 80 ms to 240 ms (i.e., 4-12 Hz), crossed the 95 % line during that period.

The relationship between single-unit activity and LFP activity was established by constructing LFP-triggered histograms of the spike activity (Destexhe et al. 1999). Each spike that occurred within 250 ms of each peak was included in a histogram plotting spike timing relative to the peak of the cycle (10 ms bins). To estimate the significance of correlations between spike timing and the LFP oscillations, for each neuron, we generated control trains of artificial spikes that had random interspike delays but retained exactly the same number of spikes as the actual spike train. For each unit, we produced 50 such different artificial spike trains and computed from them a mean and SD for all LFP-triggered artificial histograms for each 10 msec bin. We then compared the actual recorded spike data with the control spike train data for each neuron. LFP-triggered spike histogram peaks that occurred within 100 ms of the oscillation peak and that had amplitudes that exceeded those of the artificially triggered histogram by 2 SD were considered significant. These estimates were accurate only to two cycles to either side of the LFP peak in question because of the averaging and LFP peak detection method. To determine the phase relationship between the spikes of each neuron and the simultaneously recorded LFP, for each cell with a significant LFP-triggered histogram peak, we also computed the phase of each spike in the train of spikes relative to the 4-12 Hz LFP oscillation cycles. The method used was similar to that of (Perez-Orive et al. 2002), according to the following equation: phase of peak (rad) = [time of peak (in milliseconds) x 2π] /cycle time (in milliseconds). With this analysis, we produced a polar histogram of the spike–LFP phase relationship for each unit. The time domain bins were thus converted to angular values, from LFP oscillation peak (0°) to the next peak (360°- or 0°). The highest peak in this polar histogram was chosen to describe the timing relationship between the spikes of the neuron and the simultaneously recorded LFP.

Histology

After the last recording session with single electrodes, electrolytic lesions (200 μA, 45 s, anodal) were made in the cerebellar cortex at sites where oscillations or single units were found, while rats were under ketamine-xylazine anesthesia. Two days later, the rats were deeply anesthetized with ketamine-xylazine and perfused through the heart using a buffered 10% formalin – 0.9% saline solution. The brains were removed and kept in 10% formalin for at least 48 hours. They were then put in a 20% sucrose-formalin solution for another 48 hours. The brains were frozen in pulverized dry ice and then sliced in a cryostat. The 40-μm thick sections were mounted on glass slides coated with gelatin. The slides were stained using a Cresyl Violet solution. The location of the lesions were evaluated following the denomination in the Paxinos and Watson atlas (1998) and electrode tracks were reconstructed for localization of recording sites.

Results

A total of 7 rats were used in this study. The recordings were made as the animal was in a quiet, attentive state, the optimal behavior to capture cerebellar cortex GCL oscillations. The animals had been habituated to the environment, and were kept interested throughout the recording period, which could last between 5 and 20 min. Oscillations would appear in the form of spindles of 4-12 Hz oscillations on one or many electrodes or tetrodes simultaneously. Each microelectrode of the group that was implanted was individually lowered and stopped upon entering the GCL layer to witness GCL oscillations, or when capturing an isolated cell. Electrodes/tetrodes were advanced a few turns everyday, so that gradually, a large expanse of the cerebellar cortex had been recorded; the best locations for recording 4-12 Hz oscillations were deeper in the tracks, in Crus II or the paramedian lobule.

Description of cerebellar cortex GCL oscillations in the awake rodent

Fig. 1 presents an example of a Golgi cell spiking activity in relation to simultaneously recorded

LFPs at three different sites in the posterior lobe cerebellum (three LFP traces, LFP1-3, Fig. 1A). For each trace, the corresponding power spectral density signal was computed and is shown in Fig. 1B. For LFP1, single-unit activity simultaneously recorded with the LFP is shown. For this experiment, the location of electrode #1, corresponding to LFP1, was marked by an electrolytic lesion (Fig. 1C, and inset). The other recording site from a nearby electrode sharing a similar track, LFP2, is also indicated on the histological section, located 0.96 mm above the lesion, in the GCL or the GCL-white matter border. Both LFP1 and LFP2 were thus recorded in the paramedian lobule. LFP3 was recorded in a different plane, at a similar depth as the lesion, yet also in the cerebellar cortex from the neighboring multiunit activity, likely in the anterior copula of pyramis region (not shown). As can be seen from the figure, the simultaneously recorded LFP activity differed at the three individual recording sites. LFP1 and LFP2 appear more similar: these were closer and presumably both in the GCL. A period of oscillatory activity is evident around the midpoint of the recording trace, for LFP1 and LFP2. LFP3 was not oscillatory in the 4-12 Hz range. The power spectral density analysis in Fig. 1B confirms the similar oscillations on LFP1 and LFP2. Golgi unit activity simultaneously recorded with the LFP1 oscillations showed bursts occurring in-phase with the oscillation cycles.

The GCL oscillations could also affect neighboring electrodes in a synchronous manner. Next, we show an example recording from two electrodes within the posterior lobe GCL, with channel 1 in the paramedian lobule, and channel 2 in Crus II (Fig. 2). The 4-12 Hz LFP oscillations showed waxing and waning qualities, on the two channels, with a relatively fixed frequency (~ 8 Hz, both channels), as can be seen on the power spectral density spectrogram (Fig. 2A-B). Our selected time periods (see Methods) corresponding to periods of strong 4-12 Hz oscillations are shown on the two LFP channels, and two channels would often show simultaneous oscillations. In optimal conditions, these oscillation periods could last several seconds (Fig. 2). Detected spindles (which had to last longer than 3 s) would last on average 4.5 s, and would be present on average 20.9 ± 13.0 % of the total recording time (see distribution on Fig. 2E). During oscillations periods, the 4-12 Hz oscillations could be synchronized

between the two traces, as can be seen on the coherence spectrogram (Fig. 2C-D). In those periods of strong coherence, there was a stabilization of the phase relationship between the two traces. In out-of-oscillation periods, the phase would be much more variable.

Database of units

A total of 207 cells were isolated with the microelectrodes and tetrodes, and recorded simultaneously with the LFPs as the rats were quiet in their enclosure. We managed to capture 142 cells with the simultaneous presence of 4-12 Hz LFP oscillations. Descriptive data on our sample is given in Table 1.

Examples of units. The identified single units had variable extracellular firing properties. During our recordings, these were initially classified based on: (1) the location of the isolated cell with respect to the track and the background activity (i.e., the cerebellar cortex layer), with the typical GCL dense multiunit activity, or the sparser sharp fast-spiking Purkinje cell simple spikes; and (2) the action potential shape and duration, along with the co-occurrence of the occasional complex spike for Purkinje cells. Fig. 3 displays certain typical spike firing characteristics of the units. To further refine our classification, we also used an offline identification method inspired by Vos et al. (1999), which graphically compares the median of the inter-spike interval and the median absolute difference of the ISI (MAD ISI) to identify the groups of spikes corresponding to a given cell type. The median ISI was calculated for 20 consecutive bins of 10 spikes. For the same 20 consecutive bins, the MAD ISI representing the median difference between each ISI and the median ISI was obtained. Fig. 3A provides the clustered distribution of a representative sample of the Golgi and Purkinje cell types. Evident are the differences between our two identified subpopulations of spikes: the two-dimensional spread of the Golgi spike values are more spread out, while the Purkinje cell simple spike values were all aggregated towards the graph origin (Fig. 3A). A representative ISI histogram for a Golgi spike is shown in Fig. 3B, while the equivalent for a Purkinje cell simple spike is shown in Fig. 3C. Using those

methods, out of 207 recorded isolated units, spikes were classified as coming from either putative Golgi cells (n = 46) or Purkinje cells simple spikes (n = 126). Table 1 provides further details about this sample of units. The remaining 34 isolated cells were classified as coming from either Purkinje cell complex spikes (n = 3, easily identified larger spikes with after-ripples coming from Purkinje cell layer or molecular layer), mossy fibres (n = 8) or were classified as isolated spikes from unidentified cells (n = 24), as their respective 2-D median ISI vs. MAD ISI distribution was different from typical Purkinje cell simple spikes or Golgi cell spikes. Overall, our Golgi cells had a mean firing rate around 7 Hz (see Table 1) and a median ISI in the range of the samples described in Holtzman et al. (2006) and Vos et al. (1999). Simple spikes we recorded had a mean firing rate of around 24 Hz.

Spike-LFP relationship analysis: examples

We analyzed if the isolated spikes coming from the different cells followed a specific firing pattern relative to the simultaneously recorded LFP oscillatory cycles. Overall, using the spike-shuffled analysis, 29.6 % (8/27) of Golgi cells were phase-locked with the simultaneous LFP oscillations (see Table 1). A cell showing a significant relationship is shown on Fig. 4A-C. The isolated Golgi spike shows here a clear phase preference for firing in phase with the peak of the LFP (negative is up), during periods of ~ 7 Hz oscillation (Fig. 4A). From the spike-LFP cross-correlation, this cell preferentially fired spikes when the LFP reached its peak, with the hint of a cross-correlation rhythm (Fig. 4B). A similar example is given on Fig. 4D-F, The rhythmicity of the LFP was again strong ~ 7 Hz (Fig. 4D). The cell-LFP cross-correlation was weaker here.

More often located at the edge of the GCL, with the spike-shuffled cross-correlation analysis, we found that 25 % (16/64) of Purkinje cells simple spikes were phase-locked with the LFP cycle (4-12 Hz) recorded in the GCL. An example for two Purkinje simple spikes is shown in Fig. 5. The simple spike in Fig. 5A-C showed firing patterns linked with the simultaneously recorded LFP. The unit fired at a high rate: simple spikes consistently showed a higher firing rate than Golgi units. In the trace

shown (Fig. 5A), the cell fired robustly at the valley of the LFP, which was oscillatory at ~ 9 Hz. The spike-LFP cross-correlation showed many significant peaks, and strong rhythmicity, meaning that many repeated LFP peak – spike events occurred coordinated in time (Fig. 5B). The spike itself also appeared rhythmic, as shown by the multiple peaks in the autocorrelogram (~ 100 ms period, 10 Hz rhythmicity, Fig. 5C).

However, many simple spikes were also weakly or not related to the GCL LFP oscillations. Specifically, the unit shown in Fig. 5D-F fired at a high rate, and in the trace shown, the LFP was rhythmic; however, as shown by the lack of strong significant cross-correlation peaks, and the absent low-frequency rhythmicity in the spike's autocorrelogram (Fig 5E-F), it is clear that this cell was much less related to the GCL oscillatory process.

Table 1 summarizes the overall spike-LFP relationships we saw for the two different types of spikes. Golgi spikes and Purkinje cell simple spikes appeared modulated by 4-12 Hz oscillations (Table 1): About 30 % of the Golgi cells were related to the GCL oscillatory LFPs, while close to 25% of the Purkinje cell simple spikes were related to the GCL oscillatory LFPs.

Spike-LFP phase angles

Analysis of the phase-angle relationship was considered for the units that passed our criteria. The angular distribution for representative units is presented in Fig. 6, and the angular distribution for the group of LFP-related Golgi units and Purkinje simple spikes is presented in Fig. 7.

Golgi cells, example. The LFP-centered histogram and the equivalent angular distribution for the Golgi unit presented in Fig. 4A-C is shown in Fig. 6A-B. These graphs show a modulation of the spiking activity throughout the cycle, and the preferred phase for this unit almost coincident with the peak of the LFP (~ 340°). Thus, while this particular unit could thus fire at many points in the cycle, it appeared more related to the LFP peak.

Golgi cells, population. Fig. 7A-B shows the representation angular values for our sample of LFP oscillation-related Golgi units. The population angular histogram is shown in Fig. 7A. We can see

that the overall population of the Golgi units tended to discharge in phase with the peak of the LFP, even if there is a spread in the population. This population histogram was statistically different from a circular distribution (Omnibus test). The preferred phase (resultant vector for each unit) is shown in Fig. 7B, with a value of n=1 for each Golgi unit. The angular distribution shows that most resultant vectors were in the ascending to peak phase LFP cycle, providing a mean resultant value of 312° on the polar plot.

Purkinje cell simple spikes, example and population. Fig. 6 presents the same Purkinje cell simple spike unit as shown in Fig. 5A-C. This unit also had a particular phasic relationship with the simultaneously recorded LFP. Specifically, this unit tended to fire more around the valley of the cycle, at ~ 150° (Fig. 6C and D). Overall, for this simple spike sample of 30 units, the angular population histogram for Purkinje cell simple spikes is shown in Fig 7C-D. This modulation is more diverse, showing an overall tendency to fire at around 30°, 120°, and 270° values, so in a fairly spread out fashion. However, when considering the resultant vector for the 20 significantly related units, as shown in Fig. 7D, the picture is clearer. The distribution of the resultant vectors shows a greater relationship between 240° and 60°, so in a similar way in the up-phase of the cycle, up until just past the peak. The mean resultant value for this is 352°, so fairly similar to the Golgi spike-LFP relation resultant distribution.

Overall, we mainly found that the firing pattern of both types of units (Golgi and Purkinje cell simple spikes) could follow in a phase-specific fashion the LFPs, which made certain cells of both types susceptible to the oscillatory influence, but not all cells. For the unidentified units, not clearly identified to any specific subpopulation (data not shown), a phase relationship was more difficult to identify. These cells had a great dispersion in their tendency to fire around the cycle, probably due to the fact that the cell type was mixed. As a population, both Golgi units and Purkinje cell simple spikes were spread out around the cycle, but the dominant phase for both types of units was centered around the peak of the oscillation, for most cells that had a significantly related phasic pattern.

Discussion

We have shown that Golgi cells recorded in the GCL of the cerebellum, and Purkinje cell simple spikes, can show phase-locking activity with granular LFP oscillations in the 4-12 Hz frequency range. The phase relationship for both the Golgi and Purkinje cell simple spikes was around the peak of the LFP. The proportion of those cells that were phase-locked was close to or over 25-30% for both types of units, providing evidence that the LFP 4-12 Hz oscillations in the cerebellar cortex of the awake rodent have some predictive capacity in determining the timing of unit firing in the cerebellar cortex.

GCL and Golgi firing under a 4-12 Hz oscillatory influence

We found that over 30% of the Golgi cells tended to follow the 4-12 Hz LFP oscillations in a phase-specific way, and that for the overall population, the tendency was to be aligned with the peak of the LFP. These 4-12 Hz oscillations in the rodent are best recorded in the GCL (Hartmann and Bower 1998; O'Connor et al. 2002), as are the 10-25 Hz cerebellar oscillations in the primate (Courtemanche et al. 2002; Pellerin and Lamarre 1997). This layer specificity is such that during exploration and positioning of the microelectrodes, the oscillatory LFP signal corresponds distinctly in timing with multiunit firing in the GCL, as can be heard through the audio monitor when playing unit activity. This GCL multiunit activity, presumably coming from a combination of mossy fibre activity and granule cell firing, has also been well correlated with the local depolarization during those oscillatory epochs, as recorded using the monopolar LFPs (Courtemanche et al. 2002; Hartmann and Bower 1998). It appears from our current results that those oscillations are also able to trigger the firing of Golgi cells. Those oscillations affecting the Golgi cells could originate from an oscillatory afferent drive, or do so via a resonance mechanism from inside the GCL (Dugué et al. 2009).

Golgi cells receive excitatory afferent input from mossy and parallel fibers (Llinás et al. 2004). This excitation gets to the Golgi cell through a feedforward inhibitory circuit (mossy fiber – Golgi cell)

and a feedback inhibitory loop (mossy fiber – granule cell/parallel fiber – Golgi cell) (Bell and Dow 1967; Llinás et al. 2004). Both these circuits have potential resonance properties. Modelling has shown that the GCL does have 5-30 Hz resonance capacities (Dugué et al. 2009; Maex and De Schutter 2005). These circuits constitute a potential mechanism for the Golgi-LFP phase locking. Overall, this oscillatory pattern could correspond to a pattern of organization of the granule cells-Golgi cells network (D'Angelo et al. 2009; Maex and De Schutter 1998). We now propose that GCL LFP oscillations in the 4-12 Hz range provide a temporal window during which single cell activity could be enhanced, particularly in the Golgi cell network. Indeed, Golgi cell-LFP phase relationships showed that single units tended to discharge in the ascending phase and peak of the recorded cycle in the granule cell layer, which is in agreement with previous results obtained in vivo by Dugué et al. (2009). From a functional perspective, these results suggest that single cell discharge in the Golgi cell network can be predicted based on the cycle of the cerebellar granular oscillation, in the theta frequency range.

On the other hand, while oscillations in neural population can modulate Golgi cell discharges, this pattern of activity could be enhanced by intrinsic properties of elements in the GCL. Both Golgi cell and granule cell intrinsic properties could support these oscillations. Golgi cells provide rythmic inhibition on granule cells and have pacemaking activity in the theta frequency range, with a resonance for input frequencies of 4 Hz (Dieudonné 1998; Forti et al. 2006; Solinas et al. 2007). However, the amount of synaptic noise *in vivo* might obscure the rhythm-generating capacity of Golgi cells; but certainly they are capable of responding to rhythmic input particularly well (Solinas et al. 2007). Certain studies found Golgi cell rhythmicity *in vivo* in the awake animal (Edgley and Lidierth 1987), and in the anesthetized animal certain studies hint at a rhythmicity (Maex et al. 2000; Volny-Luraghi et al. 2002), or some that show clear rhythmicity (Vos et al. 1999). However, in general, Golgi cells can appear rhythmic or non-rhythmic under awake conditions. Their capacity to follow network rhythmicity, even if skipping a few cycles, might be explained by the synaptic noise that prevents reaching firing threshold in a synchronized way, while the membrane potential can follow a baseline

rhythmicity (Dugué et al. 2009). Golgi cell firing rhythmicity might require specific network conditions, such as synchronized afferent parallel fiber input (Maex et al. 2000). In addition, their capacity to be electrically coupled would greatly influence the formation of Golgi populations following the rhythm (Dugué et al. 2009). The Golgi cells, however, are not the only ones in the GCL showing certain properties conducive to oscillatory entrainment; in addition, granule cells also show specific properties of resonance at slow (best: ~ 9 Hz) frequencies (D'Angelo et al. 2001). Those cellular properties, along with local circuit connections, provide a capacity of the GCL to generate or maintain a rhythm through granule-Golgi interactions. As it was previously suggested, by controlling granular oscillations, Golgi cells could influence the spatio-temporal organization of information processing and storage in the granule cell layer (D'Angelo 2008; D'Angelo et al. 2009). While we saw only a tendency, the possibility that the faster the firing rate of a Golgi cell, the earlier that it would discharge relative to the LFP cycle warrants further study, as this phenomenon is not without reminding the one of phase precession (Pastalkova et al. 2008).

Extending further into the cerebellar cortex: Purkinje cell simple spike firing under a 4-12 Hz oscillatory influence

According to our results, the 4-12 Hz oscillatory phenomenon can influence neurons outside of the GCL, as many simultaneously recorded Purkinje cell simple spikes were phase-related to the oscillations. When related, they displayed a more varied pattern of phase-locking than the Golgi units, but still showed an overall tendency, as a population, to fire relatively in synchrony with the peak of the LFP oscillation. This has implications for the penetrability of the 4-12 Hz oscillations across the cerebellar cortex layers, a new variable to consider when evaluating cerebellar cortex output which takes place via Purkinje cells. While Purkinje cell simple spikes are clearly related to sensorimotor parameters (Ebner 1998; Heck et al. 2007; Lamarre and Chapman 1986; Shin and De Schutter 2006; Thach et al. 1992), the penetrability of the 4-12 Hz oscillatory phenomenon through the cerebellar

cortex, in a more state-dependent manner, seems apparent at this point, as they appear to be related to Purkinje cell firing. This would mean that under a strong oscillatory influence, units in the GCL and the Purkinje cell layer activity could follow the oscillatory pattern, and establish a basic attentive immobility population pattern. Within the GCL, the network properties thus seem able to receive and maintain the coherent oscillations through resonance mechanisms (D'Angelo et al. 2009). While the properties of interneuron connections emanating from the GCL directly connect could certainly influence Purkinje cell discharge and modulate cerebellar output (Barmack and Yakhnitsa 2008), a spatio-temporal concentration of activity must be operating to garner such an influence despite the divergence between the two layers. A certain amount of flow between the two layers has been established (Santamaria et al. 2007). We could posit that this GCL capacity to excite the Purkinje layer in such a coherent fashion could be related to the spatial arrangement of the connections, especially those coming from the ascending portion of the granule cell axon (Gundappa-Sulur et al. 1999; Isope and Barbour 2002; Llinás et al. 1981; Lu et al. 2005), or via the Golgi cell pattern of connection out of the GCL (Barmack and Yakhnitsa 2008; Sillitoe et al. 2008). These connections could support a coherent temporal representation within a small area between the GCL and the Purkinje layer. In effect, this coherence between the networks could display a sagittal pattern of organization at rest, an influence permeating at both the GCL level during oscillations (Courtemanche et al. 2009), and then infuence in a spatially discrete manner the Purkinje cell layer; through strong anatomical and physiological evidence, this layer has shown heavy parasagittal modularity (Herrup and Kuemerle 1997; Lang et al. 1999). In the case of our own Purkinje cell simple spike recordings, our most frequent pattern of comparison was to relate the GCL oscillations with Purkinje cell firing from a nearby electrode (e.g., from the same guide cannula, thus corresponding to the same sagittal and coronal location). This certainly could favor GCL oscillation – Purkinje simple spike synchrony.

Extending further in and out of the cerebellum

There are a series of mechanisms by which information could flow better through the cerebellar layers using an oscillatory influence (Akam and Kullmann 2010). In addition, the timing of the communication with the cerebellar nuclei could also be optimized using this form of information flow. The particular “pauses” that have been identified in the Purkinje cell firing to the deep cerebellar nuclei could be facilitated by the 4-12 Hz rhythm across the cerebellar cortex (De Schutter and Steuber 2009). This would favor synchronicity of firing towards the nuclei (Jaeger 2011; Walter et al. 2006). As an example, the inhibitory rebound in the cerebellar nuclei, lasting around 200 ms long, fits well with an underlying 5 Hz rhythmicity coming from the cerebellar cortex, as seen *in vitro* (Alvina et al. 2008). In addition, the rhythmicity also fits well with a recovery time constant of the channels CaV3.1 in those same neurons around 100 ms (De Schutter and Steuber 2009; Iftinca et al. 2006; Tadayonnejad et al. 2010). For Purkinje cells, the 10-30 Hz range would also be optimal for synaptic plasticity (Batchelor and Garthwaite 1997).

Comparison with other cerebellar cortex slow oscillatory phenomena

In the cases where one is trying to determine variations in Purkinje cell firing independent of specific movements being performed, i.e., in the cases of state changes and oscillations, Purkinje cell simple spike firing has been found to adapt to excitability state modulation and slow oscillations (Chen et al. 2009; Loewenstein et al. 2005; Ros et al. 2009; Schonewille et al. 2006). In the firing pattern of the cells, and also in the membrane potential variations, the Purkinje cells appear modulated in a bistable way (Loewenstein et al. 2005; Schonewille et al. 2006). This bistability in the awake animal has been questioned (Schonewille et al. 2006), but could by all accounts represent a mechanism influencing the firing patterns of Purkinje cell simple spikes. In a depolarized state, the firing of the Purkinje cell simple spikes would thus be favored, over an hyperpolarized state; the state-switch could be operated on via afferent input/climbing fiber firing. Another factor that appears to affect cerebellar

cortex firing are slow cerebellar oscillations, which are around or less than one Hz (Chen et al. 2009; Ros et al. 2009). The slow oscillations in the cerebellar cortex of the anesthetized rat (~ 1 Hz) and awake mouse (~2-5 Hz) recorded by Ros et al. (2009) are tightly synchronized with the the cerebral neocortical up-states and promote phase-related firing of Golgi cells, granule cells, and Purkinje cell complex spikes, during neocortical up-states. However, they did not find a phasic relationship of Purkinje cell simple spikes with those oscillations. This is in contrast with our own results, but it is unclear at this point how or if both oscillatory phenomena (slow cerebellar oscillations, and the 4-12 Hz oscillations we recorded) are related. Even slower oscillations (< 0.1 Hz) were recorded mainly in the paramedian and Crus II lobules of the tottering mouse using optical imaging, which were related to Purkinje cell firing (Chen et al. 2009). The co-occurrence and influence of all of these oscillatory processes, in various anesthetized and awake states and across species, has not been established.

As we find here that Purkinje cells simple spikes can show phasic relations with the GCL 4-12 Hz LFP oscillations, a comparison with the well-established olivocerebellar rhtyhms at similar frequencies (Lang et al. 1999; Llinás 2009) would indeed be interesting. Unfortunately, because of the small sample of Purkinje cell complex spikes we recorded (n=5), we are unable to affirm a population-level analysis for olivocerebellar activity in relation with 4-12 Hz GCL oscillations. Our small sample size is partly due to our recording context, as we were focusing on recording GCL oscillations, and corresponding unit activity when available, but also with our recording targets, going deep across the layers into the cerebellar cortex. Nevertheless, our small sample did not show phasic relation with simultaneously recorded LFP oscillations, as reported previously in the case of primate 10-25 Hz oscillations (Courtemanche et al. 2002). Similarly, as they are also situated in the Purkinje cell layer, a comparison with faster oscillatory phenomena (de Solages et al. 2008; Middleton et al. 2008) is difficult to establish at this point, but should warrant more extensive review.

In conclusion, we have found that the 4-12 Hz GCL oscillations can indeed predict the firing properties of populations from both Golgi cells and Purkinje cell simple spikes. To our surprise, the

proportion of Golgi cells and simple spikes that were related to the oscillations was remarkably similar (one method of analysis provided the Golgi units to be more strongly related, another method identified the simple spikes as the most related). This raises the non-trivial question of the penetrability of this phenomenon across the cerebellar cortex circuits. In the context of units recorded from a circuit local to the LFP oscillations, it appears as if the GCL oscillations can strongly and predictably influence cell firing, providing a better description of cerebellar cortex firing in the context of immobility, setting the stage for network changes during sensorimotor situations.

Acknowledgements

The authors wish to thank S. Dieudonné for helpful discussions. Special thanks to L. Carmant for the usage of the microscope photographic equipment, and to E. Zuccheroso for help in certain surgeries. Operating grant support for this work was provided by grants from NSERC (Canada) and NAAR/Autism Speaks (U.S.A.) to RC, and ANR grants to CL. Infrastructure support was provided by a FRSQ Group grant to the Groupe de Recherche en Neurobiologie Comportementale (CSBN). ML received FRSQ and NSERC scholarships, and is now at the Department of Neurology and Neurosurgery, Montreal Neurological Institute, McGill University. HYG received ENS scholarships. CA is now at the Dept. of Kinesiology, University of Waterloo.

Figure Captions

Fig. 1. Local field potential 4-12 Hz GCL oscillations recorded in the posterior lobe of the awake rat. A. GCL activity recorded at three different sites (three LFP traces, LFP1, 2 and 3), with corresponding single unit spike train recorded at at the same site as LFP1. Notice the relative similarity between LFP1 and LFP2, with LFP3 being relatively different. Also notice the in-phase spiking for the MU trace relative to LFP1. B: Power spectral density results for each LFP shown in A. C: Lesion made in the paramedian lobule GCL, at the site of recording for LFP1, with the relative localization of the LFP2 recording site. Inset: Magnification (2.5x) of the lesion site.

Fig. 2. Local field potential oscillations at 4-12 Hz in the cerebellar cortex GCL show variable coherence patterns across time. Simultaneous GCL LFP recordings from two microelectrodes within the same cannula, distanced ~3 mm (Chan 1 location, paramedian lobule, Chan 2 location, Crus II). A and B: Simultaneously recorded GCL LFPs (top) and corresponding frequency spectrogram (bottom) showing changes in oscillatory activity through time. LFP trace amplitude z-score normalized, in order to perform oscillatory episode detection. Detected episodes of oscillation represented by the red square box. Frequency spectrogram shown with 1-s windows. C: Coherence spectrogram, 1-s windows, showing 0-50 Hz coherence patterns in time. D: 4-12 Hz Coherence, and corresponding phase lag between the two LFP traces.

Fig. 3. Identification of the Golgi units vs. Purkinje cell simple spikes, based on the firing properties. The method follows the one used by Vos et al. (1999), based on the variability of the cell firing (MAD ISI) vs. its median firing values (Median ISI). A: Representation of two subpopulations of units, Golgi cell units (large ensemble, filled triangles, 6 cells), and Purkinje cell simple spikes (small ensemble, filled circles and losanges, 4 cells), by the relationship between their median inter-spike interval (Median ISI), and the absolute deviation of their median firing inter-spike interval (MAD ISI). B: Inter-spike interval of a representative identified Golgi cell. C: Inter-spike interval of a representative Purkinje cell simple spike.

Fig. 4. Spike-LFP relationship for two different Golgi cell spikes during 4-12 Hz oscillatory LFPs Recordings were acquired from two different animals. A-C: A Golgi spike related to the LFP. A: Simultaneously recorded spike train and LFP. Inset: Power spectral density of the LFP trace shown. B: Cell-LFP cross-correlation, zero being the time of the LFP peak, with the 2 SD dashed horizontal line. C: Cell auto-correlation (only the right side shown). D-F: A Golgi spike not related to the LFP. D: Simultaneously recorded spike train and LFP, with PSD inset. E: Cell-LFP cross-correlation. F: Cell auto-correlation.

Fig. 5. Spike-LFP relationship for two different Purkinje simple spikes during 4-12 Hz oscillatory LFPs. Recordings were acquired from the same animal but on two different days. A-C: A simple spike related to the LFP. A: Simultaneously recorded spike train and LFP. Timescale is different from preceding figure, to better show simple spike firing.

Inset: Power spectral density of the LFP trace shown. B: Cell-LFP cross-correlation, zero being the time of the LFP peak, with the 2 SD dashed horizontal line. C: Cell auto-correlation (only the right side shown). D-F: A Golgi spike not related to the LFP. D: Simultaneously recorded spike train and LFP, with PSD inset. E: Cell-LFP cross-correlation. F: Cell auto-correlation.

Fig. 6. Angular (phase) relation for Golgi units and Purkinje cell simple spikes within the LFP oscillation cycle. A-B: Relation of a Golgi unit firing vs. the LFP cycle. A. In the time domain, with the LFP peak at zero. B. In the phase domain, with the LFP peak at zero deg. This Golgi unit fired more strongly at the peak of the LFP cycle. C-D: Relation of a Purkinje cell simple spike vs. the LFP cycle. C same as in A, while D same as in B. This Purkinje cell fired more strongly at the valley of the LFP cycle.

Fig. 7. Phasic representation for the ensemble of Golgi units and Purkinje cell simple spikes in relation with the oscillatory cycle. A-B: Phase relation for the ensemble of Golgi units. A. Angular histogram for the 12 directionally related Golgi units, centered on the peak of the LFP (zero). There was a tendency for most units to fire at the around the peak of the LFP, with fewer spikes firing in the anti-phase fashion. B. Histogram of the resultant vectors for each of the 12 directionally defined Golgi units. The zero-degree phase value is even more strongly represented. C-D: Phase relation for the ensemble of Purkinje cell simple spikes. C. Angular population histogram for the 20 related units firing simple spikes. The firing pattern of the population is complex and relatively distributed. D. Histogram of the resultant vectors for each of the 20 directionally defined

simple spikes. The picture is here clearer, with most resultant vectors occurring in the ascending phase or the peak of the LFP cycle.

References

Akam T, and Kullmann DM. Oscillations and filtering networks support flexible routing of information. *Neuron* 67: 308-320, 2010.

Allen GI, and Tsukahara N. Cerebrocerebellar communication systems. *Physiological Reviews* 54: 957-1006, 1974.

Alvina K, Walter JT, Kohn A, Ellis-Davies G, and Khodakhah K. Questioning the role of rebound firing in the cerebellum. *Nat Neurosci* 11: 1256-1258, 2008.

Batchelor AM, and Garthwaite J. Frequency detection and temporally dispersed synaptic signal association through a metabotropic glutamate receptor pathway. *Nature* 385: 74-77, 1997.

Bullock TH. Signals and signs in the nervous system: The dynamic anatomy of electrical activity is probably information-rich. *Proc Natl Acad Sci USA* 94: 1-6, 1997.

Buzsaki G. *Rhythms of the Brain*. New York: Oxford University Press, 2006, p. 1-448.

Buzsaki G, and Draguhn A. Neuronal oscillations in cortical networks. *Science* 304: 1926-1929, 2004.

Chen G, Popa LS, Wang X, Gao W, Barnes J, Hendrix CM, Hess EJ, and Ebner TJ. Low-frequency oscillations in the cerebellar cortex of the tottering mouse. *J Neurophysiol* 101: 234-245, 2009.

Cheron G, Gall D, Servais L, Dan B, Maex R, and Schiffmann SN. Inactivation of calcium-binding protein genes induces 160 Hz oscillations in the cerebellar cortex of alert mice. *J Neurosci* 24: 434-441, 2004.

Courtemanche R, Chabaud P, and Lamarre Y. Synchronization in primate cerebellar granule cell layer local field potentials: Basic anisotropy and dynamic changes during active expectancy. *Front Cell Neurosci* 3: 2009.

Courtemanche R, Fujii N, and Graybiel AM. Synchronous, focally modulated beta-band oscillations characterize local field potential activity in the striatum of awake behaving monkeys. *J Neurosci* 23: 11741-11752, 2003.

Courtemanche R, and Lamarre Y. Local field potential oscillations in primate cerebellar cortex: Synchronization with cerebral cortex during active and passive expectancy. *J Neurophysiol* 93: 2039-2052, 2005.

Courtemanche R, Pellerin JP, and Lamarre Y. Local field potential oscillations in

primate cerebellar cortex: Modulation during active and passive expectancy. *J Neurophysiol* 88: 771-782, 2002.

D'Angelo E. The critical role of Golgi cells in regulating spatio-temporal integration and plasticity at the cerebellum input stage. *Front Neurosci* 2: 35-46, 2008.

D'Angelo E, and de Zeeuw CI. Timing and plasticity in the cerebellum: focus on the granular layer. *Trends Neurosci* 32: 30-40, 2009.

D'Angelo E, Koekkoek SK, Lombardo P, Solinas S, Ros E, Garrido J, Schonewille M, and De Zeeuw CI. Timing in the cerebellum: oscillations and resonance in the granular layer. *Neuroscience* 162: 805-815, 2009.

D'Angelo E, Nieus T, Maffei A, Armano S, Rossi P, Taglietti V, Fontana A, and Naldi G. Theta-frequency bursting and resonance in cerebellar granule cells: experimental evidence and modeling of a slow k+-dependent mechanism. *J Neurosci* 21: 759-770, 2001.

De Schutter E, and Steuber V. Patterns and Pauses in Purkinje Cell Simple Spike Trains: Experiments, Modeling and Theory. *Neuroscience* 2009.

de Solages C, Szapiro G, Brunel N, Hakim V, Isope P, Buisseret P, Rousseau C, Barbour B, and Lena C. High-frequency organization and synchrony of activity in the Purkinje cell layer of the cerebellum. *Neuron* 58: 775-788, 2008.

De Zeeuw CI, Hoebeek FE, Bosman LW, Schonewille M, Witter L, and Koekkoek SK. Spatiotemporal firing patterns in the cerebellum. *Nat Rev Neurosci* 12: 327-344, 2011.

de Zeeuw CI, Hoebeek FE, and Schonewille M. Causes and consequences of oscillations in the cerebellar cortex. *Neuron* 58: 655-658, 2008.

Destexhe A, Contreras D, and Steriade M. Spatiotemporal analysis of local field potentials and unit discharges in cat cerebral cortex during natural wake and sleep states. *J Neurosci* 19: 4595-4608, 1999.

Dugué GP, Brunel N, Hakim V, Schwartz EJ, Chat M, Lévesque M, Courtemanche R, Léna C, and Dieudonné S. Electrical coupling mediates tunable low-frequency oscillations and resonance in the cerebellar Golgi cell network. *Neuron* 61: 126-139, 2009.

Eccles JC, Ito M, and Szentágothai J. *The Cerebellum as a Neuronal Machine*. New

York: Spinger-Verlag, 1967, p. 335.

Forti L, Cesana E, Mapelli J, and D'Angelo E. Ionic mechanisms of autorhythmic firing in rat cerebellar Golgi cells. *J Physiol (London)* 574: 711-729, 2006.

Galliano E, Mazzarello P, and D'Angelo E. Discovery and rediscoveries of Golgi cells. *J Physiol* 588: 3639-3655, 2010.

Gao H, Solages CD, and Lena C. Tetrode recordings in the cerebellar cortex. *J Physiol Paris* 2011.

Gerstein GL. Correlation-based analysis methods for neural ensemble data. In: *Methods for Neural Ensemble Recording*, edited by Simon SA, and Nicolelis MAL. Boca Raton FL: CRC Press, 1999, p. 157-177.

Hartmann MJ, and Bower JM. Oscillatory activity in the cerebellar hemispheres of unrestrained rats. *J Neurophysiol* 80: 1598-1604, 1998.

Honda T, Yamazaki T, Tanaka S, Nagao S, and Nishino T. Stimulus-dependent state transition between synchronized oscillation and randomly repetitive burst in a model cerebellar granular layer. *PLoS Comput Biol* 7: e1002087, 2011.

Iftinca M, McKay BE, Snutch TP, McRory JE, Turner RW, and Zamponi GW. Temperature dependence of T-type calcium channel gating. *Neuroscience* 142: 1031-1042, 2006.

Isope P, Dieudonné S, and Barbour B. Temporal organization of activity in the cerebellar cortex: A manifesto for synchrony. *Annals of the New York Academy of Sciences* 978: 164-174, 2002.

Ito M. Cerebellar Cortex. In: *Handbook of Brain Microcircuits*, edited by Shepherd GM, and Grillner S. New York, NY: Oxford University Press, 2010, p. 293-300.

Jaeger D. Mini-Review: Synaptic Integration in the Cerebellar Nuclei-Perspectives From Dynamic Clamp and Computer Simulation Studies. *Cerebellum* 2011.

Lamarre Y, and Raynauld JP. Rhythmic firing in the spontaneous activity of centrally located neurons. A method of analysis. *Electroencephalography and Clinical Neurophysiology* 18: 87-90, 1965.

Lang EJ, Llinás R, and Sugihara I. Isochrony in the olivocerebellar system underlies complex spike synchrony. *J Physiol (London)* 573: 277-279, 2006.

Lang EJ, Sugihara I, Welsh JP, and Llinás R. Patterns of spontaneous Purkinje cell

complex spike activity in the awake rat. *J Neurosci* 19: 2728-2739, 1999.

Llinás RR. *I of the Vortex*. Cambridge MA: MIT Press, 2001, p. 264.

Llinás RR. Inferior olive oscillation as the temporal basis for motricity and oscillatory reset as the basis for motor error correction. *Neuroscience* 162: 797-804, 2009.

Llinás RR, Brookhart JM, and Mountcastle VB. Electrophysiology of the cerebellar networks. In: *Handbook of Physiology - The Nervous System II*. Bethesda, Maryland: American Physiological Society, 1981, p. 831-876.

Llinás RR, Walton KD, and Lang EJ. Cerebellum. In: *The Synaptic Organization of the Brain*, edited by Shepherd GM. New York, NY: Oxford University Press, 2004, p. 271-309.

Loewenstein Y, Mahon S, Chadderton P, Kitamura K, Sompolinsky H, Yarom Y, and Hausser M. Bistability of cerebellar Purkinje cells modulated by sensory stimulation. *Nature Neuroscience* 8: 202-211, 2005.

Maex R, and De Schutter E. Oscillations in the cerebellar cortex: a prediction of their frequency bands. *Prog Brain Res* 148: 181-188, 2005.

Middleton SJ, Racca C, Cunningham MO, Traub RD, Monyer H, Knopfel T, Schofield IS, Jenkins A, and Whittington MA. High-frequency network oscillations in cerebellar cortex. *Neuron* 58: 763-774, 2008.

O'Connor S, Berg RW, and Kleinfeld D. Coherent electrical activity between vibrissa sensory areas of cerebellum and neocortex is enhanced during free whisking. *J Neurophysiol* 87: 2137-2148, 2002.

Pellerin JP, and Lamarre Y. Local field potential oscillations in primate cerebellar cortex during voluntary movement. *J Neurophysiol* 78: 3502-3507, 1997.

Perez-Orive J, Mazor O, Turner GC, Cassenaer S, Wilson RI, and Laurent G. Oscillations and sparsening of odor representations in the mushroom body. *Science* 297: 359-365, 2002.

Ros H, Sachdev RN, Yu Y, Sestan N, and McCormick DA. Neocortical networks entrain neuronal circuits in cerebellar cortex. *J Neurosci* 29: 10309-10320, 2009.

Rowland NC, Goldberg JA, and Jaeger D. Cortico-cerebellar coherence and causal connectivity during slow-wave activity. *Neuroscience* 166: 698-711, 2010.

Santamaria F, Tripp PG, and Bower JM. Feedforward inhibition controls the spread of

granule cell-induced Purkinje cell activity in the cerebellar cortex. *J Neurophysiol* 97: 248-263, 2007.

Schonewille M, Khosrovani S, Winkelman BH, Hoebeek FE, De Jeu MT, Larsen IM, Van der Burg J, Schmolesky MT, Frens MA, and De Zeeuw CI. Purkinje cells in awake behaving animals operate at the upstate membrane potential. *Nature Neuroscience* 9: 459-461; author reply 461, 2006.

Senkowski D, Schneider TR, Foxe JJ, and Engel AK. Crossmodal binding through neural coherence: implications for multisensory processing. *Trends Neurosci* 31: 401-409, 2008.

Shin SL, Hoebeek FE, Schonewille M, de Zeeuw CI, Aertsen A, and De Schutter E. Regular patterns in cerebellar Purkinje cell simple spike trains. *PLoS ONE* 2: e485, 2007.

Soteropoulos DS, and Baker SN. Cortico-cerebellar coherence during a precision grip task in the monkey. *J Neurophysiol* 95: 1194-1206, 2006.

Stern EA, Jaeger D, and Wilson CJ. Membrane potential synchrony of simultaneously recorded striatal spiny neurons in vivo *Nature* 394: 475-478, 1998.

Tadayonnejad R, Anderson D, Molineux ML, Mehaffey WH, Jayasuriya K, and Turner RW. Rebound discharge in deep cerebellar nuclear neurons in vitro. *Cerebellum* 9: 352-374, 2010.

Vervaeke K, Lorincz A, Gleeson P, Farinella M, Nusser Z, and Silver RA. Rapid desynchronization of an electrically coupled interneuron network with sparse excitatory synaptic input. *Neuron* 67: 435-451, 2010.

Voogd J, and Glickstein M. The anatomy of the cerebellum. *Trends Neurosci* 21: 370-375, 1998.

Voogd J, and Paxinos G. Cerebellum. In: *The Rat Nervous System*. London, UK: Elsevier Academic Press, 2004, p. 205-242.

Walter JT, Alvina K, Womack MD, Chevez C, and Khodakhah K. Decreases in the precision of Purkinje cell pacemaking cause cerebellar dysfunction and ataxia. *Nat Neurosci* 9: 389-397, 2006.

Welsh JP, Lang EJ, Sugihara I, and Llinás R. Dynamic organization of motor control within the olivocerebellar system. *Nature* 374: 453-457, 1995.

Wilson CJ, and Kawaguchi Y. The origins of two-state spontaneous membrane

potential fluctuations of neostriatal spiny neurons. *J Neurosci* 16: 2397-2410, 1996.

Table and Table Captions

Group	n	Firing rate (spikes/s)	Units with simultaneous LFP oscillations	2 SD	Firing rate (spikes/s) for units with significant cell-LFP relation (2 SD)	Firing rate (spikes/s) for units with non- significant cell-LFP relation
Golgi	67	7.7 (± 6.0)	74 % (34/46)	29.6 % (8/27)	7.7 (± 7.7)	7.4 (± 5.6)
Pcell	12 7	43.0 (± 25.2)	65.1 % (82/126)	25 % (16/64)	30.4 (± 13.4)	43.7 (± 25.6)*

Table 1. Descriptive electrophysiological data for Golgi cells and Purkinje cell simple spikes (PcellSS). Approximately two-third of the units in our sample in each group were recorded with simultaneous LFP oscillations. We also show the number of isolated units showing a significant relation with oscillatory LFPs, as defined by the number of spike-LFP cross-correlation peaks crossing the 2 SD threshold (95$^{\#}$ percentile) and the 3 SD threshold (99$^{\#}$ percentile) within the ± two-cycle lag period (~ ± 250 ms). The average firing rate (spikes/s) was significantly higher for Purkinje cells that showed no significant cell-LFP correlations (* $p < 0.05$) compared to Purkinje cells with significant cell-LFP correlations.

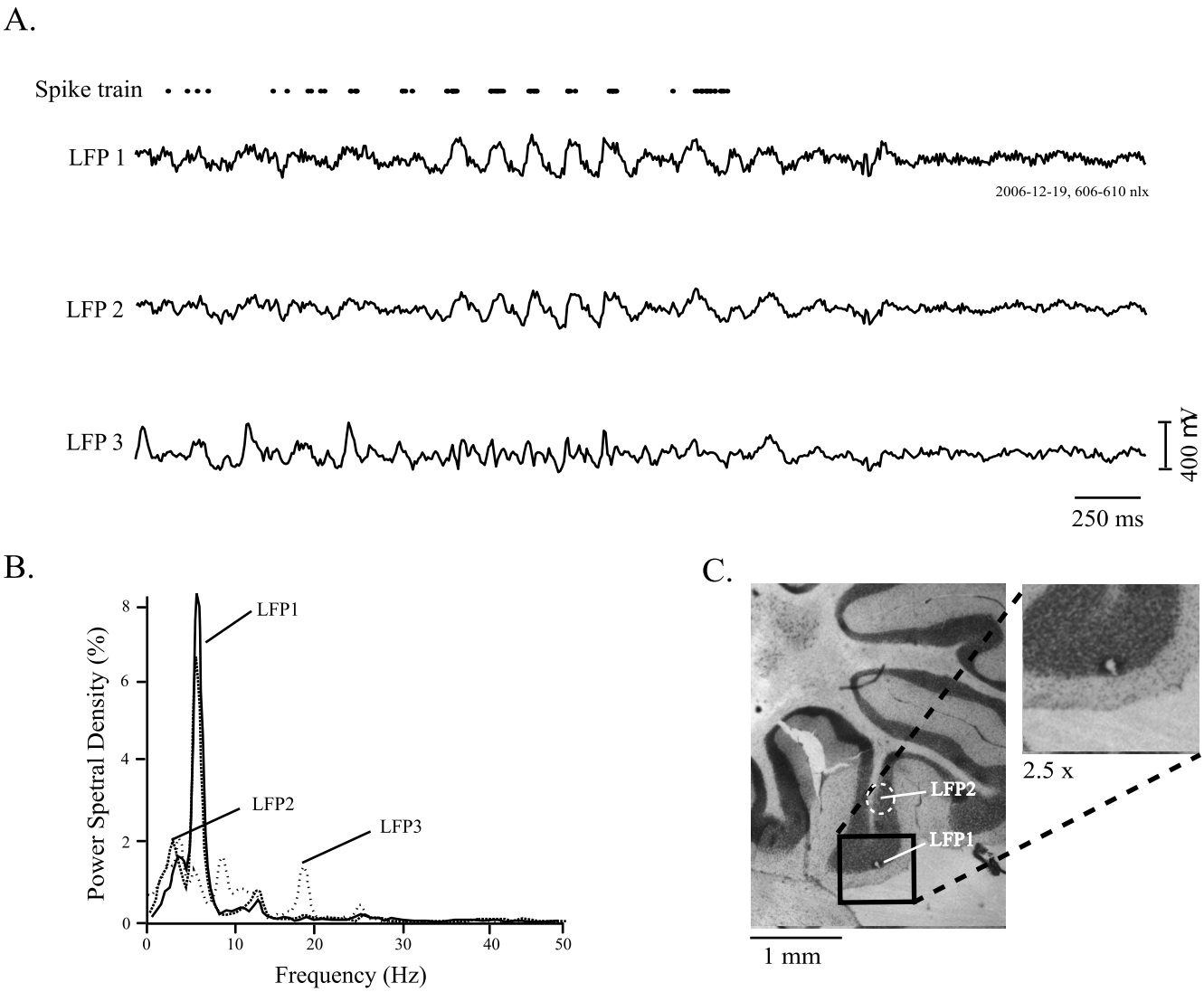
A.
Spike train
LFP 1
2006-12-19, 606-610 nlx
LFP 2
LFP 3
400 mV
250 ms
B.
Power Spetral Density (%)
LFP1
LFP2
LFP3
Frequency (Hz)
C.
LFP2
LFP1
2.5 x
1 mm

Figure 1

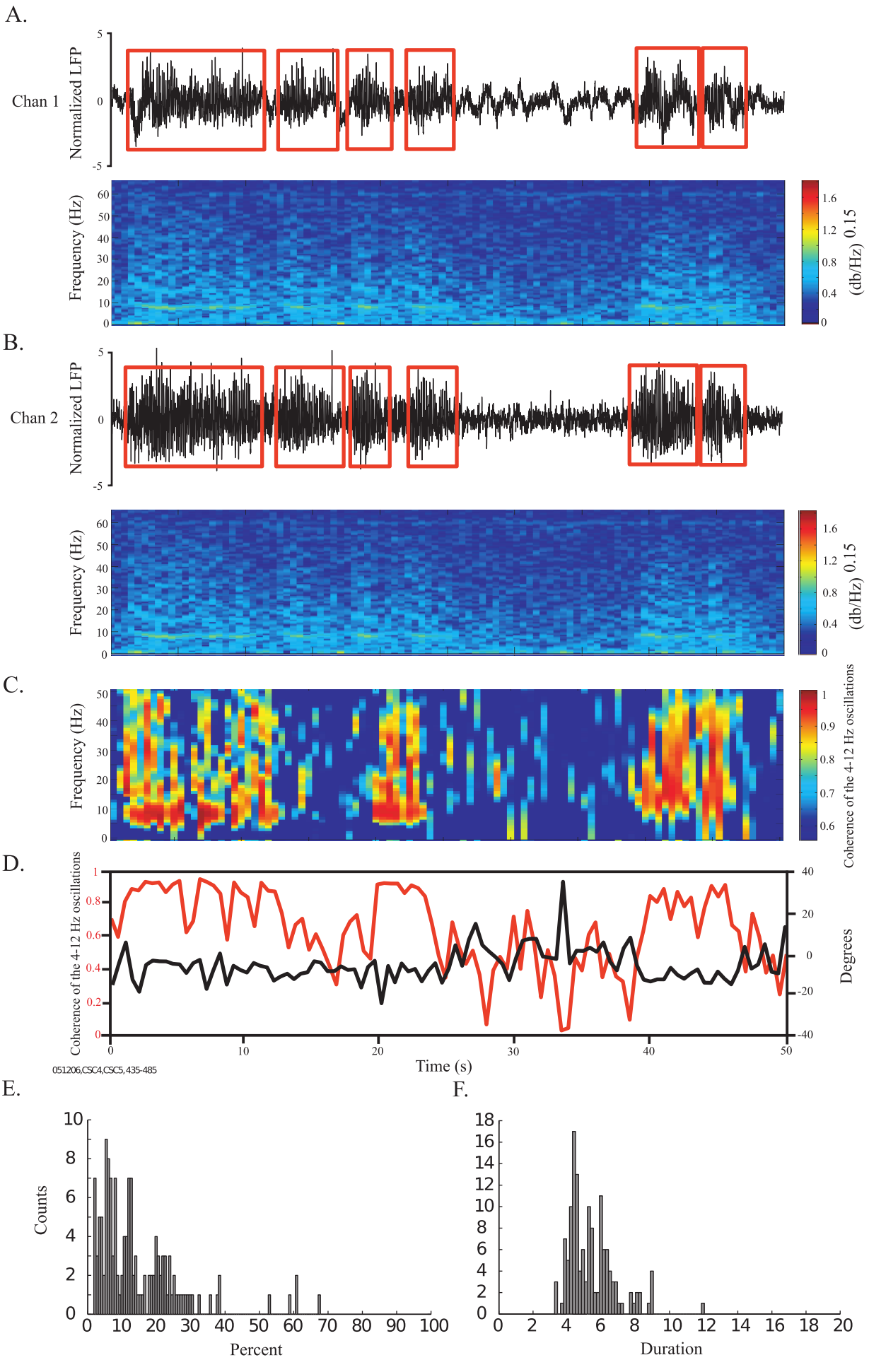
A.
Chan 1
Normalized LFP
Frequency (Hz)
(db/Hz) 0.15
B.
Chan 2
Normalized LFP
Frequency (Hz)
(db/Hz) 0.15
C.
Frequency (Hz)
Coherence of the 4-12 Hz oscillations
D.
Coherence of the 4-12 Hz oscillations
Degrees
Time (s)
051206,CSC4,CSC5, 435-485
E.
Counts
Percent
F.
Duration

Figure 2

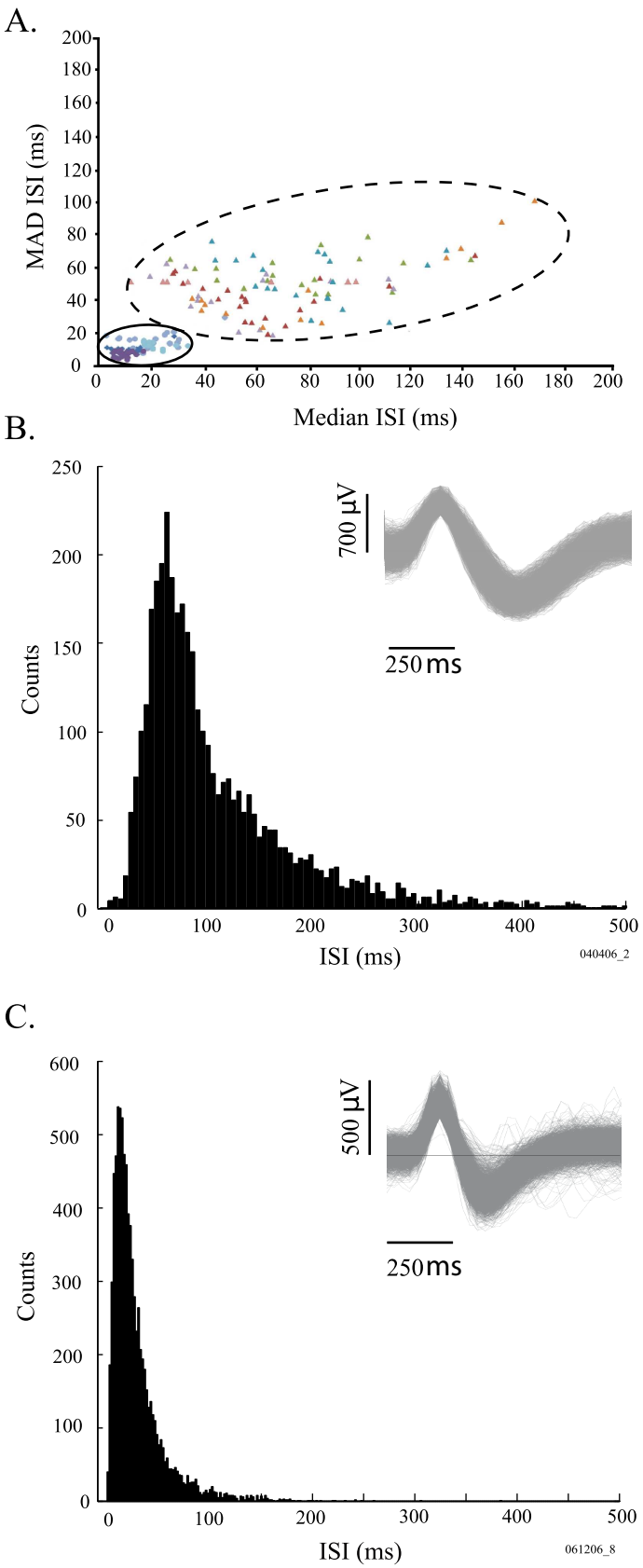
A.
MAD ISI (ms)
Median ISI (ms)
B.
Counts
ISI (ms)
700 µV
250 ms
040406_2
C.
Counts
ISI (ms)
500 µV
250 ms
061206_8

Figure 3

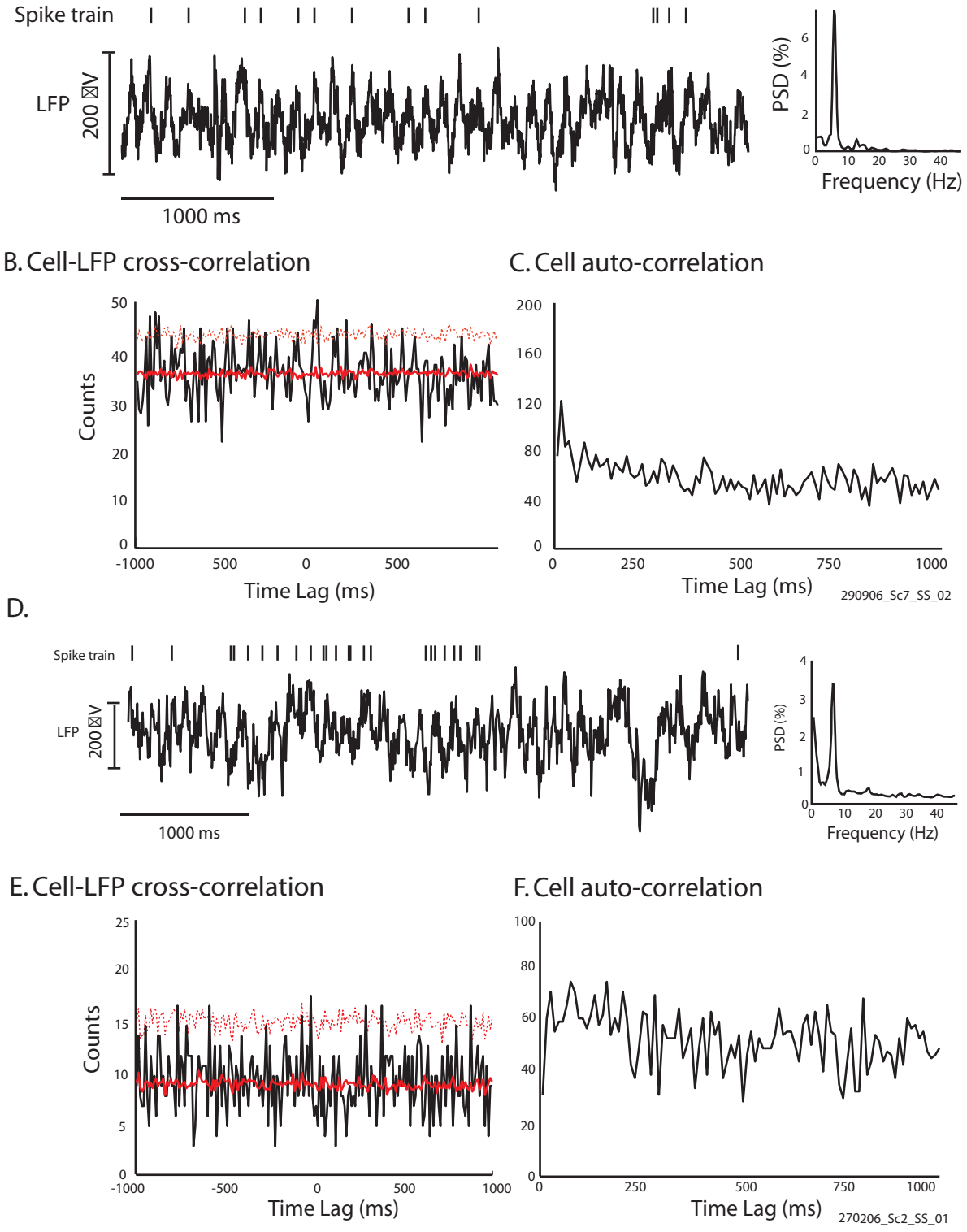
A.
Spike train
LFP
200 ⊠V
1000 ms
PSD (%)
Frequency (Hz)
B. Cell-LFP cross-correlation
Counts
Time Lag (ms)
C. Cell auto-correlation
Time Lag (ms)
290906_Sc7_SS_02
D.
Spike train
LFP
200 ⊠V
1000 ms
PSD (%)
Frequency (Hz)
E. Cell-LFP cross-correlation
Counts
Time Lag (ms)
F. Cell auto-correlation
Time Lag (ms)
270206_Sc2_SS_01

Figure 4

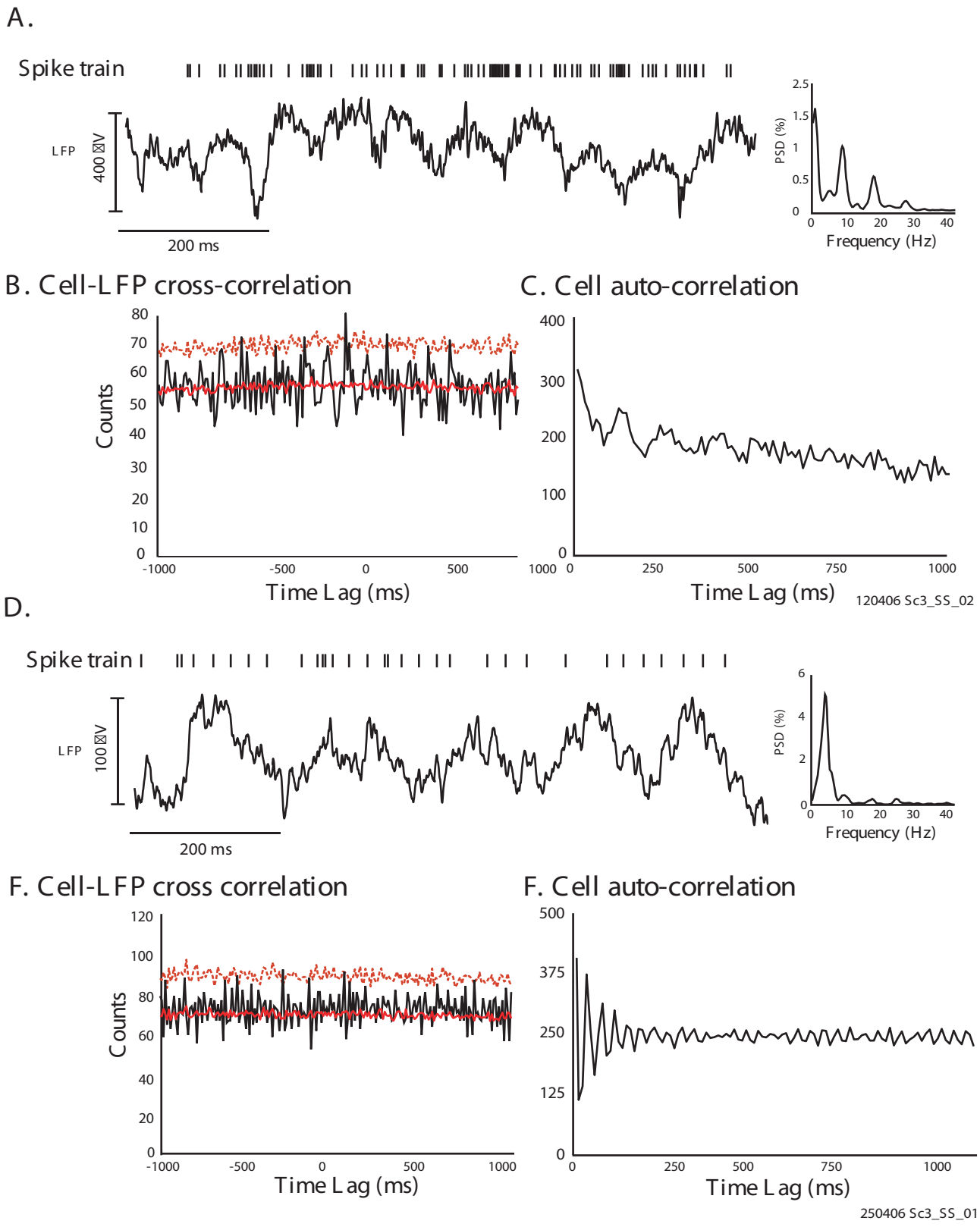
A.
Spike train
LFP
400 ⊠V
200 ms
PSD (%)
Frequency (Hz)
B. Cell-LFP cross-correlation
Counts
Time Lag (ms)
C. Cell auto-correlation
Time Lag (ms)
120406 Sc3_SS_02
D.
Spike train
LFP
100 ⊠V
200 ms
PSD (%)
Frequency (Hz)
F. Cell-LFP cross correlation
Counts
Time Lag (ms)
F. Cell auto-correlation
Time Lag (ms)
250406 Sc3_SS_01

Figure 5

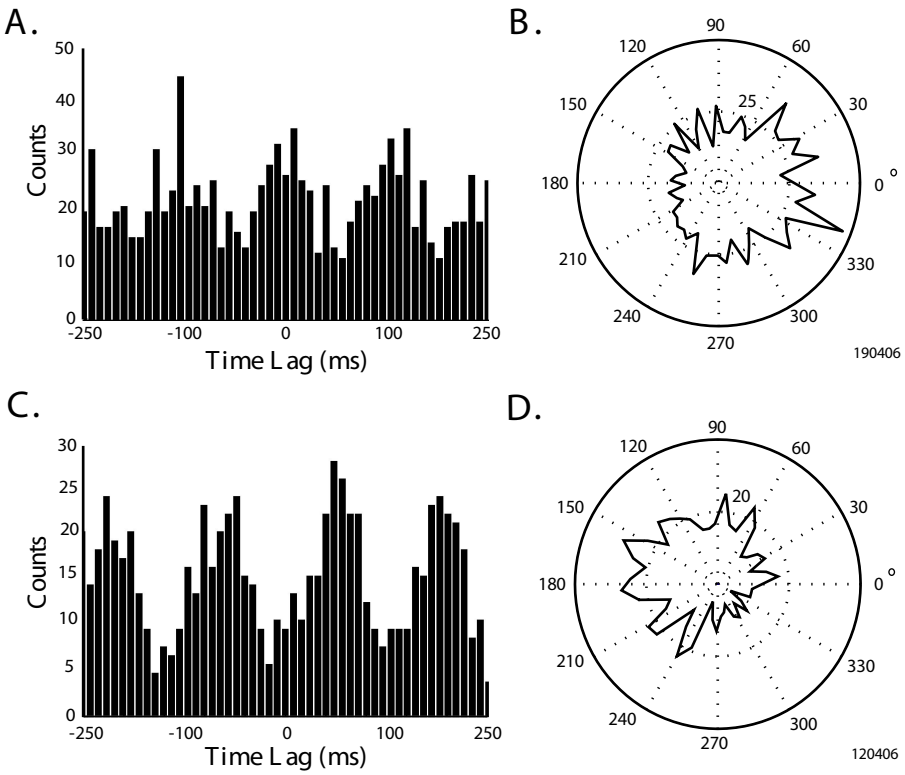
A.
B.
C.
D.
Counts
Time Lag (ms)
-250
-100
0
100
250
90
120
60
150
30
180
0 °
210
330
240
300
270
25
20
190406
120406

Figure 6

A. Golgi population

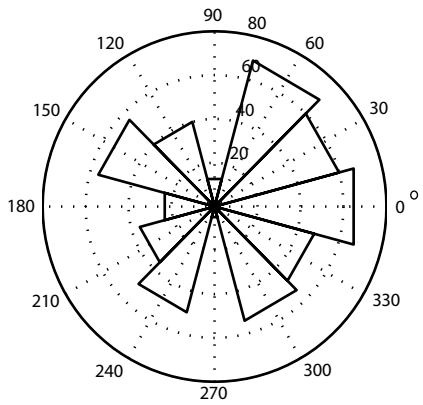

B. Golgi preferred phase

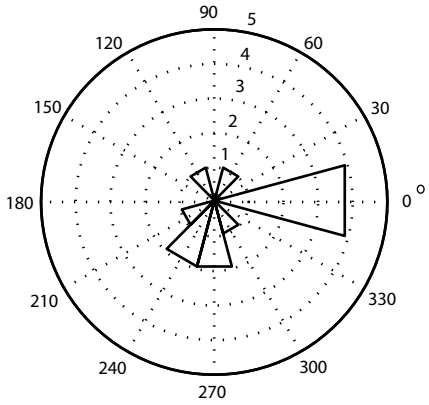

C. Purkinje cell SS population

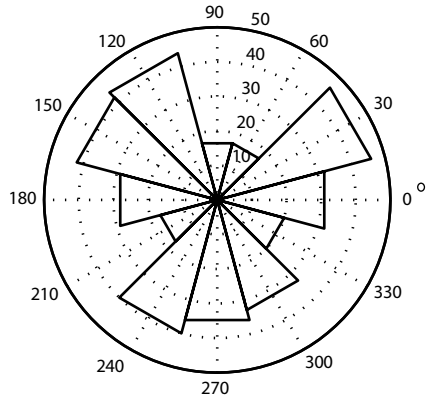

D. Purkinje cell SS preferred phase

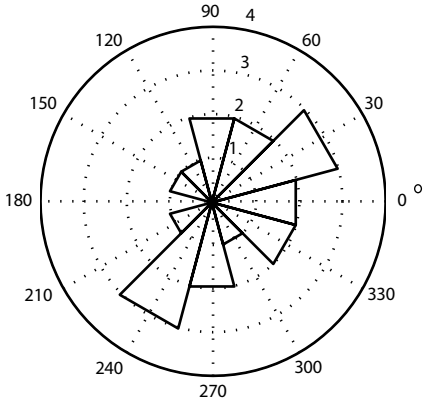

Figure 7

Other results

1 Other results in the cerebellum during the task

1.1 Phase-locking of Spikes of Purkinje cells with the local field potential

To further study the relation between Purkinje cell activities and the local oscillations, we analyzed the spike-triggered average (STA) of the local field potential around the cell spikes. We found that during both sleep and active exploration even when the cells were modulated during grasping task, there were cases in which Purkinje cells spikes were phase-locked to the negative phase of LFP. Figure 1A showed average STA of one Purkinje cell during a sleep session. For this neuron, there were high frequency oscillations before and after Purkinje cell discharges. The forward oscillation started 4.9 ms before the spikes and the oscillation afterward ended 4.6 ms after the spikes. The spectrum of the mean STA showed a peak at 238.4 Hz (Figure 1B), compatible with a phase-locking of the cells with a local oscillation. We computed the spectra of STAs for all the Purkinje cells whose LFP showed HFO peak (n=48), and found most STA sprectum peaks were also located between 200 to 300 Hz (Figure 1C), with an average of 250.84 +/- 66.16 Hz (mean +/- SD), no significant differences with the peak frequency of HFO in LFP (paired t-test, p=0.11). A STA peak between 200 to 300 Hz might still be found even if the spectrum of local field potentials did not exhibit a peak at HFO band, but there was less chance (40% (10 out 25)) compared with the population whose LFP showed a HFO peak (79% (38 out 48)) (Figure 1J). When the spikes were shifted 50ms, the relation between the spikes and the oscillation usually disappeared, and the peaks of spectra of the STA descended until less than 100Hz. The peaks of spectrum of shifted STAs and the peaks of spectrum of the original STAs showed highly significant difference ($p<0.01$) (data not showed). The chance that a STA peak in 200-300 Hz could be seen decreased when spikes were shifted no matter if the spectrum of LFP of this cell had a peak in 200-300Hz or not. Similar relationship between Purkinje cell discharge and local field potential could be found also during the animal's active spatial exploration (Figure 1DE). And chance that STA peak in 200-300 Hz could be found when LFP didn't show peak in 200-300Hz was similar with sleep state (t-test). Even just in short period of time only when cells were significant modulated during the skilled movement, the relation was still consist (Figure 1FG).

The spectrum of STA oscillation of the extracellular recording of Purkinje cells in slices showed a peak below 100 Hz instead of a peak between 200-300 Hz (Figure 1 HI) . These results

in vitro thus indicate that the high frequency peak we found in vivo was not due to the feature of extracellular action potentials of the cells but instead to the presence of fast oscillations in vivo.

1.2 Gamma oscillation observed during the task

The power of gamma band in the local oscillations were found to increase during active behavior. Figure 2A indicated the difference in the spectrogram during the rest state and the task. The power of spectrum during active behavior exhibited a peak around 100 Hz (Figure 2B), which belonged to higher gamma rhythm.

We analyzed the time course of these high gamma bands (50-100 Hz, 100-150 Hz) around the behaviour (Figure 3A), we calculated the power and found that these gamma increased in the seconds before the paw lift. One second before the lift, although there was a wide band of frequency increasing the power, there were clearly 2 peaks in the gamma bands (Figure 3C). And after lift, the power decreased (Figure 3DE). So there was transient increase in 50-150Hz power before the lift.

2 Modulation of cells in the motor cortex during a voluntary skilled movement

In 10 rats, which were trained to perform a voluntary skilled movement of grasping to retrieve food pettlets through a slot, We recorded not only cells in the cerebellar cortex, but also cells in the motor cortex. The center of the recording region is 3 mm lateral to the midline and 3.5 mm anterior to the Bregma, where was demonstrated to be responsible for the forelimb movement. Until now, we have analysed motor cells firing in 4 rats. We found most cells were modulated around 'lift'. The modulation could be an increase or/ and decrease of the firing rate relative to baseline. Figure 4A summarize the responses of 136 cells recorded in the motor cortex in 4 rats around the lift of the forelimb. The average modulation was inhibition, which started around one second before the movement (Figure 4BC).

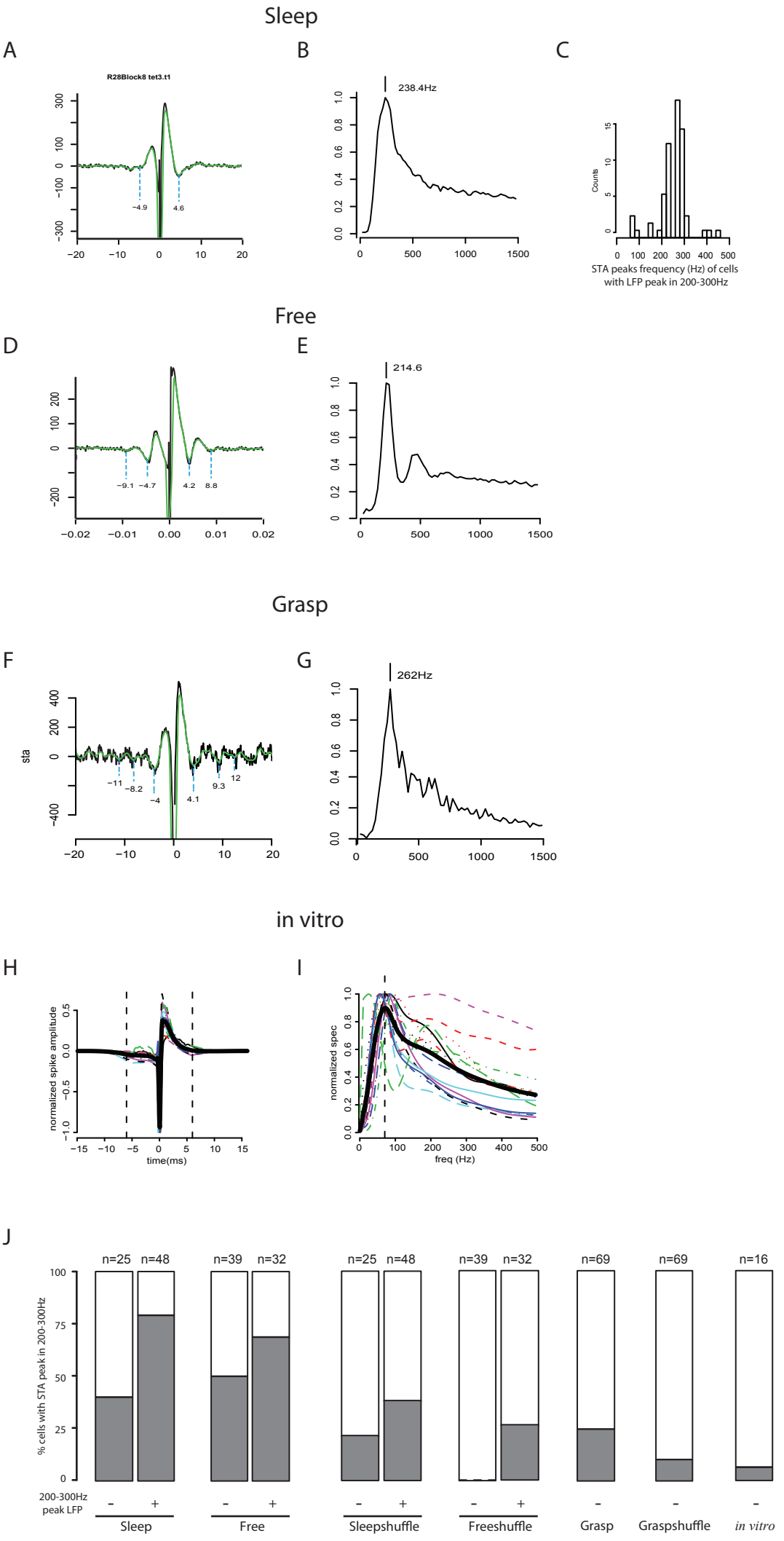
Sleep
A
B
C
R28Block8 tet3.t1
238.4Hz
Counts
STA peaks frequency (Hz) of cells with LFP peak in 200-300Hz
Free
D
E
214.6
Grasp
F
G
sta
262Hz
in vitro
H
I
normalized spike amplitude
time(ms)
normalized spec
freq (Hz)
J
n=25 n=48 n=39 n=32 n=25 n=48 n=39 n=32 n=69 n=69 n=16
% cells with STA peak in 200-300Hz
200-300Hz peak LFP
Sleep
Free
Sleepshuffle
Freeshuffle
Grasp
Graspshuffle
in vitro

Figure 1

A

LFP spectrogram

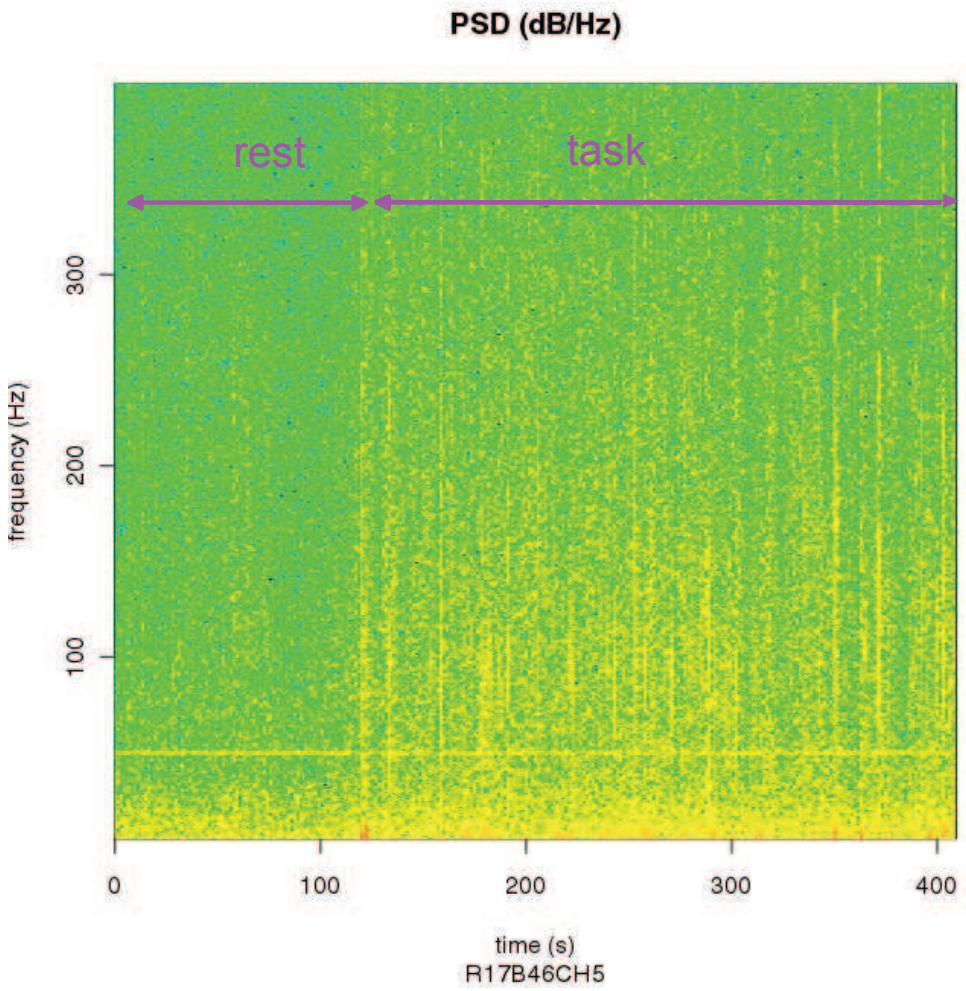

B

LFP power spectrum

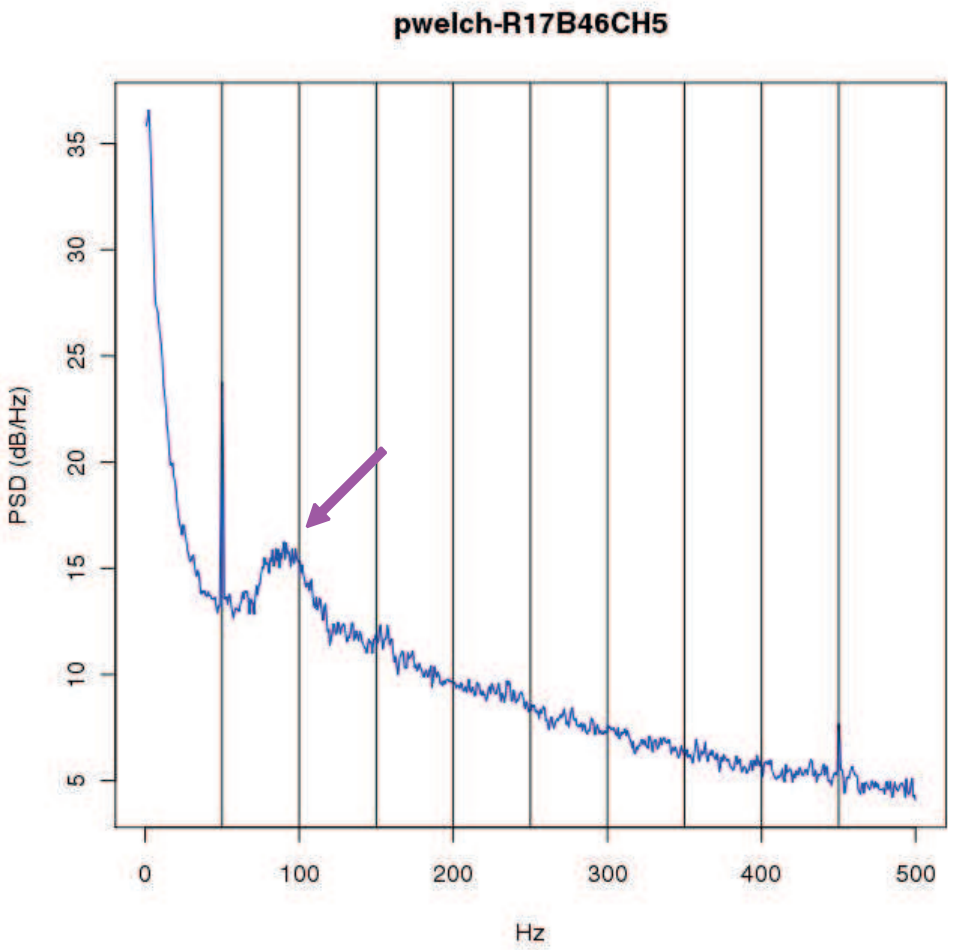

Figure 2

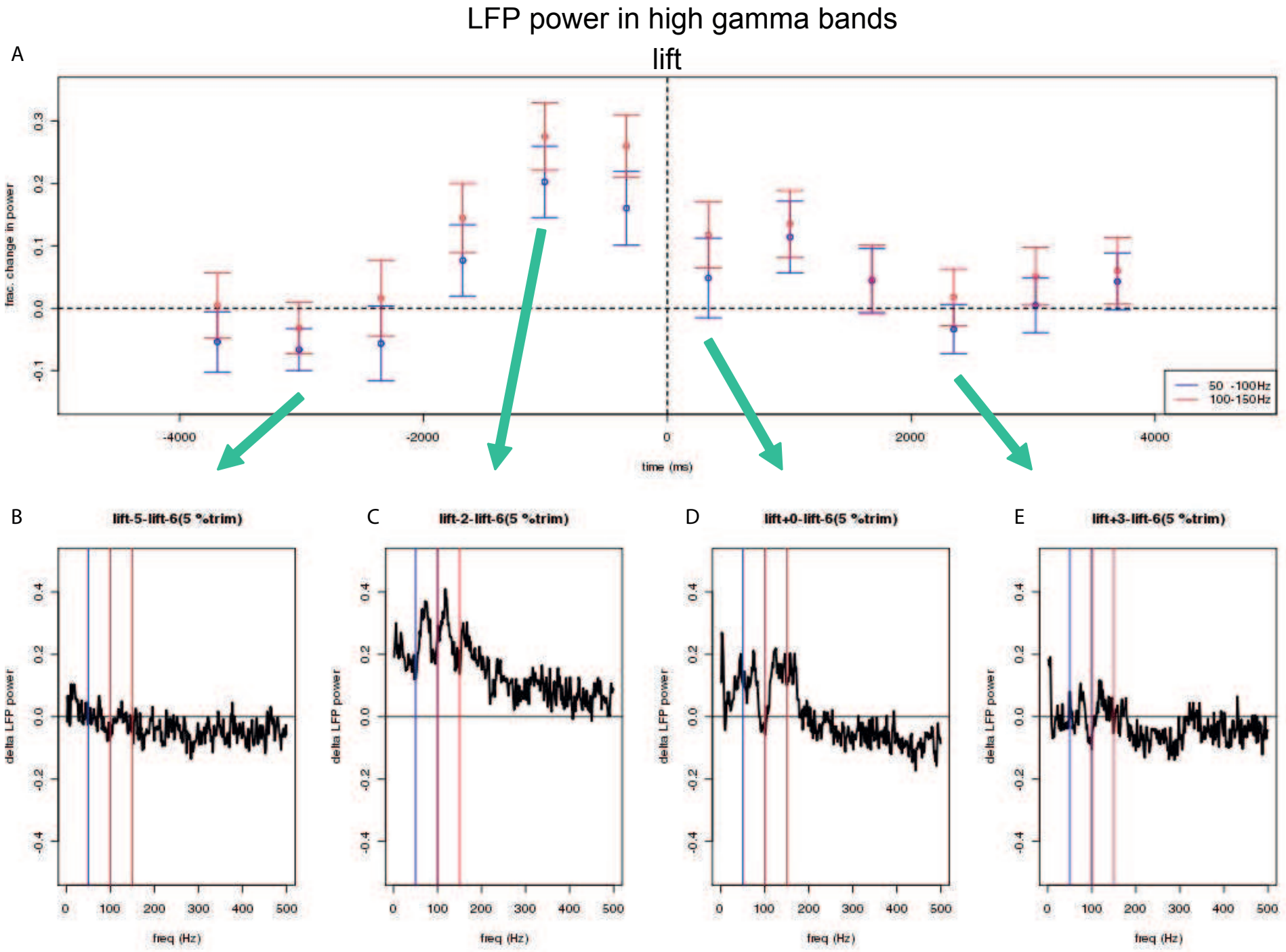
LFP power in high gamma bands
A
lift
frac. change in power
time (ms)
50 -100Hz
100-150Hz
B
lift-5-lift-6(5 %trim)
C
lift-2-lift-6(5 %trim)
D
lift+0-lift-6(5 %trim)
E
lift+3-lift-6(5 %trim)
delta LFP power
freq (Hz)

Figure 3

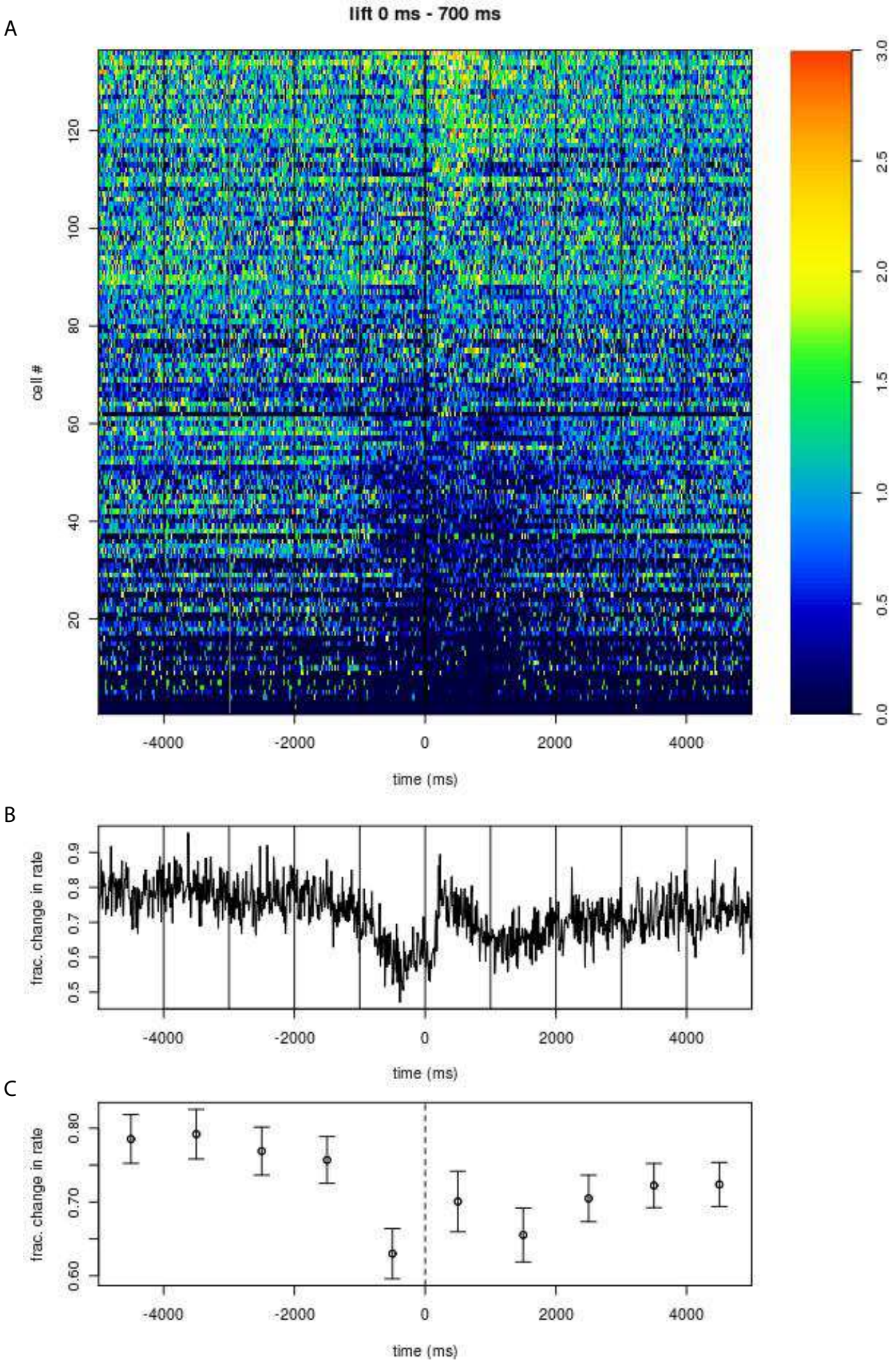
A
lift 0 ms - 700 ms
cell #
20
40
60
80
100
120
-4000
-2000
0
2000
4000
time (ms)
0.0
0.5
1.0
1.5
2.0
2.5
3.0
B
frac. change in rate
0.5
0.6
0.7
0.8
0.9
-4000
-2000
0
2000
4000
time (ms)
C
frac. change in rate
0.60
0.70
0.80
-4000
-2000
0
2000
4000
time (ms)

Figure 4

Fourth part
Discussion and perspectives

1 First article

1.1 Choice of electrode

In the first article, we proved that tetrodes provide satisfactory simultaneous recordings of multiple units in cerebellar cortex in freely-moving animals and the usage of tetrode can allow studying population activity. However, tetrodes are not the only choice of electrodes for studying cerebellar function in awake animal. Other electrodes such as linear electrodes, are well suited to identify current sources and sinks in a laminar structure such as the cerebellar cortex and have been successfully used in the study of cerebellar function (Delescluse and Pouzat, 2006; de Solages et al., 2008; Tahon et al., 2011). Therefore, the choice of electrode depends on the propose of the research.

1.2 Limitation of quartz tetrode

1.2.1 Limitation for studying the synchrony of neighboring cells under the millisecond

In the paper, we have discussed the benefits of quartz tetrode in cerebellar function research. However, tetrode recordings have also several limitations.

First, as other multiunit recording techniques, until now, it is difficult to separate overlapping spike waveforms that occur during synchronous activities under one millisecond of two or more cells recorded simultaneously: the overlap of extracellular spike waveforms will results in spikes of various amplitudes and shape depending on the individual waveforms and temporal offset between the spikes. Thus, these spikes are more likely to be identified as a separate type of spike and then be attributed to another cell during spike sorting. Thus synchronous activities of several individual cells will be either missed in spike sorting or simply discarded because of the small number of events. This limitation will prevent the study of the sub-millisecond scale synchrony of neighboring cells.

1.2.2 Fragile (special the tip) and high-cost

Second, since the material is quartz, the tetrodes are quite fragile, particularly at the level of the sharp tip. However, since the tip of the electrode is designed to optimize the metal contact spacing, and that the sharpness of the tip is critical to advance in the brain tissue, the tip is critical for obtaining good signals. Thus even a small damage of the tip will strongly affect the recording quality. Another limitation of the electrodes is their high cost; and therefore the smallest carelessness that results in the uselessness of one tetrode, will cost around 280 euros! Thus, it is better having some experience to use it, and be very careful when installing quartz tetrode into a headstage or when advancing it during or after surgery.

Perspectives:

So far, we have not implemented an algorithm to deal with overlapping waveforms; Softwares which can identify the overlapping waveforms of spikes from 2 or more cells already exist (e.g., Franke et al., 2011) but they are not yet available for commercial or public use. In near futur, it should thus be possible and more convenient to study the sub-millisecond synchrony of neighboring cells recorded in the same tetrode.

2 Second article

2.1 Synchrony is observed across states

Our experiments showed that short-term synchrony of neighboring Purkinje cells is present across different vigilance states including sleep, active awake and even when the cells are modulated during a motor skilled reaching task. We discuss below the multiple mechanism and relevance of synchrony of neighboring Purkinje cells. Neighboring Purkinje cells indeed share strong excitatory input from the climbing fibers issued from the same zone of inferior olive, share inputs

from parallel fibers, and inhibitory connections from local interneurons and from recurrent collaterals; all these mechanisms may collaborate to produce the synchrony in the small local regions. Since this phenomenon was systematically observed between neighboring Purkinje cell pairs, the local synchrony seems universal in the paramedian lobule.

2.2 Complex Spikes observed in our experiments

Both the complex spikes (Welsh et al, 1995; De zeeuw et al, 1997) and simple spikes (De zeeuw et al, 1997) of Purkinje cells are found to exhibit coordinated discharge in the cerebellar cortex. In our study, the firing rate of the Purkinje cell complex spikes is similar to the values reported in the literature and synchronous complex spikes was also present as in other studies (e.g. Wylie et al., 1995). However, the rate of synchronous spikes (~5Hz) reported in our study is 10 times higher than the rate of complex spikes (and even higher than the rate of synchronous complex spikes). According to theories of cerebellar function (see Introduction section 3.2), complex spikes are regarded to serve as 'error' signal (Ito, 1970) which can encode sensory or motor information (Jorntell et al., 1996; Mortimer, 1975), to modify synapse efficacy during learning in order to obtain an optimal movement execution. In our study, we did not observea modulation of the complex spikes during the task. This may be because of the low firing rate of complex spikes (< 1Hz) and fast action motion (around 600 ms from lift to grasp) and thus insufficient sampling of activity to detect significant modulation during the task. However, it is also possible because when we recorded the cerebellar neuronal activities, the rats were already well trained. They performed quite skillfully with very few of mistakes. Therefore, there were no need for an 'error' signal propagated by complex spikes to the cerebellum. The study of the learning of the grasping movement should more appropriate to analyze the function of complex spikes.

2.3 A potential role for the molecular layer interneurons

Modeling studies have underlined the potential synchronizing role of molecular layer interneurons (Jaeger, 2003). Molecular layer interneurons directly inhibit the Purkinje cells (Laine and Axelrad, 1998; Simat et al., 2007). Other cells such as Golgi, Lurago and globular cells can also inhibit

Purkinje cells indirectly (Hirono et al., 2012). The inhibition to Purkinje cells can cause a short pause of firing, and raise the probability of firing after inhibition, therefore increase the synchrony of neighboring Purkinje cells, which receive the similar inhibition (Shin and de Schutter, de Solage et al., in preparation). Unfortunately, we did not obtain combined recordings of interneurons and Purkinje cells to assess the contribution of the interneurons to the synchronization of Purkinje cells.

2.4 High frequency oscillation

Our results indicated that short-term synchrony of population is consistent across states, which may causes HFO around 250 Hz (de Solages et al., 2008), even though the firing rates significantly vary because of either different states or modulation during a motor task. There seems to be an internal organization in a local zone in Purkinje cell layer. This local organization of Purkinje cell population can be displayed as local high frequency oscillation, which sometimes can be observed in LFP. However, when the animal is active, the network is more active than during sleep or resting. The Purkinje cells receive more excitation information from precerebellar nuclei and inferior olive, the network noise decreased the possibility of observation this organization in local field potential, without shifting the frequency bands. This may be a reason why the HFO was also not observed in wildtype mouse (Cheron et al., 2008). In our cases, when rats were during active exploration, the chance to observe the HFO in LFP decreased and the peak amplitude of HFO is significant smaller than during sleep. However, whether or not the HFO could be observed in LFP or how big is the HFO, stableness of local Purkinje cells population short-term synchrony across different states is demonstrated by our experiments.

2.5 Functional relevance of Purkinje cell synchrony

Purkinje cells are the sole output of cerebellar cortex and their activities represent the integrated results of the whole cerebellar cortex processing. Purkinje cells send their signals to cerebellar deep nuclei cells, which are the final output of the cerebellum. The impact of the cortex on the deep cerebellar nuclei is determined by the population activity of the cortex instead of single Purkinje cell (Thier et al., 2000). Anatomical experiments have also demonstrated that tens to

several hundreds of Purkinje cells from single microzones converge upon a single cerebellar nuclei neuron (De Zeeuw and Berrebi, 1995; Person and Raman, 2011). Thus, Purkinje cell synchrony is likely to substantially affect strongly the timing of spike activity in the downstream structure (Gauck and Jaeger, 2000; Person and Raman, 2011), at a short time scales.

Perspectives:

To answer the questions that if synchrony of neighboring Purkinje cells will help precisely control timing of cerebellar deep nuclei cells firing and that if interneuron can sharpen synchrony during task, one way is recording of different kinds of cerebellar cortex cells during the task. Indeed,nterneurons and DCN cells are accessible to recordings. However, since in my project, we focus more on the Purkinje cells. We recorded neither the interneurons nor DCN cells during movement. Thus, further investigations are required to analyze the effect of short-term synchrony of neighboring Purkinje cells on their target, DCN cells, and the probable effect of local interneuron firing on timing the synchrony of neighboring Purkinje cells.

The second way to study the relationship of synchrony of Purkinje cells and DCN cells druing movement is to use an animal model with optogenetical technique. In these animals, Purkinje cells, which express Channelrhodopsin, can be excited by pulses of light. Since one microzone can be targeted by the illumination, a large fraction of Purkinje cells of one microzone can be active simultaneously. Thus, recording in the DCN the action of light-gated synchronous activation of neighboring Purkinje cells should allow studying the function of synchrony of neighboring Purkinje cell to their downstream DCN cells.

On the other side, how the synchrony changes during learning is also unclear. The amplitude of short-term synchrony during modulation is almost twice bigger as during rest. However, we recorded just after rats had already well learned the task, Thus, this increase of the synchrony power happens before, during or just after well trained is unclear. To uncover the answer, we need to observe the process of learning. Another benefit of recordings of the whole learning process is that during learning, there will be a lot of mistakes, whose data can help us explore the behaviour and function of complex spikes.

3 Third article

Prominent theta oscillations can easily been recorded in the granule layer of quiet awake rats. They originate in the granular layer and these oscillations influence local cell firing. However, we have found that not only neurons in the granular layer can operate in the theta bands. Other loops in the cerebellum may be also involved in operation of the same frequency range.

3.1 Effect of oscillation to DCN

Before our study, there was no evidence of a propagation of theta oscillation beyond the granular layer (Kanichay and Silver, 2008). Our results indeed demonstrated the presence of theta oscillation in the Purkinje cell layer. Furthermore, the pause of Purkinje cell firing to the deep cerebellar nuclei could be facilitated by the theta rhythm (De Schutter and Steuber, 2009). However, if these oscillation will continue to propagate in downstream structures and have effect on cells in these structure, such as DCN cells, remains to be established.

3.2 Putative mechanisms at work and link with the climbing fiber activity

We found that Purkinje cell simple spikes are modulated in phase with the granular layer theta oscillations. Feedback loops (via mossy fiber-granule cell-Golgi cell interactions) and feed-forward circuits (via mossy fiber-Golgi cell-granule cell interactions) could generate theta oscillations or at least resonate in response to entraining excitation. Moreover, it has been proposed previously that the electric coupling between Golgi cell may play an important role in theta-resonnance to rhythmic inputs. Thus, the theta oscillation propagation from the granular layer to Purkinje cell layer is probably by the parallel fibers. The mossy fiber and the climbing fiber are two main inputs to Purkinje cells. Climbing Fibers send output directly and indirectly to the Golgi cells, thus the granular layer may also be tuned toward the dominant frequencies of the olivo-cerebellar modules. The climbing fiber may also contribute to the propagation of theta oscillations. But we did not obtain enough samples to analyze the relationship with Purkinje cell

complex spikes. The climbing fibers have been reported to exhibit theta oscillations activities generated in the inferior olive (Van Der Giessen et al., 2008). Study the relationship of complex spikes and theta oscillation in GCL will help to answer the question how these oscillations affect the propagation of GCL theta oscillation to PCL.

Perspectives:

To solve these questions, more recording samples of complex spikes and DCN cells are necessary. Our quartz tetrodes can indeed record good signal of complex spikes of Purkinje cells. We may do more rats and record simultaneously granular local field potentials and complex spikes, together with DCN cells.

4 Other results

4.1 Spike triggered oscillations imply the local high frequency oscillation

It's difficult to observe HFO in local field potentials during task, as discussed above. However, the oscillations reflect the local population cell activities. Thus, examining population activity of Purkinje cells is one way to reveal the HFO. The synchrony of neighboring cells at around 4ms can be one means of indication of HFO during the task. Another way to study the HFO is to analyse the STA. Our results of STA indicate also the phase-locking relationship of spikes and oscillation, and from one side, proved the existence of HFO during task.

4.2 How the gamma oscillation affect movement

We observed gamma oscillations in the Purkinje cell layer during the task. Gamma oscillation has already been reported in the cerebellum (Niedermeyer, 2004). A combined input from GABAergic interneurons and Purkinje cells is suggested to be required to generate the gamma field potentials (Middleton et al., 2008). However, where and how gamma band oscillations are generated is still unclear. Moreover, the function of gamma oscillations in the cerebellum has been seldom studied.

In our experiments, the power of gamma oscillations increased before the onset of paw movement during reach to grasp task, which suggests the relationship of gamma oscillation with preparation of execution. In the cerebral cortex, the dynamic synchronization of gamma rhythms is linked to precision sensorimotor task (Tecchio et al., 2007) and event-related synchrony at gamma frequencies is observed during the onset and execution of motor commands (Szurhaj et al., 2005).

4.3 Relationship of the cerebellum and the motor cortex

In our experiments, the motor cortex cells are also modulated during movement. These preliminary results indicated that besides of the cerebellum, the motor cortex is also involved in the task. In the theory of internal models, the motor cortex works together with the cerebellum, sends motor command for controlling movements of muscles, and therefore achieve the motor action. The cerebellar neurons have been demonstrated to project to M1 at the single neuron level during a reaching and button pressing task (Hodefer et al., 2000). Moreover, a remarkable coherence in theta oscillations between the sensorimotor cortex and cerebellum has been observed in the rat and monkey performing an active movement (Courtemanche et al., 2002), which represent the communication between cerebral-cerebellar system.

Perspectives:

We have already data of cells spiking and LFP in the motor cortex. The preliminary results indicate the involvement of the motor cortex in the task, which brings the high possibility of cooperation of the motor cortex and the cerebellum during the task. The further analysis of coherence of these two regions and the relationship of activities of cells in the two structures can help to uncover how these two structures works functionally during the task.

Conclusion:

The work during my Ph.D. study focused on the presence and characteristics of the

organization of cerebellar cortex in freely-moving rats, especially when they perform a reach-to-grasp task. My results demonstrated the existence of strong discharge coordination of local Purkinje cells across states and its relationship to other elements, such as Golgi cells, in the cerebellar cortex. I found local oscillations shift its main power bands in different states, which may have its function in information processing. Overall, my work has identified and characterized a number of state-dependent population activity patterns in the cerebellar cortex. How these patterns impact on the motor system remains to be examined in future studies.

References

Ackermann, H., Gräber, S., Hertrich, I. & Daum, I. Categorical speech perception in cerebellar disorders. Brain and language 60, 323-31 (1997).
Ackermann, H., Mathiak, K. & Riecker, A. The contribution of the cerebellum to speech production and speech perception: clinical and functional imaging data. Cerebellum (London, England) 6, 202-13 (2007).
Adrian, E.D. Discharge frequencies in the cerebral and cerebellar cortex. *J. Physiol. (London)* **83**, 32-33 (1935).
Akemann, W., Middleton, S.J. & Knöpfel, T. Optical imaging as a link between cellular neurophysiology and circuit modeling. *Frontiers in cellular neuroscience* **3**, 5 (2009).
Akkal, D., Dum, R.P. & Strick, P.L. Supplementary motor area and presupplementary motor area: targets of basal ganglia and cerebellar output. *The Journal of neuroscience : the official journal of the Society for Neuroscience* **27**, 10659-73 (2007).
Alaverdashvili, M. & Whishaw, I.Q. Motor cortex stroke impairs individual digit movement in skilled reaching by the rat. *The European journal of neuroscience* **28**, 311-22 (2008).
Albus, J. A theory of cerebellar function. *Mathematical Biosciences* **10**, 25-61 (1971).
Allen, G.I. & Tsukahara, N. Cerebrocerebellar communication systems. *Physiological reviews* **54**, 957-1006 (1974).
Allen, G., Buxton, R.B., Wong, E.C. & Courchesne, E. Attentional activation of the cerebellum independent of motor involvement. *Science (New York, N.Y.)* **275**, 1940-3 (1997).
Aoki, E., Semba, R. & Kashiwamata, S. New candidates for GABAergic neurons in the rat cerebellum: an immunocytochemical study with anti-GABA antibody. *Neuroscience letters* **68**, 267-71 (1986).
Apps, R., Atkins, M.J. & Garwicz, M. Gating of cutaneous input to cerebellar climbing fibres during a reaching task in the cat. *The Journal of physiology* **502 (Pt 1**, 203-14 (1997).
Apps, R. & Garwicz, M. Anatomical and physiological foundations of cerebellar information processing. *Nat. Rev. Neurosci.* **6**, 297-311 (2005).
Apps, R. & Hawkes, R. Cerebellar cortical organization: a one-map hypothesis. *Nature reviews. Neuroscience* **10**, 670-81 (2009).
Atkins, M.J., van Alphen, A.M. & Simpson, J.I. Characteristics of putative Golgi cells in the rabbit cerebellar flocculus. *Soc Neurosci Abstr* **23**, 1287 (1997).
Babiloni, C. *et al.* Human movement-related potentials vs desynchronization of EEG alpha rhythm: a high-resolution EEG study. *NeuroImage* **10**, 658-65 (1999).
Ballermann, M., McKenna, J. & Whishaw, I.Q. A grasp-related deficit in tactile discrimination following dorsal column lesion in the rat. *Brain research bulletin* **54**, 237-42 (2001).
Barbour, B. Synaptic currents evoked in Purkinje cells by stimulating individual granule cells. *Neuron* **11**, 759-69 (1993).
Barmack, N.H. & Yakhnitsa, V. Functions of interneurons in mouse cerebellum. *The Journal of neuroscience : the official journal of the Society for Neuroscience* **28**, 1140-52 (2008).
Bartos, M., Vida, I. & Jonas, P. Synaptic mechanisms of synchronized gamma oscillations in inhibitory interneuron networks. *Nature reviews. Neuroscience* **8**, 45-56 (2007).
Bauer, M., Oostenveld, R., Peeters, M. & Fries, P. Tactile spatial attention enhances gamma-band activity in somatosensory cortex and reduces low-frequency activity in parieto-occipital areas. *The Journal of neuroscience : the official journal of the Society for Neuroscience* **26**, 490-501 (2006).
Bell, C.C. & Grimm, R.J. Discharge properties of Purkinje cells recorded on single and double microelectrodes. *Journal of neurophysiology* **32**, 1044-55 (1969).
Bell, C.C., Han, V.Z., Sugawara, Y. & Grant, K. Synaptic plasticity in a cerebellum-like structure depends on temporal order. *Nature* **387**, 278-81 (1997).
Bengtsson, F., Ekerot, C.-F. & Jörntell, H. In vivo analysis of inhibitory synaptic inputs and rebounds in deep cerebellar nuclear neurons. *PloS one* **6**, e18822 (2011).
Bennett, K.M., O'Sullivan, J.D., Peppard, R.F., McNeill, P.M. & Castiello, U. The effect of unilateral posteroventral pallidotomy on the kinematics of the reach to grasp movement. *Journal of neurology, neurosurgery, and psychiatry* **65**, 479-87 (1998).
Bosman, L.W.J. *et al.* Encoding of whisker input by cerebellar Purkinje cells. *The Journal of physiology* **588**, 3757-83 (2010).

Bower, J.M. & Woolston, D.C. Congruence of spatial organization of tactile projections to granule cell and Purkinje cell layers of cerebellar hemispheres of the albino rat: vertical organization of cerebellar cortex. *Journal of neurophysiology* **49**, 745-66 (1983).
Boyden, E.S., Katoh, A. & Raymond, J.L. Cerebellum-dependent learning: the role of multiple plasticity mechanisms. *Annual review of neuroscience* **27**, 581-609 (2004).
Brand, S., Dahl, A.L. & Mugnaini, E. The length of parallel fibers in the cat cerebellar cortex. An experimental light and electron microscopic study. *Experimental Brain Research* **26**, (1976).
Brandauer, B., Timmann, D., Häusler, A. & Hermsdörfer, J. Influences of load characteristics on impaired control of grip forces in patients with cerebellar damage. *Journal of neurophysiology* **103**, 698-708 (2010).
BROOKHART, J.M., MORUZZI, G. & SNIDER, R.S. Origin of cerebellar waves. *Journal of neurophysiology* **14**, 181-90 (1951).
Brown, E.N., Kass, R.E. & Mitra, P.P. Multiple neural spike train data analysis: state-of-the-art and future challenges. *Nature neuroscience* **7**, 456-61 (2004).
Brunel, N., Hakim, V., Isope, P., Nadal, J.-P. & Barbour, B. Optimal information storage and the distribution of synaptic weights: perceptron versus Purkinje cell. *Neuron* **43**, 745-57 (2004).
Bureau, I., Dieudonne, S., Coussen, F. & Mulle, C. Kainate receptor-mediated synaptic currents in cerebellar Golgi cells are not shaped by diffusion of glutamate. *Proceedings of the National Academy of Sciences of the United States of America* **97**, 6838-43 (2000).
Buzsáki, G. & Draguhn, A. Neuronal oscillations in cortical networks. *Science (New York, N.Y.)* **304**, 1926-9 (2004).
Canolty, R.T. *et al.* High gamma power is phase-locked to theta oscillations in human neocortex. *Science (New York, N.Y.)* **313**, 1626-8 (2006).
Chadderton, P., Margrie, T.W. & Häusser, M. Integration of quanta in cerebellar granule cells during sensory processing. *Nature* **428**, 856-60 (2004).
Chapman, P.F., Atkins, C.M., Allen, M.T., Haley, J.E. & Steinmetz, J.E. Inhibition of nitric oxide synthesis impairs two different forms of learning. *Neuroreport* **3**, 567-70 (1992).
Cheron, G., Servais, L. & Dan, B. Cerebellar network plasticity: from genes to fast oscillation. *Neuroscience* **153**, 1-19 (2008).
Cheron, G., Servais, L., Wagstaff, J. & Dan, B. Fast cerebellar oscillation associated with ataxia in a mouse model of Angelman syndrome. *Neuroscience* **130**, 631-637 (2005).
Cheron, G. *et al.* Inactivation of calcium-binding protein genes induces 160 Hz oscillations in the cerebellar cortex of alert mice. *The Journal of neuroscience : the official journal of the Society for Neuroscience* **24**, 434-41 (2004).
Clower, D.M., West, R.A., Lynch, J.C. & Strick, P.L. The inferior parietal lobule is the target of output from the superior colliculus, hippocampus, and cerebellum. *The Journal of neuroscience : the official journal of the Society for Neuroscience* **21**, 6283-91 (2001).
Coenen, D.P. & D., O.J.-M. Model of granular layer encoding in the cerebellum. *Neurocomputing* **58-60**, 575-580 (2004).
Coesmans, M., Weber, J.T., De Zeeuw, C.I. & Hansel, C. Bidirectional parallel fiber plasticity in the cerebellum under climbing fiber control. *Neuron* **44**, 691-700 (2004).
Cohen, D. & Yarom, Y. Patches of synchronized activity in the cerebellar cortex evoked by mossy-fiber stimulation: questioning the role of parallel fibers. *Proceedings of the National Academy of Sciences of the United States of America* **95**, 15032-6 (1998).
Coltz, J.D., Johnson, M.T. & Ebner, T.J. Cerebellar Purkinje cell simple spike discharge encodes movement velocity in primates during visuomotor arm tracking. *The Journal of neuroscience : the official journal of the Society for Neuroscience* **19**, 1782-803 (1999).
Courtemanche, R., Chabaud, P. & Lamarre, Y. Synchronization in primate cerebellar granule cell layer local field potentials: basic anisotropy and dynamic changes during active expectancy. *Frontiers in cellular neuroscience* **3**, 6 (2009).
Courtemanche, R. & Lamarre, Y. Local field potential oscillations in primate cerebellar cortex: synchronization with cerebral cortex during active and passive expectancy. *Journal of neurophysiology* **93**, 2039-52 (2005).

Courtemanche, R., Pellerin, J.-P. & Lamarre, Y. Local field potential oscillations in primate cerebellar cortex: modulation during active and passive expectancy. *Journal of neurophysiology* **88**, 771-82 (2002).
Dagher, A., Owen, A.M., Boecker, H. & Brooks, D.J. Mapping the network for planning: a correlational PET activation study with the Tower of London task. *Brain : a journal of neurology* **122 (Pt 1**, 1973-87 (1999).
Dalal, S.S. *et al.* Five-dimensional neuroimaging: localization of the time-frequency dynamics of cortical activity. *NeuroImage* **40**, 1686-700 (2008).
Damji, K.F. *et al.* Periodic vestibulocerebellar ataxia, an autosomal dominant ataxia with defective smooth pursuit, is genetically distinct from other autosomal dominant ataxias. *Archives of neurology* **53**, 338-44 (1996).
D'Angelo, E. *et al.* Timing in the cerebellum: oscillations and resonance in the granular layer. *Neuroscience* **162**, 805-15 (2009).
D'Angelo, E. *et al.* Theta-frequency bursting and resonance in cerebellar granule cells: experimental evidence and modeling of a slow k+-dependent mechanism. *The Journal of neuroscience : the official journal of the Society for Neuroscience* **21**, 759-70 (2001).
D'Angelo, E. The critical role of Golgi cells in regulating spatio-temporal integration and plasticity at the cerebellum input stage. *Frontiers in neuroscience* **2**, 35-46 (2008).
De Schutter, E. & Bjaalie, J.G. Coding in the granular layer of the cerebellum. *Progress in brain research* **130**, 279-96 (2001).
De Schutter, E. Cerebellar cortex: computation by extrasynaptic inhibition? *Current biology : CB* **12**, R363-5 (2002).
de Solages, C. *et al.* High-frequency organization and synchrony of activity in the purkinje cell layer of the cerebellum. *Neuron* **58**, 775-88 (2008).
De Zeeuw, C.I. & Berrebi, A.S. Postsynaptic targets of Purkinje cell terminals in the cerebellar and vestibular nuclei of the rat. *The European journal of neuroscience* **7**, 2322-33 (1995).
De Zeeuw, C.I., Koekkoek, S.K., Wylie, D.R. & Simpson, J.I. Association between dendritic lamellar bodies and complex spike synchrony in the olivocerebellar system. *Journal of neurophysiology* **77**, 1747-58 (1997).
De Zeeuw, C.I. *et al.* Morphological correlates of bilateral synchrony in the rat cerebellar cortex. *The Journal of neuroscience : the official journal of the Society for Neuroscience* **16**, 3412-26 (1996).
De Zeeuw, C.I. *et al.* Microcircuitry and function of the inferior olive. *Trends in neurosciences* **21**, 391-400 (1998).
De Zeeuw, C.I. *et al.* Spatiotemporal firing patterns in the cerebellum. *Nature reviews. Neuroscience* **12**, 327-44 (2011).
De Zeeuw, C.I., Hoebeek, F.E. & Schonewille, M. Causes and consequences of oscillations in the cerebellar cortex. *Neuron* **58**, 655-8 (2008).
Dean, P., Porrill, J. & Stone, J.V. Decorrelation control by the cerebellum achieves oculomotor plant compensation in simulated vestibulo-ocular reflex. *Proceedings. Biological sciences / The Royal Society* **269**, 1895-904 (2002).
DeCoteau, W.E. *et al.* Learning-related coordination of striatal and hippocampal theta rhythms during acquisition of a procedural maze task. *Proceedings of the National Academy of Sciences of the United States of America* **104**, 5644-9 (2007).
Delescluse, M. & Pouzat, C. Efficient spike-sorting of multi-state neurons using inter-spike intervals information. *Journal of neuroscience methods* **150**, 16-29 (2006).
Destexhe, A. & Contreras, D. Neuronal computations with stochastic network states. *Science (New York, N.Y.)* **314**, 85-90 (2006).
Deubel, H. Separate adaptive mechanisms for the control of reactive and volitional saccadic eye movements. *Vision research* **35**, 3529-40 (1995).
Diana, M.A. *et al.* T-type and L-type Ca2+ conductances define and encode the bimodal firing pattern of vestibulocerebellar unipolar brush cells. *The Journal of neuroscience : the official journal of the Society for Neuroscience* **27**, 3823-38 (2007).
Dieudonne, S. Submillisecond kinetics and low efficacy of parallel fibre-Golgi cell synaptic currents in the rat cerebellum. *The Journal of physiology* **510 (Pt 3**, 845-66 (1998).

Dieudonné, S. & Dumoulin, A. Serotonin-driven long-range inhibitory connections in the cerebellar cortex. *The Journal of neuroscience : the official journal of the Society for Neuroscience* **20**, 1837-48 (2000).
Diño, M.R., Perachio, A.A. & Mugnaini, E. Cerebellar unipolar brush cells are targets of primary vestibular afferents: an experimental study in the gerbil. *Experimental brain research. Experimentelle Hirnforschung. Expérimentation cérébrale* **140**, 162-70 (2001).
Dow, R.S. The electrical activity of the cerebellum and its functional significance. *The Journal of physiology* **94**, 67-86 (1938).
Dugué, G.P. Etude fonctionnelle d'un interneurone inhibiteur du cortex cérébelleux: la cellule de Golgi. (2006).
Dugué, G.P. *et al.* Electrical coupling mediates tunable low-frequency oscillations and resonance in the cerebellar Golgi cell network. *Neuron* **61**, 126-39 (2009).
Dum, R.P. & Strick, P.L. An unfolded map of the cerebellar dentate nucleus and its projections to the cerebral cortex. *Journal of neurophysiology* **89**, 634-9 (2003).
Dumoulin, A., Triller, A. & Dieudonné, S. IPSC kinetics at identified GABAergic and mixed GABAergic and glycinergic synapses onto cerebellar Golgi cells. *The Journal of neuroscience : the official journal of the Society for Neuroscience* **21**, 6045-57 (2001).
Ebner, T.J. & Bloedel, J.R. Correlation between activity of Purkinje cells and its modification by natural peripheral stimuli. *Journal of neurophysiology* **45**, 948-61 (1981).
Ebner, T.J., Johnson, M.T.V., Roitman, A. & Fu, Q. What do complex spikes signal about limb movements? *Annals of the New York Academy of Sciences* **978**, 205-18 (2002).
Eccles, J.C., Llinás, R. & Sasaki, K. The mossy fibre-granule cell relay of the cerebellum and its inhibitory control by Golgi cells. *Experimental brain research. Experimentelle Hirnforschung. Expérimentation cérébrale* **1**, 82-101 (1966).
Eccles, J.C., Sasaki, K. & Strata, P. Interpretation of the potential fields generated in the cerebellar cortex by a mossy fibre volley. *Experimental brain research. Experimentelle Hirnforschung. Expérimentation cérébrale* **3**, 58-80 (1967).
Eccles, J.C., Ito, M. & Szentágothai, J. *The Cerebellum as a Neuronal Machine. Science* **158**, 1439-1440 (Springer-Verlag, New York: 1967).
Edge, A.L., Marple-Horvat, D.E. & Apps, R. Lateral cerebellum: functional localization within crus I and correspondence to cortical zones. *The European journal of neuroscience* **18**, 1468-85 (2003).
Ekerot, C.F. & Jörntell, H. Parallel fibre receptive fields of Purkinje cells and interneurons are climbing fibre-specific. *The European journal of neuroscience* **13**, 1303-10 (2001).
Ekerot, C.F., Jörntell, H. & Garwicz, M. Functional relation between corticonuclear input and movements evoked on microstimulation in cerebellar nucleus interpositus anterior in the cat. *Experimental brain research. Experimentelle Hirnforschung. Expérimentation cérébrale* **106**, 365-76 (1995).
Ekerot, C.F. & Larson, B. Branching of olivary axons to innervate pairs of sagittal zones in the cerebellar anterior lobe of the cat. *Experimental brain research. Experimentelle Hirnforschung. Expérimentation cérébrale* **48**, 185-98 (1982).
Ekerot, C.F. & Larson, B. The dorsal spino-olivocerebellar system in the cat. I. Functional organization and termination in the anterior lobe. *Experimental brain research. Experimentelle Hirnforschung. Expérimentation cérébrale* **36**, 201-17 (1979).
Ekerot, C.-F. & Larson, B. Branching of olivary axons to innervate pairs of sagittal zones in the cerebellar anterior lobe of the cat. *Experimental Brain Research* **48**, (1982).
Ekerot, C.-F. & Jörntell, H. Parallel fiber receptive fields: a key to understanding cerebellar operation and learning. *Cerebellum (London, England)* **2**, 101-9 (2003).
Espinoza, E. & Smith, A.M. Purkinje cell simple spike activity during grasping and lifting objects of different textures and weights. *Journal of neurophysiology* **64**, 698-714 (1990).
Evarts, E.V. & Tanji, J. Reflex and intended responses in motor cortex pyramidal tract neurons of monkey. *Journal of neurophysiology* **39**, 1069-80 (1976).
Fang, P.-C., Stepniewska, I. & Kaas, J.H. Ipsilateral cortical connections of motor, premotor, frontal eye, and posterior parietal fields in a prosimian primate, Otolemur garnetti. *The Journal of comparative neurology* **490**, 305-33 (2005).

Fee, M.S., Mitra, P.P. & Kleinfeld, D. Automatic sorting of multiple unit neuronal signals in the presence of anisotropic and non-Gaussian variability. *Journal of neuroscience methods* **69**, 175-88 (1996).
Forti, L., Cesana, E., Mapelli, J. & D'Angelo, E. Ionic mechanisms of autorhythmic firing in rat cerebellar Golgi cells. *The Journal of physiology* **574**, 711-29 (2006).
Fortier, P.A., Kalaska, J.F. & Smith, A.M. Cerebellar neuronal activity related to whole-arm reaching movements in the monkey. *Journal of neurophysiology* **62**, 198-211 (1989).
FOX, C.A. & BARNARD, J.W. A quantitative study of the Purkinje cell dendritic branchlets and their relationship to afferent fibres. *Journal of anatomy* **91**, 299-313 (1957).
Fox, P.T. *et al.* Brain correlates of stuttering and syllable production. A PET performance-correlation analysis. *Brain : a journal of neurology* **123 (Pt 1**, 1985-2004 (2000).
Franke, F., Natora, M., Boucsein, C., Munk, M.H.J. & Obermayer, K. An online spike detection and spike classification algorithm capable of instantaneous resolution of overlapping spikes. *Journal of computational neuroscience* **29**, 127-48 (2010).
Fu, Q.G., Flament, D., Coltz, J.D. & Ebner, T.J. Relationship of cerebellar Purkinje cell simple spike discharge to movement kinematics in the monkey. *Journal of neurophysiology* **78**, 478-91 (1997).
Gancarz, G. & Grossberg, S. A neural model of saccadic eye movement control explains task-specific adaptation. *Vision research* **39**, 3123-43 (1999).
Gao, H., Solages, C. de & Lena, C. Tetrode recordings in the cerebellar cortex. *Journal of physiology, Paris* (2011).doi:10.1016/j.jphysparis.2011.10.005
Gao, J.H. *et al.* Cerebellum implicated in sensory acquisition and discrimination rather than motor control. *Science (New York, N.Y.)* **272**, 545-7 (1996).
Garwicz, M. Cerebellar control of forelimb movements: modular organization revealed by nociceptive and tactile climbing fibre input. (1992).
Garwicz, M., Ekerot, C.-F. & Schouenborg, J. Distribution of Cutaneous Nociceptive and Tactile Climbing Fibre Input to Sagittal Zones in Cat Cerebellar Anterior Lobe. *The European journal of neuroscience* **4**, 289-295 (1992).
Garwicz, M. & Ekerot, C.F. Topographical organization of the cerebellar cortical projection to nucleus interpositus anterior in the cat. *The Journal of physiology* **474**, 245-60 (1994).
Garwicz, M., Jörntell, H. & Ekerot, C.F. Cutaneous receptive fields and topography of mossy fibres and climbing fibres projecting to cat cerebellar C3 zone. *The Journal of physiology* **512 (Pt 1**, 277-93 (1998).
Garwicz, M., Levinsson, A. & Schouenborg, J. Common principles of sensory encoding in spinal reflex modules and cerebellar climbing fibres. *The Journal of physiology* **540**, 1061-9 (2002).
Gauck, V. & Jaeger, D. The control of rate and timing of spikes in the deep cerebellar nuclei by inhibition. *The Journal of neuroscience : the official journal of the Society for Neuroscience* **20**, 3006-16 (2000).
Georgopoulos, A.P., Kalaska, J.F., Caminiti, R. & Massey, J.T. On the relations between the direction of two-dimensional arm movements and cell discharge in primate motor cortex. *The Journal of neuroscience : the official journal of the Society for Neuroscience* **2**, 1527-37 (1982).
Geurts, F.J., De Schutter, E. & Dieudonné, S. Unraveling the cerebellar cortex: cytology and cellular physiology of large-sized interneurons in the granular layer. *Cerebellum (London, England)* **2**, 290-9 (2003).
Gharbawie, O.A., Karl, J.M. & Whishaw, I.Q. Recovery of skilled reaching following motor cortex stroke: do residual corticofugal fibers mediate compensatory recovery? *The European journal of neuroscience* **26**, 3309-27 (2007).
Gharbawie, O.A., Williams, P.T.J.A., Kolb, B. & Whishaw, I.Q. Transient middle cerebral artery occlusion disrupts the forelimb movement representations of rat motor cortex. *The European journal of neuroscience* **28**, 951-63 (2008).
Gholamrezaei, G. & Whishaw, I.Q. Individual differences in skilled reaching for food related to increased number of gestures: evidence for goal and habit learning of skilled reaching.

Behavioral neuroscience **123**, 863-74 (2009).
Gibson, A.R., Horn, K.M., Pong, M. & Van Kan, P.L. Construction of a reach-to-grasp. *Novartis Foundation symposium* **218**, 233-45; discussion 245-51 (1998).
Glickstein, M., May, J.G. & Mercier, B.E. Corticopontine projection in the macaque: the distribution of labelled cortical cells after large injections of horseradish peroxidase in the pontine nuclei. *The Journal of comparative neurology* **235**, 343-59 (1985).
Glickstein, M. & Doron, K. Cerebellum: connections and functions. *Cerebellum (London, England)* **7**, 589-94 (2008).
Gomi, H. *et al.* Temporal firing patterns of Purkinje cells in the cerebellar ventral paraflocculus during ocular following responses in monkeys I. Simple spikes. *Journal of neurophysiology* **80**, 818-31 (1998).
González, B., Rodríguez, M., Ramirez, C. & Sabaté, M. Disturbance of motor imagery after cerebellar stroke. *Behavioral neuroscience* **119**, 622-6 (2005).
Goossens, J. *et al.* Expression of protein kinase C inhibitor blocks cerebellar long-term depression without affecting Purkinje cell excitability in alert mice. *The Journal of neuroscience : the official journal of the Society for Neuroscience* **21**, 5813-23 (2001).
Green, E.C. *Anatomy of the rat.* 370 (Hafner Publishing: New York, 1963).
Grill, J. *et al.* Critical risk factors for intellectual impairment in children with posterior fossa tumors: the role of cerebellar damage. *Journal of neurosurgery* **101**, 152-8 (2004).
Gross, J. *et al.* The neural basis of intermittent motor control in humans. *Proceedings of the National Academy of Sciences of the United States of America* **99**, 2299-302 (2002).
Gunji, A., Ishii, R., Chau, W., Kakigi, R. & Pantev, C. Rhythmic brain activities related to singing in humans. *NeuroImage* **34**, 426-34 (2007).
Hámori, J. & Szentágothai, J. Participation of Golgi neuron processes in the cerebellar glomeruli: an electron microscope study. *Experimental brain research. Experimentelle Hirnforschung. Expérimentation cérébrale* **2**, 35-48 (1966).
Hartmann, J. & Konnerth, A. Determinants of postsynaptic Ca2+ signaling in Purkinje neurons. *Cell calcium* **37**, 459-66 (2005).
Hartmann, M.J. & Bower, J.M. Oscillatory activity in the cerebellar hemispheres of unrestrained rats. *Journal of neurophysiology* **80**, 1598-604 (1998).
Häusser, M. & Clark, B.A. Tonic synaptic inhibition modulates neuronal output pattern and spatiotemporal synaptic integration. *Neuron* **19**, 665-78 (1997).
Hawkes, R. & Leclerc, N. Purkinje cell axon collateral distributions reflect the chemical compartmentation of the rat cerebellar cortex. *Brain research* **476**, 279-90 (1989).
Hazan, L., Zugaro, M. & Buzsáki, G. Klusters, NeuroScope, NDManager: a free software suite for neurophysiological data processing and visualization. *Journal of neuroscience methods* **155**, 207-16 (2006).
Heck, D.H., Thach, W.T. & Keating, J.G. On-beam synchrony in the cerebellum as the mechanism for the timing and coordination of movement. *Proceedings of the National Academy of Sciences of the United States of America* **104**, 7658-63 (2007).
Heine, S.A., Highstein, S.M. & Blazquez, P.M. Golgi cells operate as state-specific temporal filters at the input stage of the cerebellar cortex. *The Journal of neuroscience : the official journal of the Society for Neuroscience* **30**, 17004-14 (2010).
Hermer-Vazquez, L. Distinct temporal activity patterns in the rat M1 and red nucleus during skilled versus unskilled limb movement. *Behavioural Brain Research* **150**, 93-107 (2004).
Herrero, L., Pardoe, J. & Apps, R. Pontine and lateral reticular projections to the c1 zone in lobulus simplex and paramedian lobule of the rat cerebellar cortex. *Cerebellum (London, England)* **1**, 185-99 (2002).
Hoebeek, F.E. *et al.* Increased noise level of purkinje cell activities minimizes impact of their modulation during sensorimotor control. *Neuron* **45**, 953-65 (2005).
Holdefer, R.N., Miller, L.E., Chen, L.L. & Houk, J.C. Functional connectivity between cerebellum and primary motor cortex in the awake monkey. *Journal of neurophysiology* **84**, 585-90 (2000).
Holtzman, T., Mostofi, A., Phuah, C.L. & Edgley, S.A. Cerebellar Golgi cells in the rat receive multimodal convergent peripheral inputs via the lateral funiculus of the spinal cord. *The*

Journal of physiology **577**, 69-80 (2006).
Hopp, J.J. & Fuchs, A.F. The characteristics and neuronal substrate of saccadic eye movement plasticity. *Progress in neurobiology* **72**, 27-53 (2004).
Horn, K.M., Pong, M. & Gibson, A.R. Functional relations of cerebellar modules of the cat. *The Journal of neuroscience : the official journal of the Society for Neuroscience* **30**, 9411-23 (2010).
Hull, C. & Regehr, W.G. Identification of an inhibitory circuit that regulates cerebellar Golgi cell activity. *Neuron* **73**, 149-58 (2012).
Hyland, B.I. & Jordan, V.M.B. Muscle activity during forelimb reaching movements in rats. *Behavioural Brain Research* **85**, 175-186 (1997).
Ito, M. Neurophysiological aspects of the cerebellar motor control system. *International journal of neurology* **7**, 162-76 (1970).
Ito, M. & Kano, M. Long-lasting depression of parallel fiber-Purkinje cell transmission induced by conjunctive stimulation of parallel fibers and climbing fibers in the cerebellar cortex. *Neuroscience letters* **33**, 253-8 (1982).
Ito, M., Sakurai, M. & Tongroach, P. Climbing fibre induced depression of both mossy fibre responsiveness and glutamate sensitivity of cerebellar Purkinje cells. *The Journal of physiology* **324**, 113-34 (1982).
Ito, M. & Yoshida, M. The cerebellar-evoked monosynaptic inhibition of Deiters' neurones. *Experientia* **20**, 515-6 (1964).
Ito, M., Yoshida, M. & Obata, K. Monosynaptic inhibition of the intracerebellar nuclei induced from the cerebellar cortex. *Cerebellum (London, England)* **6**, 103-4 (2007).
Ito, M. Cerebellar circuitry as a neuronal machine. *Progress in neurobiology* **78**, 272-303 (2006).
Ito, M. *the Cerebellum and Neural Control*. (Raven Press, New York: New York, 1984).
Ito, M. Control of mental activities by internal models in the cerebellum. *Nature reviews. Neuroscience* **9**, 304-13 (2008).
Ito, M. Bases and implications of learning in the cerebellum--adaptive control and internal model mechanism. *Progress in brain research* **148**, 95-109 (2005).
Ivry, R.B. & Keele, S.W. Timing Functions of The Cerebellum. *Journal of Cognitive Neuroscience* **1**, 136-152 (1989).
Iwaniuk, A.N. & Whishaw, I.Q. On the origin of skilled forelimb movements. *Trends in neurosciences* **23**, 372-6 (2000).
Jacobs, J., Kahana, M.J., Ekstrom, A.D. & Fried, I. Brain oscillations control timing of single-neuron activity in humans. *The Journal of neuroscience : the official journal of the Society for Neuroscience* **27**, 3839-44 (2007).
Jaeger, D. No parallel fiber volleys in the cerebellar cortex: evidence from cross-correlation analysis between Purkinje cells in a computer model and in recordings from anesthetized rats. *Journal of computational neuroscience* **14**, 311-27 (2003).
Jarratt, H. & Hyland, B. Neuronal activity in rat red nucleus during forelimb reach-to-grasp movements. *Neuroscience* **88**, 629-42 (1999).
Jones, M.S. & Barth, D.S. Spatiotemporal organization of fast (>200 Hz) electrical oscillations in rat Vibrissa/Barrel cortex. *Journal of neurophysiology* **82**, 1599-609 (1999).
Jörntell, H., Ekerot, C., Garwicz, M. & Luo, X.L. Functional organization of climbing fibre projection to the cerebellar anterior lobe of the rat. *The Journal of physiology* **522 Pt 2**, 297-309 (2000).
Jörntell, H., Garwicz, M. & Ekerot, C.F. Relation between cutaneous receptive fields and muscle afferent input to climbing fibres projecting to the cerebellar C3 zone in the cat. *The European journal of neuroscience* **8**, 1769-79 (1996).
Jörntell, H. & Ekerot, C.-F. Reciprocal bidirectional plasticity of parallel fiber receptive fields in cerebellar Purkinje cells and their afferent interneurons. *Neuron* **34**, 797-806 (2002).
JOYNT, R.J. Micro-electrode studies of cerebellar electrical activity in the frog. *The Journal of physiology* **144**, 23-37 (1958).
Kanichay, R.T. & Silver, R.A. Synaptic and cellular properties of the feedforward inhibitory circuit within the input layer of the cerebellar cortex. *The Journal of neuroscience : the official journal of the Society for Neuroscience* **28**, 8955-67 (2008).

Kassel, J., Shambes, G.M. & Welker, W. Fractured cutaneous projections to the granule cell layer of the posterior cerebellar hemisphere of the domestic cat. *The Journal of comparative neurology* **225**, 458-68 (1984).
Kawato, M. Internal models for motor control and trajectory planning. *Current opinion in neurobiology* **9**, 718-27 (1999).
Kawato, M., Furukawa, K. & Suzuki, R. A hierarchical neural-network model for control and learning of voluntary movement. *Biological cybernetics* **57**, 169-85 (1987).
Kawato, M. & Gomi, H. A computational model of four regions of the cerebellum based on feedback-error learning. *Biological cybernetics* **68**, 95-103 (1992).
Kazantsev, V.B., Nekorkin, V.I., Makarenko, V.I. & Llinás, R. Self-referential phase reset based on inferior olive oscillator dynamics. *Proceedings of the National Academy of Sciences of the United States of America* **101**, 18183-8 (2004).
Keating, J.G. & Thach, W.T. Nonclock behavior of inferior olive neurons: interspike interval of Purkinje cell complex spike discharge in the awake behaving monkey is random. *Journal of neurophysiology* **73**, 1329-40 (1995).
Kelly, R.M. & Strick, P.L. Cerebellar loops with motor cortex and prefrontal cortex of a nonhuman primate. *The Journal of neuroscience : the official journal of the Society for Neuroscience* **23**, 8432-44 (2003).
Khosrovani, S., Van Der Giessen, R.S., De Zeeuw, C.I. & De Jeu, M.T.G. In vivo mouse inferior olive neurons exhibit heterogeneous subthreshold oscillations and spiking patterns. *Proceedings of the National Academy of Sciences of the United States of America* **104**, 15911-6 (2007).
Kim, J.J. *et al.* Direct comparison of the neural substrates of recognition memory for words and faces. *Brain : a journal of neurology* **122 (Pt 6**, 1069-83 (1999).
Kim, K.H. & Kim, S.J. Method for unsupervised classification of multiunit neural signal recording under low signal-to-noise ratio. *IEEE transactions on bio-medical engineering* **50**, 421-31 (2003).
Kim, S.G., Uğurbil, K. & Strick, P.L. Activation of a cerebellar output nucleus during cognitive processing. *Science (New York, N.Y.)* **265**, 949-51 (1994).
King, V.M., Armstrong, D.M., Apps, R. & Trott, J.R. Numerical aspects of pontine, lateral reticular, and inferior olivary projections to two paravermal cortical zones of the cat cerebellum. *The Journal of comparative neurology* **390**, 537-51 (1998).
Kistler, W.M. & De Zeeuw, C.I. Time windows and reverberating loops: a reverse-engineering approach to cerebellar function. *Cerebellum (London, England)* **2**, 44-54 (2003).
Kitazawa, S., Kimura, T. & Yin, P.B. Cerebellar complex spikes encode both destinations and errors in arm movements. *Nature* **392**, 494-7 (1998).
Kitazawa, S. & Yin, P.-B. Prism adaptation with delayed visual error signals in the monkey. *Experimental brain research. Experimentelle Hirnforschung. Expérimentation cérébrale* **144**, 258-61 (2002).
Kobayashi, Y. *et al.* Temporal firing patterns of Purkinje cells in the cerebellar ventral paraflocculus during ocular following responses in monkeys II. Complex spikes. *Journal of neurophysiology* **80**, 832-48 (1998).
Kolb, F.P., Arnold, G., Lerch, R., Straka, H. & Büttner-Ennever, J. Spatial distribution of field potential profiles in the cat cerebellar cortex evoked by peripheral and central inputs. *Neuroscience* **81**, 1155-81 (1997).
Lainé, J. & Axelrad, H. Extending the cerebellar Lugaro cell class. *Neuroscience* **115**, 363-74 (2002).
Lang, C.E. & Bastian, A.J. Cerebellar damage impairs automaticity of a recently practiced movement. *Journal of neurophysiology* **87**, 1336-47 (2002).
Lang, E.J., Sugihara, I., Welsh, J.P. & Llinás, R. Patterns of spontaneous purkinje cell complex spike activity in the awake rat. *The Journal of neuroscience : the official journal of the Society for Neuroscience* **19**, 2728-39 (1999).
Lang, E.J., Sugihara, I. & Llinás, R. Olivocerebellar modulation of motor cortex ability to generate vibrissal movements in rat. *The Journal of physiology* **571**, 101-20 (2006).
Larkin, M. Cerebellar damage limits some, but not all, motor-control functions. *Lancet neurology*

2, 389 (2003).
Lawrence, D.G. & Kuypers, H.G. The functional organization of the motor system in the monkey. I. The effects of bilateral pyramidal lesions. *Brain : a journal of neurology* **91**, 1-14 (1968).
Legg, C.R., Mercier, B. & Glickstein, M. Corticopontine projection in the rat: the distribution of labelled cortical cells after large injections of horseradish peroxidase in the pontine nuclei. *The Journal of comparative neurology* **286**, 427-41 (1989).
Leiner, H.C., Leiner, A.L. & Dow, R.S. Cognitive and language functions of the human cerebellum. *Trends in neurosciences* **16**, 444-7 (1993).
Leiner, H.C., Leiner, A.L. & Dow, R.S. The human cerebro-cerebellar system: its computing, cognitive, and language skills. *Behavioural brain research* **44**, 113-28 (1991).
Lev-Ram, V., Wong, S.T., Storm, D.R. & Tsien, R.Y. A new form of cerebellar long-term potentiation is postsynaptic and depends on nitric oxide but not cAMP. *Proceedings of the National Academy of Sciences of the United States of America* **99**, 8389-93 (2002).
Lewicki, M.S. A review of methods for spike sorting: the detection and classification of neural action potentials. *Network (Bristol, England)* **9**, R53-78 (1998).
Llinás, R.R. Inferior olive oscillation as the temporal basis for motricity and oscillatory reset as the basis for motor error correction. *Neuroscience* **162**, 797-804 (2009).
Llinas, R., Walton, K. & Lang, E. Ch. 7 Cerebellum. *The Synaptic Organization of the Brain* (2004).
Llinás, R. & Welsh, J.P. On the cerebellum and motor learning. *Current opinion in neurobiology* **3**, 958-65 (1993).
Long, M.A., Deans, M.R., Paul, D.L. & Connors, B.W. Rhythmicity without synchrony in the electrically uncoupled inferior olive. *The Journal of neuroscience : the official journal of the Society for Neuroscience* **22**, 10898-905 (2002).
Lotze, M. *et al.* Activation of cortical and cerebellar motor areas during executed and imagined hand movements: an fMRI study. *Journal of cognitive neuroscience* **11**, 491-501 (1999).
Maex, R. & De Schutter, E. Synchronization of golgi and granule cell firing in a detailed network model of the cerebellar granule cell layer. *Journal of neurophysiology* **80**, 2521-37 (1998).
Maex, R. & De Schutter, E. Oscillations in the cerebellar cortex: a prediction of their frequency bands. *Progress in brain research* **148**, 181-8 (2005).
Mangels, J.A., Ivry, R.B. & Shimizu, N. Dissociable contributions of the prefrontal and neocerebellar cortex to time perception. *Brain research. Cognitive brain research* **7**, 15-39 (1998).
Manni, E. & Petrosini, L. A century of cerebellar somatotopy: a debated representation. *Neuroscience* **5**, 1-9 (2004).
Mann-Metzer, P. & Yarom, Y. Electrotonic coupling interacts with intrinsic properties to generate synchronized activity in cerebellar networks of inhibitory interneurons. *The Journal of neuroscience : the official journal of the Society for Neuroscience* **19**, 3298-306 (1999).
Mano, N. & Yamamoto, K. Simple-spike activity of cerebellar Purkinje cells related to visually guided wrist tracking movement in the monkey. *Journal of neurophysiology* **43**, 713-28 (1980).
Marani, E. & Voogd, J. An acetylcholinesterase band-pattern in the molecular layer of the cat cerebellum. *Journal of anatomy* **124**, 335-45 (1977).
Marani, E. Topographic enzyme histochemistry of the mammalian. (1982).
Marple-Horvat, D.E. & Stein, J.F. Cerebellar neuronal activity related to arm movements in trained rhesus monkeys. *The Journal of physiology* **394**, 351-66 (1987).
Marr, D. A theory of cerebellar cortex. *The Journal of physiology* **202**, 437-70 (1969).
Martin, J.H., Cooper, S.E., Hacking, A. & Ghez, C. Differential effects of deep cerebellar nuclei inactivation on reaching and adaptive control. *Journal of neurophysiology* **83**, 1886-99 (2000).
Maruta, J., Hensbroek, R.A. & Simpson, J.I. Intraburst and interburst signaling by climbing fibers. *The Journal of neuroscience : the official journal of the Society for Neuroscience* **27**, 11263-70 (2007).
Mathiak, K., Hertrich, I., Grodd, W. & Ackermann, H. Cerebellum and speech perception: a

functional magnetic resonance imaging study. *Journal of cognitive neuroscience* **14**, 902-12 (2002).
Mauk, M.D., Medina, J.F., Nores, W.L. & Ohyama, T. Cerebellar function: coordination, learning or timing? *Current biology : CB* **10**, R522-5 (2000).
Medina, J.F. & Lisberger, S.G. Encoding and decoding of learned smooth-pursuit eye movements in the floccular complex of the monkey cerebellum. *Journal of neurophysiology* **102**, 2039-54 (2009).
Metz, G.A. & Whishaw, I.Q. Skilled reaching an action pattern: stability in rat (Rattus norvegicus) grasping movements as a function of changing food pellet size. *Behavioural brain research* **116**, 111-22 (2000).
Miall, R.C., Keating, J.G., Malkmus, M. & Thach, W.T. Simple spike activity predicts occurrence of complex spikes in cerebellar Purkinje cells. *Nature neuroscience* **1**, 13-5 (1998).
Middleton, F.A. & Strick, P.L. Cerebellar output: motor and cognitive channels. *Trends in cognitive sciences* **2**, 348-54 (1998).
Middleton, F.A. & Strick, P.L. Cerebellar projections to the prefrontal cortex of the primate. *The Journal of neuroscience : the official journal of the Society for Neuroscience* **21**, 700-12 (2001).
Middleton, S.J. *et al.* High-frequency network oscillations in cerebellar cortex. *Neuron* **58**, 763-74 (2008).
Miles, F.A., Fuller, J.H., Braitman, D.J. & Dow, B.M. Long-term adaptive changes in primate vestibuloocular reflex. III. Electrophysiological observations in flocculus of normal monkeys. *Journal of neurophysiology* **43**, 1437-76 (1980).
Mittmann, W., Koch, U. & Häusser, M. Feed-forward inhibition shapes the spike output of cerebellar Purkinje cells. *The Journal of physiology* **563**, 369-78 (2005).
Moon, S.-K., Alaverdashvili, M., Cross, A.R. & Whishaw, I.Q. Both compensation and recovery of skilled reaching following small photothrombotic stroke to motor cortex in the rat. *Experimental neurology* **218**, 145-53 (2009).
Mortimer, J.A. Cerebellar responses to teleceptive stimuli in alert monkeys. *Brain research* **83**, 369-90 (1975).
Mugnaini, E. The length of cerebellar parallel fibers in chicken and rhesus monkey. *The Journal of comparative neurology* **220**, 7-15 (1983).
Muthukumaraswamy, S.D. Functional properties of human primary motor cortex gamma oscillations. *Journal of neurophysiology* **104**, 2873-85 (2010).
Napper, R.M. & Harvey, R.J. Number of parallel fiber synapses on an individual Purkinje cell in the cerebellum of the rat. *The Journal of comparative neurology* **274**, 168-77 (1988).
Napper, R.M. & Harvey, R.J. Quantitative study of the Purkinje cell dendritic spines in the rat cerebellum. *The Journal of comparative neurology* **274**, 158-67 (1988).
Niedermeyer, E. The electrocerebellogram. *Clinical EEG and neuroscience : official journal of the EEG and Clinical Neuroscience Society (ENCS)* **35**, 112-5 (2004).
Nikkhah, G., Rosenthal, C., Hedrich, H.J. & Samii, M. Differences in acquisition and full performance in skilled forelimb use as measured by the "staircase test" in five rat strains. *Behavioural brain research* **92**, 85-95 (1998).
O'Connor, S.M., Berg, R.W. & Kleinfeld, D. Coherent electrical activity between vibrissa sensory areas of cerebellum and neocortex is enhanced during free whisking. *Journal of neurophysiology* **87**, 2137-48 (2002).
O'Donoghue, D.L. & Bishop, G.A. A quantitative analysis of the distribution of Purkinje cell axonal collaterals in different zones of the cat's cerebellum: an intracellular HRP study. *Experimental brain research. Experimentelle Hirnforschung. Expérimentation cérébrale* **80**, 63-71 (1990).
Orduz, D. & Llano, I. Recurrent axon collaterals underlie facilitating synapses between cerebellar Purkinje cells. *Proceedings of the National Academy of Sciences of the United States of America* **104**, 17831-6 (2007).
Oscarsson, O. Spatial distribution of mossy and climbing fiber inputs into the cerebellar cortex. *Exp Brain Res [Suppl]* **1**, 36-42 (1976).
Oscarsson, O. & Sjölund, B. The ventral spino-olivocerebellar system in the cat. I. Identification

of five paths and their termination in the cerebellar anterior lobe. *Experimental brain research. Experimentelle Hirnforschung. Expérimentation cérébrale* **28**, 469-86 (1977).
Ozden, I., Sullivan, M.R., Lee, H.M. & Wang, S.S.-H. Reliable coding emerges from coactivation of climbing fibers in microbands of cerebellar Purkinje neurons. *The Journal of neuroscience : the official journal of the Society for Neuroscience* **29**, 10463-73 (2009).
Palay, S. & Chan-Palay, V. The Cerebellar Cortex. *Springer-Verlag, New York* (1974).
Pardoe, J. & Apps, R. Structure-function relations of two somatotopically corresponding regions of the rat cerebellar cortex: olivo-cortico-nuclear connections. *Cerebellum (London, England)* **1**, 165-84 (2002).
Parsons, L.M. *et al.* Neuroimaging evidence implicating cerebellum in support of sensory/cognitive processes associated with thirst. *Proceedings of the National Academy of Sciences of the United States of America* **97**, 2332-6 (2000).
Parsons, L.M. *et al.* Use of implicit motor imagery for visual shape discrimination as revealed by PET. *Nature* **375**, 54-8 (1995).
Pasalar, S., Roitman, A.V., Durfee, W.K. & Ebner, T.J. Force field effects on cerebellar Purkinje cell discharge with implications for internal models. *Nature neuroscience* **9**, 1404-11 (2006).
Passingham, R.E., Perry, V.H. & Wilkinson, F. The long-term effects of removal of sensorimotor cortex in infant and adult rhesus monkeys. *Brain : a journal of neurology* **106 (Pt 3)**, 675-705 (1983).
Peeters, R.R. *et al.* A patchy horizontal organization of the somatosensory activation of the rat cerebellum demonstrated by functional MRI. *The European journal of neuroscience* **11**, 2720-30 (1999).
Pei, X. *et al.* Spatiotemporal dynamics of electrocorticographic high gamma activity during overt and covert word repetition. *NeuroImage* **54**, 2960-72 (2011).
Pellerin, J.P. & Lamarre, Y. Local field potential oscillations in primate cerebellar cortex during voluntary movement. *Journal of neurophysiology* **78**, 3502-7 (1997).
Pellet, J., Tardy, M.F., Dubrocard, S. & Harlay, F. Phasic electrical activity of the cerebellar cortex during sleep and wakefulness. *Arch. Ital. Biol.* **112**, 163-195 (1974).
Perrett, S.P., Ruiz, B.P. & Mauk, M.D. Cerebellar cortex lesions disrupt learning-dependent timing of conditioned eyelid responses. *The Journal of neuroscience : the official journal of the Society for Neuroscience* **13**, 1708-18 (1993).
Pfurtscheller, G. Central beta rhythm during sensorimotor activities in man. *Electroencephalography and clinical neurophysiology* **51**, 253-64 (1981).
Pichitpornchai, C., Rawson, J.A. & Rees, S. Morphology of parallel fibres in the cerebellar cortex of the rat: an experimental light and electron microscopic study with biocytin. *The Journal of comparative neurology* **342**, 206-20 (1994).
Pijpers, A., Apps, R., Pardoe, J., Voogd, J. & Ruigrok, T.J.H. Precise spatial relationships between mossy fibers and climbing fibers in rat cerebellar cortical zones. *The Journal of neuroscience : the official journal of the Society for Neuroscience* **26**, 12067-80 (2006).
Pijpers, A., Voogd, J. & Ruigrok, T.J.H. Topography of olivo-cortico-nuclear modules in the intermediate cerebellum of the rat. *The Journal of comparative neurology* **492**, 193-213 (2005).
Porrill, J., Dean, P. & Stone, J.V. Recurrent cerebellar architecture solves the motor-error problem. *Proceedings. Biological sciences / The Royal Society* **271**, 789-96 (2004).
Pouzat, C., Delescluse, M., Viot, P. & Diebolt, J. Improved spike-sorting by modeling firing statistics and burst-dependent spike amplitude attenuation: a Markov chain Monte Carlo approach. *Journal of neurophysiology* **91**, 2910-28 (2004).
Price, C.J., Green, D.W. & von Studnitz, R. A functional imaging study of translation and language switching. *Brain : a journal of neurology* **122 (Pt 1**, 2221-35 (1999).
Prsa, M. & Thier, P. The role of the cerebellum in saccadic adaptation as a window into neural mechanisms of motor learning. *The European journal of neuroscience* **33**, 2114-28 (2011).
Purves, D. *et al. Neuroscience.* (Sinauer Associates, Inc.: 2007).
Purves, D. *et al. Neuroscience.* (2001).
Raman, I.M. & Bean, B.P. Ionic currents underlying spontaneous action potentials in isolated

cerebellar Purkinje neurons. *The Journal of neuroscience : the official journal of the Society for Neuroscience* **19**, 1663-74 (1999).
Rand, M.K., Shimansky, Y., Stelmach, G.E., Bracha, V. & Bloedel, J.R. Effects of accuracy constraints on reach-to-grasp movements in cerebellar patients. *Experimental Brain Research* **135**, 179-188 (2000).
Robinson, F.R. & Fuchs, A.F. The role of the cerebellum in voluntary eye movements. *Annual review of neuroscience* **24**, 981-1004 (2001).
Roitman, A.V., Pasalar, S., Johnson, M.T.V. & Ebner, T.J. Position, direction of movement, and speed tuning of cerebellar Purkinje cells during circular manual tracking in monkey. *The Journal of neuroscience : the official journal of the Society for Neuroscience* **25**, 9244-57 (2005).
Ros, H., Sachdev, R.N.S., Yu, Y., Sestan, N. & McCormick, D.A. Neocortical networks entrain neuronal circuits in cerebellar cortex. *The Journal of neuroscience : the official journal of the Society for Neuroscience* **29**, 10309-20 (2009).
Rossi, D.J., Alford, S., Mugnaini, E. & Slater, N.T. Properties of transmission at a giant glutamatergic synapse in cerebellum: the mossy fiber-unipolar brush cell synapse. *Journal of neurophysiology* **74**, 24-42 (1995).
Ruigrok, T.J.H. Ins and outs of cerebellar modules. *Cerebellum (London, England)* **10**, 464-74 (2011).
Ruigrok, T.J.H., Pijpers, A., Goedknegt-Sabel, E. & Coulon, P. Multiple cerebellar zones are involved in the control of individual muscles: a retrograde transneuronal tracing study with rabies virus in the rat. *The European journal of neuroscience* **28**, 181-200 (2008).
Sahin, M. & Hockfield, S. Molecular identification of the Lugaro cell in the cat cerebellar cortex. *The Journal of comparative neurology* **301**, 575-84 (1990).
Sakai, K. *et al.* What and when: parallel and convergent processing in motor control. *The Journal of neuroscience : the official journal of the Society for Neuroscience* **20**, 2691-700 (2000).
Sanchez, M. *et al.* Compartmentation of the rabbit cerebellar cortex. *The Journal of comparative neurology* **444**, 159-73 (2002).
Sato, Y., Miura, A., Fushiki, H. & Kawasaki, T. Short-term modulation of cerebellar Purkinje cell activity after spontaneous climbing fiber input. *Journal of neurophysiology* **68**, 2051-62 (1992).
SCHEIBEL, M.E. & SCHEIBEL, A.B. Observations on the intracortical relations of the climbing fibers of the cerebellum; a Golgi study. *The Journal of comparative neurology* **101**, 733-63 (1954).
Schmahmann, J.D. From movement to thought: anatomic substrates of the cerebellar contribution to cognitive processing. *Human brain mapping* **4**, 174-98 (1996).
Schmahmann, J.D. The cerebrocerebellar system: anatomic substrates of the cerebellar contribution to cognition and emotion. *International Review of Psychiatry* **13**, 247-260 (2001).
Schulman, J.A. & Bloom, F.E. Golgi cells of the cerebellum are inhibited by inferior olive activity. *Brain research* **210**, 350-5 (1981).
Schultz, S.R., Kitamura, K., Post-Uiterweer, A., Krupic, J. & Häusser, M. Spatial pattern coding of sensory information by climbing fiber-evoked calcium signals in networks of neighboring cerebellar Purkinje cells. *The Journal of neuroscience : the official journal of the Society for Neuroscience* **29**, 8005-15 (2009).
Schwartzman, R.J. A behavioral analysis of complete unilateral section of the pyramidal tract at the medullary level in Macaca mulatta. *Annals of neurology* **4**, 234-44 (1978).
Schwarz, C. & Welsh, J.P. Dynamic modulation of mossy fiber system throughput by inferior olive synchrony: a multielectrode study of cerebellar cortex activated by motor cortex. *Journal of neurophysiology* **86**, 2489-504 (2001).
Servais, L. *et al.* Mono- and dual-frequency fast cerebellar oscillation in mice lacking parvalbumin and/or calbindin D-28k. *The European journal of neuroscience* **22**, 861-70 (2005).
Servais, L. & Cheron, G. Purkinje cell rhythmicity and synchronicity during modulation of fast cerebellar oscillation. *Neuroscience* **134**, 1247-1259 (2005).
Servais, L. *et al.* Purkinje cell dysfunction and alteration of long-term synaptic plasticity in fetal

alcohol syndrome. *Proceedings of the National Academy of Sciences of the United States of America* **104**, 9858-63 (2007).
Shibuki, K. & Okada, D. Endogenous nitric oxide release required for long-term synaptic depression in the cerebellum. *Nature* **349**, 326-8 (1991).
Shidara, M., Kawano, K., Gomi, H. & Kawato, M. Inverse-dynamics model eye movement control by Purkinje cells in the cerebellum. *Nature* **365**, 50-2 (1993).
Shin, S.-L. & De Schutter, E. Dynamic synchronization of Purkinje cell simple spikes. *Journal of neurophysiology* **96**, 3485-91 (2006).
Shin, S.-L. *et al.* Regular patterns in cerebellar Purkinje cell simple spike trains. *PloS one* **2**, e485 (2007).
Shoham, S., Fellows, M.R. & Normann, R.A. Robust, automatic spike sorting using mixtures of multivariate t-distributions. *Journal of neuroscience methods* **127**, 111-22 (2003).
Sillitoe, R.V., Chung, S.-H., Fritschy, J.-M., Hoy, M. & Hawkes, R. Golgi cell dendrites are restricted by Purkinje cell stripe boundaries in the adult mouse cerebellar cortex. *The Journal of neuroscience : the official journal of the Society for Neuroscience* **28**, 2820-6 (2008).
Sillitoe, R.V. & Hawkes, R. Whole-mount immunohistochemistry: a high-throughput screen for patterning defects in the mouse cerebellum. *The journal of histochemistry and cytochemistry : official journal of the Histochemistry Society* **50**, 235-44 (2002).
Sillitoe, R.V., Hulliger, M., Dyck, R. & Hawkes, R. Antigenic compartmentation of the cat cerebellar cortex. *Brain research* **977**, 1-15 (2003).
Simat, M., Parpan, F. & Fritschy, J.-M. Heterogeneity of glycinergic and gabaergic interneurons in the granule cell layer of mouse cerebellum. *The Journal of comparative neurology* **500**, 71-83 (2007).
Smith, A.M. & Bourbonnais, D. Neuronal activity in cerebellar cortex related to control of prehensile force. *Journal of neurophysiology* **45**, 286-303 (1981).
Solinas, S. *et al.* Fast-reset of pacemaking and theta-frequency resonance patterns in cerebellar golgi cells: simulations of their impact in vivo. *Frontiers in cellular neuroscience* **1**, 4 (2007).
Sotelo, C. & Llinás, R. Specialized membrane junctions between neurons in the vertebrate cerebellar cortex. *The Journal of cell biology* **53**, 271-89 (1972).
Sotelo, C., Llinas, R. & Baker, R. Structural study of inferior olivary nucleus of the cat: morphological correlates of electrotonic coupling. *Journal of neurophysiology* **37**, 541-59 (1974).
Soteropoulos, D.S. & Baker, S.N. Cortico-cerebellar coherence during a precision grip task in the monkey. *Journal of neurophysiology* **95**, 1194-206 (2006).
Stone, L.S. & Lisberger, S.G. Visual responses of Purkinje cells in the cerebellar flocculus during smooth-pursuit eye movements in monkeys. I. Simple spikes. *Journal of neurophysiology* **63**, 1241-61 (1990).
Strick, P.L., Dum, R.P. & Fiez, J.A. Cerebellum and nonmotor function. *Annual review of neuroscience* **32**, 413-34 (2009).
Sugihara, I. & Shinoda, Y. Molecular, topographic, and functional organization of the cerebellar cortex: a study with combined aldolase C and olivocerebellar labeling. *The Journal of neuroscience : the official journal of the Society for Neuroscience* **24**, 8771-85 (2004).
Sultan, F. Distribution of mossy fibre rosettes in the cerebellum of cat and mice: evidence for a parasagittal organization at the single fibre level. *The European journal of neuroscience* **13**, 2123-30 (2001).
Szurhaj, W. *et al.* Intracerebral study of gamma rhythm reactivity in the sensorimotor cortex. *The European journal of neuroscience* **21**, 1223-35 (2005).
Tahon, K., Volny-Luraghi, A. & De Schutter, E. Temporal characteristics of tactile stimuli influence the response profile of cerebellar Golgi cells. *Neuroscience letters* **390**, 156-61 (2005).
Takahashi, S., Anzai, Y. & Sakurai, Y. Automatic sorting for multi-neuronal activity recorded with tetrodes in the presence of overlapping spikes. *Journal of neurophysiology* **89**, 2245-58 (2003).

Tanji, J. & Evarts, E.V. Anticipatory activity of motor cortex neurons in relation to direction of an intended movement. *Journal of neurophysiology* **39**, 1062-8 (1976).
Tecchio, F. *et al.* Somatosensory dynamic gamma-band synchrony: a neural code of sensorimotor dexterity. *NeuroImage* **35**, 185-93 (2007).
Tesche, C.D. & Karhu, J.J. Anticipatory cerebellar responses during somatosensory omission in man. *Human brain mapping* **9**, 119-42 (2000).
Thier, P., Dicke, P.W., Haas, R. & Barash, S. Encoding of movement time by populations of cerebellar Purkinje cells. *Nature* **405**, 72-6 (2000).
Timmann, D., Watts, S. & Hore, J. Failure of cerebellar patients to time finger opening precisely causes ball high-low inaccuracy in overarm throws. *Journal of neurophysiology* **82**, 103-14 (1999).
Timofeev, I. & Steriade, M. Fast (mainly 30-100 Hz) oscillations in the cat cerebellothalamic pathway and their synchronization with cortical potentials. *The Journal of physiology* **504 (Pt 1**, 153-68 (1997).
Toyama, K., Tsukahara, N., Kosaka, K. & Matsunami, K. Synaptic excitation of red nucleus neurones by fibres from interpositus nucleus. *Experimental brain research. Experimentelle Hirnforschung. Expérimentation cérébrale* **11**, 187-98 (1970).
Tsukahara, N. & Kosaka, K. The mode of cerebral excitation of red nucleus neurons. *Experimental brain research. Experimentelle Hirnforschung. Expérimentation cérébrale* **5**, 102-17 (1968).
Usowicz, M.M., Sugimori, M., Cherksey, B. & Llinás, R. P-type calcium channels in the somata and dendrites of adult cerebellar Purkinje cells. *Neuron* **9**, 1185-99 (1992).
Van Der Giessen, R.S. *et al.* Role of olivary electrical coupling in cerebellar motor learning. *Neuron* **58**, 599-612 (2008).
van Kan, P.L., Gibson, A.R. & Houk, J.C. Movement-related inputs to intermediate cerebellum of the monkey. *Journal of neurophysiology* **69**, 74-94 (1993).
VandenBerg, P.M., Hogg, T.M., Kleim, J.A. & Whishaw, I.Q. Long-Evans rats have a larger cortical topographic representation of movement than Fischer-344 rats: a microstimulation study of motor cortex in naïve and skilled reaching-trained rats. *Brain research bulletin* **59**, 197-203 (2002).
Vargas-Irwin, C. & Donoghue, J.P. Automated spike sorting using density grid contour clustering and subtractive waveform decomposition. *Journal of neuroscience methods* **164**, 1-18 (2007).
Voogd, J., Hess, D.T. & Marani, E. The parasagittal zonation of the cerebellar cortex in cat and monkey: topography, distribution of acetyhcholinesterase, and development. *New Concepts in Cerebellar Neurobiology.* 183-220 (1987).
Voogd, J. The cerebellum of the Cat. Structure and Fibre Connections. (1964).
Voogd, J. The importance of fiber connections in the comparative anatomy of the mammalian cerebellum. *Neurobiology of Cerebellar Evolution and Development* 493—54 (1969).
Vos, B.P., Maex, R., Volny-Luraghi, A. & De Schutter, E. Parallel fibers synchronize spontaneous activity in cerebellar Golgi cells. *The Journal of neuroscience : the official journal of the Society for Neuroscience* **19**, RC6 (1999).
Vos, B.P., Volny-Luraghi, A. & De Schutter, E. Cerebellar Golgi cells in the rat: receptive fields and timing of responses to facial stimulation. *The European journal of neuroscience* **11**, 2621-34 (1999).
Vos, B.P., Volny-Luraghi, A., Maex, R. & De Schutter, E. Precise spike timing of tactile-evoked cerebellar Golgi cell responses: a reflection of combined mossy fiber and parallel fiber activation? *Progress in brain research* **124**, 95-106 (2000).
Watanabe, D. & Nakanishi, S. mGluR2 postsynaptically senses granule cell inputs at Golgi cell synapses. *Neuron* **39**, 821-9 (2003).
Welker, W., Blair, C. & Shambes, G.M. Somatosensory projections of cerebellar granule cell layer of giant bushbaby, Galago crassicaudatus. *Brain, behavior and evolution* **31**, 150-60 (1988).
Welsh, J.P., Lang, E.J., Suglhara, I. & Llinás, R. Dynamic organization of motor control within the olivocerebellar system. *Nature* **374**, 453-7 (1995).

Wenger, K.K., Musch, K.L. & Mink, J.W. Impaired reaching and grasping after focal inactivation of globus pallidus pars interna in the monkey. *Journal of neurophysiology* **82**, 2049-60 (1999).
Whishaw, I.Q. An endpoint, descriptive, and kinematic comparison of skilled reaching in mice (Mus musculus) with rats (Rattus norvegicus). *Behavioural brain research* **78**, 101-11 (1996).
Whishaw, I.Q. Loss of the innate cortical engram for action patterns used in skilled reaching and the development of behavioral compensation following motor cortex lesions in the rat. *Neuropharmacology* **39**, 788-805 (2000).
Whishaw, I.Q. & Gorny, B. Does the red nucleus provide the tonic support against which fractionated movements occur? A study on forepaw movements used in skilled reaching by the rat. *Behavioural brain research* **74**, 79-90 (1996).
Whishaw, I.Q., O'Connor, W.T. & Dunnett, S.B. The contributions of motor cortex, nigrostriatal dopamine and caudate-putamen to skilled forelimb use in the rat. *Brain : a journal of neurology* **109 (Pt 5**, 805-43 (1986).
Whishaw, I.Q. & Pellis, S.M. The structure of skilled forelimb reaching in the rat: a proximally driven movement with a single distal rotatory component. *Behavioural brain research* **41**, 49-59 (1990).
Whishaw, I.Q., Pellis, S.M., Gorny, B., Kolb, B. & Tetzlaff, W. Proximal and distal impairments in rat forelimb use in reaching follow unilateral pyramidal tract lesions. *Behavioural brain research* **56**, 59-76 (1993).
Whishaw, I.Q. & Tomie, J.A. Olfaction directs skilled forelimb reaching in the rat. *Behavioural brain research* **32**, 11-21 (1989).
Whishaw, I.Q., Tomie, J.A. & Ladowsky, R.L. Red nucleus lesions do not affect limb preference or use, but exacerbate the effects of motor cortex lesions on grasping in the rat. *Behavioural brain research* **40**, 131-44 (1990).
Whishaw, I.Q., Gorny, B., Foroud, A. & Kleim, J.A. Long-Evans and Sprague-Dawley rats have similar skilled reaching success and limb representations in motor cortex but different movements: some cautionary insights into the selection of rat strains for neurobiological motor research. *Behavioural brain research* **145**, 221-32 (2003).
Wiesendanger, R., Wiesendanger, M. & Rüegg, D.G. An anatomical investigation of the corticopontaine projection in the primate (Macaca fascicularis and Saimiri sciureus)--II. The projection from frontal and parental association areas. *Neuroscience* **4**, 747-65 (1979).
Winkelman, B. & Frens, M. Motor coding in floccular climbing fibers. *Journal of neurophysiology* **95**, 2342-51 (2006).
Wise, A.K., Cerminara, N.L., Marple-Horvat, D.E. & Apps, R. Mechanisms of synchronous activity in cerebellar Purkinje cells. *The Journal of physiology* **588**, 2373-90 (2010).
Womack, M.D. & Khodakhah, K. Somatic and dendritic small-conductance calcium-activated potassium channels regulate the output of cerebellar Purkinje neurons. *The Journal of neuroscience : the official journal of the Society for Neuroscience* **23**, 2600-7 (2003).
Wulff, P. *et al.* Synaptic inhibition of Purkinje cells mediates consolidation of vestibulo-cerebellar motor learning. *Nature neuroscience* **12**, 1042-9 (2009).
Wylie, D.R., De Zeeuw, C.I. & Simpson, J.I. Temporal relations of the complex spike activity of Purkinje cell pairs in the vestibulocerebellum of rabbits. *The Journal of neuroscience : the official journal of the Society for Neuroscience* **15**, 2875-87 (1995).
Xu, W. & Edgley, S.A. Climbing fibre-dependent changes in Golgi cell responses to peripheral stimulation. *The Journal of physiology* **586**, 4951-9 (2008).
Yanagihara, D. & Kondo, I. Nitric oxide plays a key role in adaptive control of locomotion in cat. *Proceedings of the National Academy of Sciences of the United States of America* **93**, 13292-7 (1996).
Zackowski, K.M., Thach, W.T. & Bastian, A.J. Cerebellar subjects show impaired coupling of reach and grasp movements. *Experimental brain research. Experimentelle Hirnforschung. Expérimentation cérébrale* **146**, 511-22 (2002).